UNIVERSITY OF CALIFORNIA
RIVERSIDE

Selective C–H Functionalization of Diamondoids Using Photocatalysis,
Total Synthesis of the Earthworm Metabolite Malylglutamate,
and
Investigations Toward the Synthesis of the Flavalin Family of Natural Products

A Dissertation submitted in partial satisfaction
of the requirements for the degree of

Doctor of Philosophy

in

Chemistry

by

Abigail Feceu

September 2019

Dissertation Committee:
        Dr. Dave B. C. Martin, Chairperson
        Dr. Christopher Switzer
        Dr. Kevin Kou

The Dissertation of Abigail Feceu is approved:

_____

_____

_____

Committee Chairperson

University of California, Riverside

ACKNOWLEDGEMENT

ABSTRACT OF THE DISSERTATION

Selective C–H Functionalization of Diamondoids Using Photocatalysis,
Total Synthesis of the Earthworm Metabolite Malylglutamate,
and
Investigations Toward the Synthesis of the Flavalin Family of Natural Products

by

Abigail Feceu

Doctor of Philosophy, Graduate Program in Chemistry
University of California, Riverside, September 2019
Dr. Dave B. C. Martin, Chairperson

Diamondoids are a fascinating class of caged hydrocarbons unique in structure with properties unlike other alkanes and have proven to be useful scaffolds in medicinal chemistry, catalysis and nanomaterials. One inherent property of diamondoids is their strong C–H bonds making this class an excellent target for investigating selective and direct C–H functionalization. Chapter 1 of this dissertation focuses on previous methods used to directly transform adamantanes to functional molecules *via* radical methods. In Chapter 2, a direct and selective alkylation method of adamantanes using a dual-photocatalytic C–H activation method is reported. This selective functionalization relies both on a visible light absorbing photocatalyst and a quinuclidine based hydrogen atom transfer (HAT) catalyst.

Optimization studies, syntheses of adamantane derivatives and an in-depth mechanistic study will be discussed. The direct acetylation of the second higher ordered diamondoid, diamantane *via* photocatalytic C–H functionalization, is also investigated.

In Chapter 3, the total synthesis and structural reassignment of the newly identified natural product, malylglutamate, an earthworm metabolite, is reported. A traditional peptide coupling approach is utilized for assembling the amide from a protected malate and glutamate. Finally, in Chapter 4, the synthesis of a family of bioactive sesquiterpene natural products, known as the flavalins, are investigated. The initial proposed synthesis relies on a key 6π-electrocyclization as the final step in generating the flavalin core. The synthesis of the flavalin precursor, an electron deficient triene, leads to unexpected results during typical Suzuki cross-coupling conditions, ultimately precluding the synthesis of these natural products.

Table of Contents

LIST OF SCHEMES

LIST OF FIGURES

LIST OF TABLES

LIST OF ACRONYMS AND ABBREVIATIONS

Ac   acetyl

Acac   acetylacetone

Acr   acridinium

AIBN   azobisisobutyronitrile

Ar   aryl

BDE   bond dissociation energy

BHT   butylated hydroxytoluene

Boc   *tert*-butyloxycarbonyl

Bn   benzyl

BnOH   benzyl alcohol

Bn_2O dibenzyl ether

BnBr   benzylbromide

BPO   benzoyl peroxide

Bpy   2,2'-bipyridine

BzPy   4-benzoylpyridine

CSA   camphorsulfonic acid

Cat   catalyst

CuTC   copper(I) thiophene-2-carboxylate

COSY   correlation spectroscopy

DBU   1,8-diazabicyclo[5.4.0]undec-7-ene

DCC   *N,N'*-dicyclohexylcarbodiimide

DCE   1,2-dichloroethane

DCM   dichloromethane

DIBAL   diisobutylaluminium hydride

DIC   *N,N'*-diisopropylcarbodiimide

DMF   dimethylformamide

DMSO   dimethylsulfoxide

Dtbbpy   4,4'-di-*tert*-butyl-2,2'-dipyridyl

DTBP   di-*tert*-butyl peroxide

DTMP   thymidine monophosphate

EDCl 1-ethyl-3-(3-dimethylaminopropyl)carbodiimide hydrochloride

ESI electrospray ionization

Et. Al. et alli

EY eyosin Y

FDA U.S. food and drug administration

FID flame ionization detector

FPP farnesyl pyrophosphate

FT-IR Fourier-transform infrared spectroscopy

GC gas chromatography

g.l.c. gas-liquid chromatography

HAT hydrogen atom transfer

HCTU 2-(6-chloro-1-H-benzotriazole-1-yl)-1,1,3,3-tetramethyluronium hexafluorophosphate

HMPA hexamethylphosphoramide

HOBT *N*-hydroxybenzotriazole

HOMO highest occupied molecular orbital

HRMS high-resolution mass spectrometry

HWE Horner-wadsworth-emmons

hυ light

IPMN isopropylydene malononitrile

ISC intersystem crossing

KIE kinetic isotope effect

LC-MS liquid chromatography-mass spectrometry

LDA lithium diisopropylamide

LED light-emitting diode

LUMO lowest unoccupied molecular orbital

MDPT   4-mesityl-2,6-diphenylpyrylium tetrafluoroborate

MIDA   *N*-methyliminodiacetic acid

MLCT   metal-to-ligand charge transfer

NAAG   *N*-acetylaspartylglutamate

NHC   *N*-heterocyclic carbene

NHPI   *N*-hydroxyphthalimide

NMI   *N*-methylimidazole

NMM   *N*-methylmaleimide

NMR   nuclear magnetic resonance spectroscopy

NOE   nuclear overhauser effect

NOESY nuclear overhauser effect spectroscopy

PIFA   (bis(trifluoroacetoxy)iodobenzene

PINO   phthalimide-*N*-oxyl

Ppy   2-phenylpyridine

PT   5,7,12,14-pentacenetetraone

PTC   phase transfer catalyst

SCE   saturated calomel electrode

SET   single electron transfer

SPhos   2-dicyclohexylphosphino-2',6'-dimethoxybiphenyl

TBADT   tetrabutylammonium decatungstate

TBHN   di-*tert*-butyl hyponitrite

TCB   1,2,4,5-benzenetetracarbonitrile

TCFH   tetramethylchloroformamidinium hexafluorophosphate

TEMPO 2,2,6,6-tetramethylpiperidine *N*-oxide

TFA   trifluoroacetic acid

TFAA   trifluoroacetic anhydride

TFE   2,2,2-trifluoroethanol

THF   tetrahydrofuran

THP   tetrahydropyran

TLC   thin layer chromatography

TPT   triphenylpyrylium

tetrafluoroborate

TsOH   *p*-toluenesulfonic acid

UV   ultraviolet

Cl$_4$NHPI tetrachloro-*N*-

hydroxyphthalimide

XPhos   2-dicyclohexylphosphino-

2',4',6'-triisopropylbiphenyl

PUBLICATIONS

Abigail Feceu, Lauren E. Sangster, David B. C. Martin, *"Unexpected Alkene Isomerization During Iterative Cross-Coupling To Form Hindered, Electron-Deficient Trienes." Org. Lett.,* **2018***, 20,* 3151-3155.

Abigail Feceu, Corey M. Griffith, Cynthia K. Larive, David B. C. Martin*, "Synthesis and Structure Reassignment of Malylglutamate, a Recently Discovered Earthworm Metabolite" J. Nat. Prod.,* **2019***, 82*, 417-421.

Hai-Bin Yang, Abigail Feceu, David B.C. Martin, *"Catalyst-Controlled C–H Functionalization of Adamantanes Using Selective H-Atom Transfer." ACS Catal.,* **2019***, 9,* 5708-5715**.**

Chapter 1 - Selective Radical Functionalization Methods to Access Substituted

Adamantanes and Diamondoids

1.1 - Introduction

Diamondoids are a fascinating class of caged hydrocarbons unique in structure with properties unlike other alkanes. The name originates from the Greek translation of diamond as these aliphatic caged hydrocarbons resemble the hydrogen-terminated diamond lattice. The lower-ordered members of this family adamantane (**1.01**), diamantane (**1.02**) and triamantane **(1.03)** each have a single isomer and of the higher-ordered diamondoids, only *anti*-tetramantane **(1.04)** has been synthesized, albeit in low yields (Figure 1.1).[1] Tetramantane possesses four different isomers, *iso-, anti-* and two enantiomeric *skew*-tetramantanes, shown in Figure 1.1. As the size of the diamondoids increase, so do the number of isomers; pentamantane has 10 isomers, hexamantanes have 24 isomers, and heptamantane has nearly one hundred isomers.[2–7] In Nature, the formation of these diamondoids occur *via* thermodynamically controlled carbocation rearrangements[8,9] and although this method has been used to synthesize the lower ordered members, carbocation rearrangements have failed in the production of higher diamondoids.
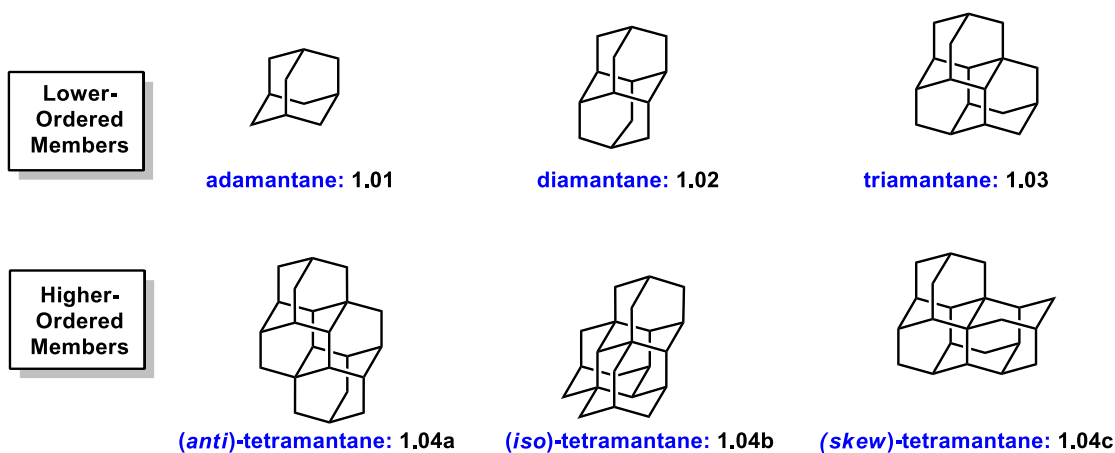
Figure 1.1 Selected lower- and higher-ordered diamondoids

1.1.1 - Background

In 1933, the first member of the diamondoid family, adamantane, was discovered from the Hodonin oil field in Moravia, Czechoslovakia by Landa and Machacek from crude oil (Figure 1.2).[10] Naturally occurring diamondoids have been isolated from crude oil, natural gas and sediments with the highest member identified as dodecamantane ($C_{54}H_{60}$).[11] Unfortunately, isolation of these hydrocarbons from the natural source has shown to be problematic as diamondoids are scarce and comprises only approximately 0.0004% of petroleum content.[12] This called for the development of synthetic approaches for the diamondoids. Adamantane was first synthesized by Prelog and Seiwerth in 1941; however the yield was initially a low 6.5% over multiple steps.[13] Inspired by Nature's way of making these particular scaffolds, Schleyer devised a simplified synthetic route to making adamantane *via* a Lewis acid-promoted rearrangement of tetrahydrodicyclopentadiene (**1.05**) and was able to improve the yield to 60-62% (Figure 1.2).[14] This process is thought to be thermodynamically controlled and successful due to the high stability of adamantane relative to the intermediate **1.05.** The mechanism involves a series of carbocation intermediates that undergo rearrangements *via* 1,2 bond migrations and hydride shifts.[15]

The study of adamantane and its functionalization was limited until adamantane became more readily available through Schleyer's synthesis. However, soon following Schleyer's report, a number of adamantyl derivatives were synthesized *via* halogenations, amidations, carboxylations and more.[2-4] The halogenation of adamantanes became an attractive target in the late 1950's due to their ease of functionalization. In 1954, the first

bromination of adamantane was performed but it was not until 1959 that 1-bromoadamantane (**1.06**) was successfully synthesized and confirmed by Stetter *et. al.* in a reported 85% yield.[16] In 1961, Haaf *et. al.* reported the first known amidation of adamantane using *tert*-butanol, sulfuric acid and hydrogen cyanide to give the desired formamide in 76% yield.[17] This was followed by hydrolysis to give 1-aminoadamantane. This led to the discovery of pharmaceutical drugs containing this particular amine scaffold.[18]

1-Aminoadamantane, also formally known as amantadine (**1.07**), was the first pharmaceutical derived from the adamantane scaffold and was found to display potent anti-*influenza* A properties in 1964.[19] Amantadine was officially FDA approved for treatment in 1967. Following the success of amantadine, other adamantane containing drug candidates were quickly synthesized. A year after amantadine was approved for treatment, memantine, was synthesized and patented by Eli Lilly and Company in 1968 for its antiviral properties. Ultimately, it was approved by the FDA as an anti-dementia drug for the treatment of Alzheimer's disease in 2003.[20]
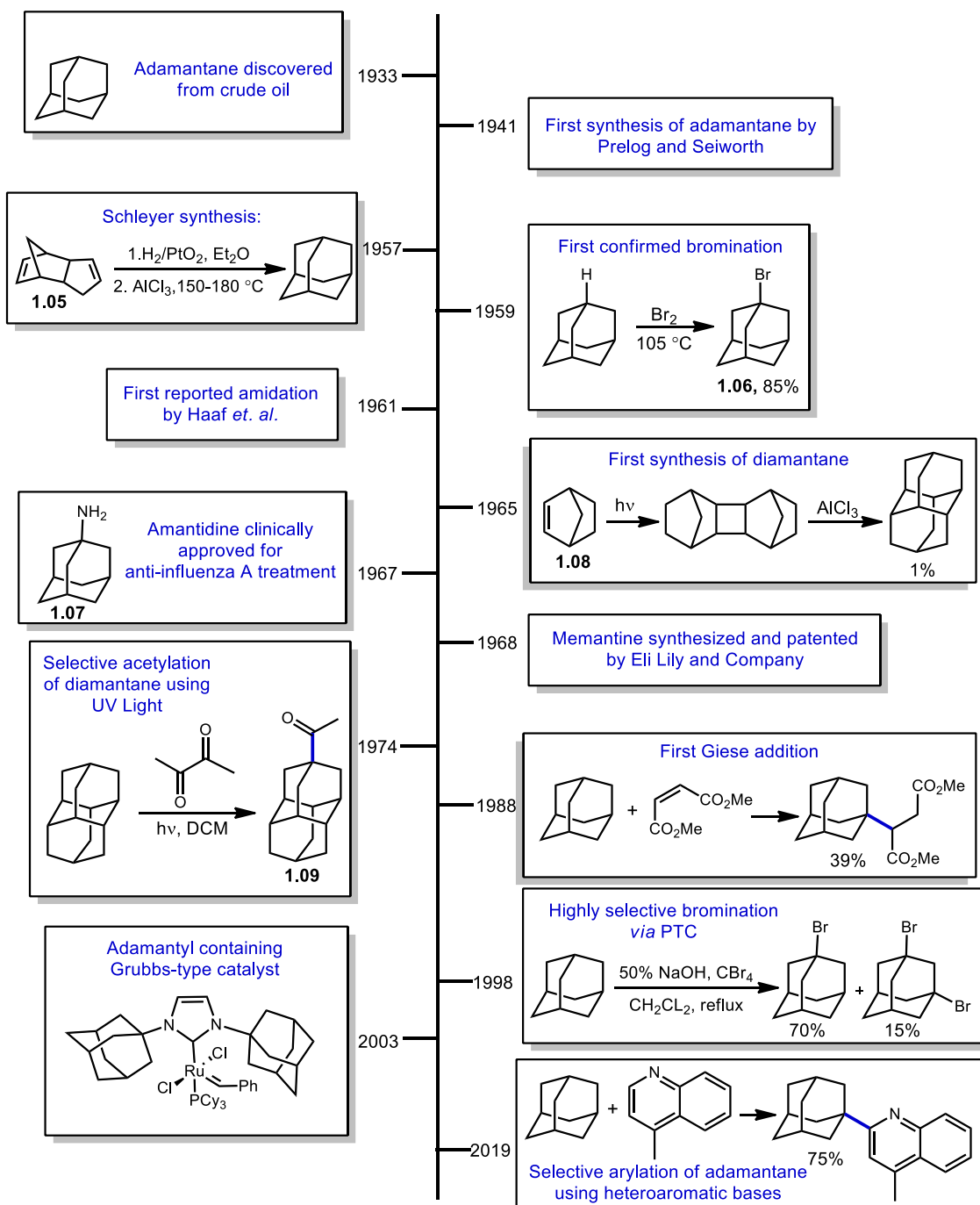
Figure 1.2 Timeline and history of diamondoids

The second member of the diamondoid family, diamantane, originally known as congressane[21,22] was first synthesized by Cupas *et. al.* in 1965 through a [2+2] dimerization of norbornene (**1.08**) followed by a rearrangement using AlCl$_3$ resulting in a 1% isolated yield (Figure 1.2)[22]; it was not isolated naturally from petroleum until a year later in 1966. In 1974, Tabushi and coworkers selectively acetylated diamantane at the apical position using biacetyl and UV light.[23] This was followed by selective acetylation of the higher diamondoids in 2006 by Schreiner and coworkers.[2,5] The first Giese-like addition performed on adamantane using unsaturated compounds, was done by Fukunishi and Tabushi in 1988.[24] This reaction allowed for the direct functionalization of C–H bonds to generate C–C bonds with high regioselectivity.

In 1998, Schreiner *et. al.* invented a selective method for the direct bromination of adamantane using phase-transfer conditions. Adamantane and tetrabromomethane were refluxed in DCM at 40℃ in the presence of 50% aqueous NaOH using triethylbenzylammonium chloride as the phase transfer catalyst.[25] Under these reaction conditions, a 70% yield of the mono-brominated product was obtained with a 15% yield of the byproduct, bis-brominated adamantane. In 2003, Mol *et. al.* utilized the adamantane scaffold in synthesizing *N*-heterocyclic carbenes (NHC) bearing these substituents.[26]

Typically, mesityl substituted NHC ligands are commonly used however adamantanes' bulky properties were hypothesized to reduce decomposition of the metal catalyst and help induce rapid dissociation of the phosphine ligand on the Grubbs catalyst. The direct and selective C–H functionalization of adamantanes has been of interest since Schleyer's method however methods for synthesizing diverse adamantane products in high

yield as a single regioisomer has more recently been investigated. One example by Togo *et. al.* reports the functionalization of heteroaromatic bases with adamantane in a selective fashion generating the arylated products in high yields (Figure 1.2).[27]

1.1.2 - Properties of Adamantanes

Diamondoids are highly symmetrical saturated hydrocarbons that are comprised of almost perfectly tetrahedral geometries about their carbon atoms and three or more fused cyclohexane rings in the chair conformation. Although not completely strain free, diamondoids possess low strain energy resulting in more stable and rigid structures. Since all carbon atoms in adamantane are tetrahedral, the molecule is free from angle strain. Also, all C–C bonds are staggered making the molecule free from torsional strain.[28] Adamantane is a $C_{10}H_{16}$ molecule with T_d symmetry (Figure 1.3) that possesses one type of tertiary C–H bond and one type of secondary C–H bond. The bond dissociation energy (BDE) of the C–H bonds are relatively high; the secondary position has a BDE of 96 kcal/mol and the tertiary position has a BDE of 99 kcal/mol. Due to their high C–H BDE's, diamondoids are a compelling substrate class for the investigation of selective C–H functionalization
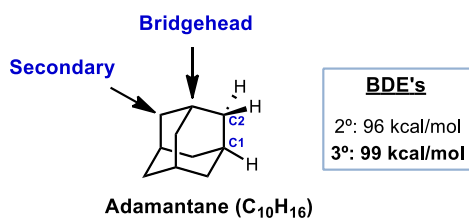
Figure 1.3 Properties of adamantane

1.1.3 - Functionalization of Diamondoids

Adamantane is the most studied member of the diamondoids with applications varying from nanomaterials and catalysis to medicinal chemistry and drug delivery.[18,29–31] Compared to higher members, adamantane is the simplest to functionalize as it possesses only one kind of tertiary C–H bond and one secondary. Diamantane is more challenging to selectively functionalize because it has two different types of tertiary C–H bonds in which six of the positions are about the central cyclohexane and are termed "medial" and two are located at both the top and bottom of diamantane and are called "apical".

Typical functionalization of diamondoids relies on radical, ionic or oxidative transformations for which single electron oxidations are usually the most selective. In this chapter, we provide an overview of the different types of C–H to C–C transformations using direct functionalization *via* radical chemistry. Hydrogen atom abstraction methods that directly generate the adamantyl radical include halogen and alkoxyl radicals, as well as catalytic hydrogen atom transfer (HAT) species such as diarylketone and decatungstate photocatalysts (Figure 1.4).[24,32–39] The high reactivity of these abstractors results in variable, often low selectivity between different types of C–H bonds, making them impractical for many applications.
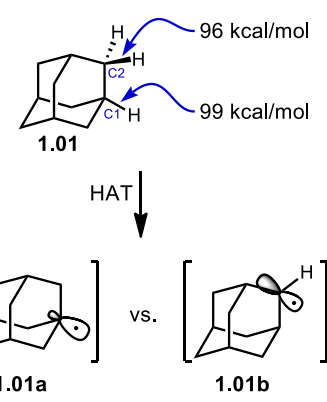
Figure 1.4 C–H Activation species of adamantanes

1.2 - Acylations

Introducing an acyl group to alkanes especially adamantanes was a challenging transformation in early organic synthesis.[40] Acyladamantanes are useful intermediates that can be further functionalized and are defined here as a compound featuring a direct C–C bond between adamantane and the carbonyl of a ketone, ester or aldehyde. Acyladamantanes have been shown to be useful precursors for compounds possessing biological activity.[41,42] While many methods have been developed to synthesize various acyladamantanes over the years, most rely on a pre-functionalized adamantyl substrate and/or harsh conditions. Currently, there are few reports of direct and selective acylations of adamantanes under irradiation or by a radical initiatior.[43,44] Therefore, direct methods for forging C–C bonds with adamantanes eliminate the need to use pre-functionalized substrates are desirable. Use of the reactive adamantyl radical has been used to achieve direct acylations and shall be detailed herein.

1.2.1 - Chlorocarbonylation

Tabushi was well known for his early work with functionalizing admantanes *via* acylation reactions. In 1968, Tabushi *et. al.* reported a free-radical chlorocarbonylation of adamantane using oxalyl chloride (**1.11**) and a benzoyl radical initiator which led to chlorocarbonylated intermediate **1.13** (shown in Table 1.1). Following methanolysis, a mixture of methyl 1- and 2-adamantanecarboxylates **1.12** and **1.12'** (55:45 r.r., respectively) was obtained in an 82% yield based on recovered starting material. After statistical correction, this distribution of regioisomers indicated a reactivity ratio of 3.67:1

favoring the tertiary adamantyl positions.[45] This preferential tertiary reactivity of adamantanes was also observed in prior radical halogenations by Smith and Williams.[46]

Table 1.1 Chlorocarbonylation of adamantane
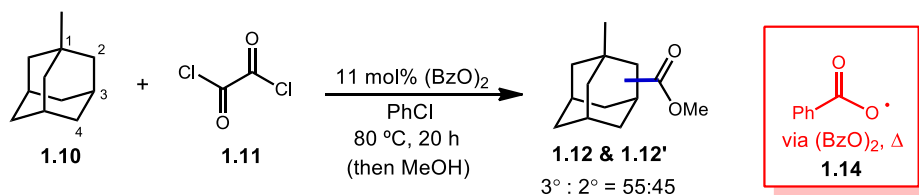
R	3° : 2° ratio
CH$_3$	2.3 : 1
H	1.2 : 1
OCH$_3$	5.7 : 1
CO$_2$CH$_3$	4.4 : 1
CN	1.4 : 1

Acyl Intermediate 1.13

1.2.2 - Formylation

Recently, Kamijo *et. al.* have reported a photochemically induced method for the formylation of unactivated C(sp^3)–H bonds in many substrates including adamantane using an aldoxime functional group.[47] Using a mercury lamp to generate a photoexcited 4-benzoylpyridine (4-BzPy) (**1.15**) to act as the C–H abstractor for adamantane, Kamijo showed that the resulting adamantly radical can readily intercept a formylating agent (Scheme 1.1). Using an *O*-benzyl aldoxime with an arylsulfonyl substituent **1.16** as a good leaving group leads to adamantyl *O*-benzylaldoxime precursor (**1.17**). The aldoxime can then be converted to aldehyde (**1.18**) using a solution of formaldehyde in aqueous HCl. Under these conditions the methine position of adamantane was formylated with a high regioselectivity (95:5).

11
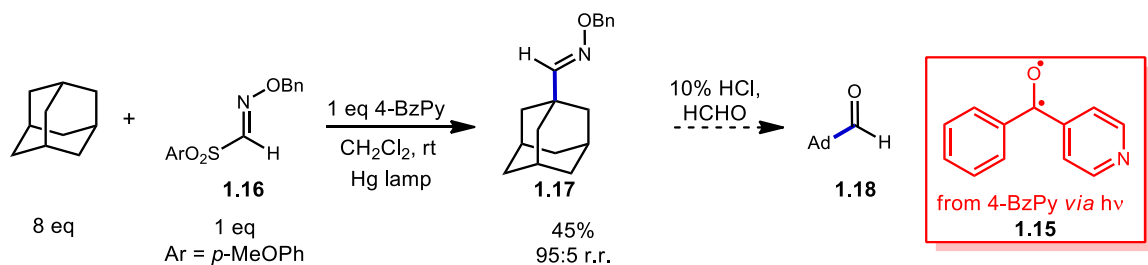
Scheme 1.1 Formylation of adamantane

1.2.3 - Acetylation

Tabushi *et. al.* selectively acetylated adamantane using an excess of biacetyl **1.18** under high energy UV irradiation in dichloromethane[48] to give 1-acetyladamantane (**1.19**) as the sole regioisomer (Table 1.2).[43] The C–H abstracting species is believed to be triplet biacetyl **1.20** since no acetylation occurred in the presence of pyrene, a known quencher of biacetyl phosphorescence *via* energy transfer.[49] Despite also being a potential quencher, oxygen instead increased the rate of acetylation and both the 1- and 2-acetyladamantane products were observed as was 1-adamantanol, the autooxidation product.

The increase in the photoacetylation rate and loss of selectivity is attributed to the generation of reactive methyl radicals which are formed in a decarboxylative process after oxygen and biacetyl react with each other. In higher ordered diamondoids, photoacetylation remains selective for the methine positions. However, unlike adamantane which features four equivalent methine positions, higher ordered diamondoids possess multiple nonequivalent positions

Table 1.2 Photoacetylation of adamantane
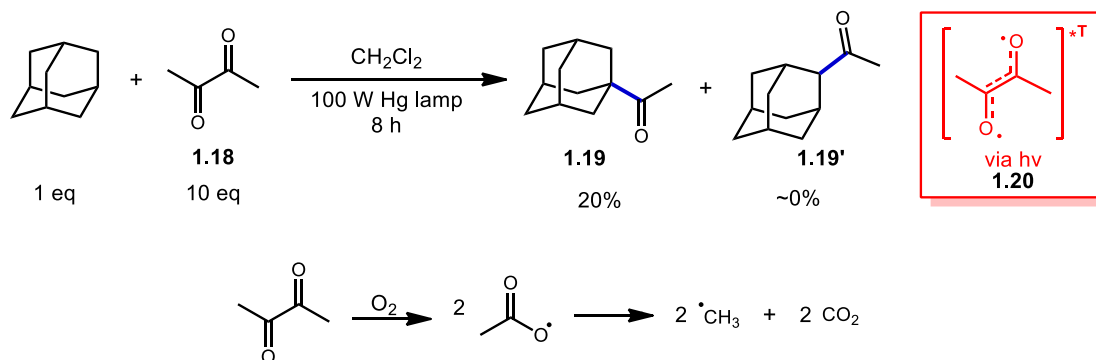
Conditions	1-acetyl adamantane (%)	2-acetyl adamantane (%)	1-adamantanol (%)
N_2	13.8	--	--
N_2, pyrene	0	--	--
O_2	28.6	12.3	8.3

.   For diamantane featuring two apical and 6 medial positions, photoacetlyation using biacetyl favored mono-acetylation at the apical position (**1.21**) over the medial position in a 5.5:1 ratio (17:1 after statistical correction, Figure 1.5). Acetylation of the methylene positions and bis-addition products were not observed.[23] This apical selectivity is still maintained in even higher ordered tri-, tetra- and pentamantanes (**1.22-1.27**) despite an increase in the number of possible functionalization positions. For instance, despite the unique number of different 3º C–H positions increasing from two in diamantane to four in triamantane and [121]tetramantane, acetylation of apical position is still favored over the other medial positions in an ~5:1 ratio.[2] Even higher apical selectivity is observed in [1(2)3]tetramantane and [123]tetramantane despite having six unique C–H positions).[50] [1(2,3)4]pentamantane showed near complete apical selectivity and resulted in a significant amount of bis-acetylated product as well.
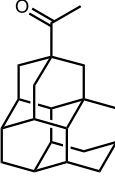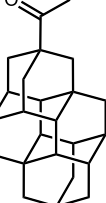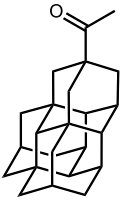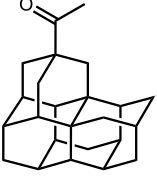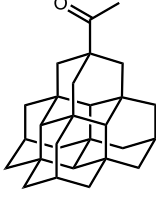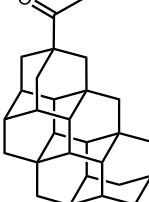
Diamondoid	acetylated product (apical)	Yield	apical:nonapical ratio
diamantane: **1.21**		53%	82:18
triamantane: **1.22**		43%	88:12
[121] (*anti*) tetramantane: **1.23**		57%	82:18
[1(2)3] (*iso*) tetramantane: **1.24**		53%	95:5
[123] (*skew*) tetramantane: **1.25**		58%	90:10
[1(2,3)4]pentamantane: **1.26**		45% (+ 40% bis)	~100
[1212]pentamantane: **1.27**		51%	85:15

Figure 1.5 Selectivity of the photoacetylation of higher diamondoids

1.3 - Carbonylation

1.3.1 - Carboxylation using NHPI

C–H functionalization of saturated hydrocarbons incorporating carbon monoxide, although attractive in synthetic methods, is quite challenging due to challenges of selectivity and low conversion of starting material.[51–53] Work done by Ishii in 1998 showed that oxidation of polycyclic alkanes in the presence of O_2 can produce carboxylated products using a catalytic free-radical method. *N*-hydroxyphthalimide (NHPI) is used as a radical catalyst to generate PINO radical **1.28** without photoactivation and under mild conditions.[33] However, when using adamantane as the hydrocarbon, multiple products are generated when O_2 or CO is introduced into the reaction as shown in Scheme 1.2.
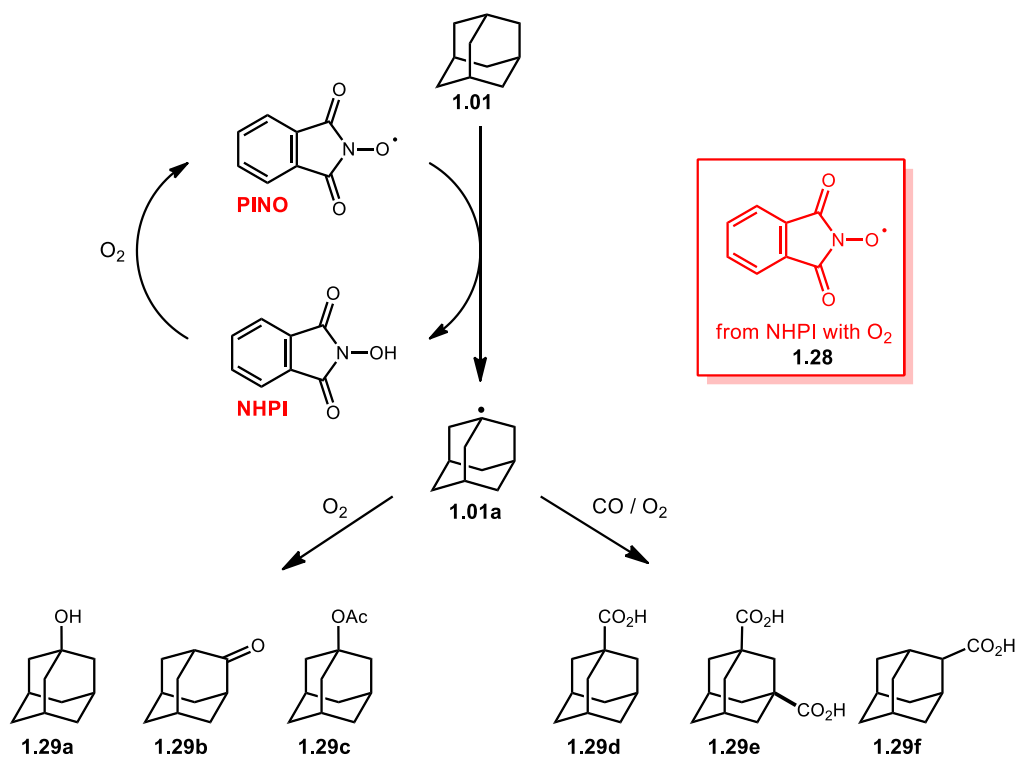
Scheme 1.2 NHPI-catalyzed oxidation and carboxylation

A conceivable mechanism begins with generating the reactive intermediate, phthalimide-*N*-oxyl (PINO) **1.28** from NHPI in the presence of O_2. The PINO radical formed will then do C–H abstraction preferentially at the tertiary position of adamantane **(1.01)** to give the intermediate, adamantyl radical **1.01a**. Radical **1.01a** can then react with O_2 to give the oxygenated products 1-adamantanol **1.29a**, 2-adamantanone **1.29b**, and 1-acetoxyadamantane **1.29c.** Alternatively, radical **1.01a** is readily trapped with CO which upon subsequent reaction with O_2, eventually generates carboxylic acids **1.29d-f**. Selectivity varies depending on reaction conditions and in all cases, there is recovery of starting material.

1.3.2 - Photocatalyzed Carbonylation
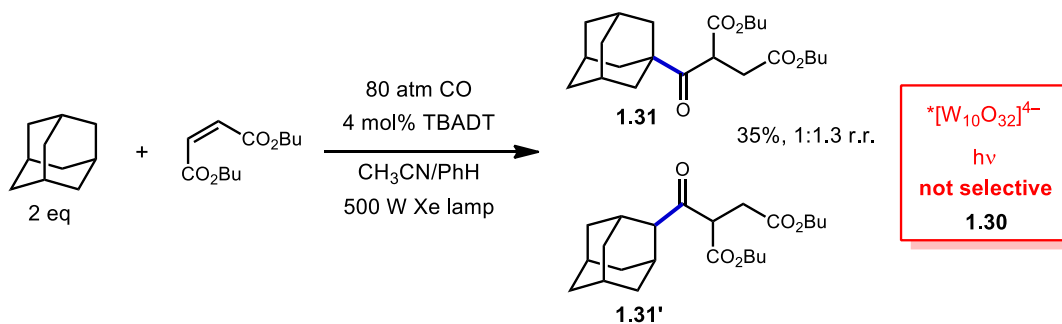
Scheme 1.3 Photocatalyzed carbobylation using decatungstate

In 2011, Ryu and Albini reported a three-component coupling reaction using photocatalytic methods based on previous work by Albini and others.[38] This multi-component process generated unsymmetrical ketones with tetrabutylammonium decatungstate (TBADT) **1.30** as the photocatalyst and a xenon lamp as their UV light source. The carbonylation of adamantane proceeded using a 1:1 mixture of acetonitrile and benzene as solvent and 2 equivalents of adamantane resulting in poor selectivity and

16

relatively low yields as shown in Scheme 1.3. A l:1.3 mixture of the 1- and 2- carbonylated products **1.31-131'** were obtained with an overall yield of 35% after 48% conversion of the alkene starting material. Higher yields and selectivities were reported for non-adamantane substrates.
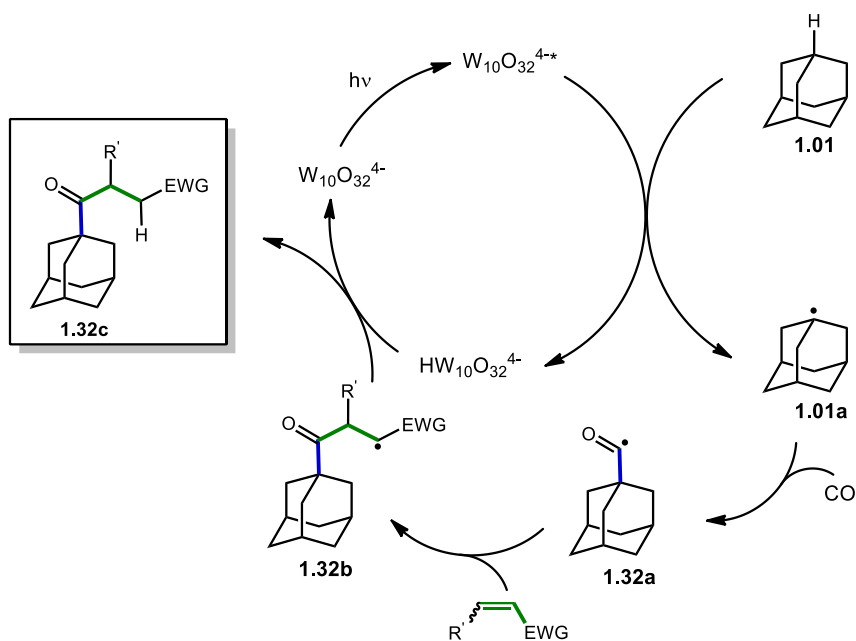
Scheme 1.4 TBADT catalyzed carbonylation

Scheme 1.4 shows the proposed catalytic cycle for the C–H functionalization of adamantane using the three-component system. Upon irradiation of TBADT, the excited photocatalyst **1.30** abstracts the hydrogen from adamantane **1.01** generating adamantyl radical **1.01a**. Carbonylation results in the acyl radical **1.32a** followed by a Giese-like addition to give intermediate **1.32b**. Intermediate **1.32b** is reduced by the photocatalyst, completing the catalytic cycle, and is followed by protonation to afford the desired functionalized adamantane product **1.32c.**

17

1.3.3 - Transition Metal Carbonylation

The use of transition metals for C–H activation *via* carbonylation is an attractive method for generating compounds containing carbonyl compounds. However, commonly used second- and third- row transition metals such as ruthenium and rhodium are expensive and can lead to complicated substrate syntheses limiting their use.[54–56] First row transition metals akin to nickel and copper are attractive alternative options due to their low toxicity, abundance and low cost.[57]

With this in mind, Wu *et. al.* reported the first copper-catalyzed carbonylative C–H activation in 2016 using a variety of alkanes and amides to generate imides.[58] Wu employed a Cu(I) species and di-*tert*-butyl peroxide (DTBP) to selectively functionalize adamantane at the tertiary position; generating imide **1.34** in 31% yield (Scheme 1.5a). While other alkanes were used in excess and cyclohexane was used as solvent, a 1:1 ratio of adamantane and *N*-methylacetamide **1.33** gave the desired product when (trifluoromethyl)benzene (PhCF$_3$) was used as solvent. The C–H abstracting species is likely the *tert*-butyloxy radical **1.35**, although the participation of copper cannot be ruled out.
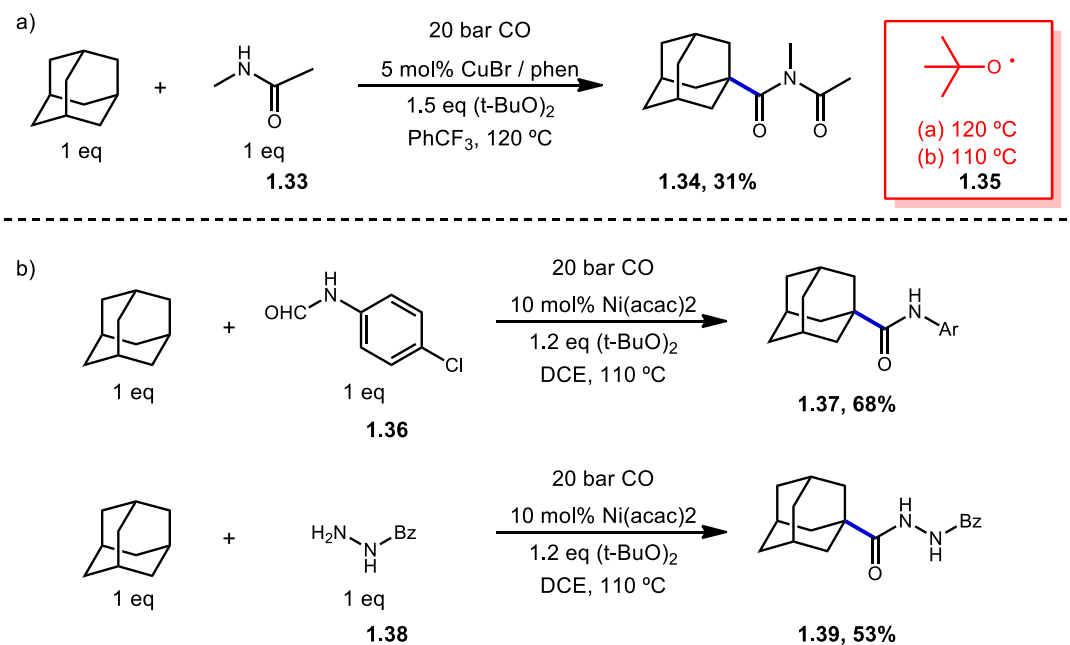
Scheme 1.5 Transition metal carbonylation

Nickel-based catalysis has previously been reported to be successful in the activation of inert $C(sp^3)$–H bonds, often through a directing group effect.[59] Recently, Li *et. al.* developed a Ni-catalyzed carbonylation of unreactive alkanes with formanilide to obtain amide products.[60] Scheme 1.5b illustrates two selective carbonylations both using adamantane. The first reaction uses an equimolar amount of formanilide **1.36** to give a modest 68% yield of compound **1.37** while the second utilizes benzohydrazide **1.38** which gave the corresponding di-acylhydrazines **1.39** in 53% yield. In both cases, selectivity favored the methine position. Similar to the work done by Wu and coworkers, DTBP is homolytically cleaved with the help of the transition metal, in this case Ni, to form the key reactive intermediate, the *tert*-butyloxy radical **1.35**.

1.3.4 - Metal-free Radical Oxidative Carbonylation

Although transition metal carbonylation is a commonly used approach in C–H activation reactions, an alternative to obtaining carbonyl derivatives is *via* a radical carbonylation method.[61] Lei *et. al*. reported a novel oxidant induced alkane C–H bond activation using amide and alcohols as nucleophiles. They obtained a variety of esters and imides using carbon monoxide for the carbonylation step and di-*tert*-butylperoxide (DTBP) as oxidant.[62] A variety of alkanes were used to synthesize benzyl esters but Scheme 1.6 specifically shows carbonylation using adamantane as substrate and benzyl alcohol (**1.40**) as nucleophile. Ultimately, C_1 and C_2 carbonylated products **1.41** and **1.41'** were obtained in a 2:1 r.r. in 77% yield. The key reactive species is considered to be *tert*-butyloxy radical **1.35** which abstracts the hydrogen from adamantane generating adamantyl radical **1.01a** and **1.01b**.
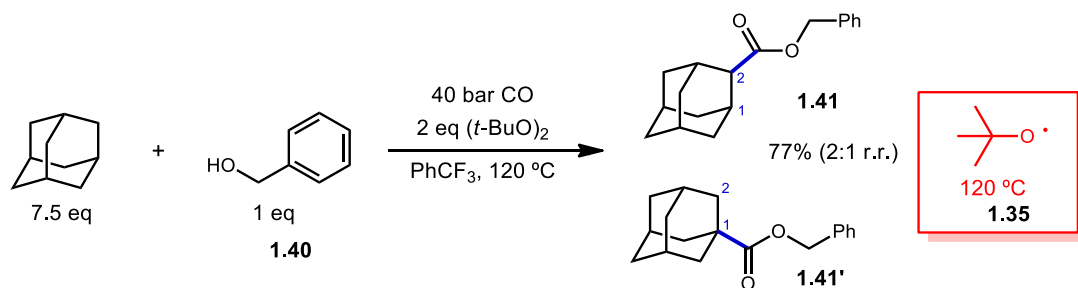
Scheme 1.6 Metal free radical oxidative carbonylation

1.4 - Alkene Additions (Michael / Giese)

Accessing functionalized adamantanes is challenging due to the necessity of performing multiple steps leading to more waste generation. However, directly functionalizing adamantane in one step *via* free radical reactions is of high interest to avoid

pre-functionalization. The radical addition of adamantanes to alkenes is a useful process especially when it proceeds with high regioselectivity and diastereoselectivity. The first Giese-type addition performed on adamantane and substituted adamantanes using different unsaturated compounds was done by Fukunishi and Tabushi in 1988 and gave products **1.42a-e** in moderate yields (Table 1.3).[24] The reactive species is once again *tert*-butyloxy radical **1.35** and is generated at high temperatures using di- *tert*-butylperoxide.

Table 1.3 Alkylation via olefin functionalization
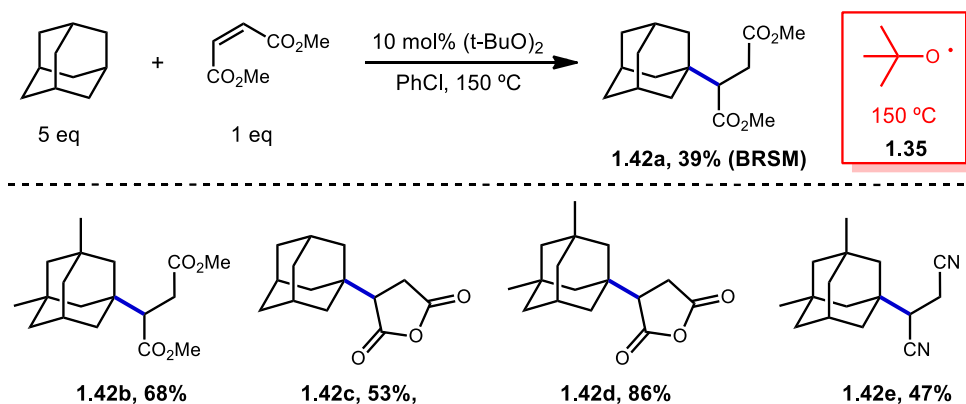
a-Thiosulfones are convenient synthetic intermediates that can be used for several key transformations. e.g. desulfurization[63] and pyrolysis to obtain carbonyl derivatives.[64] Albini and coworkers developed a photochemical radical alkylation to access *a*-thiosulfones from ketene dithioacetal *S,S*-dioxides.[34] With stoichiometric amounts of benzophenone, 1 eq of (E)-1-(methylthio)-1-[(4-methylphenyl)-sulfonyl)]propene **1.44**, excess adamantane and UV light, the thiosulfone product **1.45** was obtained in 90% yield as a single isomer (Scheme 1.7a). The selectivity of the alkylation was at the tertiary bridgehead position and trace amounts of phenyladamantane, bis-adamantane, 1-adamantanol, and 2-adamantanone was observed.
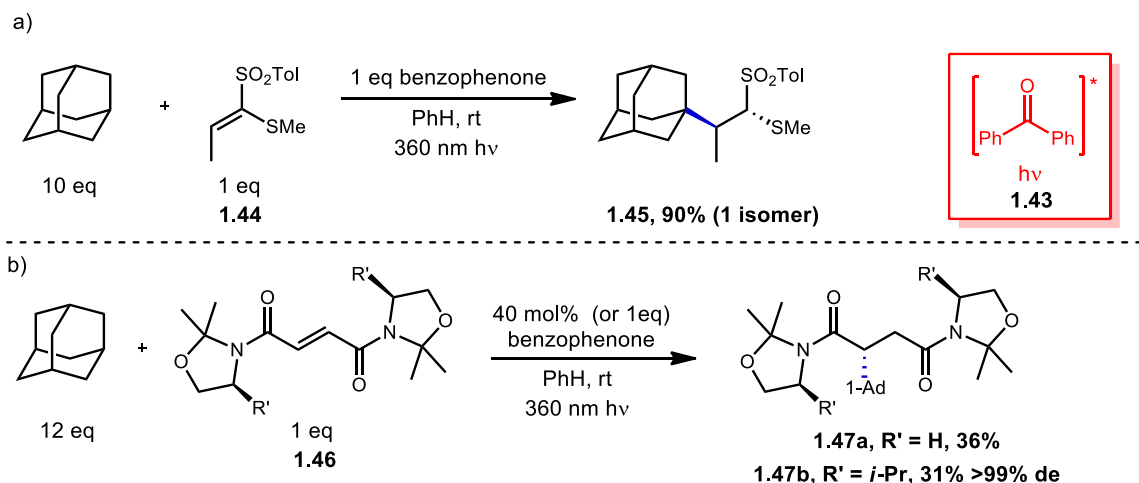
Scheme 1.7 Alkene addition using benzophenone

Albini *et. al*. further studied radical additions to olefins with fumaric acid diamides and oxazolidine chiral auxiliaries to generate functionalized products with a high degree of diastereoselectivity.[35] As shown in (Scheme 1.7b), two oxazolidines, one achiral and one achiral, were tested with excess adamantane and benzophenone as photosensitizer. Irradiation at 360 nm resulted in the triplet excited state of benzophenone **1.43** which then abstracts the hydrogen from adamantane, generating the adamantyl radical **1.01a** exclusively at the tertiary position. Addition to the fumaryloxazolidines **1.46** gave desired functionalized adamantane products **1.47a-b** in moderate yields and high diastereoselectivity.

Natural products possessing nitrile moieties, including metabolites, are of interest but accessing them directly through radical methods has limitations due to toxicity of the cyanide salts used.[65–68] Scheme 1.8a shows work done by Albini's group who used benzophenone to generate the triplet excited state with UV light.[69] Cyanoethyl adamantanes were synthesized using 100 mol% photosensitizer, excess adamantane and

one equivalent of acrylonitrile resulting in the two regioisomers **1.48** and **1.48'** in a 6:1 r.r.

ratio. Yields were determined by GC and the isolated yield was somewhat lower. An

alternative to benzophenone was the use of xanthone (**1.49**) as photosensitizer. However,

the reaction was unproductive due to solubility and isolation issues.
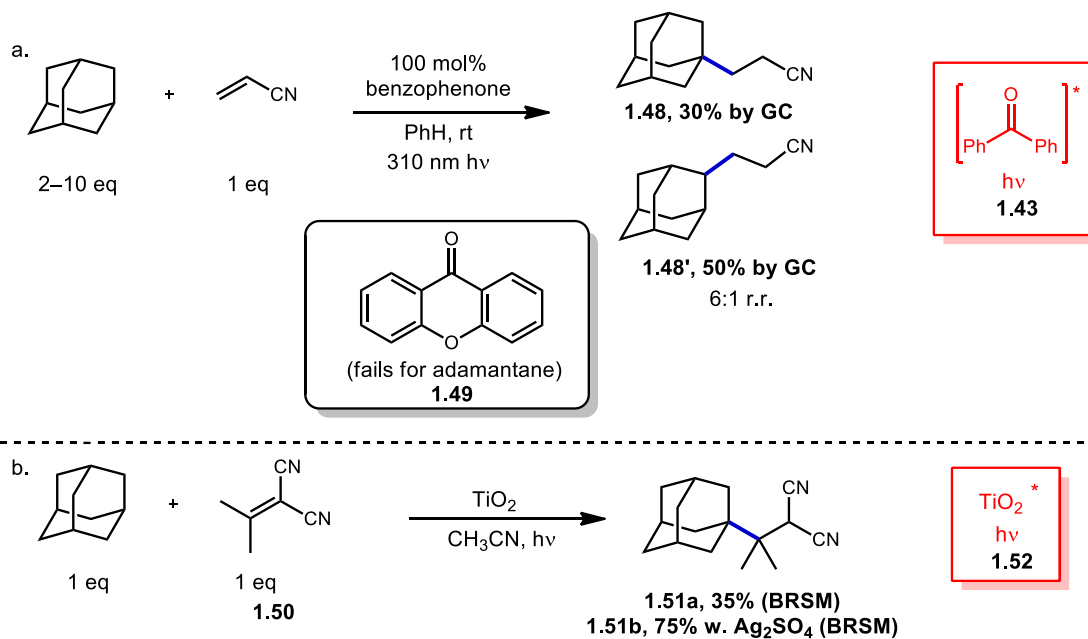
Scheme 1.8 Alkene additions using nitriles

As an alternative to using benzophenone as the photocatalyst, Albini tested TiO_2, a

known photo-oxidant.[70] As shown in Scheme 1.8b isopropylidene malononitrile (**1.50**)

and adamantane were treated with TiO_2 and irradiated under UV light. This reaction was

subjected to longer irradiation times than other TiO_2-mediated reactions in order to have

decent conversion. A yield of 35% of product **1.51a** was obtained based on recovered

starting material. Oxygenated products were observed which were attributed to remaining

oxygen. A higher yield was obtained (**1.51b)** when using silver sulfate but did require

longer reaction time.
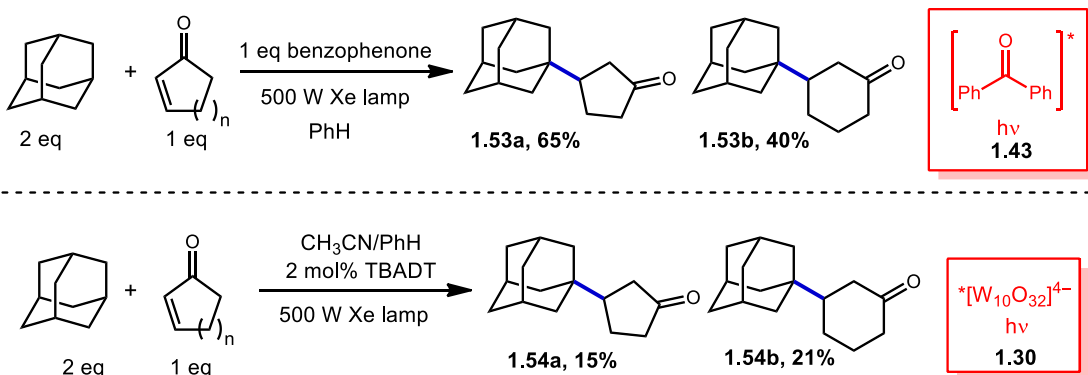
Scheme 1.9 Synthesis of β-cycloalkyl products

In 2006, Albini and coworkers synthesized β-alkylketones using photomediated radical addition (Scheme 1.9).[37] Beginning with the adamantane, the adamantyl radical was generated *via* hydrogen atom abstraction (HAT) by either benzophenone or TBADT. When using benzophenone as catalyst, only 1-adamantyl derivatives were observed and cyclopentanone product **1.53a** was generated in 65% yield while the cyclohexanone product **1.53b** was obtained in a lower 40% yield. When using the alternative method with TBADT as photocatalyst, the yields were lower, with cyclopentanone product **1.54a** in 15% yield and the cyclohexanone product **1.54b** in 21% yield. The reaction mechanism was hypothesized to be induced by a direct hydrogen abstraction as opposed to energy or electron transfer.

The first catalytic oxyalkylation of alkenes with alkanes was reported by Ishii *et. al*[36] who used the PINO radical **1.28** as the reactive intermediate, cobalt as co-catalyst and molecular oxygen. This reaction resulted in two different products in high yields when adamantane is used as the hydrocarbon. Under optimized conditions, methyl fumarate and adamantane gave 98% conversion with a 78% yield (71/29 ratio of hydroxy product **1.55a**

versus ketone product **1.55b**) (Table 1.4). A variety of alkenes were also tested using dimethyl adamantane with yields ranging from modest to excellent however in most cases, a mixture of products was observed (**1.55b-d**).

Table 1.4 NHPI induced oxyalkylation

1.55b, 42% yield (60/40)*   1.55c, 78% yield (92/8)*   1.55d, 96% yield
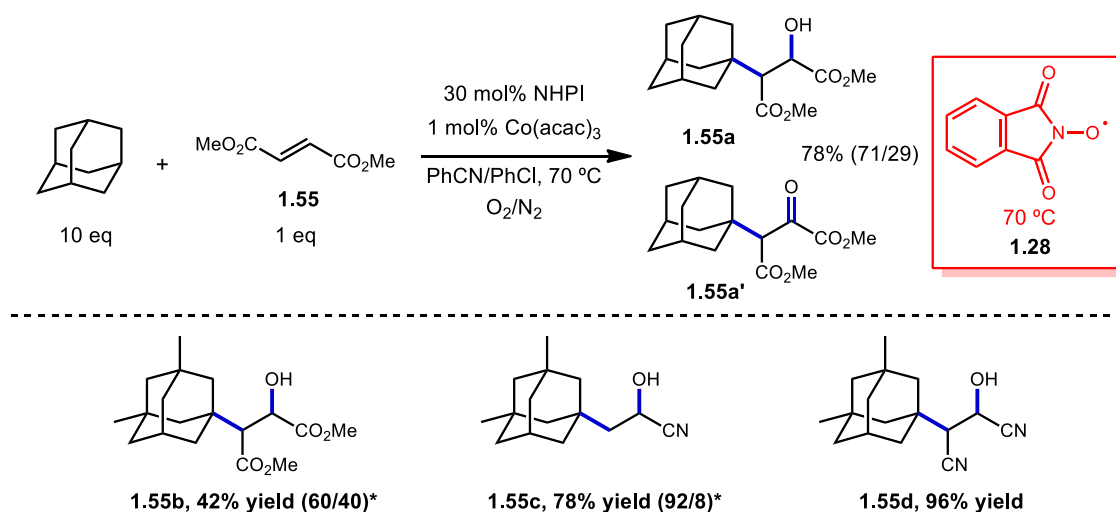
*Ratio of alcohol to ketone product

A metal free radical-chain functionalization was investigated using an oxiranylcarbinyl derivative by Roberts and coworkers.[71] Previously, Roberts used an analogue of this reagent as a source of allyloxyl radicals with the intention of doing direct C–H abstraction. They focused their studies on *O*-oxiranylcarbinyl *O*-silyl ketene acetal **A** (Scheme 1.10)**.** This particular acetal was used due to the commercial availability of starting material, isophorone oxide, and its inability to do a rearrangement once the radical intermediate is generated. The reaction of interest involved excess adamantane, 0.2 eq of di-*tert*-butyl hyponitrite (TBHN) which was used as a source for *tert*-butoxyl radicals, 1.0 eq of acetal reagent **A**, and N-methylmaleimide (NMM) **(1.56)** as the acceptor. With

adamantane, a mixture of two isomers **1.57** and **1.57'** was obtained with a combined yield of 50% in a 79:21 ratio favoring the tertiary position.
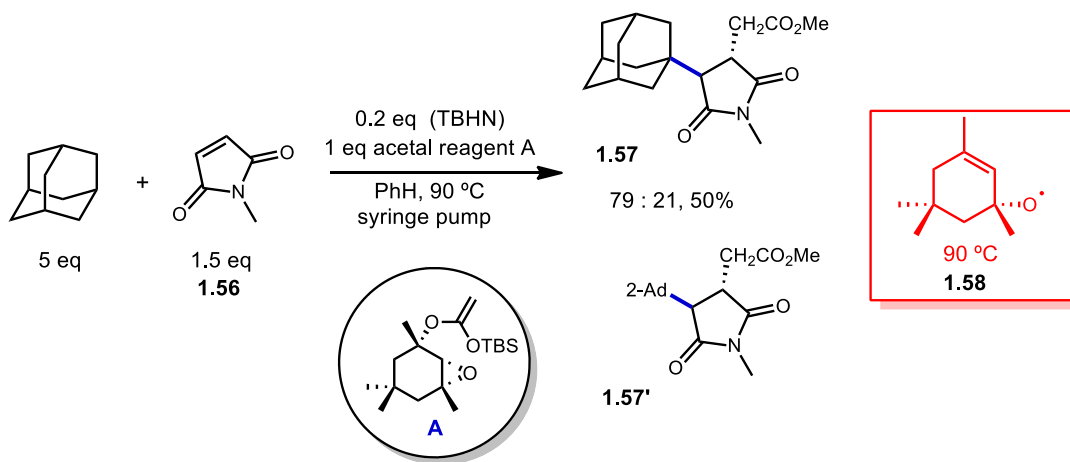
Scheme 1.10 Metal free C–H functionalization

More recently, in 2018 Nicewicz and Alexanian proposed a general strategy for organic photoredox-catalyzed C–H abstraction which was followed by direct C–H diversification to directly convert C–H bonds to a variety of C–N, C–X and C–C bonds (Scheme 1.11).[72] Herein, a highly oxidizing acridinium photocatalyst (**1.59**), shown in Scheme 11, was used to oxidatively generate heteroatom-centered radicals capable of doing C–H abstraction of aliphatic compounds. In this case, the reactive phosphate radical **1.60** was generated upon oxidation by the acridinium photocatalyst. When using aryl-adamantyl derivative **1.62**, alkylation was selective for the tertiary position giving product **1.61** in a 45% yield.
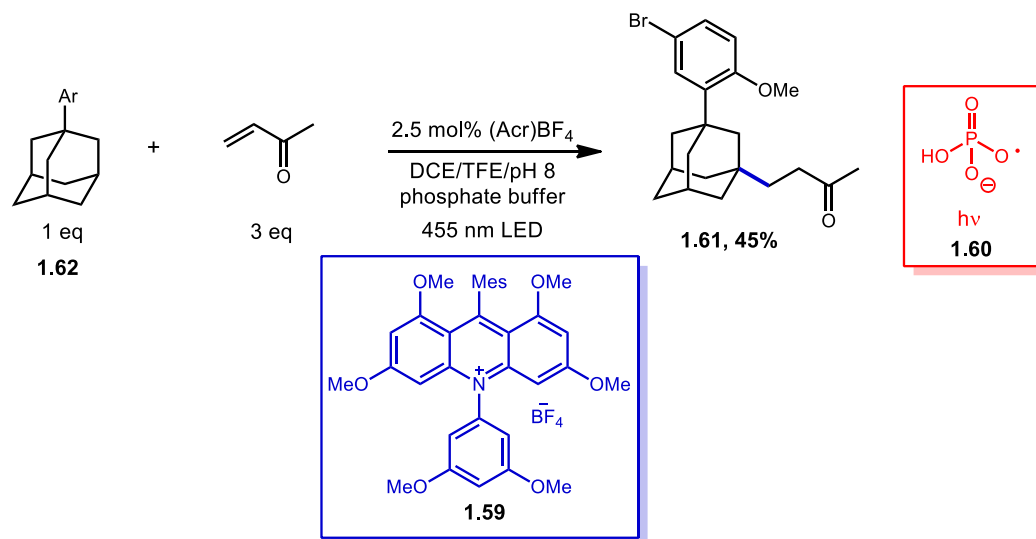
Scheme 1.11 Organic photoredox-catalyzed Giese addition

1.5 - Addition-Fragmentation

The addition-fragmentation sequence, shown in Scheme 1.12, is a common practice in the realm of radical chemistry to effect vinylation, among others.[74] As such, this mode of reactivity has been reported in a variety of cases involving the adamantyl radical. Generally speaking, this process begins by using some means of H–atom abstraction to generate a reactive adamantyl radical intermediate (II). Common radical acceptors will feature an electron withdrawing group to aid in stabilizing radical intermediate III as well as a leaving group that promotes a facile fragmentation immediately following addition giving the desired substituted alkene product IV. In addition to vinylation, examples of decarboxylation and allylation reactions are described below.
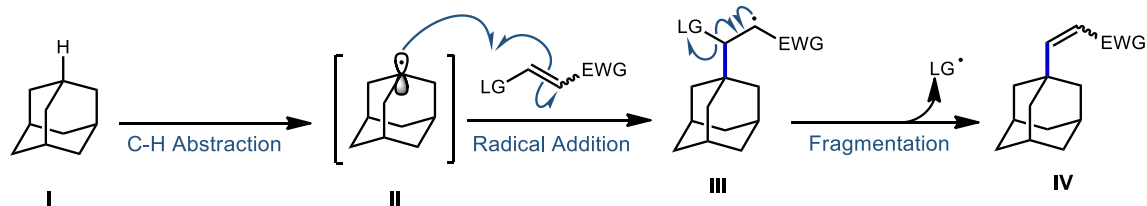
Scheme 1.12 General radical addition-fragmentation sequence

1.5.1 - Decarboxylative alkylation

Sun *et al.* demonstrated that styrenyl adamantanes can be made using cinnamic acids (**1.63**) in the presence of di-*tert*-butyl peroxide (DTBP) and heat (Scheme 1.13).[75] In this case, homolytic thermolysis of DTBP results in *tert*-butoxy radical **1.35** that acts as the C-H abstractor giving rise to the reactive adamantyl radical. This reaction is then thought to proceed through a radical addition to give a stabilized benzylic radical **1.64** followed by decarboxylative fragmentation. This addition-fragmentation process is selective for the methine position on adamantane, favoring it over the methylene position in an 83:17 ratio and a 59% yield is obtained.
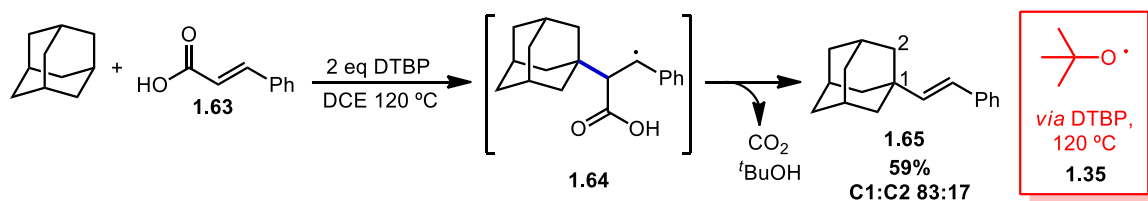
Scheme 1.13 Peroxide promoted decarboxylative alkylation of cinnamic acids to form alkenes or ketones

1.6 - Allylation

Adamantyl allylation has been demonstrated using 1,2-bis(phenylsulfonyl) propene **1.66** as an allylating agent (Table 1.5).[76] Using 5 mol% 5,7,12,14-pentacenetetraone (PT, **1.68**) as the photocatalyst, 1.1 equiv K_2CO_3, excess adamantane and visible light, both the

C1 and C2 products (**1.67** and **1.67'**) can be obtained in 63% yield and 90:10 r.r. The reaction tolerates substituted adamantanes giving yields between 42-67% for products **1.67a-e.**

Table 1.5 Aryl ketone catalyzed radical allylation
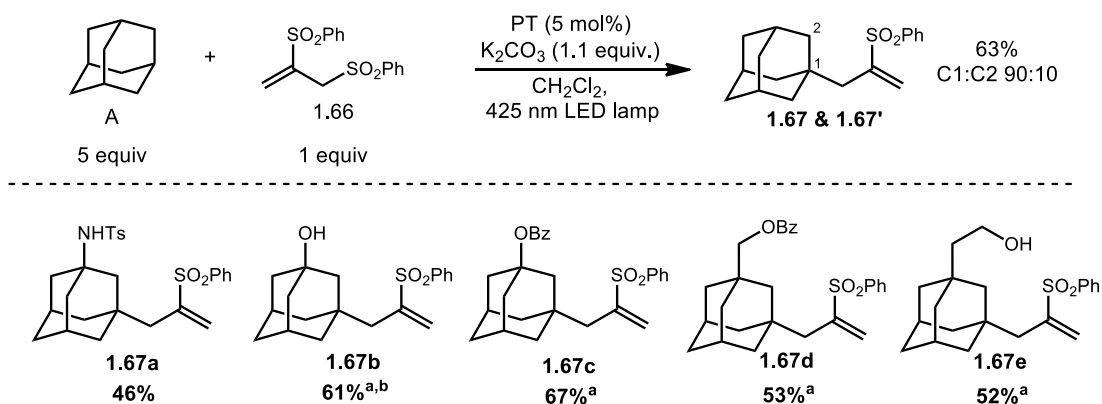
^{a}less than 4% of the methylene addition product observed. ^{b}ran without use of K_2CO_3.

The adamantyl radical **1.01a** is generated using 5,7,12,14-pentacenetetraone (**1.68**) and a visible light source. The radical generated by irradiating the PT catalyst is a competent C–H abstractor leading to semiquinone form **1.68'**.[77–79] Adamantyl radical then intercepts the sulfonylated propene (**1.66**) to generate radical intermediate **1.69**. Fragmentation and re-oxidation of the PT catalyst results in allylated adamantyl phenylsulphone, **1.67a**. Under these conditions, **1.67a** was isolated in 63% yield with the allylated methine being favored in a 9:1 ratio over the methylene position. While a strong electron-withdrawing group (sulfone) is required on the alkene **1.66**, the reaction was successful for a range of substituted adamantanes as shown in Table 1.5.
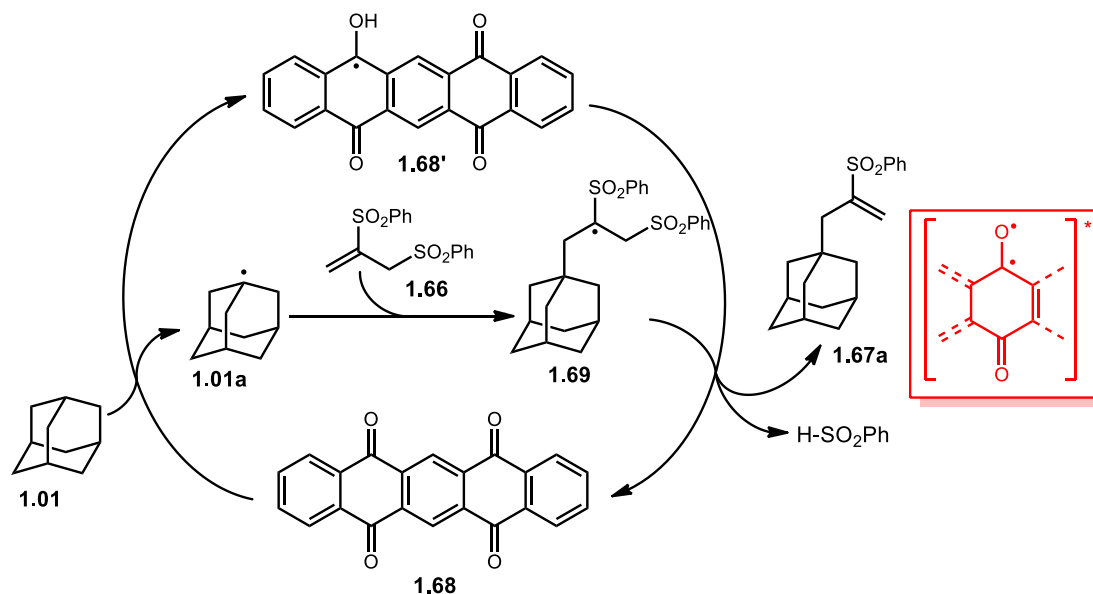
Scheme 1.14 Adamantyl allylation using PT

Wang and coworkers recently developed a method for the directed allylation of adamantane using remote amidyl radical **1.73** (Figure 1.6). This remote amidyl radical is generated photocatalytically using green LEDs to excite the photocatalyst, eyosin Y (EY) (**1.70**), which undergoes single electron transfer (SET) with a pre-functionalized adamantane featuring dinitroaryloxy amide **1.71**. The resulting radical anion, **1.72,** then fragments to give the key amidyl radical **1.73**. Similar to a Hofmann–Löffler–Freytag reaction, remote amidyl radical **1.73** was used to generate the adamantyl radical **1.74** *via* a 1,5 C-H abstraction.[80] Interception of the adamantyl radical by allylic sulphone **1.75** and subsequent fragmentation of **1.77** gives the final allylated adamantane **1.76.** Like many related processes of this type, the reaction was very selective for 1,5-H-atom transfer to functionalize either a $3°$ or $2°$ position selectively, depending on the substrate.

30
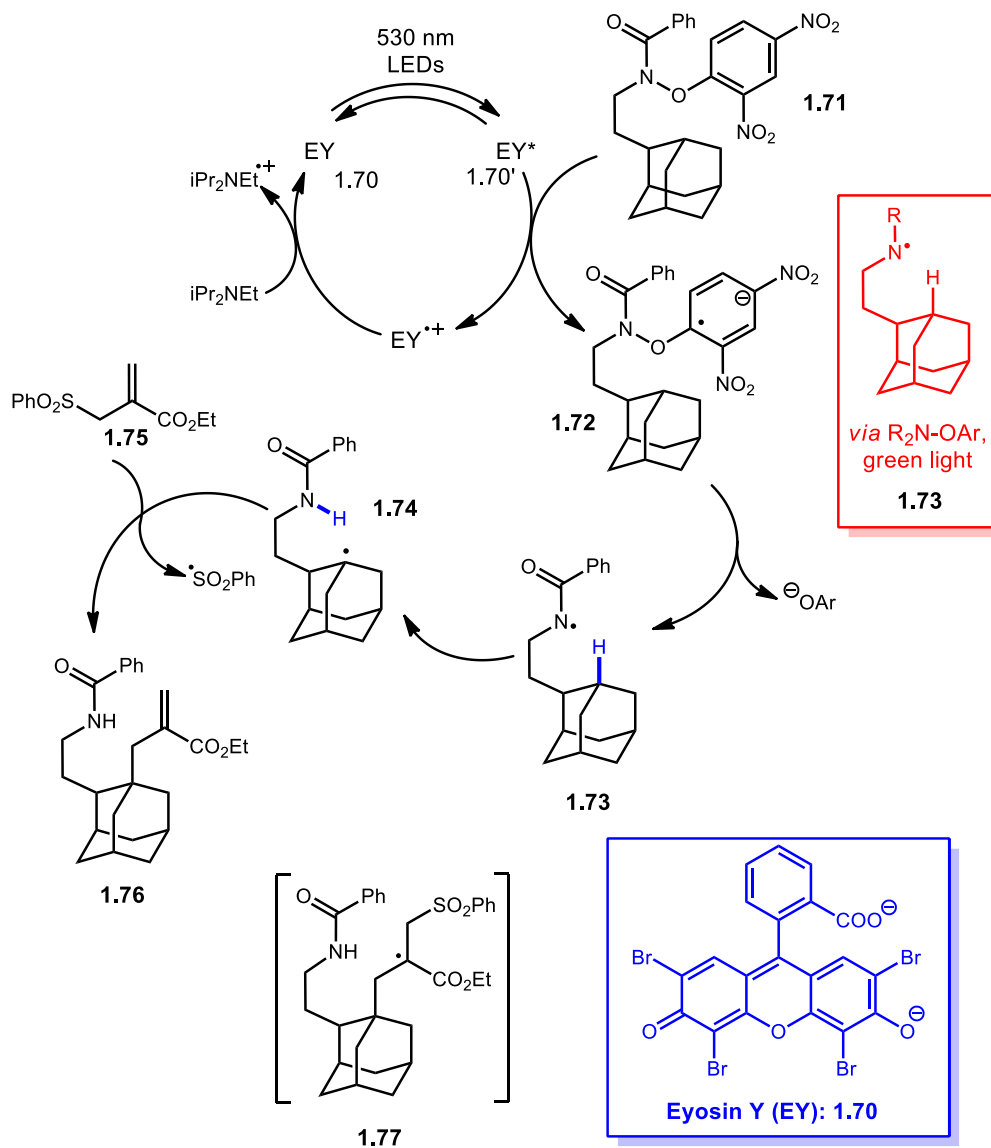
Figure 1.6 Amidyl radical directed allylation

1.7 - Arylation

1.7.1 - Photooxidation of Diamondoids using TCB

In 1996, Albini proposed an arylation reaction using 1,2,4,5-benzenetetracarbonitrile (TCB) **1.78**.[81,82] TCB was utilized due to its ability to become an extremely strong single electron oxidant upon irradiation.[83] Upon irradiation, the radical

anion of TCB **1.78'** and the adamantyl radical cation **1.01c** is generated. In the presence of a base, the adamantyl radical cation is easily deprotonated at the bridgehead position resulting in a coupling reaction with the radical anion of TCB.
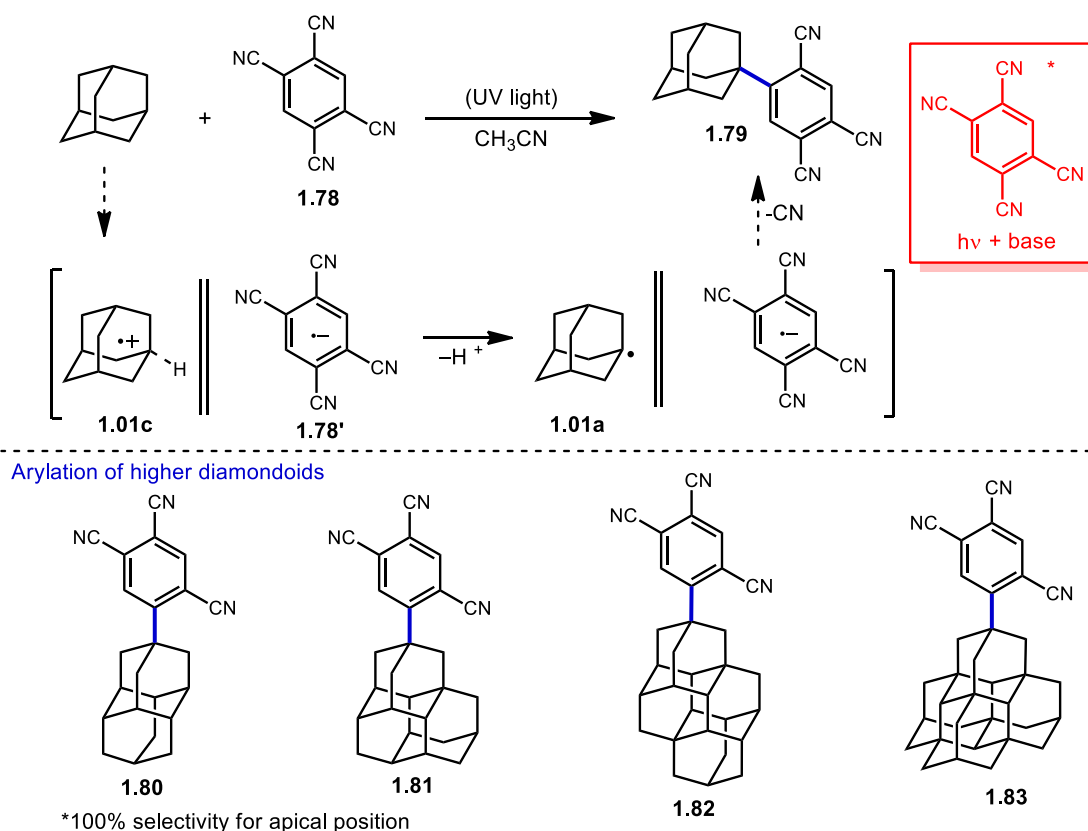
Figure 1.7 Arylation of diamondoids with TCB

Irradiation of adamantane and TCB in acetonitrile led to the formation of single adamantyl product **1.79**. By prolonging the reaction time, although it led to higher conversion of starting material, a small amount of the bis-arylated product was observed. This arylation method was also used with higher diamondoids, shown in Figure 1.7, to give the desired product with high selectivity for the apical position in all cases (**1.80-1.83**).[2,5,84] Arylation beyond pentamantane has not been investigated as of yet.

1.7.2 - Minisci-Type Arylation of Adamantane

In 2013, Antonchick and coworkers developed a Minisci-type arylation reaction using a selective oxidative cross-coupling approach.[85] One example, shown in Scheme 1.15, shows the arylation of adamantane using 4,7-dichloroquinoline (**1.84**) in the presence of [bis(trifluoracetoxy)iodo]benzene (PIFA) as oxidant and NaN$_3$, as a critical additive. The key H-atom abstractor is likely the azide radical **1.86** and the corresponding arylated product **1.85** was obtained in an 84% yield as a single isomer. Overall, Antonchick *et. al.* used this oxidative cross-coupling approach of heteroarenes and alkanes to obtain arylated products under mild conditions, with short reaction times and in high yields.
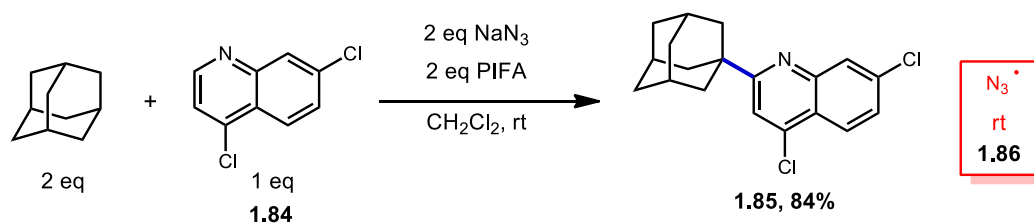
Scheme 1.15 Arylation of adamantane

1.7.3 - Dual-Catalytic Arylation

In 2018, another direct arylation was performed by MacMillan and coworkers using a dual catalytic system with decatungstate and a nickel catalyst (Scheme 1.16).[39] Adamantane derivatives underwent arylation predominantly at the methylene position for both 2-adamantanone (**1.87**) and bromo-adamantanone (**1.90**) to give a 48% and 53% yield, respectively. The high regioselectivity can be rationalized *via* reversible radical capture and selectivity-determining reductive elimination.[86] The proposed mechanism begins with the photoexcitation of TBADT followed by intersystem crossing giving the triplet

excited state. This is followed by HAT abstraction from a hydrocarbon like adamantanone by the excited TBADT catalyst ultimately reducing the catalyst and generating the adamantyl radical at the secondary position. Disproportionation of the singly reduced decatungstate would regenerate the active HAT catalyst and form a doubly reduced decatungstate species. Following single-electron reduction of a nickel catalyst to give Ni^0 species, the alkyl substrate is captured, followed by oxidative addition of the aryl bromide **1.88**, reductive elimination to give the desired cross-coupled arylated product, and a final single-electron step between the active nickel catalyst and reduced TBADT catalyst to complete both catalytic cycles.
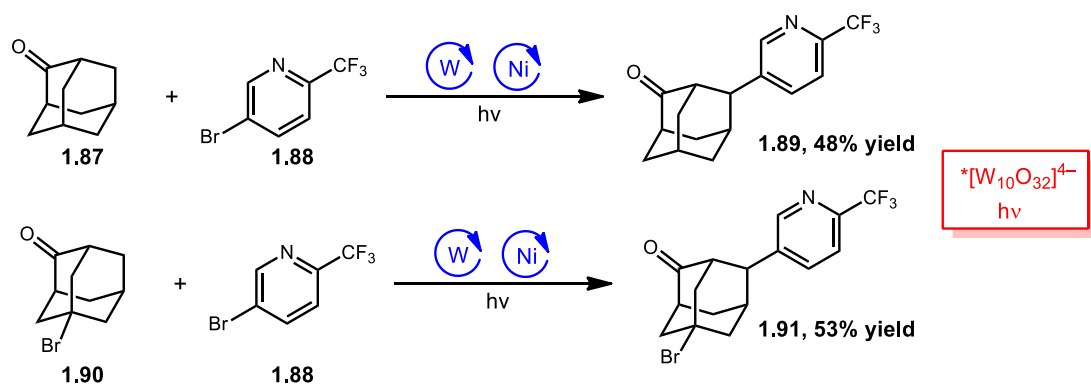
Scheme 1.16 Dual catalytic arylation

1.7.4 - Transition Metal-Free Arylation using Heteroaromatic Bases

This year, Togo *et. al.* studied the introduction of heteroaromatic bases onto hydrocarbons using benzoyl peroxide, BPO, under transition-metal-free and irradiation-free conditions.[27] When 5 equivalents of adamantane and 1.3 equivalents of BPO and trifluoroacetic acid in benzene was treated with the nitrogen containing compound, lepidine

(**1.92**), the desired methylquinoline product **1.93** was obtained in 75% yield (Scheme 1.17). Other heteroaromatic bases also produced the arylated product in good yields (**1.94-1.96; 63%-86%**). The reaction relies on the formation of reactive benzoyl radical **1.14** which is formed from BPO under thermal conditions which then abstracts the hydrogen generating the adamantyl radical. Subsequent nucleophilic radical addition with a protonated heteroaromatic base and oxidation of the benzenecarboxyl radical forms the protonated product. After quenching with aqueous NaHCO₃, the desired arylated product is obtained.
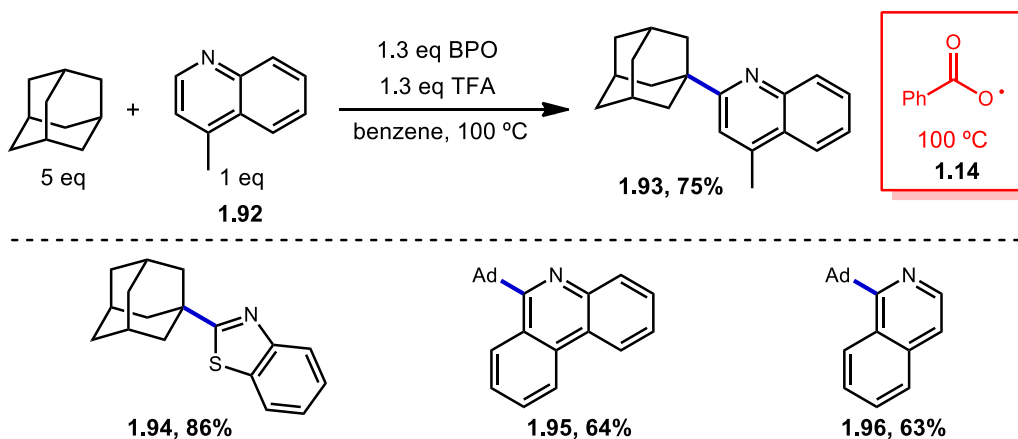
Scheme 1.17 Arylation via thermal conditions

1.8 - Alkynylation

Alkynes are valuable building blocks in organic synthesis and are important structural compounds in both materials science and chemical biology.[87–89] The use of pre-functionalized substrates[90,91] or transition-metal-catalyzed alkynylations[92–95] have been extensively reported however metal-free conditions are of interest due to the current necessity of developing "greener" reactions.

1.8.1 - Metal-free Direct Alkynylations

In 1996, a direct trifluoromethyl radical mediated C–H alkynylation reaction is reported by Fuchs *et. al.* using TIPS-substituted acetylenic triflones.[96,97] The reaction proceeds by a radical C–H abstraction with an electrophilic trifluoromethyl radical intermediate **1.101** to generate the adamantyl radical. Following the addition into the acetylenic triflone **1.97** at the α-position, elimination and fragmentation generates the trifluoromethyl radical and the desired alkynylated adamantane product shown in Scheme 1.18 is obtained in a 60% yield when 0.2 equivalents of AIBN is used as the radical initiator. Other substituted triflates gave moderate yields (**1.99**, 40% yield and **1.100**, 50% yield).
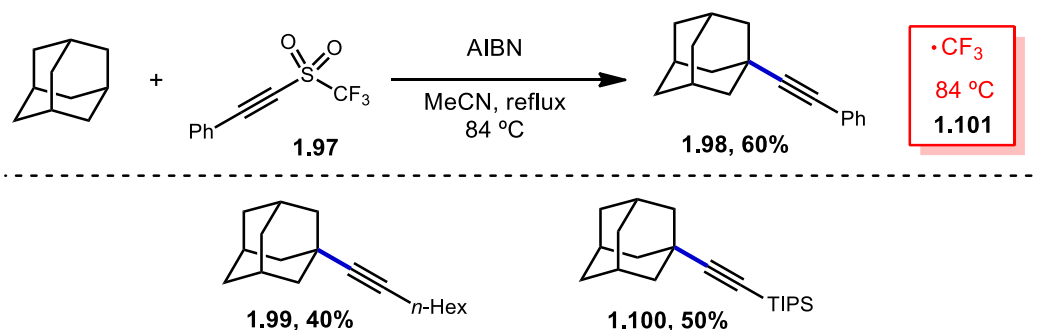
Scheme 1.18 Alkynylation with acetylenic triflones

A photochemically induced alkynylation of adamantane was developed by Inoue and coworkers.[98] Benzophenone was employed as an oxyl radical precursor and 1-tosyl-2-(trimethylsilyl)acetylene **1.103** as the alkynylating agent. Upon excitation with UV light, an electrophilic oxyl radical is generated which then abstracts a hydrogen atom from the tertiary position of adamantane generating the adamantyl radical. This intermediate then reacts with the electron-deficient alkyne and subsequent release of the toluenesulfinyl

radical generates the alkynylated adamantyl product. When adamantanol (**1.102**) and Boc protected amantadine **(1.105)** were used, the reaction proceeded exclusively at the tertiary position in 86% and 73% yield, respectively with loss of the Boc group.
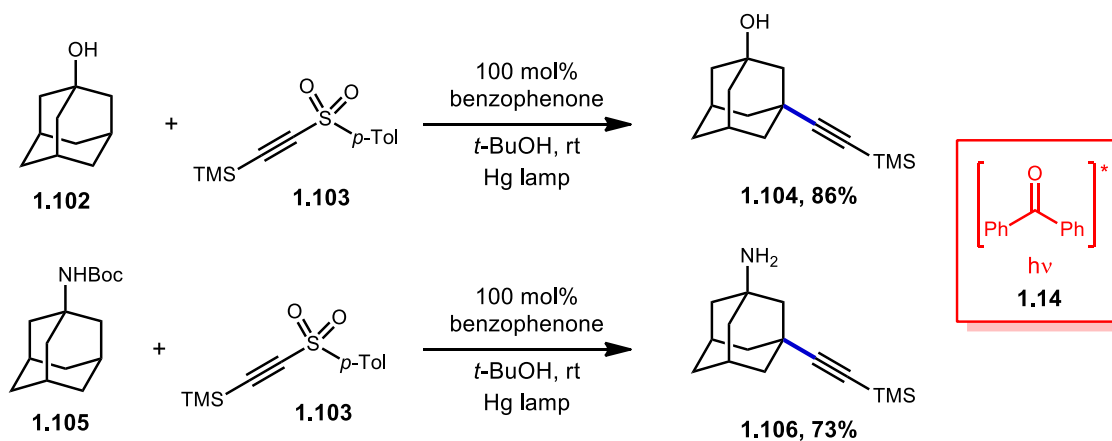
Scheme 1.19 Alkynylation using benzophenone **1.14**

In 2016, Xu and coworkers investigated an efficient method for the direct alkynylation of substrates containing unactivated $C(sp^3)$–H bonds under metal-free conditions (Scheme 1.20).[99] Notably, when adamantane was used, C–H functionalization was selective for the tertiary position over the secondary and a 59% yield was reported for the desired adamantyl product. 1-[(triisopropylsilyl)-ethynyl]-1,2-benziodoxol-3(1H)-one was required along with an oxidant and high temperature to generate the adamantyl radical. When testing the radical trapping agent, TEMPO, the reaction was completely suppressed and the alkyl-TEMPO product was observed suggesting the reaction proceeds *via* a radical intermediate. A plausible mechanism begins with generation of the *tert*-butoxy radical from homolytic cleavage of di-*tert*-butylperoxide (DTBP) which reacts with adamantane giving the adamantyl radical. This is followed by addition to the triple bond of hypervalent

iodine reagent **1.107** and subsequent β-elimination gives the final alkynylated product **1.108**.
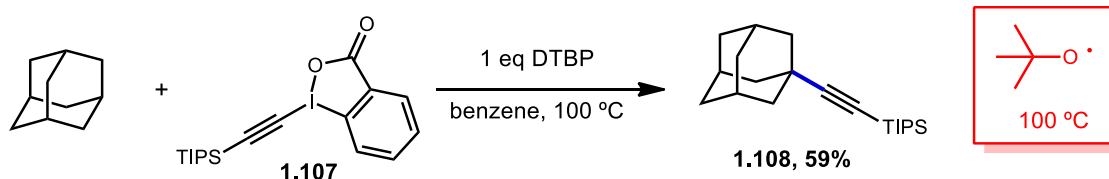
Scheme 1.20 Alkynylation with ethynylbenziodoxolones

1.8.2 - Metal-Catalyzed C–H Functionalization

The first Cu-catalyzed radical addition/cyclization with diaryl(arylethynyl)-phosphine oxides has been developed by Zhao (Scheme 1.21).[100] Herein, unactivated hydrocarbons were used as a general, one-step method to synthesize benzophosphole oxides using C-H functionalization in a highly regioselective manner. Using 10 mol% CuBr and DTBP, the adamantyl functionalized product was obtained at the tertiary position in 42% yield. The reactive intermediate, *tert*-butoxy radical, was generated when heated with the active Cu^I species. As in previous methods, this radical then abstracts the hydrogen from adamantane generating the adamantyl radical which adds to the alkyne and undergoes cyclization to give the desired adamantyl-benzo[*b*]phospholes.
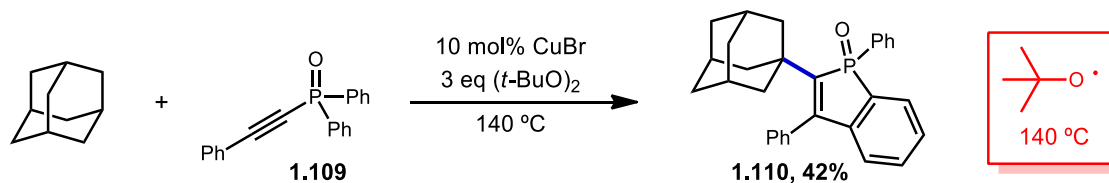
Scheme 1.21 Metal-mediated alkynylation

1.9 - Conclusion

The direct functionalization of aliphatic C–H bonds is of great interest to the scientific community and although there have been significant advances in the area, it is still in need of more selective methods that proceed under mild conditions. Since the synthesis of adamantane *via* Schleyers method in 1957, diamondoids have fascinated synthetic organic chemists leading to the synthesis of functionalized substrates containing the adamantyl scaffold and thusto a wide array of applications in nanomaterials, catalysis and pharmaceutical agents. Diamondoids, a special class of hydrocarbons with unique characteristics, have been shown to be excellent substrates for the investigation of direct and selective C–H activation. Herein, different types of C–H to C–C bond transformations of diamondoids using direct functionalization *via* radical chemistry has been discussed.

1.10 - References

[1] W. Burns, T. R. B. Mitchell, M. A. McKervey, J. J. Rooney, G. Ferguson, P. Roberts, *J. Chem. Soc. Chem. Commun.* **1976**, 893–895.

[2] P. R. Schreiner, N. A. Fokina, B. A. Tkachenko, H. Hausmann, M. Serafin, J. E. P. Dahl, S. Liu, R. M. K. Carlson, A. A. Fokin, *J. Org. Chem.* **2006**, *71*, 6709–6720.

[3] A. A. Fokin, B. A. Tkachenko, N. A. Fokina, H. Hausmann, M. Serafin, J. E. P. Dahl, R. M. K. Carlson, P. R. Schreiner, *Chem. – Eur. J.* **2009**, *15*, 3851–3862.

[4] P. R. Schreiner, A. A. Fokin, H. P. Reisenauer, B. A. Tkachenko, E. Vass, M. M. Olmstead, D. Bläser, R. Boese, J. E. P. Dahl, R. M. K. Carlson, *J. Am. Chem. Soc.* **2009**, *131*, 11292–11293.

[5] A. A. Fokin, P. R. Schreiner, N. A. Fokina, B. A. Tkachenko, H. Hausmann, M. Serafin, J. E. P. Dahl, S. Liu, R. M. K. Carlson, *J. Org. Chem.* **2006**, *71*, 8532–8540.

[6] J. E. P. Dahl, J. M. Moldowan, T. M. Peakman, J. C. Clardy, E. Lobkovsky, M. M. Olmstead, P. W. May, T. J. Davis, J. W. Steeds, K. E. Peters, et al., *Angew. Chem. Int. Ed.* **2003**, *42*, 2040–2044.

[7] A. T. Balaban, P. V. Ragé Schleyer, *Tetrahedron* **1978**, *34*, 3599–3609.

[8] O. Farooq, S. M. F. Farnia, M. Stephenson, G. A. Olah, *J. Org. Chem.* **1988**, *53*, 2840–2843.

[9] E. Osawa, A. Furusaki, N. Hashiba, T. Matsumoto, V. Singh, Y. Tahara, E. Wiskott, M. Farcasiu, T. Iizuka, *J. Org. Chem.* **1980**, *45*, 2985–2995.

[10] S. Landa, V. Macháček, *Collect. Czechoslov. Chem. Commun.* **1933**, *5*, 1–5.

[11] A. Shimoyama, H. Yabuta, *Geochem. J.* **2002**, *36*, 173–189.

[12] R. C. Fort, P. von R. Schleyer, *Chem. Rev.* **1964**, *64*, 277–300.

[13] V. Prelog, R. Seiwerth, *Berichte Dtsch. Chem. Ges. B Ser.* **1941**, *74*, 1644–1648.

[14] P. von R. Schleyer, *J. Am. Chem. Soc.* **1957**, *79*, 3292–3292.

[15] M. A. Mckervey, *Tetrahedron* **1980**, *36*, 971–992.

[16] H. Stetter, M. Schwarz, A. Hirschhorn, *Chem. Ber.* **1959**, *92*, 1629–1635.

[17] W. Haaf, *Angew. Chem.* **1961**, *73*, 144–144.

[18] L. Wanka, K. Iqbal, P. R. Schreiner, *Chem. Rev.* **2013**, *113*, 3516–3604.

[19] G. Jackson, R. Muldoon, L. Akers, *Antimicrob. Agents Chemother.* **1963**, *161*, 703–707.

[20] J. M. Reddy, G. Prasad, V. Raju, M. Ravikumar, V. Himabindu, G. M. Reddy, *Org. Process Res. Dev.* **2007**, *11*, 268–269.

[21] V. Prelog, *Pure Appl. Chem.* **1963**, *6*, 545–560.

[22] C. Cupas, P. von R. Schleyer, D. J. Trecker, *J. Am. Chem. Soc.* **1965**, *87*, 917–918.

[23] I. Tabushi, S. Kojo, P. v R. Schleyer, T. M. Gund, *J. Chem. Soc. Chem. Commun.* **1974**, 591–591.

[24] K. Fukunishi, I. Tabushi, *Synthesis* **1988**, *1988*, 826–827.

[25] P. R. Schreiner, O. Lauenstein, I. V. Kolomitsyn, S. Nadi, A. A. Fokin, *Angew. Chem. Int. Ed.* **1998**, *37*, 1895–1897.

[26] M. B. Dinger, P. Nieczypor, J. C. Mol, *Organometallics* **2003**, *22*, 5291–5296.

[27] L. Zhou, H. Togo, *Eur. J. Org. Chem.* **2019**, *2019*, 1627–1634.

[28] "(8) (PDF) Molecular Structure and Chemistry of Diamondoids," can be found under https://www.researchgate.net/publication/286145976_Molecular_Structure_and_Chemistry_of_Diamondoids,

[29] Q. Fang, S. Gu, J. Zheng, Z. Zhuang, S. Qiu, Y. Yan, *Angew. Chem. Int. Ed.* **2014**, *53*, 2878–2882.

[30] Q. Li, C. Jin, P. A. Petukhov, A. V. Rukavishnikov, T. O. Zaikova, A. Phadke, D. H. LaMunyon, M. D. Lee, J. F. W. Keana, *J. Org. Chem.* **2004**, *69*, 1010–1019.

[31] T. P. Stockdale, C. M. Williams, *Chem. Soc. Rev.* **2015**, *44*, 7737–7763.

[32] I. Tabushi, K. Fukunishi, *J. Org. Chem.* **1974**, *39*, 3748–3750.

[33] S. Kato, T. Iwahama, S. Sakaguchi, Y. Ishii, *J. Org. Chem.* **1998**, *63*, 222–223.

[34] A. M. González-Cameno, M. Mella, M. Fagnoni, A. Albini, *J. Org. Chem.* **2000**, *65*, 297–303.

[35] G. Campari, M. Fagnoni, M. Mella, A. Albini, *Tetrahedron Asymmetry* **2000**, *11*, 1891–1906.

[36] T. Hara, T. Iwahama, S. Sakaguchi, Y. Ishii, *J. Org. Chem.* **2001**, *66*, 6425–6431.

[37] D. Dondi, A. M. Cardarelli, M. Fagnoni, A. Albini, *Tetrahedron* **2006**, *62*, 5527–5535.

[38] I. Ryu, A. Tani, T. Fukuyama, D. Ravelli, M. Fagnoni, A. Albini, *Angew. Chem. Int. Ed.* **2011**, *50*, 1869–1872.

[39] I. B. Perry, T. F. Brewer, P. J. Sarver, D. M. Schultz, D. A. DiRocco, D. W. C. MacMillan, *Nature* **2018**, *560*, 70.

[40] A. Kishi, S. Kato, S. Sakaguchi, Y. Ishii, *Chem. Commun.* **1999**, 1421–1422.

[41] A. Kolocouris, K. Dimas, C. Pannecouque, M. Witvrouw, G. B. Foscolos, G. Stamatiou, G. Fytas, G. Zoidis, N. Kolocouris, G. Andrei, et al., *Bioorg. Med. Chem. Lett.* **2002**, *12*, 723–727.

[42] N. V. Makarova, M. N. Zemtsova, I. K. Moiseev, A. A. Ozerov, V. I. Petrov, I. A. Grigor'ev, *Pharm. Chem. J.* **2000**, *34*, 293–296.

[43] I. Tabushi, S. Kojo, Z. Yoshida, *Tetrahedron Lett.* **1973**, *14*, 2329–2332.

[44] W. G. Bentrude, K. R. Darnall, *J. Am. Chem. Soc.* **1968**, *90*, 3588–3589.

[45] I. Tabushi, J. Hamuro, R. Oda, *J. Org. Chem.* **1968**, *33*, 2108–2109.

[46] G. W. SMITH, H. D. WILLIAMS, *J. Org. Chem.* **1961**, *26*, 2207–2212.

[47] S. Kamijo, G. Takao, K. Kamijo, M. Hirota, K. Tao, T. Murafuji, *Angew. Chem. Int. Ed.* **2016**, *55*, 9695–9699.

[48] I. Tabushi, Y. Aoyama, *J. Org. Chem.* **1973**, *38*, 3447–3454.

[49] I. Tabushi, S. Kojo, K. Fukunishi, *J. Org. Chem.* **1978**, *43*, 2370–2374.

[50] A. A. Fokin, P. A. Gunchenko, A. A. Novikovsky, T. E. Shubina, B. V. Chernyaev, J. E. P. Dahl, R. M. K. Carlson, A. G. Yurchenko, P. R. Schreiner, *Eur. J. Org. Chem.* **2009**, *2009*, 5153–5161.

[51] D. H. R. Barton, D. Doller, *Acc. Chem. Res.* **1992**, *25*, 504–512.

[52] J. Sommer, J. Bukala, *Acc. Chem. Res.* **1993**, *26*, 370–376.

[53] B. A. Arndtsen, R. G. Bergman, T. A. Mobley, T. H. Peterson, *Acc. Chem. Res.* **1995**, *28*, 154–162.

[54] Q. Liu, H. Zhang, A. Lei, *Angew. Chem. Int. Ed.* **2011**, *50*, 10788–10799.

[55] X.-F. Wu, H. Neumann, *ChemCatChem* **2012**, *4*, 447–458.

[56] X.-F. Wu, H. Neumann, M. Beller, *Chem. Rev.* **2013**, *113*, 1–35.

[57] S. E. Allen, R. R. Walvoord, R. Padilla-Salinas, M. C. Kozlowski, *Chem. Rev.* **2013**, *113*, 6234–6458.

[58] Y. Li, K. Dong, F. Zhu, Z. Wang, X.-F. Wu, *Angew. Chem. Int. Ed.* **2016**, *55*, 7227–7230.

[59] L. C. M. Castro, N. Chatani, *Chem. Lett.* **2015**, *44*, 410–421.

[60] Z. Han, D. Chaowei, L. Lice, M. Hongfei, B. Hongzhong, L. Yufeng, *Tetrahedron* **2018**, *74*, 3712–3718.

[61] I. Ryu, *Chem. Soc. Rev.* **2001**, *30*, 16–25.

[62] L. Lu, D. Cheng, Y. Zhan, R. Shi, C.-W. Chiang, A. Lei, *Chem. Commun.* **2017**, *53*, 6852–6855.

[63] K. Ogura, A. Kayano, N. Sumitani, M. Akazome, M. Fujita, *J. Org. Chem.* **1995**, *60*, 1106–1107.

[64] B. Wladislaw, L. Marzorati, R. B. Uchôa, *Synthesis* **1986**, *1986*, 964–965.

[65] P. J. Scheuer, *Acc. Chem. Res.* **1992**, *25*, 433–439.

[66] D. P. Curran, S. Hadida, *J. Am. Chem. Soc.* **1996**, *118*, 2531–2532.

[67] H. I. Tashtoush, R. Sustmann, *Chem. Ber.* **1992**, *125*, 287–289.

[68] B. Giese, H. Harnisch, S. Lachhein, *Synthesis* **1983**, *1983*, 733–733.

[69] A. M. Cardarelli, M. Fagnoni, M. Mella, A. Albini, *J. Org. Chem.* **2001**, *66*, 7320–7327.

[70] L. Cermenati, D. Dondi, M. Fagnoni, A. Albini, *Tetrahedron* **2003**, *59*, 6409–6414.

[71] Y. Cai, H.-S. Dang, B. P. Roberts, *Tetrahedron Lett.* **2004**, *45*, 4405–4409.

[72] K. A. Margrey, W. L. Czaplyski, D. A. Nicewicz, E. J. Alexanian, *J. Am. Chem. Soc.* **2018**, *140*, 4213–4217.

[73] H.-B. Yang, A. Feceu, D. B. C. Martin, *ACS Catal.* **2019**, *9*, 5708–5715.

[74] A. Studer, D. P. Curran, *Angew. Chem. Int. Ed.* **2016**, *55*, 58–102.

[75] J. Ji, P. Liu, P. Sun, *Chem. Commun.* **2015**, *51*, 7546–7549.

[76] S. Kamijo, K. Kamijo, K. Maruoka, T. Murafuji, *Org. Lett.* **2016**, *18*, 6516–6519.

[77] M. W. Forkner, L. L. Miller, S. F. Rak, *Synth. Met.* **1990**, *36*, 65–73.

[78] J. E. Almlof, M. W. Feyereisen, T. H. Jozefiak, L. L. Miller, *J. Am. Chem. Soc.* **1990**, *112*, 1206–1214.

[79] I. Baxter, D. W. Cameron, R. B. Titman, *J. Chem. Soc. C Org.* **1971**, 1253–1256.

[80] K. Wu, L. Wang, S. Colón-Rodríguez, G.-U. Flechsig, T. Wang, *Angew. Chem. Int. Ed.* **2019**, *58*, 1774–1778.

[81] M. Mella, M. Freccero, T. Soldi, E. Fasani, A. Albini, *J. Org. Chem.* **1996**, *61*, 1413–1422.

[82] M. Mella, M. Freccero, A. Albini, *Tetrahedron* **1996**, *52*, 5533–5548.

[83] A. Albini, M. Mella, M. Freccero, *Tetrahedron* **1994**, *50*, 575–607.

[84] A. A. Fokin, B. A. Tkachenko, P. A. Gunchenko, D. V. Gusev, P. R. Schreiner, *Chem. – Eur. J.* **2005**, *11*, 7091–7101.

[85] A. P. Antonchick, L. Burgmann, *Angew. Chem. Int. Ed.* **2013**, *52*, 3267–3271.

[86] O. Gutierrez, J. C. Tellis, D. N. Primer, G. A. Molander, M. C. Kozlowski, *J. Am. Chem. Soc.* **2015**, *137*, 4896–4899.

[87] Z.-Z. Zhang, B. Liu, C.-Y. Wang, B.-F. Shi, *Org. Lett.* **2015**, *17*, 4094–4097.

[88] W. Liu, Z. Chen, L. Li, H. Wang, C.-J. Li, *Chem. – Eur. J.* **2016**, *22*, 5888–5893.

[89] "Acetylene Chemistry: Chemistry, Biology and Material Science," can be found under https://www.wiley.com/en-us/Acetylene+Chemistry%3A+Chemistry%2C+Biology+and+Material+Science-p-9783527307814,

[90] C. W. Cheung, P. Ren, X. Hu, *Org. Lett.* **2014**, *16*, 2566–2569.

[91] G. A. Russell, Preecha. Ngoviwatchai, H. I. Tashtoush, *Organometallics* **1988**, *7*, 696–702.

[92] G. A. Molander, K. M. Traister, *Org. Lett.* **2013**, *15*, 5052–5055.

[93] H. Ohmiya, H. Yorimitsu, K. Oshima, *Org. Lett.* **2006**, *8*, 3093–3096.

[94] J. Yi, X. Lu, Y.-Y. Sun, B. Xiao, L. Liu, *Angew. Chem. Int. Ed.* **2013**, *52*, 12409–12413.

[95] G. Cahiez, O. Gager, J. Buendia, *Angew. Chem. Int. Ed.* **2010**, *49*, 1278–1281.

[96] J. Xiang, W. Jiang, P. L. Fuchs, *Tetrahedron Lett.* **1997**, *38*, 6635–6638.

[97] J. Gong, P. L. Fuchs, *J. Am. Chem. Soc.* **1996**, *118*, 4486–4487.

[98] T. Hoshikawa, S. Kamijo, M. Inoue, *Org. Biomol. Chem.* **2012**, *11*, 164–169.

[99] Z.-F. Cheng, Y.-S. Feng, C. Rong, T. Xu, P.-F. Wang, J. Xu, J.-J. Dai, H.-J. Xu, *Green Chem.* **2016**, *18*, 4185–4188.

[100] D. Ma, J. Pan, L. Yin, P. Xu, Y. Gao, Y. Yin, Y. Zhao, *Org. Lett.* **2018**, *20*, 3455–3459.

Chapter 2 - Selective C–H Functionalization of Diamondoids Using Photocatalysis

2.1 - Background

2.1.1 - Introduction

Diamondoids are an interesting class of hydrocarbons in which their carbon-carbon framework constitutes the fundamental repeating unit in the diamond lattice structure. These compounds are distinct due to their unique structure and chemical properties.[1] As discussed in Chapter 1, one inherent property that sets these particular hydrocarbons apart from others is the high $3°$ C–H bond dissociation energy (BDE) of 99 kcal/mol which exceeds the $2°$ C–H BDE of 96 kcal/mol as shown in Figure 2.1.[2] These properties, which result from the rigid caged structures, make this class an excellent target for investigating selective and direct C–H functionalization.[3–6] Diamondoids, especially adamantane, have many applications in nanoscale frameworks, drug delivery, and clinically approved drugs (e.g. memantine, an anti-dementia drug).[7–15]

Diamondoids possess low strain energy making them quite stable. Since all carbon atoms are perfectly tetrahedral and all C–C bonds are perfectly staggered, the molecule is free from both angle strain and torsional strain.[1] However, despite their chemical and thermal stability and lack of notable strain, their inherent properties pose significant challenges. One major difficulty is chemoselectively functionalizing adamantanes, a challenge which increases with each increasing adamantane unit due to similar types of C–H bonds.[1,6] When hydrogen atom transfer (HAT) catalysis is used, two reactive species can be generated making selective functionalization difficult (Figure 2.1d).[16] Also, traditional methods of functionalization can require harsh conditions, typically requires multiple steps and generate waste (Figure 2.1e).[17–21] Therefore, a mild, atom-economical

method for selectively functionalizing adamantanes is of interest. The selective functionalization of one type of C–H bond in the presence of a variety of different C–H bonds is a grand challenge in the field of catalysis.[22–25]

Figure 2.1 Smallest members of diamondoid family, specific examples, and difficulties in functionalization

2.2 - Motivation: C–H functionalization of diamondoids

The direct functionalization of aliphatic C–H bonds has been an attractive and difficult strategy that typically employs the reactivity of weak or activated C–H bonds (ex. Tertiary, benzylic or heteroatom-substituted positions) in comparison to diamondoids.[26–30] The functionalization of unactivated C–H bonds still poses a challenge today. Specifically, the selective activation of strong alkane C–H bonds is difficult due to the high kinetic barrier associated with their cleavage. New methods that favor unactivated aliphatic positions would broaden the applications of C–H functionalization. A compelling candidate for testing direct C–H functionalization is the diamondoids. Here we discuss two different functionalization reaction of diamondoids (alkylation and acylation).
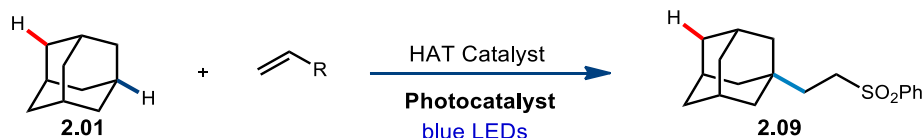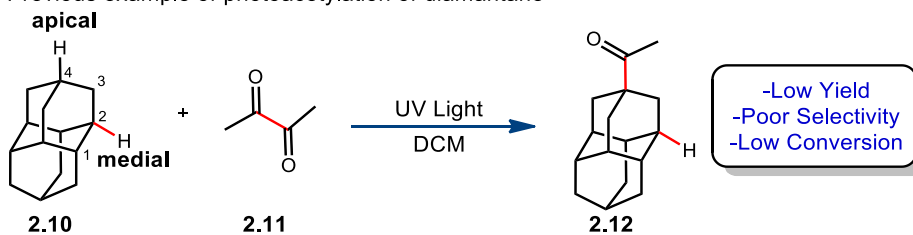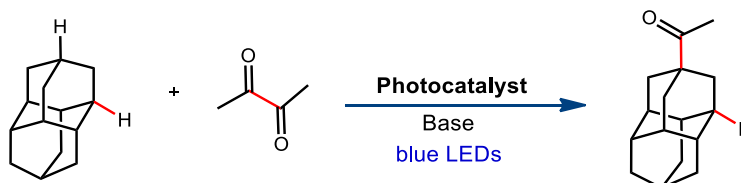
Figure 2.2 Proposed idea for selective C–H functionalization of diamondoids

Our motivation was to overcome previous limitations though the systematic study of adamantanes by identifying a catalyst system that can target strong C–H bonds in the presence of weaker activated bonds. Although there are two different types of C–H bonds in adamantane, we were interested in selectively mono-functionalizing diamondoids at the tertiary position. For the first part of this chapter, we will discuss a new alkylation method for the direct functionalization of diamondoids that is highly selective for the tertiary position on adamantane (**2.11**).[31]

Figure 2.2a shows the proposed idea in which both photoredox and H–atom transfer catalysis are necessary for excellent chemoselectivity for the strong 3° C–H bonds using a Giese-type reaction. We evaluated a variety of alkene substrates and substituted adamantanes in the alkylation reaction as well as investigated the reaction mechanism. The mechanistic proposal is shown in Scheme 2.1. Following HAT, the adamantyl radical **2.13** adds to an alkene to generate a new radical species **2.14**. This is then reduced to give anion intermediate **2.15** followed by protonation to give the desired product.
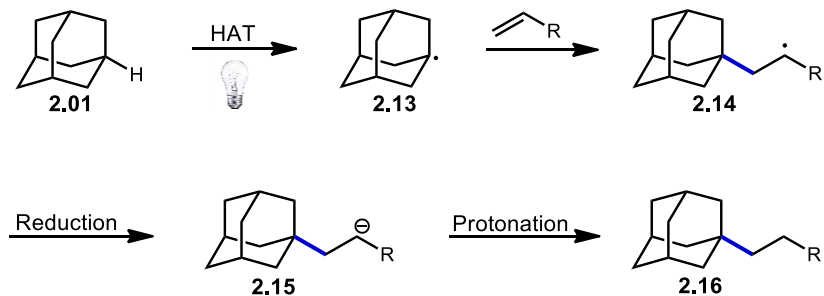
Scheme 2.1 Mechanistic proposal for functionalized adamantanes

50

The second part of this chapter focuses on the selective acetylation of diamantane **(2.10)** (Figure 2.2b). As opposed to adamantane, which has one type of tertiary position due to symmetry, diamantane becomes increasingly more difficult to selectively functionalize due to its two distinct tertiary positions, referred to as apical (C4) and medial (C1). This substrate is also much less explored than the smallest diamondoid, adamantane and has potential application in medicinal chemistry and nanomaterials. There is currently only one selective and direct C–H acetylation of diamantane.[32] However, this particular reaction requires the use of high energy ultra-violet (UV) irradiation and is low yielding. We propose a photoacetylation reaction that proceeds *via* a different mechanism and provides different selectivity with diamantane.

2.3 - Alkylation: Results and Discussion

2.3.1 - Optimization Studies/Control Experiments

Inspired by reports of C–H functionalization reactions *via* heteroatom-stabilized radicals by MacMillan and coworkers, we focused our attention on optimizing around quinuclidines as HAT catalysts due to the strong N-H bond generated (> 100 kcal/mol) and either a transition metal or organic photocatalyst.[33–36] A few examples of the catalysts investigated (including non-quinuclidine based catalysts) are shown in Figure 2.3.

51
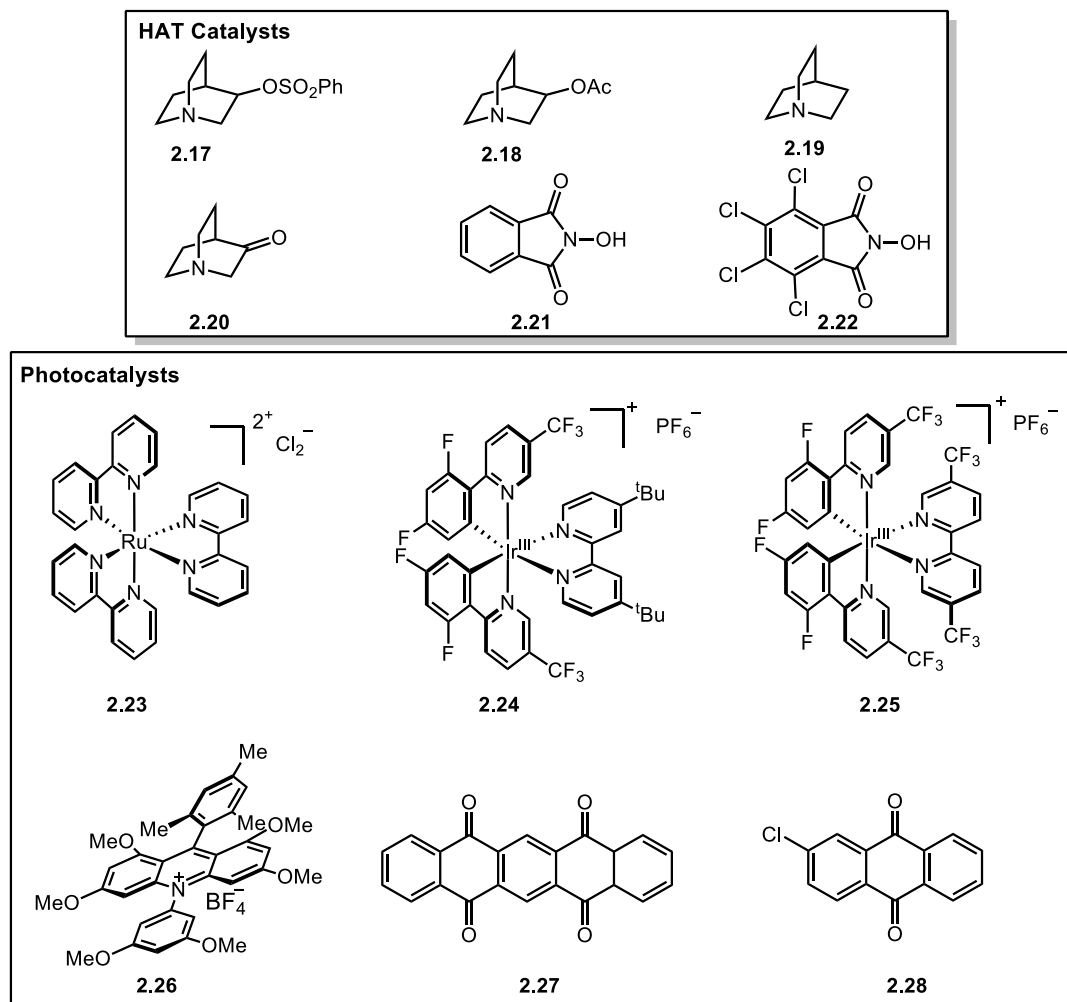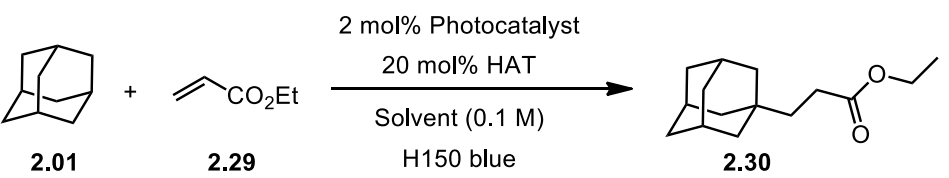
Figure 2.3 Investigated HAT and photoredox catalysts

We began the investigation with ethyl acrylate **(2.29)** as the alkene substrate of choice. Different solvents, HAT catalysts and photocatalysts were tested (shown in Table 2.1). An issue that arose was the insolubility of adamantane in many of the more polar solvents (e.g. DMF or DMSO). Entries 1-3 tested different solvents commonly used in photocatalytic reactions and known to improve the solubility of adamantane. In all cases, conversion of starting materials were low and the desired product was not obtained. We continued the investigation with DCE as the solvent due to improved solubility of all

reagents. With Ru(bpy)$_3$Cl$_2$ **(2.23)** as the photocatalyst (Entries 1-4), the functionalized adamantane product **2.30** was not observed and only polymerization of ethyl acrylate was detected. This was most likely due to incompatible redox potentials and the high reactivity of ethyl acrylate.

Table 2.1 Optimization with ethyl acrylate

Entry	Solvent	HAT Catalyst	Photocatalyst	% Product
1	DCE	**2.19**	**2.23**	0
2	MeCN	**2.19**	**2.23**	0
3	PhCF$_3$	**2.19**	**2.23**	0
4[a]	DCE	**2.21**	**2.23**	0
5[a]	DCE	**2.21**	**2.24**	0
6[a]	DCE	**2.22**	**2.24**	2
7	DCE	**2.18**	**2.24**	17
8	DCE	**2.19**	**2.24**	19

a) Used 20 mol% K$_2$HPO$_4$

N-hydroxyphthalimide (NHPI) **(2.21)** and tetrachloro-*N*-hydroxyphthalimide (Cl$_4$NHPI) **(2.22)** were used as a non-quinuclidine based hydrogen atom transfer catalyst in conjunction with K$_2$HPO$_4$ as base. The role of the base was to deprotonate NHPI, making it easier to oxidize to the more reactive PINO radical which can then participate in HAT catalysis. This particular HAT catalyst was unsuccessful directing us back to the amine based quinuclidine catalysts. We then tested different iridium based photocatalysts **(2.24 and 2.25)** and HAT catalysts **(2.17 – 2.22)** previously shown to undergo C–H abstraction.[18,36,37] To our delight, a dual catalytic system using a quinuclidine catalyst in combination with Ir((df(CF$_3$)ppy)$_2$dtbbpy)PF$_6$ **(2.25)** gave improved yields of 17% for

acetoxy-quinuclidine **(2.18)** and 19% for quinuclidine **(2.19)**. Unfortunately, due to low starting material conversion and high polymerization of ethyl acrylate when exposed to light, we directed our attention to determining a more promising alkene substrate for optimization.

With a potential dual catalytic system using an iridium photocatalyst and a quinuclidine based catalyst in mind, Dr. Haibin Yang tested a variety of alkene substrates and ultimately, vinyl sulfonyl benzene **2.31** was the ideal alkene of choice due to its benchtop stability and ease of handling. A variety of solvents were tested (Table 2.2, Entries 1-7) and although trifluorotoluene seemed promising (Entry 6), the optimal solvent was DCE due to higher yields and increased solubility of adamantane (Entry 7). In all cases except when using acetonitrile as solvent, both unsaturated product **2.32** and decomposition product **2.33** was observed albeit in low yields. Interestingly, the proper combination of catalyst affected both yield and conversion of starting material indicating a synergistic relationship between the two catalysts. When using the HAT catalyst quinuclidine **2.19** with Ir catalyst **2.24** (Entry 7), we obtained a 30% yield but the previously reported acetoxy quinuclidine **2.18** with iridium catalyst **2.24** lowered the conversion to 97% and yield to 27% (Entry 8).

In Entry 9, the yield reduced to 18% when **2.17** was used and there was a slight increase in the unsaturated product **2.32** and decomposition product **2.33**. An alternative, more oxidizing iridium photocatalyst **2.25** was synthesized using known procedures and then tested with three different quinuclidine based catalysts (Entry 10-12). With this particular photocatalyst, a synergistic effect with a quinuclidine base was observed. In

combination with photocatalyst **2.24**, quinuclidine **2.18** gave the desired product but in low yield. A synergistic effect was observed with **2.19** and **2.18**. **2.17** was a better quinuclidine catalyst for this transformation, giving the desired product in 62% yield in a dual catalytic reaction with photocatalyst **2.25**.

Table 2.2 Optimization using vinyl sulfonyl benzene
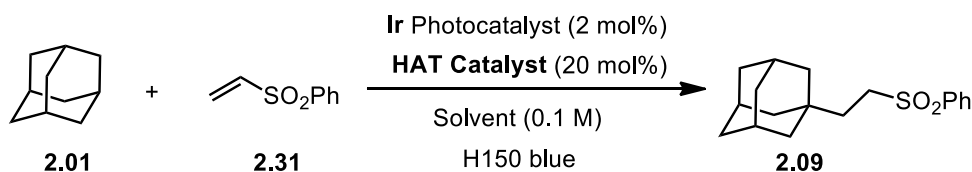
Entry	Solvent	HAT Catalyst	Photocatalyst	% Conversion	% Product
1	DMSO	**2.19**	**2.24**	78	13
2	DMF	**2.19**	**2.24**	76	16
3	DCM	**2.19**	**2.24**	82	17
4	CH3CN	**2.19**	**2.24**	71	18
5	t-BuOH	**2.19**	**2.24**	87	23
6	PhCF$_3$	**2.19**	**2.24**	100	27
7	DCE	**2.19**	**2.24**	97	30
8	DCE	**2.18**	**2.24**	100	27
9	DCE	**2.17**	**2.24**	100	18
10	DCE	**2.19**	**2.25**	33	9
11	DCE	**2.18**	**2.25**	97	57
12	DCE	**2.17**	**2.25**	99	62

* Based on GC Yields
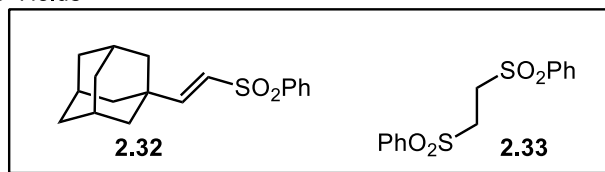
We then proceeded to test different light sources using excess adamantane, acrylonitrile **2.34** as the alkene source and the optimized catalytic system. The initial light source, the Kessil H150 blue LED lamp, seemed like a viable candidate due to its widespread emission in the visible region however we were interested in determining the optimal wavelength to further optimize the reaction. When using a single wavelength

(Kessil PR 160 LED light sources), 390 nm was the least successful of the tested wavelengths (Table 2.3, Entry 2) giving low conversion and a 14% yield. Conversion and yield increased as the wavelength increased however the optimal wavelength was irradiating the reaction with 456 nm for 48 hours which gave a 99% conversion of acrylonitrile and a 90% yield.

Table 2.3 Evaluation of different light sources
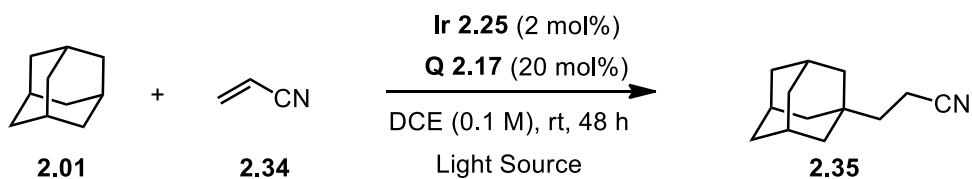
Entry	Light Source	% Conversion	% Product
1	H150 blue	64	60
2	390 nm	50	14
3	440 nm	53	17
4	456 nm	99	90
5	467 nm	83	71
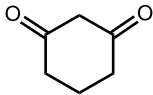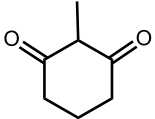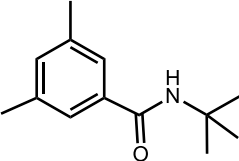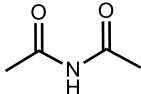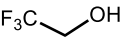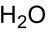
* NMR yields based on Bn$_2$O as internal standard

Although optimistic about the current optimized conditions, we were interested in whether an additive would improve reaction yields, in particular for slower and more difficult substrates. With the help of Dr. Haibin Yang, an extensive protic additive screen was performed (Examples shown in Table 2.4) using 2 mol% Ir **2.24**, 20 mol% **2.19** HAT catalyst and 1 equivalent of additive. Both diones **2.36** and **2.37** were unsuccessful giving no desired product and with benzamide **2.38**, the yield was 27%. *N*-acetylamide **2.39** increased the yield to 43% while trifluoroethanol **2.40** gave a promising yield of 63%. We tested water **2.41** as an additive and saw a greater improvement to 73% yield using one equivalent of water. After testing different equivalents of water, we discovered that 2

56

equivalents was optimal. Without water, the yield decreased to 50%. We hypothesized that the protic additive potentially acts as a proton shuttle. This was further studied in deuterium labeling studies described below.

Table 2.4 Investigation of different additives

Next, a variety of organic and transition-metal photocatalysts were screened with quinuclidine as HAT catalyst (some examples shown in Table 2.5). Ru(bpy)$_3$Cl$_2$ **2.23** was the first catalyst tested with the ethyl acrylate system but was not successful and when tested in the new system, desired product was not observed. Ir **2.24** was the initial iridium catalyst of choice and the first successful photocatalyst however when tested under standard conditions, the conversion was high (97%) but the yield was only 60% for functionalized product **2.09**. Both the unsaturated product **2.32** and decomposition product **2.33** were observed in lower yields. Inspired by the photocatalytic C–H functionalization

reported by Nicewicz *et. al.*[38], we explored the highly oxidizing acridinium photocatalyst, **2.26**. Unfortunately, it provided 77% conversion of starting material, but we observed the desired product in very low yields (1%). Other organic photocatalysts such as pentacenetetrone **2.27** and 2-chloroanthroquinone **2.28** were also unsuccessful with the substrates studied.

Table 2.5 Evaluation of different photocatalysts
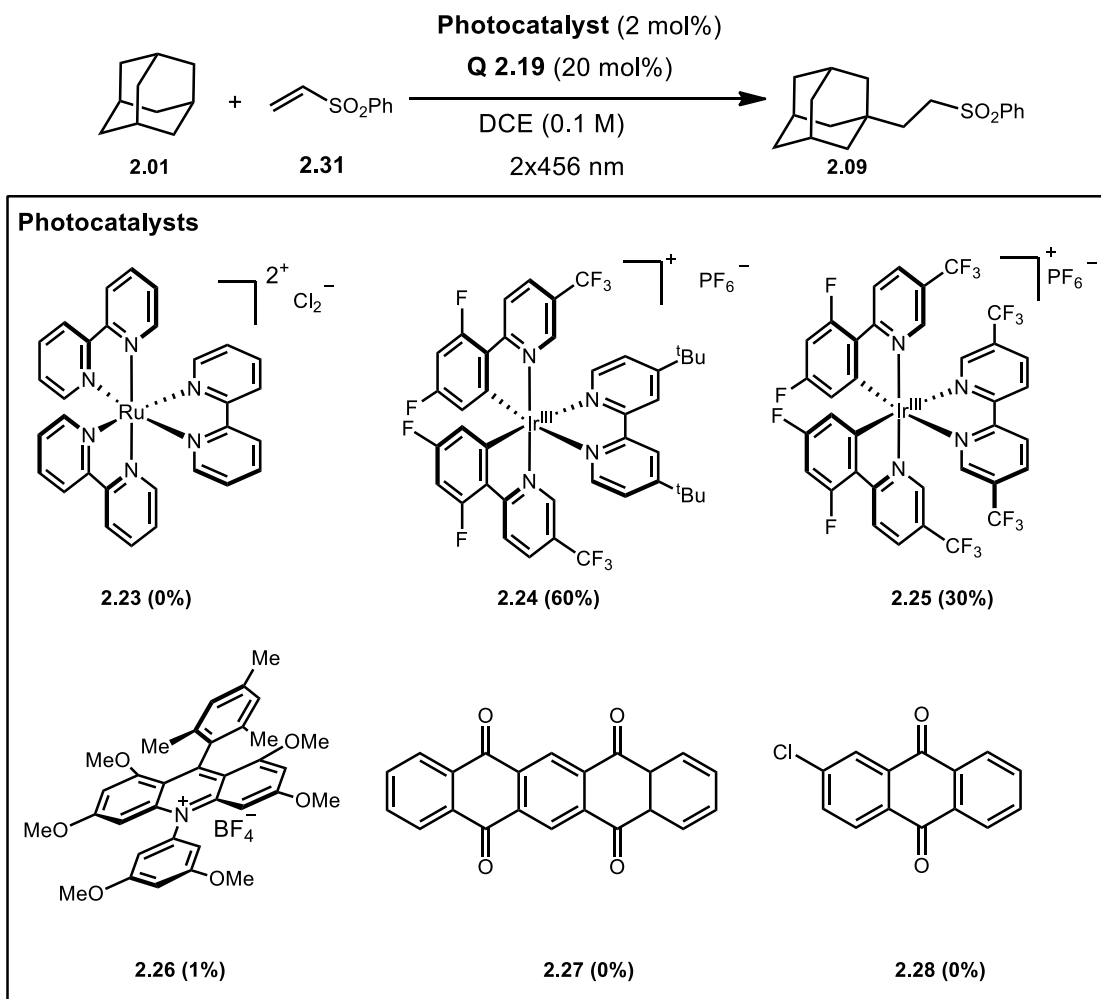
An alternative quinuclidine based HAT catalyst **2.17** was synthesized and tested against the photocatalysts in Table 2.5. The results were similar however when used

simultaneously with Iridium catalyst **2.25**, the yields improved to 72%. Further studies were performed using this catalytic system. Ultimately, the two catalytic systems shown in Figure 2.4 were identified as being optimal, depending on the substrate used in the reaction and therefore the potential required in the key redox steps.

Figure 2.4 Dual catalytic systems

Finally, control reactions were run to test the limitations of the catalytic system using excess adamantane (3 equivalents), 1 equiv. phenyl vinyl sulfone **2.31** and DCE as solvent (Table 2.6). Without the iridium photocatalyst or quinuclidine HAT catalyst, conversions were 36% and 30%, respectively and product was not observed. This indicates both are required for the reaction to produce the expected product, however some background side-reaction of the sulfone can occur. With both catalysts present and no light source, conversion of starting material was a rather low 6% and the desired product was

not observed. Pleasingly, the photocatalyst, HAT catalyst and light are all necessary for the

reaction to proceed efficiently.

Table 2.6 Control reactions
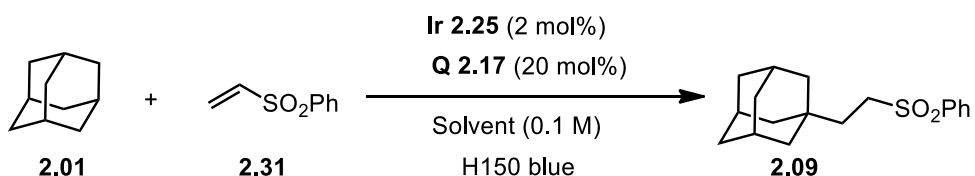
Entry	Reaction Conditions	% Conversion	% Product
1	no Ir catalyst	36	0
2	no HAT catalyst	30	0
3	no light	6	0

A summary of the optimization studies is shown in Table 2.7. Standard conditions

employ the catalysts system 1; HAT catalyst **2.17** and iridium photocatalyst **2.25** (Entry 1),

using 3 eq. of adamantane, phenyl vinyl sulfone **2.31** as the limiting reagent, 2 equiv of

water as an additive. When using the catalyst system 2 with this particular alkene, the yield

was slightly reduced to 66% (Entry 2). Solvent was a key variable in the reaction as shown

in Entry 2. DCE was the optimal solvent as it readily solubilized adamantane; upon

switching to acetonitrile, both the yield and conversion lowered. The additive (H_2O)

improved the reaction and is hypothesized to act as a proton shuttle.

The combination of photocatalyst and HAT catalyst was important as shown in

Entries 5 and 6. Using a ruthenium based photocatalyst was unsuccessful (Entry 7) and

gave no desired product. Redox potentials were an important aspect of this catalytic system

and due to $Ru(bpy)_3Cl_2$'s lower oxidation potential (less positive), the reaction was

unsuccessful when compared to the highly oxidizing iridium catalysts. Another important

feature was the stoichiometry of the reagents. Optimal results were obtained with 3 equivalents of adamantane and phenyl vinyl sulfone as the limiting reagent. When reversing the stoichiometry (Entry 8) the yield reduced to 55% with decomposition product **2.33** as the byproduct. To our delight, when reducing the catalyst loading to 0.5 mol%, the yield was still very good (Entry 9).

Table 2.7 Summary of optimization studies and variation from optimal conditions

Entry	Variation from "standard" conditions	% Conversion	% Product
1	none	100	79
2	Ir **2.24** + Q **2.19** instead of Ir **2.25** + Q **2.17**	100	66
3	CH_3CN instead of DCE	89	54
4	without H_2O	82	50
5	Q **2.19** instead of Q **2.17**	100	74
6	Ir **2.24** instead of Ir **2.25**	89	16
7	Ru(bpy)$_3$Cl$_2$ instead of Ir **2.25**	2	0
8	adamantane (1 equiv) and alkene(2 equiv)	94	55
9	Ir-1 (0.5 mol%)	100	73

2.3.2 - Substrate Scope

With optimal catalytic conditions in hand, we investigated the scope of the alkylation reaction. A number of alkenes with different electron withdrawing groups including sulfones, nitriles, ketones and esters were effective coupling partners giving a single regioisomer of product (**2.09**, **2.42-2.52,** Table 2.8). In all examples functionalization occurred at the tertiary position with no indication of alkylation at the secondary position. When using vinyl sulfonyl benzene **2.31** as alkene, the product **2.09** was obtained in an isolated yield of 72% and when using 1.5 equivalents of adamantane, the yield was reduced to 64% indicating that the reaction was still effective with excess starting material. Although ethyl acrylate was an issue in the beginning of the optimization studies, when applied to the optimized conditions, it was much more successful (product **2.45**). In this case we employed the second catalyst system (Ir **2.24** and Q **2.19**) to provide a 57% yield. When using the first catalyst system, the yield was reduced to 48% yield. We hypothesize that this particular catalytic system helped facilitate the more challenging reduction step (**2.14 – 2.15, Scheme 2.1**).

Other alkenes were also investigated and high yields were obtained. When using cyclohexenone as substrate, the desired product **2.44** was isolated in 65% yield. A dehydroalanine derivative **2.47** was an excellent substrate in this C–H alkylation, giving amino acid derivative **2.47** in 89% yield. Olefins with two electron withdrawing groups were effective including the more sterically hindered 1,2-disubstituted and trisubstituted variants (**2.46-2.52**, 82-94% yield). Adjacent tertiary and quaternary centers are formed, which highlights the power of radical chemistry to generate highly congested centers.

Overall, the isolated yields were quite high (57- 94%) and all products are formed as a single regioisomer.

Table 2.8 Substrate scope: Testing of different alkenes

2.09: 72%	2.42: 91%	2.43: 84%	2.44: 65%
2.45: 57%	2.46: 87%	2.47: 89%	2.48: 94%
2.49: 87%	2.50: 82%	2.51: 93%	2.52: 86%
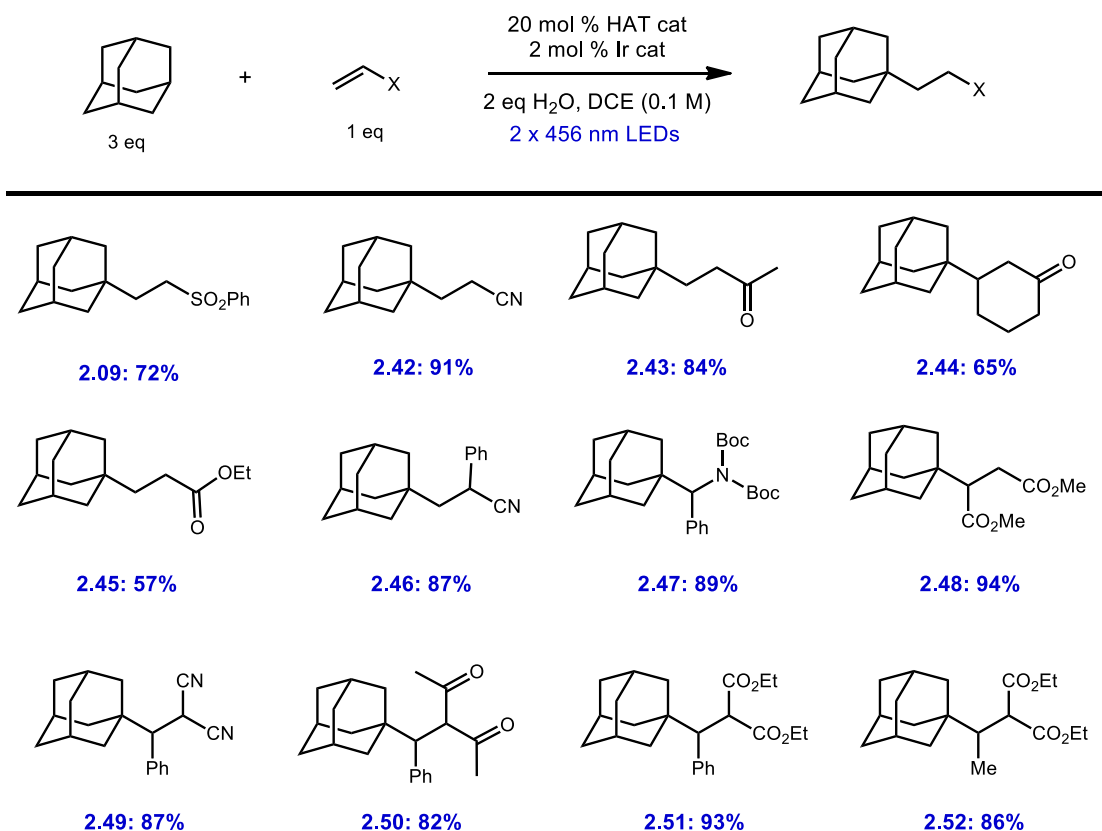
We also investigated the scope of adamantane coupling partners using vinyl sulfonyl benzene as the alkene partner as shown in Table 2.9. A broad range of substituted adamantanes were well tolerated including dimethyl adamantane **2.53** which gave an isolated yield of 69%. When 1.5 equivalents of this adamantane was used, the yield was not affected (68% yield). Arylated (**2.54** and **2.57)**, hydroxylated **(2.56)** and halogenated adamantanes **(2.59)** were also well tolerated and gave the desired alkylated product in good yields (70%-72%). Cyanoadamantane product **2.58** was successfully isolated in 64% yield

when the reaction was performed in acetonitrile. Electron-deficient 2-adamantanone **2.60** and 1-acetyladamantane **2.61**, also performed in acetonitrile as solvent, were alkylated in 60% and 75% yield, respectively.

Table 2.9 Substrate scope: Testing of substituted adamantanes

2.53: 69% (68%)   2.54: 66%   2.56: 72% (66%)   2.57: 72% (67%)

2.58: 64%   2.59: 70%   2.60: 60%   2.61: 75%
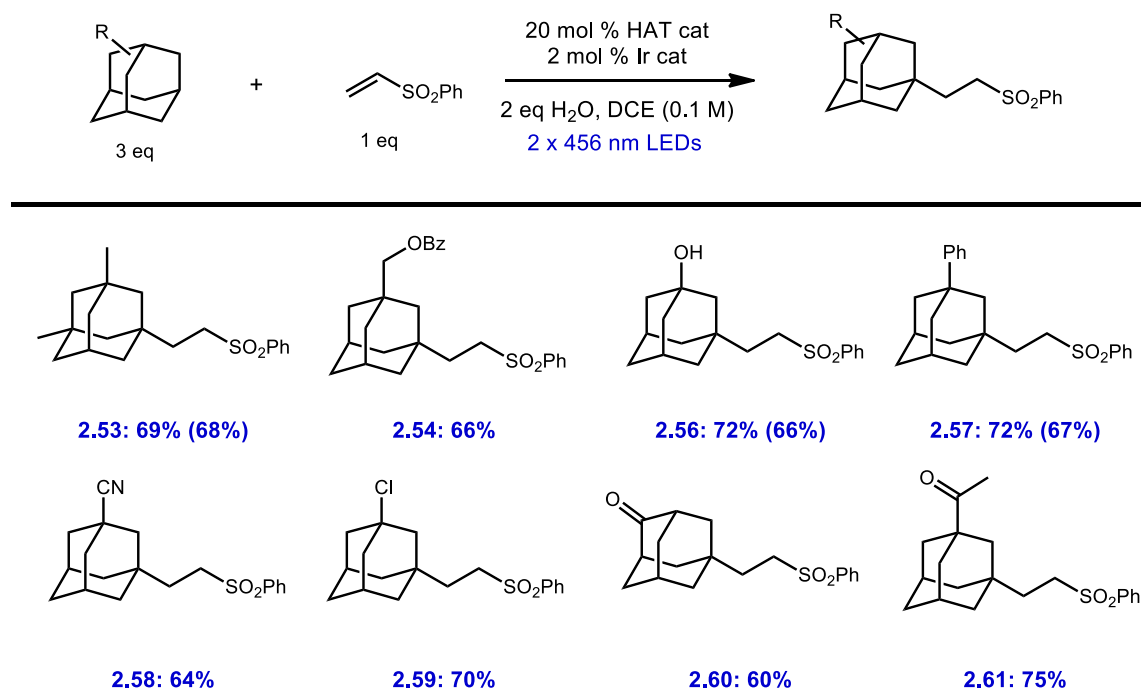
We then turned our attention to more complicated diamondoid structures as shown in Table 2.10. Clinically approved drug derivatives **2.62-2.64** were initially investigated. We employed *N*-Boc protected amantadine **2.62** and memantine **2.63** which gave the desired alkylated product in 63% and 74% yields, respectively. N-Boc-memantine **2.63** was used as the limiting reagents with two equivalents of vinyl sulfonyl benzene in acetonitrile as solvent and at elevated temperatures (38 ℃) as the reaction proceeded more efficiently. A precursor to the anti-acne medication differin **2.64** underwent alkylation at the tertiary position using the second catalytic system and without significant interference

of the electron rich aryl and methoxy groups (51% yield). Next, we tested the selectivity of the amine catalyst Q **2.17** on polyfunctional substrates **2.65-2.67** to investigate whether the reaction conditions were still selective for the tertiary position on adamantane in the presence of multiple $C(sp^3)$–H bonds.

Boc-protected rimantadine **2.65** was monoalkylated in 68% yield with no functionalization at the tertiary position adjacent to the *N*-Boc group. Interestingly, an adamantane ester **2.66**, which possesses an additional tertiary site and functionalizable secondary position adjacent to the ester oxygen, underwent selective alkylation on the adamantane group to produce **2.66** in a 70% yield (>20:1 r.r). Aldehyde **2.67** was monoalkylated in 70% yield with only 3% of the ketone product resulting from activation of the weak aldehyde C–H bond. Functionalization at the secondary position adjacent to the ester was not observed. Notably, Glorius and coworkers described a carboxyl radical HAT system that shows the opposite selectivity in closely related substrates, favoring activation of the weaker aldehyde and 3° C–H bonds.[39] Diamantane, the simplest higher ordered diamondoid, gave the corresponding sulfone product **2.68** and **2.68'** in 62% yield and succinate product **2.69** and **2.69'** in 65% yield as a 1.1-1.2:1 mixture of regioisomers. This implies a moderate inherent selectivity (~3:1) for the apical position.

Table 2.10 Substrate scope: synthesis of other diamondoids
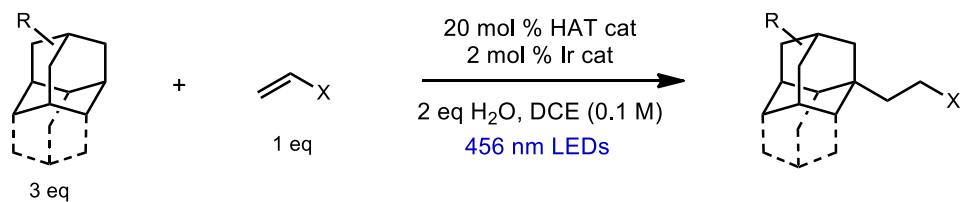
Drug derivatives
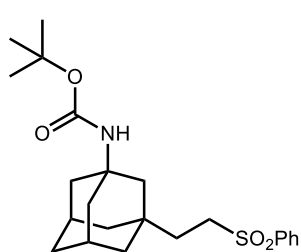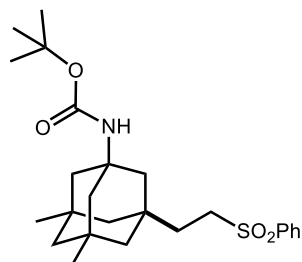
Amantadine 2.62: 63%   **Memantine 2.63: 74%**   **Differin Precursor 2.64: 51%**
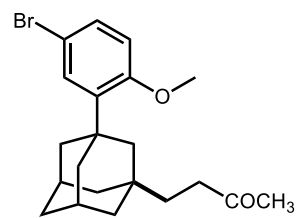
Polyfunctional substrates
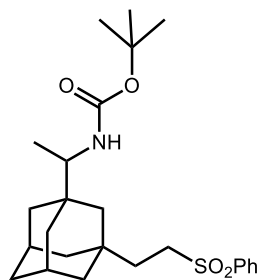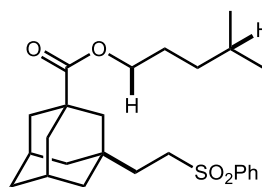
Rimantadine 2.65: 68%   **2.66: 70% (>20:1 r.r.)**   **2.67: 70% (>20:1 r.r.)**
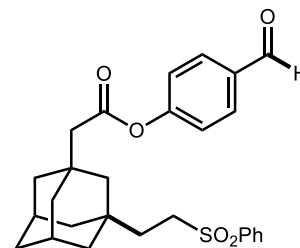
Diamantane
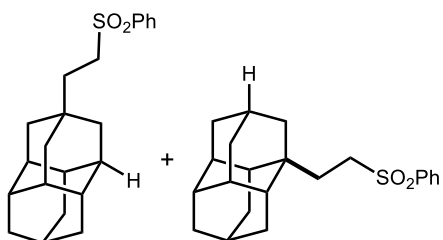
2.68   **2.68'**   **2.69**   **2.69'**
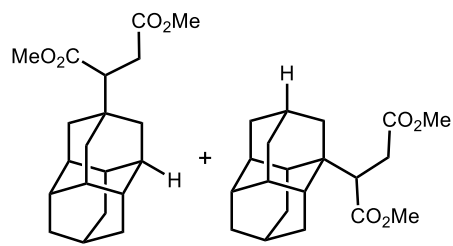
62% (1.2:1 ratio)   **65% (1.1:1 ratio)**

2.3.3 - Intermolecular Competition Experiments

Intermolecular competition experiments were performed with prototypical substrates for HAT methodologies including alkanes, ethers, aldehydes and amides (**2.70-2.77,** Table 2.11). In all cases, the reactivity of adamantane was dominant and 46-80% of alkylation product **2.09** was obtained. Other tertiary C–H bonds such as those in norbornane **2.72** and 2,2,4-trimethylpentane **2.73** were virtually unreactive. Only octanal **2.75**, THF **2.76** and isopropanol **2.77** gave significant amounts of product (14-27%), but alkylated adamantane product **2.09** was still the major product. This increase in yield was attributed to their very electronically activated C–H bonds.

We then performed a competition experiment with polyfunctional natural products and observed high chemoselectivity. Menthol **(2.78)** was essentially unreactive, providing only 4% of the corresponding product along with 75% of **2.09.** Sclareolide, progesterone and limonin **(2.79-2.81)** were also tested and no alkylation products detected using catalyst Q **2.17** instead only the adamantane product **2.09**. The wide range of C–H bonds that remain untouched in favor of adamantanes is an interesting demonstration of the chemoselectivity that is unique to the quinuclidine catalyst system.

Table 2.11 Intermolecular competition studies
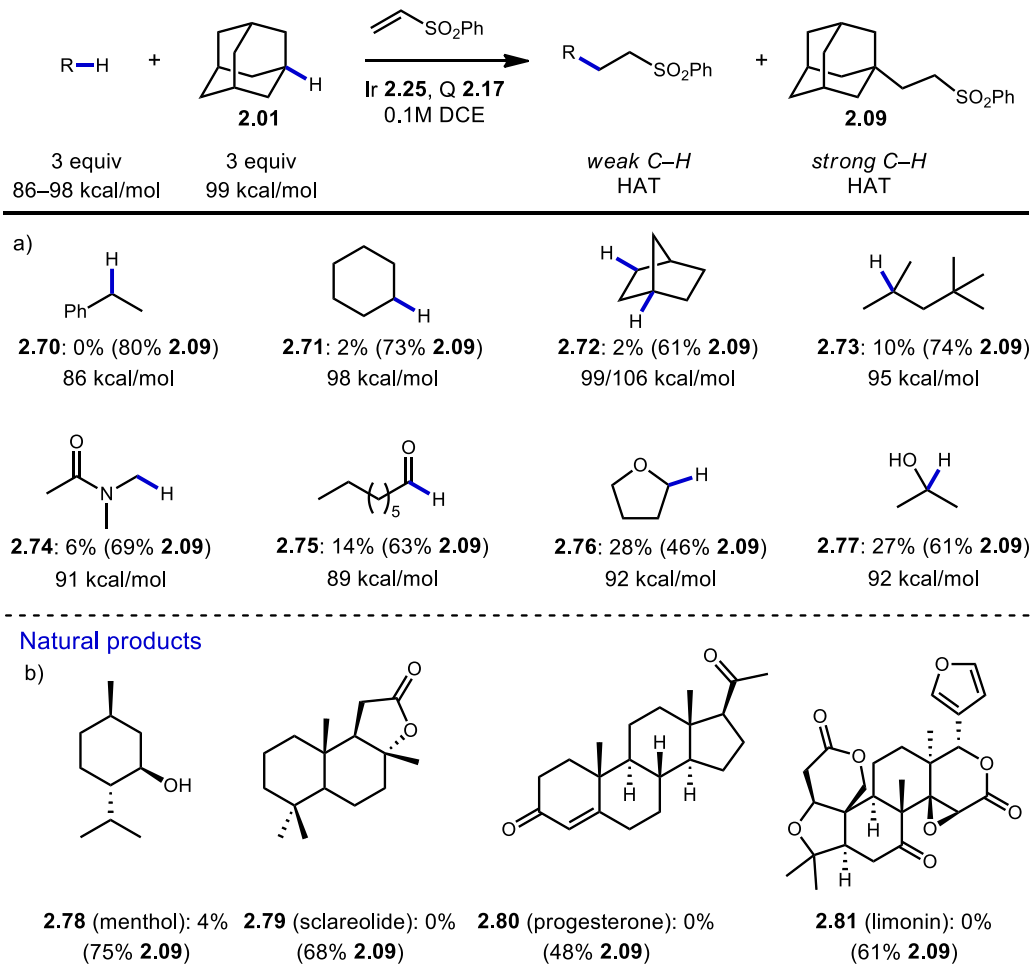
Afterwards, we compared the chemoselectivity of amine catalyst **2.17** for the strong bonds of adamantane to several previously reported photocatalytic HAT systems (Table 2.12) using both octanal and THF in separate competition experiments. In the first study, we added 3 equivalents each of adamantane and octanal and subjected them under typical catalytic conditions. Yields were based on GC results using Bn$_2$O as internal standard and selectivity was determined by ^{1}H NMR. Both dual catalytic systems using an iridium photocatalyst paired with a quinuclidine based catalyst (Entries 1-2, Table 2.12) provided

selectivity for adamantane in a 4.5:1 and 4.2:1 ratio, respectively. The yields for the

adamantane product was quite high while the ketone product **2.75**, although generated, was

significantly lower. However, all other catalysts investigated were either poorly selective

or favored functionalization of the weaker C–H bond. The decatungstate photocatalyst

(TBADT) and carboxyl radical gave moderate yields for the ketone products but a 1:5 ratio

favoring octanal. For the acridinium catalyst **2.26** and phosphate base, very low yields were

shown for both the adamantane product and ketone product with a 1:1 selectivity.

Table 2.12 Competition experiments with octanal
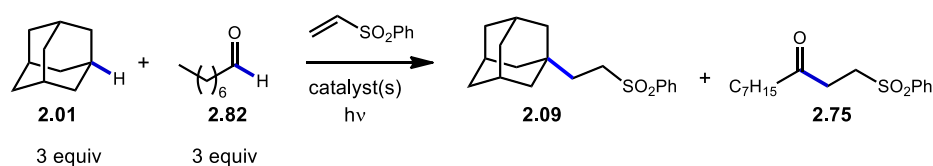
Entry	Catalyst system	Light Source	Yield adapdt	Yield Ketone pdt	Selectivity
1	Ir **2.25**, Q **2.17**	456 nm	63%	14%	4.5:1
2	Ir **2.24**, Q **2.19**	456 nm	55%	13%	4.2:1
3	2-Cl-AQ	390 nm	11%	24%	1:2.2
4	PT	390 nm	13%	26%	1:2
5	TBADT	390 nm	8%	41%	1:5.1
6	Ir **2.24**, NBu$_4$OBz	456 nm	7%	34%	1:4.9
7	Acr^e, HPO$_4^{2-}$	456 nm	7%	7%	1:1
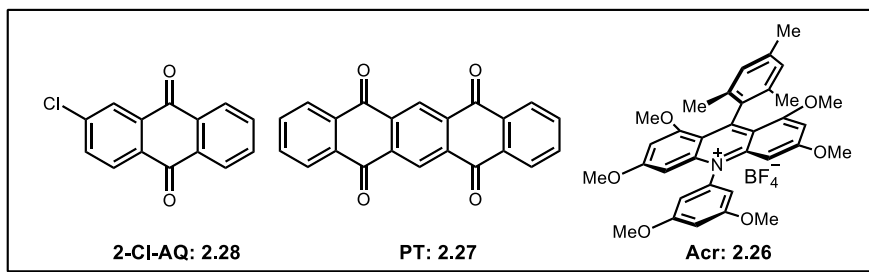
Similar results were observed in THF competitions experiments with the results

shown in Table 2.13. As with the competition experiments with octanal, the two dual

catalytic system were both selective for/towards adamantane giving the functionalized

69

adamantane product **2.09** in 46% yield for system 1 (Entry 1) and a 45% for system 2

(Entry 2). Compared to octanal, the yields were higher for the THF products **2.76**. One

thing to note is that although adamantane is still more reactive than THF using quinuclidine

HAT catalysts, the selectivity decreased significantly to a 1.6:1 and 1.8:1 ratio. With all

other catalyst systems, the yields are low for adamantane product **2.09** and THF product

2.76 but favor THF. Overall, these results indicate that the iridium photocatalyst in

combination with a quinuclidine HAT catalyst is rather unique. All other catalyst systems

show a completely different selectivity and only the catalytic system is selective for

adamantane.

Table 2.13 Intermolecular studies with THF
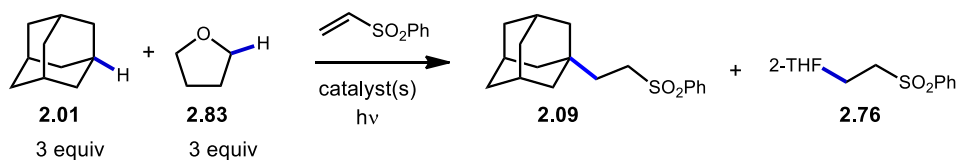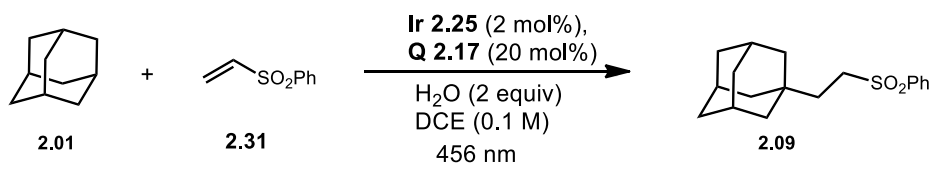
Entry	Catalyst system	Light Source	Yield **2.09**	Yield **2.76**	Selectivity
1	Ir **2.25**, Q **2.17**	456 nm	46%	28%	1.6:1
2	Ir **2.24**, Q **2.19**	456 nm	45%	25%	1.8:1
3	benzophenone	390 nm	13%	11%	1.2:1
4	2-Cl-AQ	390 nm	3%	34%	1:11
5	PT	427 nm	2%	25%	1:12.5
6	TBADT	390 nm	7%	30%	1:4.3
7	Ir **2.24**, NBu$_4$OBz	456 nm	4%	5%	1:1.25
8	Acr, HPO$_4{}^{2-}$	456 nm	18%	15%	1.2:1
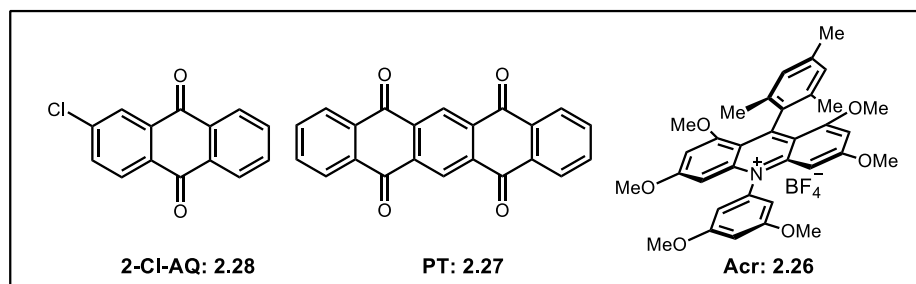
2.4 - Mechanistic Studies

In order to understand this new photoredox catalyzed reaction, a series of mechanistic experiments were performed including radical trapping, fluorescence studies, deuterium labeling and kinetic isotope effect experiments. We began by investigating the effect of radical scavengers. When butylated hydroxytoluene (BHT) was used, alkylation was inhibited giving a 6% yield of alkylated product **2.09** (shown in Entry 1, Table 2.14). When the radical trapping agent, TEMPO, was used, it completely inhibited generation of product **2.09** and TEMPO trapped adamantane adduct **2.84** was confirmed by mass spectrometry. These two results support the proposal that an adamantyl radical intermediate is generated in the reaction.

Table 2.14 Radical trapping experiments

Entry	Radical Scavenger	% Conversion	% Product
1	BHT	16	6
2	TEMPO	37	0
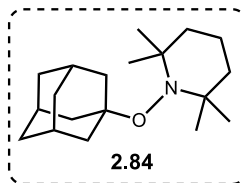
We then performed Stern–Volmer fluorescence quenching experiments to determine what is most likely interacting with the photocatalyst excited state. When irradiated at 420 nm, luminescence studies shown no quenching by adamantane **2.01** or

71

phenyl vinyl sulfone **2.31** as expected. However, studies showed that the HAT catalyst Q **2.17** did quench the photocatalyst **Ir 2.25** and resulted in a significant decrease in luminescence. Results from the Stern−Volmer studies are consistent with the redox potentials of these species. Cyclic voltammetry experiments were performed on the newly synthesized amine catalyst **2.17** and the oxidative potential increased compared to quinuclidine **2.19** due to the introduction of the electron withdrawing group.

For catalyst system 1, shown in Figure 2.5, the excited photocatalyst Ir **2.25*** ($E_{1/2}^{red}$ (*IrIII/IrII)) = +1.68V vs. saturated calomel electrode (SCE in CH_3CN) is a sufficiently strong oxidant to generate the radical cation from quinuclidine Q **2.17** ($E_{1/2}^{red}$ = +1.41V vs SCE in CH_3CN). Similarly for catalyst system 2, photocatalyst Ir **2.24** is well matched with quinuclidine Q **2.19**. The direct oxidation of adamantane by the photocatalyst or quinuclidine radical cation is not favorable ($E_{1/2}^{red}$ = +2.72V vs SCE in CH_3CN), rendering a direct oxidation/deprotonation unlikely.

Catalyst System 1   **Catalyst System 2**

Photocatalyst

Ir 2.25   Ir 2.24

Redox Potentials

$*Ir^{III}/Ir^{II} = +1.68V$
$Ir^{III}/Ir^{II} = -0.69V$

$*Ir^{III}/Ir^{II} = +1.21V$
$Ir^{III}/Ir^{II} = -1.37V$

HAT Catalyst

Q 2.17   Q 2.19

$E_{1/2}{}^{red} = +1.41V$ $E_{1/2}{}^{red} = +1.10V$
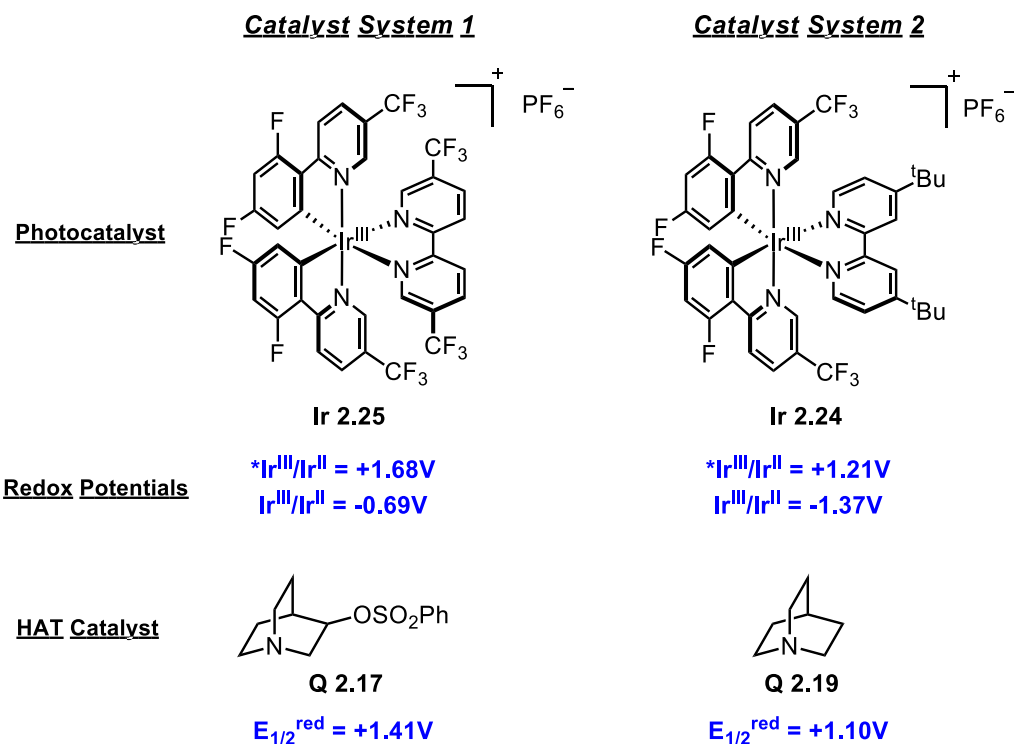
Figure 2.5 Catalyst systems and their redox potentials

We then performed deuterium labeling experiments to investigate the HAT step and probe the reversibility of C–H abstraction (Scheme 2.2 Deuterium labeling experiment and KIE experiment). The proton exchange between the ammonium salt generated from quinuclidine and D_2O should result in the corresponding deuterated ammonium salt **2.86-D**. The tertiary position in the adamantane motif of the starting material or product would be partially deuterated if C–H abstraction is a reversible process. However, no incorporation of deuterium into the starting material or adamantyl C–H bonds of the product were observed, suggesting that HAT is irreversible. The deuterated experiment yielded a 75% with 39% deuteration at the alpha-position only (product **2.85**).
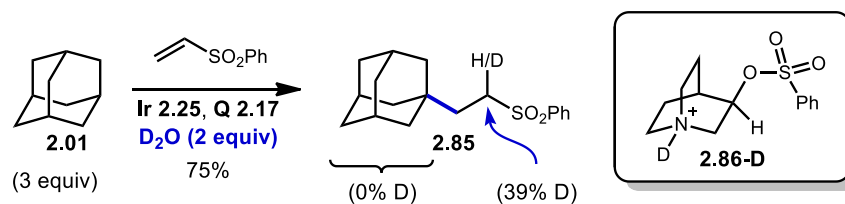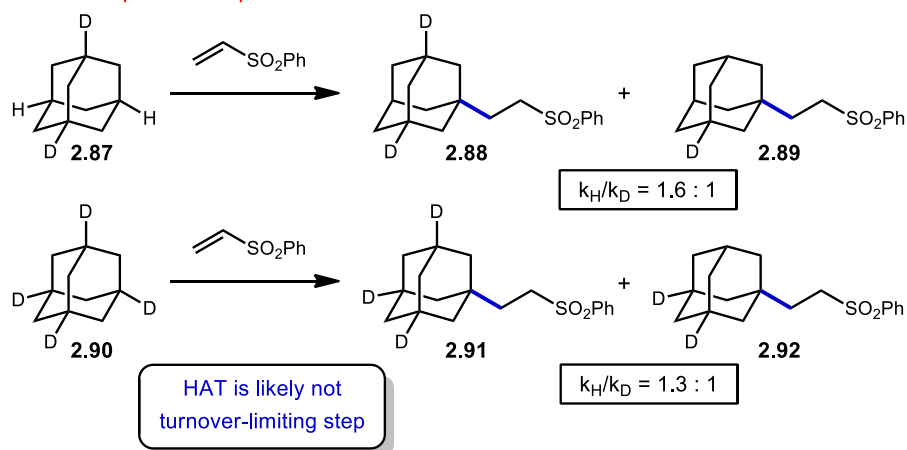
Scheme 2.2 Deuterium labeling experiment and KIE experiment

Both di-deuterated (**2.87**) and tetra-deuterated (**2.90**) adamantane were prepared, tested and compared in kinetic isotope effect experiments. When adamantane and deuterated adamantane were subjected under normal reaction conditions, aliquots were carefully removed at ten minute time intervals and analyzed by gas chromatography (GC). Small kinetic isotope effect (KIE) values obtained from an intramolecular competition experiment with **2.87** ($k_H/k_D = 1.6$) and intermolecular competition experiments in parallel with tetra-deuterated adamantane gave a KIE of 1.3 indicating that the HAT process is likely not the turnover-limiting step in the catalytic cycle. These data are consistent with HAT as an irreversible process with an early transition state.

2.5 - Proposed Mechanism

Based on the evidence above, the proposed mechanism is shown in Figure 2.6. Upon irradiation (**Step A**), the iridium photocatalyst **2.25** is excited to give **2.95** which then oxidizes the quinuclidine HAT catalyst Q **2.17** generating the radical cation **2.93 (Step B)**. Hydrogen abstraction from adamantane **2.01 (Step C)** by the radical cation intermediate **2.93** gives the corresponding ammonium **2.94** and adamantyl radical **2.13**, which rapidly adds to the electron-deficient olefin **(Step D)**, in this case ethyl acrylate, to generate αlpha-acyl radical intermediate **2.14**. The reduction of radical **2.14** by iridium (II) intermediate **2.96 (Step E)** and protonation by either quinuclidinium **2.94** or water as a proton shuttle provides the final product **2.45** and closes both catalytic cycles.
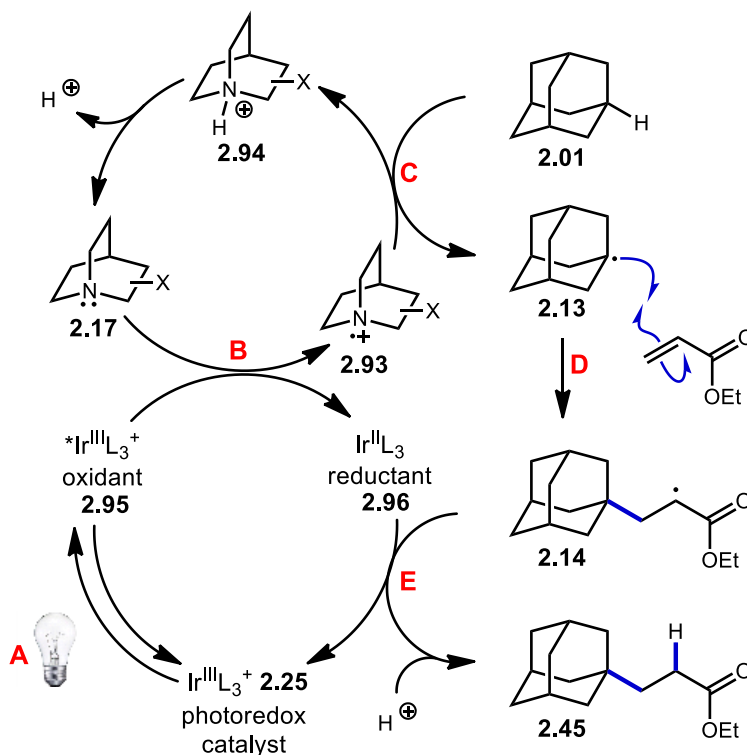
Figure 2.6 Proposed catalytic cycle

2.6 - Conclusions

Herein, we have developed a highly selective C–H functionalization strategy for the direct alkylation of adamantanes. Following extensive optimization studies, we have developed two catalytic systems involving an iridium catalyst and amine-based HAT catalyst. Importantly, we observed a synergistic effect between the photocatalyst and electron-deficient quinuclidine HAT catalyst for the first time. A broad scope of over 25 diamondoid containing compounds including substituted adamantanes, medicinal precursors and diamantanes were synthesized in high yields. Mechanistic studies were explored and support a dual catalytic process.
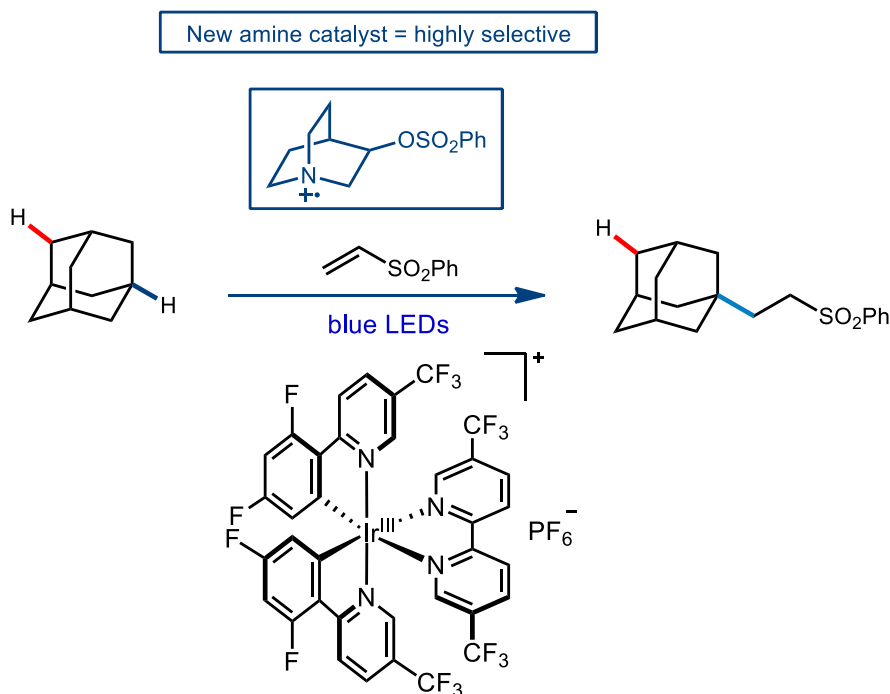
Figure 2.7 Alkylation reaction of adamantane to generate functionalized products

76

2.7 - Introduction−Acetylation of Diamondoids

As stated before, the selective functionalization of diamondoids poses challenges due to their inherent properties. Although there have been previous strategies for direct C–H functionalization of these rigid structures, more methods need to be developed to expand the synthetic toolbox. As outlined above, we have developed a new method for directly functionalizing a variety of adamantanes *via* a dual catalytic alkylation reaction. However, we were interested in directly functionalizing the second higher ordered diamondoid, diamantane, at the apical position using photocatalytic methods.

Each successively higher diamondoid increases in structural complexity, however there have been some examples of their applications in different fields of science and technology like drug delivery and polymer synthesis. Diamantane, the second member of the diamondoid family has been shown to be advantageous in polymer chemistry to provide increased stiffness and thermal stability.[6] Although potentially useful in a variety of applications, directly functionalizing diamantane has previously been shown to be challenging. Figure 2.8 shows some of difficulties in functionalizing this higher diamondoid. One challenge is the increased number of similar C–H bonds present in diamantane. Diamantane has two tertiary positions known as apical and medial and there are currently two examples of selective functionalization at the apical position. However, these reactions have low conversion, are low yielding and requires high-energy UV light. Other methods are poorly selective and lead to multiple inseparable isomers. Another issue is the multiple isomers associated with higher diamondoids like tetramantane, making selective functionalization increasingly difficult.
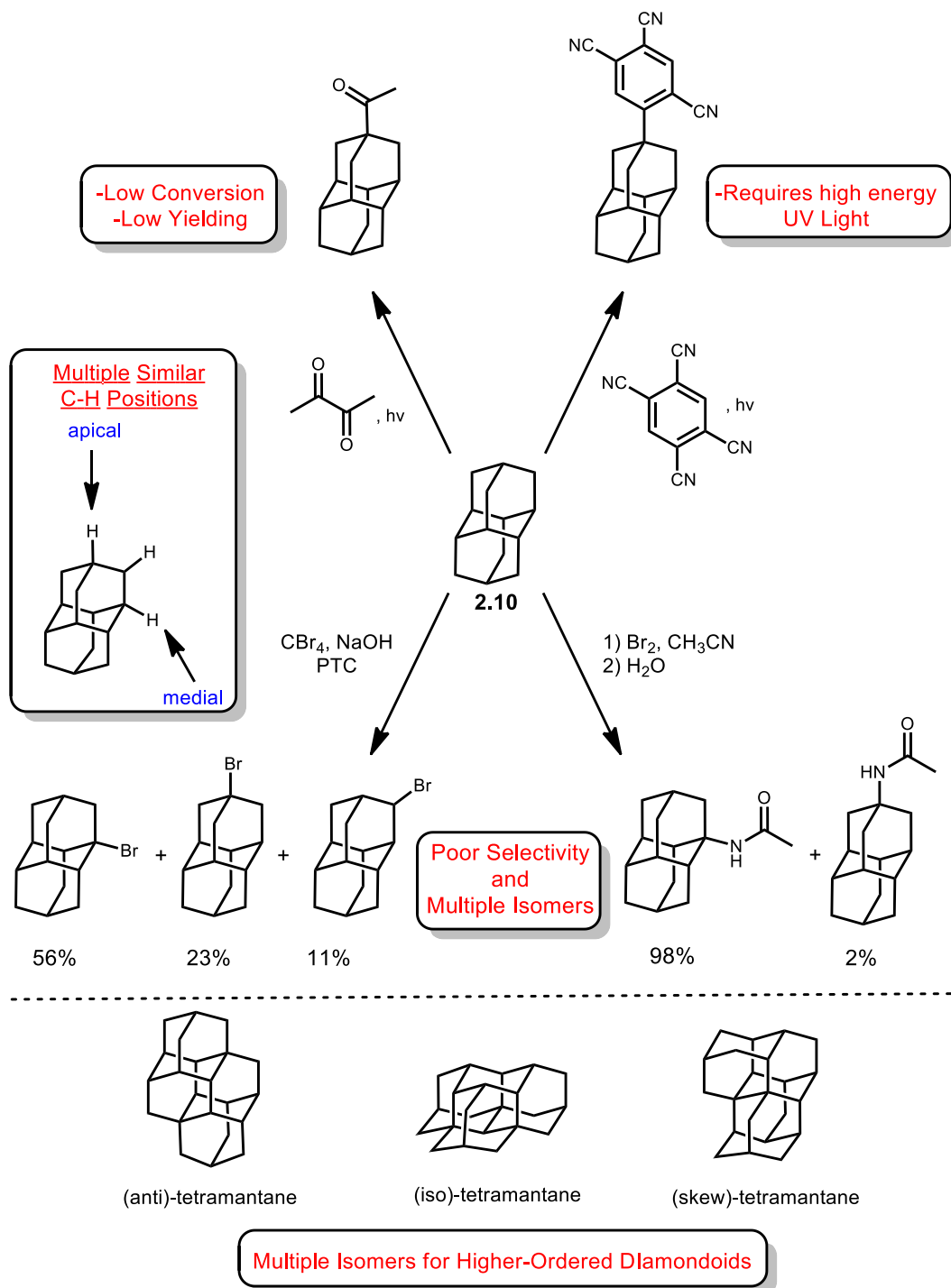
Figure 2.8 Difficulties in functionalizing higher diamondoids

As outlined in Chapter 1, acylated diamondoids are useful intermediates that can be further functionalized, for example through a reductive amination or Baeyer–Villager oxidation.[40,41] Previous methods that have been developed require a pre-functionalized substrate and/or harsh conditions. One method in which adamantane is selectively acylated as a single regioisomer is by using excess biacetyl under high energy ultraviolet photolysis conditions.[17,42] However, the acylation of diamantane has been shown to have low conversion of starting material and is low yielding.[32] In higher ordered diamondoids, photoacetylation remains selective for the methine (apical) position but is consistently low yielding (~20%).[43]

Unlike adamantane, which features four equivalent methine positions, higher ordered diamondoids possess two nonequivalent methine positions for a total of eight potential methine functionalization sites. For diamantane, which features two apical and six medial positions, photoacetylation using biacetyl favored mono-acetylation at the apical position over the medial in a 5.5:1 ratio. This method requires an excessive amount of biacetyl **2.11** (46 equivalents) and relies on the use of UV light. We propose a C–H functionalization approach using visible light *via* an oxidation/deprotonation method that is selective for the apical position (Scheme 1.1). Here, an investigation into different

reaction conditions lead to a new functionalization of diamantane that proceeds with high selectivity.

2.10   **2.11**   **2.12**
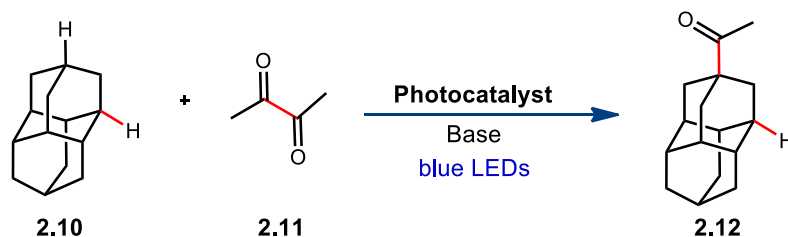
Scheme 2.3 Proposed acetylation strategy with diamantane

One pathway to functionalize adamantane is to directly oxidize the substrate making it more susceptible to reactivity (such as deprotonation) however the oxidation potential of adamantane is quite high ($E_{1/2}^{red} = +2.72V$ vs SCE in CH_3CN) making this method challenging. Inspired by the work done by Beeler *et. al*[16] with pyrylium photocatalysts, we sought to develop a photocatalyst with the oxidative ability to directly oxidize adamantane. Triphenylpyrylium tetrafluoroborate (TPT) **2.97** is a known photooxidant[45] with an oxidation potential ($E_{1/2}^{red} = +2.55V$ vs SCE in CH_3CN) and although it has one of the highest redox potentials and absorbs light in the visible region, it remains highly susceptible to homocoupling or nucleophilic/radical addition. Beeler and coworkers considered whether TPT could be chemically modified to make a more robust catalyst with an oxidation potential that has the capability of oxidizing more challenging reactions and is less susceptible toward unwanted reactivity.

TPT: 2.97

Protective activity

Mes-Acr-Me: 2.99

MDPT: 2.98

Absorbs visible light
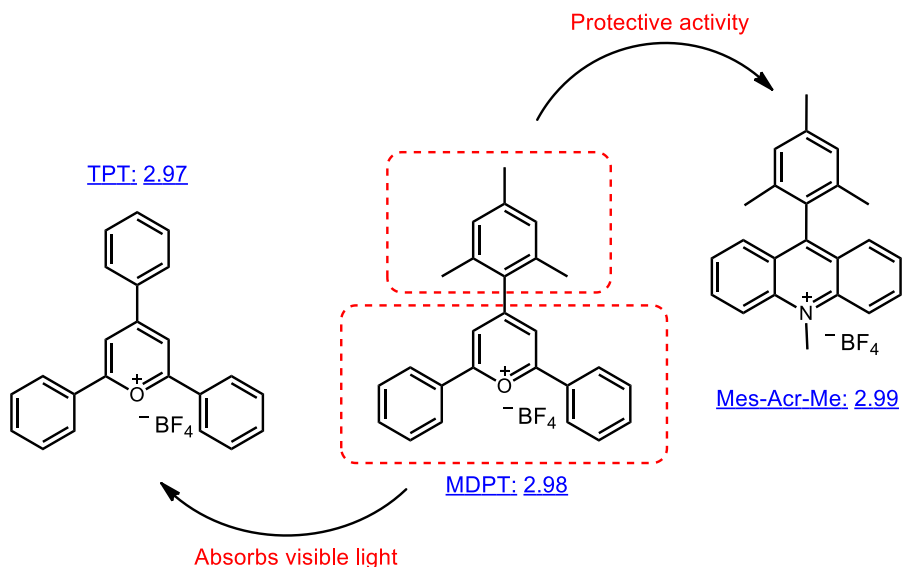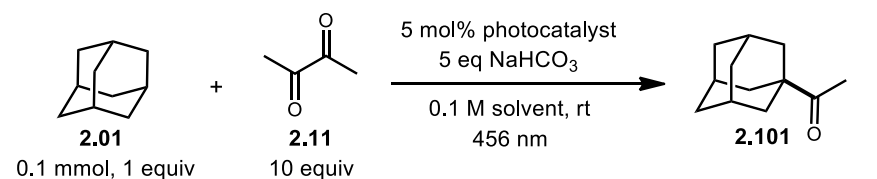
Scheme 2.4 Design of the MDPT catalyst

A photocatalyst developed by Fukuzumi and popularized by Nicewicz,[38,46] *N*-methylmesitylacridinium **2.99** has a lower excited state oxidation potential than TPT, however it possesses an orthogonal mesityl group which has a protective function for the catalyst by minimizing undesirable reactivity towards nucleophiles and transient radicals at the acridinium chromophore. It was hypothesized that by replacing the 4-aryl group on TPT with a mesityl group, the new photocatalyst will not only possess high photophysical properties but a protective environment from the mesityl group. With that in mind, the 4-mesityl-2,6-diphenylpyrylium tetrafluoroborate (MDPT) **2.98** shown in Scheme 2.4 was synthesized and studied for its redox capabilities. MDPT has been shown to have one of the highest oxidation potential known with an $E_{1/2}^{red} = +2.62V$ vs SCE in CH_3CN.[2] Therefore, we moved forward with the hopes of directly functionalizing diamondoids *via* an oxidation with the highly oxidizing MDPT photocatalyst.

2.8 - Results and Discussion

Before testing diamantane directly, we sought to optimize reaction conditions using adamantane as substrate. A variety of catalysts including TPT **2.97**, MDPT **2.98** and an MDPT derivative **2.100** (Table 2.15) were initially tested among a variety of solvents and bases.

Table 2.15 Initial optimization studies

Entry	Solvent	Photocatalyst	% Product
1	Acetone	**A**	0
2	Acetone	**B**	0
3	Acetone	**C**	0
4	THF	**A**	0
5	THF	**B**	0
6	THF	**C**	4
7	MeCN	**A**	3
8	MeCN	**B**	7
9	MeCN	**C**	11
10	DCM	**A**	12
11	DCM	**B**	21
12	DCM	**C**	18
13	DCE	**A**	31
14	DCE	**B**	40
15	DCE	**C**	64
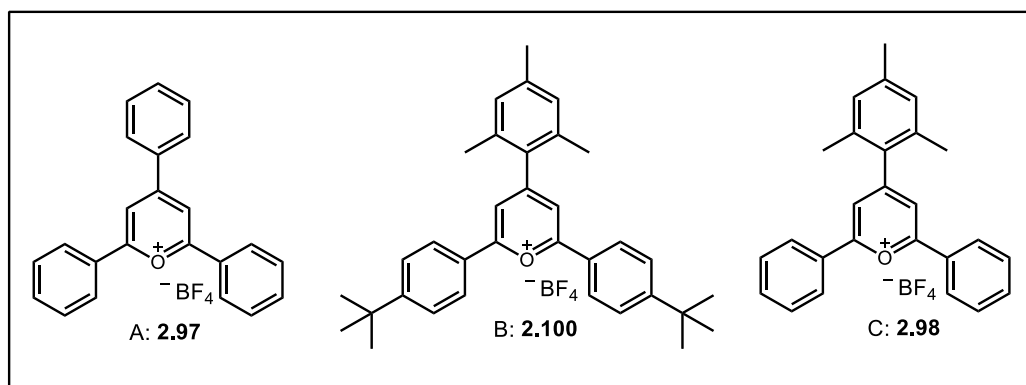
We tested a variety of protic and aprotic solvents with pyrylium photocatalysts A-C (Table 2.15). Acetone, THF and MeOH were unsuccessful as shown in Entries 1-9 however we did see an improvement using DCM which was expected as it is the solvent used in the photoacetylation reaction. Dichloroethane (DCE) was the optimal solvent yielding 31%, 40% and 64% yield for photocatalysts A, B and C, respectively. Excited with these new results, we moved forward with the MDPT photocatalyst and DCE as solvent. We then performed an extensive base screen with some results shown in Table 2.16. A base was hypothesized to increase reactivity by potentially promoting deprotonation of the reactive species. Using 10 equivalents of biacetyl, 5 mol% of photocatalyst MDPT and 5 equivalents of base, we tested a variety of inorganic bases including phosphates and carbonates but interestingly, NaF gave the best results with a yield of 67% (entry 9).

Table 2.16 Base and wavelength screen

Entry	Base	Wavelength	% Product
1	KCN	456	10
2	NaBr	456	11
3	LiCl	456	16
4	K_2PO4	456	17
5	Na_3PO4	456	18
6	Na_2CO_3	456	34
7	$NaHCO_3$	456	64
8	NaOAc	456	54
9	NaF	456	67
10	NaF	390	37
11	NaF	427	37
12	NaF	440	42
13	NaF	456	68
14	NaF	tuna	8

In entries 10-14, a wavelength screen was investigated using both UV light and visible light sources. Following a UV-Vis experiment, the MDPT catalyst was shown to absorb light at 420 nm however the optimal wavelength was at 456 nm giving a 68% yield by gas chromatography (GC). This was followed by testing the equivalents of base, shown in Table 2.17. Although, the reaction does work poorly without base, increasing the base loading significantly affected the yield. Optimal results are shown in Entry 5 using 7 equivalents on NaF which gave a 71% yield by GC. Both reaction concentration and catalyst loading did not affect the yield. Also, control reactions were performed and the reaction does not proceed without light, while without base or catalyst, the reaction proceeds poorly.

Table 2.17 Optimization with equivalents of base

Entry	Equiv Base	% Product
1	0	12
2	1	18
3	3	43
4	5	50
5	7	71
6	9	62
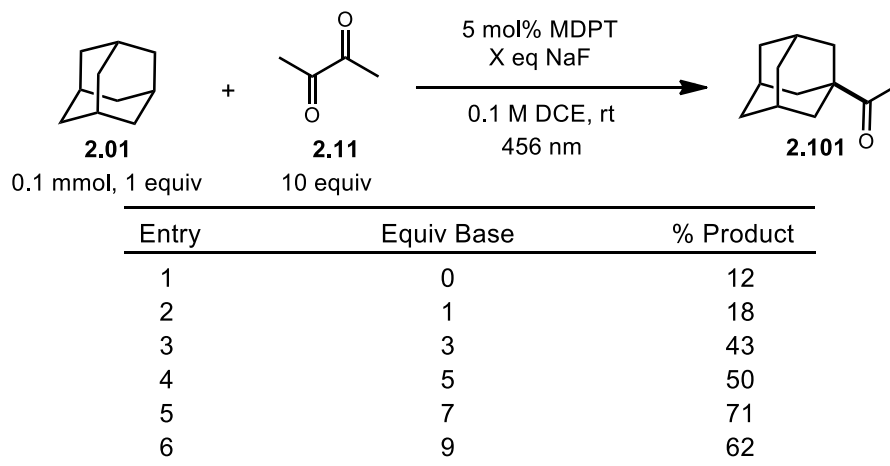
With these optimized conditions in hand, we moved forward with the acetylation of diamantane. The reactions were monitored by GC and performed on a 0.1 mmol scale. After 24 hours, two new peaks appeared by GC at about 10 minutes which was hypothesized to be the two regioisomers of the diamantane product **2.12**. Initial isolation procedures were unsuccessful as conversion of the starting material was low and diamantane was not easily separated from the potential product. By scaling the reaction to 0.5 mmol and a carefully crafted purification system, acetyldiamantane **2.12** was successfully isolated in 48% yield with a regioisomeric ratio of 8:1 favoring the apical position over the medial.
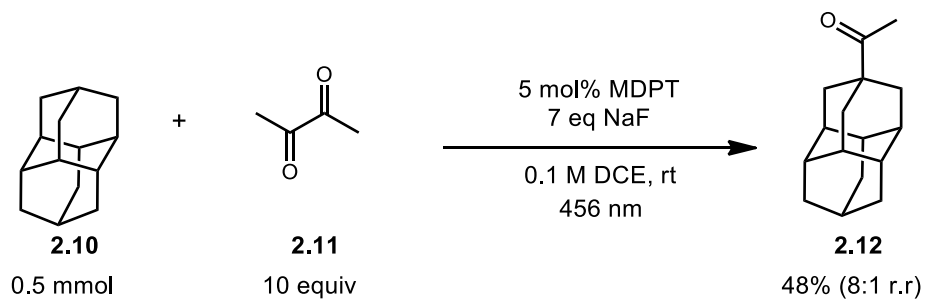
Scheme 2.5 Photoacetylation of diamantane

2.9 - Future Work / Conclusion

Despite successful functionalization and isolation of acetyldiamantane **2.12**, the reaction pathway has not been conclusively determined. Future studies would involve investigating the limitations of this reaction by employing various substrates. An in-depth mechanistic study needs to be performed in order to better understand this transformation and to determine the role of biacetyl, photocatalyst and the base NaF. We hypothesize that the proposed oxidation/deprotonation mechanism is responsible for the high apical selectivity observed.

2.10 - Experimental

2.10.1 - Materials and Methods:

^{1}H and ^{13}C NMR spectra were recorded on a Varian Inova 400 MHz spectrometer unless otherwise indicated and were internally referenced to residual protio solvent signal (note: CDCl$_3$ referenced at δ7.26 ppm for ^{1}H NMR and δ77.16 ppm for ^{13}C NMR, respectively). Data for ^{1}H NMR are reported as follows: chemical shift (δ ppm), integration, multiplicity (s = singlet, d = doublet, t = triplet, q = quartet, m = multiplet), and coupling constant (Hz). Data for ^{13}C NMR are reported in terms of chemical shift and no special nomenclature is used for equivalent carbons. IR spectra were recorded on a Bruker Alpha FT-IR Spectrometer. High-resolution mass spectrometry data were recorded on an Agilent LCTOF instrument using direct injection of samples in dichloromethane into the electrospray source (ESI) with positive ionization. GC was performed on a SHIMADZU GC-2010 Plus instrument equipped with a flame-ionization detector (FID). Stern-Volmer experiments were conducted on a QuantaMaster^{TM} 400 Fluorometer. Cyclic voltammetry experiments were performed using a Pine AFP1 potentiostat.

All reactions were carried out under an inert atmosphere of nitrogen in oven dried or flame dried glassware with magnetic stirring, unless otherwise noted. DCE was distilled from NaH and *t*-BuOH was distilled from Na. Other solvents were dried by passage through columns of activated alumina. All starting materials were prepared according to known literature procedures or used as obtained from commercial sources, unless otherwise indicated. LEDs were purchased from Kessil (http://www.kessil.com/photoredox/Products.php). Reactions were monitored by thin-

layer chromatography (TLC) and carried out on 0.25 mm coated commercial silica gel plates (Analtech TLC Uniplates, F254 precoated glass plates) using UV light as visualizing agent and KMnO$_4$ and heat as a developing agent. Flash chromatography was performed on silica gel (Silicycle, SiliaFlash P60, 230-400 mesh).

2.10.2 - Optimization Details

To an 8-mL glass vial equipped with a magnetic stir bar were sequentially added photoredox catalyst (2 mol%), hydrogen atom transfer catalyst (20 mol%), adamantane (0.750 mmol, 3.0 equiv), phenyl vinyl sulfone or acrylonitrile (0.250 mmol, 1.0 equiv) and solvent (2.5 mL). The vial was sealed with a Teflon septum. The resulting mixture was degassed via three cycles of "freeze, pump, thaw" operation. The vial was further sealed with parafilm and placed approximately 2 inches away from one Kessil® LED (model 456 blue) or Precise Wavelengths PR160 LED (http://www.kessil.com/photoredox/Products.php). The reaction mixture was stirred and irradiated for 48 h. The internal temperature was maintained at approximately 28 °C by an electric fan placed approximately 5 inches above the vial. After 48 h, the yield was determined by GC using Bn_2O as an internal standard.

GC conditions: The initial oven temperature was set to 100 °C, and the ramp rate was programmed to 3 °C/min until reaching 250 °C. The temperature is held at 250 °C for 10 minutes before concluding the run. Retention time: t (**2.31**) = 8.9 min, t (Bn_2O) = 15.3 min, t (**2.09**) = 45.1 min, t (**2.32**) = 45.4 min, t (**2.33**) = 45.8 min. Relative response factor: Rf phenyl vinyl sulfone = 0.630, Rf (Bn_2O) = 1, Rf (**2.09**) = 1.393, Rf (**2.32**) = 0.945, Rf (**2.33**) = 0.350.

2.10.3 - Control Experiments

"Standard" procedure: To an 8-mL glass vial equipped with a magnetic stir bar were sequentially added **Ir 2.25** (11.5 mg, 0.010 mmol, 2 mol%), **Q 2.17** (26.7 mg, 0.100 mmol, 20 mol%), adamantane (204.4 mg, 1.500 mmol, 3.0 equiv), phenyl vinyl sulfone (84.1 mg, 0.500 mmol, 1.0 equiv), water (18.0 µL, 1.00 mmol, 2.0 equiv) and DCE (5.0 mL). The vial was sealed with a Teflon septum. The resulting mixture was degassed via three cycles of "freeze, pump, thaw" operation. The vial was further sealed with parafilm and placed approximately 4 inches away from two Kessil® LEDs (456 nm). The reaction mixture was stirred and irradiated for 48 h. The internal temperature was maintained at approximately 28 °C by an electric fan placed approximately 5 inches above the vial. After 8 h, the yield was determined by GC using Bn_2O as an internal standard. Control experiments were done to explore the effect of reaction parameters.

2.10.4 - Synthesis and Characterization of Ir complexes and quinuclidine derivatives

Ir 2.25, **Ir 2.24** and **Q 2.18** were synthesized according to the literature.[47–49]
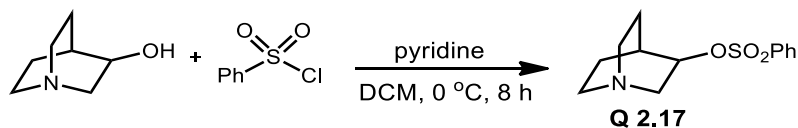
(±)-Quinuclidin-3-yl benzenesulfonate (**Q 2.17**)

To a solution of quinuclidin-3-ol (1.27 g, 10.000 mmol, 1.0 equiv) and pyridine (1.58 g, 20.000 mmol, 2.0 equiv) in DCM (10.0 mL) were added benzenesulfonyl chloride (1.76 g, 10.000 mmol, 1.0 equiv) via syringe at 0 °C. The mixture was further stirred at 0 °C for 8 h, and then concentrated in vacuo. The residue was diluted with DCM (30.0 mL), and washed with saturated aqueous solution of K_2CO_3 (10.0 mL). The volatiles was removed in vacuo and the crude material was purified using silica gel chromatography (eluent: 20:1 dichloromethane/ethanol to 100:10:1 dichloromethane: ethanol: 30% ammonia solution) to provide **Q 2.17** (white solid, 1.20 g, 45% yield). IR (film) 2940, 2868, 1446, 1360, 1186, 1170, 1094, 928, 884, 814, 764, 718, 690, 621, 577, 549 cm^{-1}; ^{1}H NMR (400 MHz, CDCl$_3$) δ 7.92-7.89 (m, 2H), 7.64 (td, J = 8.0, 1.3 Hz, 1H), 7.54 (t, J = 8.0 Hz, 2H), 4.65-4.61 (m, 1H), 3.07 (ddd, J = 15.1, 8.3, 2.3 Hz, 1H), 2.92-2.58 (m, 5H), 2.01-1.97 (m, 1H), 1.89-1.80 (m, 1H), 1.66 (ddt, J = 14.3, 10.1, 4.4 Hz, 1H), 1.48-1.31 (m, 2H); ^{13}C NMR (100 MHz, CDCl$_3$) δ 137.37, 133.80, 129.39, 127.69, 79.77, 55.05, 47.30, 46.27, 26.26, 24.52, 18.76; HRMS (ESI) m/z calcd for C$_{13}$H$_{18}$NO$_3$S (M+H)$^+$ 268.1002, found 268.0992.

2.10.5 - Synthesis and Characterization of Products
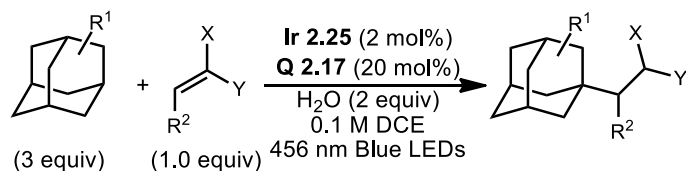
General Procedure: To an 8-mL glass vial equipped with a magnetic stir bar were sequentially added **Ir 2.25** (11.5 mg, 0.010 mmol, 2 mol%), **Q 2.17** (26.7 mg, 0.100 mmol, 20 mol%), adamantane (1.500 mmol, 3.0 equiv), alkene (0.500 mmol, 1.0 equiv), water (18.0 µL, 1.000 mmol, 2.0 equiv) and DCE (5.0 mL). The vial was sealed with a Teflon septum. The resulting mixture was degassed via three cycles of "freeze, pump, thaw" operation. The vial was further sealed with parafilm and placed approximately 4 inches away from two Kessil® LEDs (456 nm). The reaction mixture was stirred and irradiated for the specified time. The solvent was removed in vacuo and the crude residue was purified using silica gel chromatography to provide products (**2.09, 2.42-2.69**)
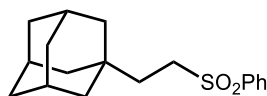
1-(2-(Phenylsulfonyl)ethyl)adamantane (2.09)

Prepared according to General Procedure using adamantane and phenyl vinyl sulfone as the substrates. Reaction time: 8 h. The crude residue was purified by column chromatography on silica gel (EtOAc/Hexanes = 1/5) to afford **2.09** (110.0 mg, 72% yield), IR (film) 2896, 2845, 1445, 1299, 1144, 1084, 786, 747, 728, 685, 614, 548, 531 cm^{-1}; NMR data are in accordance with literature values:[50] ^{1}H NMR (400 MHz, CDCl$_3$) δ 7.89-

7.87 (m, 2H), 7.63 (td, J = 7.6, 1.5 Hz, 1H), 7.55 (t, J = 7.6 Hz, 2H), 3.06-3.01 (m, 2H), 1.91 (brs, 3H), 1.65 (d, J = 12.0 Hz, 3H), 1.54 (d, J = 12.0 Hz, 3H), 1.47-1.43 (m, 2H), 1.38-1.37 (m, 6H); ^{13}C NMR (100 MHz, CDCl$_3$) δ 139.29, 133.63, 129.29, 128.04, 51.30, 41.95, 36.83, 35.89, 31.87, 28.45. HRMS (ESI) m/z calcd for C$_{18}$H$_{25}$O$_2$S (M+H)$^+$ 305.1570, found 305.1569.
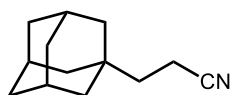
3-(Adamantan-1-yl)propanenitrile (2.42)

Prepared according to General Procedure using adamantane and acrylonitrile as the substrates. Reaction time: 48 h. The crude residue was purified by column chromatography on silica gel (EtOAc/Hexanes = 1/10) to afford **2.42** (86.0 mg, 91% yield), IR (film) 2897, 2846, 2242, 1448, 1360, 1100 cm^{-1}; NMR data are in accordance with literature values[3]: ^{1}H NMR (400 MHz, CDCl$_3$) δ 2.25 (t, J = 8.0 Hz, 2H), 1.96 (brs, 3H), 1.70 (d, J = 12.0 Hz, 3H), 1.60 (d, J = 12.0 Hz, 3H), 1.48-1.44 (m, 8H); ^{13}C NMR (100 MHz, CDCl$_3$) δ 120.95, 41.67, 39.50, 36.86, 32.15, 28.42, 11.00. HRMS (ESI) m/z calcd for C$_{13}$H$_{20}$N (M+H)$^+$ 190.1590, found 190.1295
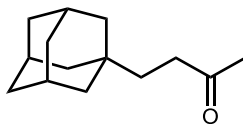
4-(Adamantan-1-yl)butan-2-one (**2.43**)

Prepared according to General Procedure using adamantane and methyl vinyl ketone as the substrates. Reaction time: 24 h. The crude residue was purified by column chromatography on silica gel (EtOAc/Hexanes = 1/10) to afford **2.43** (86.2 mg, 84% yield). IR (film) 2896, 2844, 1715, 1450, 1361, 1157, 548 cm^{-1}; NMR data are in accordance with literature values[2]: ^{1}H NMR (400 MHz, CDCl$_3$) δ 2.36-2.32 (m, 2H), 2.11 (s, 3H), 1.91 (brs, 3H), 1.67 (d, *J* = 12.4 Hz, 3H), 1.58 (d, *J* = 12.4 Hz, 3H), 1.42-1.41 (m, 6H), 1.33-1.29 (m, 2H); ^{13}C NMR (100 MHz, CDCl$_3$) δ 209.96, 42.23, 37.82, 37.51, 37.15, 31.83, 29.93, 28.68.
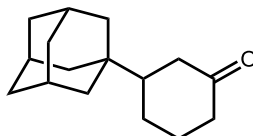
3-(Adamantan-1-yl)cyclohexanone (2.44)

Prepared according to General Procedure with slight modification (Reaction vial was placed approximately 2 inches away from two Kessil® LEDs which led to a higher temperature (38 °C)), using adamantane and cyclohex-2-enone as the substrates. Reaction time: 84 h. The crude residue was purified by column chromatography on silica gel (EtOAc/Hexanes = 1/10) to afford **2.44** (75.2 mg, 65% yield). IR (film) 2894, 2843, 1707, 1448, 1346, 1228, 523 cm^{-1}; NMR data are in accordance with literature values[50]: ^{1}H NMR

(400 MHz, CDCl$_3$) δ 2.41-2.37 (m, 1H), 2.33-2.28 (m, 1H), 2.23-2.14 (m, 1H), 2.09-1.87 (m, 6H), 1.67 (d, J = 12.3 Hz, 3H), 1.58 (d, J = 12.3 Hz, 3H), 1.54-1.43 (m, 7H), 1.34-1.22 (m, 2H); ^{13}C NMR (100 MHz, CDCl$_3$) δ 213.44, 49.74, 42.17, 41.62, 39.49, 37.28, 34.51, 28.71, 25.76, 24.66.
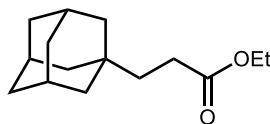
Ethyl 3-(adamantan-1-yl)propanoate (2.45)

Prepared according to General Procedure with slight modification (**Ir 2.25**+**Q 2.17** were replaced by **Ir 2.24**+**Q 2.19**), using adamantane and ethyl acrylate as the substrates. Reaction time: 24 h. The crude residue was purified by column chromatography on silica gel (EtOAc/Hexanes = 1/30) to afford **2.45** (66.8 mg, 57% yield). IR (film) 2898, 2846, 1733, 1450, 1301, 1151, 1103, 1024 cm^{-1}; NMR data are in accordance with literature values[4]: ^{1}H NMR (400 MHz, CDCl$_3$) δ 4.10 (q, J = 7.1 Hz, 2H), 2.25-2.21 (m, 2H), 1.93 (brs, 1H), 1.68 (d, J = 11.9 Hz, 3H), 1.60 (d, J = 12.1 Hz, 3H), 1.44-1.38 (m, 8H), 1.23 (t, J = 7.2 Hz, 3H); ^{13}C NMR (100 MHz, CDCl$_3$) δ 174.80, 60.30, 42.14, 39.08, 37.18, 32.01, 28.71, 28.30, 14.34.
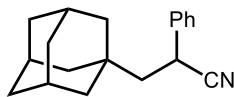
3-(Adamantan-1-yl)-2-phenylpropanenitrile (2.46)

Prepared according to General Procedure using adamantane and 2-phenylacrylonitrile as the substrates. Reaction time: 36 h. The crude residue was purified by column chromatography on silica gel (EtOAc/Hexanes = 1/25) to afford **2.46** (115.4mg, 87% yield), IR (film) 3069, 3035, 2897, 2848, 2239, 1600, 1495, 1452, 1347, 1101, 1031, 748, 713, 694, 586, 491, 463 cm^{-1}; NMR data are in accordance with literature values[5]: ^{1}H NMR (400 MHz, CDCl3) δ 7.30-7.17 (m, 5H), 3.71 (dd, J = 10.4, 3.4 Hz, 1H), 1.93 (brs, 3H), 1.85 (dd, J = 14.3, 10.4 Hz, 1H), 1.67 – 1.55 (m, 12H), 1.42 (dd, J = 14.3, 3.4 Hz, 1H); ^{13}C NMR (100 MHz, CDCl$_3$) δ 138.15, 129.21, 127.85, 127.24, 122.46, 51.18, 42.28, 36.89, 33.11, 31.42, 28.56; HRMS (ESI) m/z calcd for C$_{19}$H$_{23}$NNa (M+Na)$^+$ 288.1723, found 288.1729.
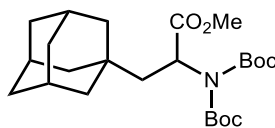
Methyl 2-(di(tert-butoxycarbonyl)amino)-3-adamantan-1-yl)-propanoate (2.47)

Prepared according to General Procedure using adamantane and methyl (tert-butoxycarbonyl)-L-serinate as the substrates. Reaction time: 24 h. The crude residue was purified by column chromatography on silica gel (EtOAc/Hexanes = 1/10) to afford **2.47** (194.3 mg, 89% yield). IR (film) 2979, 2900, 2847, 1744, 1698, 1453, 1366, 1137, 1002,

855, 731 cm^{-1}; ^{1}H NMR (400 MHz, CDCl$_3$) δ 4.93 (dd, J = 7.3, 3.6 Hz, 1H), 3.64 (s, 3H), 2.06 (dd, J = 15.2, 3.6 Hz, 1H), 1.89 (brs, 3H), 1.64 (d, J = 12.3 Hz, 3H), 1.56 (d, J = 12.3 Hz, 3H), 1.52-1.41 (m, 25H); ^{13}C NMR (100 MHz, CDCl$_3$) δ 172.36, 152.00, 82.90, 54.07, 52.28, 44.76, 42.14, 36.97, 32.16, 28.57, 28.05; HRMS (ESI) m/z calcd for C$_{24}$H$_{39}$NO$_6$Na (M+Na)$^+$ 460.2670, found 460.2677.

Dimethyl 2-(adamantan-1-yl)succinate (2.48)

Prepared according to General Procedure using adamantane and (Z)-dimethyl maleate as the substrates. Reaction time: 24 h. The crude residue was purified by column chromatography on silica gel (EtOAc/Hexanes = 1/5) to afford **2.48** (132.2 mg, 94% yield). IR (film) 2901, 2847, 1726, 1438, 1340, 1304, 1195, 1160, 988, 845 cm^{-1}; NMR data are in accordance with literature values[51]: ^{1}H NMR (400 MHz, CDCl$_3$) δ 3.64 (s, 3H), 3.60 (s, 3H), 2.70 (dd, J = 17.1, 12.3 Hz, 1H), 2.48-2.43 (m, 2H), 1.93 (brs, 3H), 1.66-1.55 (m, 9H), 1.43-1.40 (m, 3H); ^{13}C NMR (100 MHz, CDCl$_3$) δ 174.32, 173.36, 52.29, 51.75, 51.28, 39.99, 36.78, 34.42, 30.98, 28.53.

2-(Adamantan-1-yl(phenyl)methyl)malononitrile (**2.49**)

Prepared according to General Procedure using adamantane and 2-benzylidenemalononitrile as the substrates. Reaction time: 24 h. The crude residue was purified by column chromatography on silica gel (EtOAc/Hexanes = 1/10) to afford **2.49** (126.9 mg, 87% yield), IR (film) 2903, 2852, 2250, 1499, 1453, 1346, 1315, 975, 711, 646, 567, 497 cm^{-1}; NMR data are in accordance with literature values[50]: ^{1}H NMR (400 MHz, CDCl$_3$) δ 7.42-7.37 (m, 5H), 4.27 (d, J = 5.4 Hz, 1H), 2.82 (d, J = 5.4 Hz, 1H), 2.03 (brs, 3H), 1.72-1.58 (m, 12H); ^{13}C NMR (100 MHz, CDCl$_3$) δ 135.39, 129.73, 128.59, 128.51, 113.62, 113.46, 57.93, 40.35, 36.54, 36.36, 28.40, 23.80.
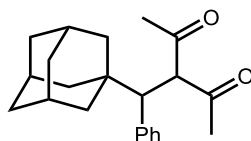
**3-(Adamantan-1-yl(phenyl)methyl)pentane-2,4-dione** (**2.50**)

Prepared according to General Procedure using adamantane and 3-benzylidenepentane-2,4-dione as the substrates. Reaction time: 48 h. The crude residue was purified by column chromatography on silica gel (EtOAc/Hexanes = 1/10) to afford **2.50** (132.2 mg, 82% yield). IR (film) 2973, 2898, 2844, 1693, 1453, 1353, 1141, 1087, 1046, 880, 768, 717, 534, 471 cm^{-1}; ^{1}H NMR (400 MHz, CDCl$_3$) δ 7.21-7.10 (m, 4H), 6.86 (brs, 1H), 4.43 (d, J = 11.0 Hz, 1H), 3.45 (d, J = 11.0 Hz, 1H), 2.30 (s, 3H), 1.88 (brs, 3H),

1.58 (d, J = 15.6 Hz, 3H), 1.48-1.37 (m, 9H), 1.32 (d, J = 13.9 Hz, 3H); ^{13}C NMR (100 MHz, CDCl$_3$) δ 204.28, 203.65, 138.58, 132.58, 129.29, 127.69, 126.70, 72.44, 55.52, 40.49, 36.71, 36.40, 30.53, 28.59, 26.74; HRMS (ESI) m/z calcd for C$_{22}$H$_{28}$O$_2$Na (M+Na)$^+$ 347.1982, found 347.1988.
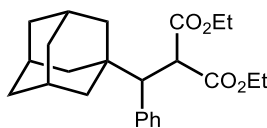
Diethyl 2-(adamantan-1-yl(phenyl)methyl)malonate (2.51)

Prepared according to General Procedure using adamantane and diethyl 2-benzylidenemalonate as the substrates. Reaction time: 48 h. The crude residue was purified by column chromatography on silica gel (EtOAc/Hexanes = 1/20) to afford **2.51** (178.5 mg, 93% yield), IR (film) 2972, 2901, 2852, 1754, 1722, 1448, 1366, 1305, 1249, 1169, 1120, 1032, 775, 708, 626, 611, 556 cm^{-1}; NMR data are in accordance with literature values[50]: ^{1}H NMR (400 MHz, CDCl$_3$) δ 7.20-7.07 (m, 5H), 4.26-4.12 (m, 2H), 3.97 (d, J = 10.7 Hz, 1H), 3.72-3.60 (m, 2H), 3.31 (d, J = 10.7 Hz, 1H), 1.88 (brs, 3H), 1.58 (d, J = 12.3 Hz, 3H), 1.50-1.46 (m, 9H), 1.26 (t, J = 7.1 Hz, 3H), 0.75 (t, J = 7.1 Hz, 3H); ^{13}C NMR (100 MHz, CDCl$_3$) δ 169.59, 168.32, 138.82, 127.20, 126.44, 61.64, 61.09, 56.07, 53.55, 39.92, 36.72, 36.11, 28.58, 13.96, 13.39.

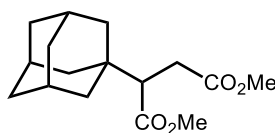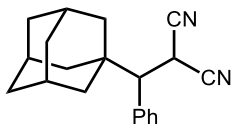**Diethyl 2-(1-(adamantan-1-yl)ethyl)malonate (2.52)**

Prepared according to General Procedure using adamantane and diethyl 2-ethylidenemalonate as the substrates. Reaction time: 48 h. The crude residue was purified by column chromatography on silica gel (EtOAc/Hexanes = 1/20) to afford **2.52** (138.5 mg, 86% yield), IR (film) 2980, 2901, 2848, 1752, 1728, 1447, 1367, 1147, 1031 cm^{-1}; NMR data are in accordance with literature values[50]: ^{1}H NMR (400 MHz, CDCl$_3$) δ 4.17-4.10 (m, 4H), 3.52 (d, *J* = 5.0 Hz, 1H), 2.02 (qd, *J* = 7.3, 5.0 Hz, 1H), 1.92 (brs, 3H), 1.64 (d, *J* = 12.4 Hz, 3H), 1.56 (d, *J* = 12.4 Hz, 3H), 1.51-1.43 (m, 6H), 1.22 (q, *J* = 7.0 Hz, 6H), 0.94 (d, *J* = 7.3 Hz, 3H); ^{13}C NMR (100 MHz, CDCl$_3$) δ 170.38, 169.78, 61.32, 60.88, 51.85, 43.12, 39.41, 37.07, 35.27, 28.66, 14.10, 14.07, 10.40.
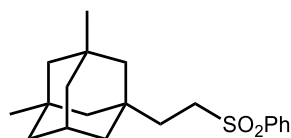
1,3-Dimethyl-5-(2-(phenylsulfonyl)ethyl)adamantane (2.53)

Prepared according to General Procedure using 1,3-dimethyladamantane and phenyl vinyl sulfone as the substrates. Reaction time: 24 h. The crude residue was purified by column chromatography on silica gel (EtOAc/Hexanes = 1/5) to afford **2.53** (114.7 mg, 69% yield), IR (film) 2941, 2891, 2838, 1448, 1303, 1147, 1087, 807, 739, 690, 609, 533, 432 cm^{-1}; ^{1}H NMR (400 MHz, CDCl$_3$) δ 7.88 (d, *J* = 7.1 Hz, 2H), 7.63 (t, *J* = 7.4 Hz, 1H),

7.54 (t, J = 7.6 Hz, 2H), 3.05-3.01 (m, 2H), 1.99 (h, J = 3.2 Hz, 1H), 1.51-1.47 (m, 2H), 1.28-1.20 (m, 6H), 1.11-0.94 (m, 6H), 0.75 (s, 6H); ^{13}C NMR (100 MHz, CDCl$_3$) δ 139.32, 133.64, 129.30, 128.05, 51.47, 50.97, 48.30, 43.07, 40.55, 35.20, 33.56, 31.24, 30.51, 29.52; HRMS (ESI) *m/z* calcd for C$_{20}$H$_{28}$O$_2$SNa (M+Na)$^+$ 355.1702, found 355.1709.
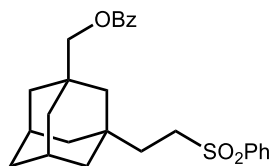
(3-(2-(Phenylsulfonyl)ethyl)adamantan-1-yl)methyl benzoate (**2.54**)

Prepared according to General Procedure using adamantan-1-ylmethyl benzoate and phenyl vinyl sulfone as the substrates. Reaction time: 24 h. The crude residue was purified by column chromatography on silica gel (EtOAc/Hexanes = 1/5) to afford **2.54** (145.7 mg, 66% yield), IR (film) 2900, 2847, 1713, 1447, 1304, 1268, 1147, 1113, 1069, 1025, 710, 687, 619, 533 cm^{-1}; ^{1}H NMR (400 MHz, CDCl$_3$) δ 8.00 (d, J = 7.6 Hz, 2H), 7.88 (d, J = 7.7 Hz, 2H), 7.63-7.40 (m, 6H), 3.89 (s, 2H), 3.07-3.03 (m, 2H), 2.05 (brs, 2H), 1.62-1.23 (m, 14H); ^{13}C NMR (100 MHz, CDCl$_3$) δ 166.48, 139.12, 133.64, 132.93, 130.33, 129.49, 129.26, 128.40, 127.98, 73.72, 51.19, 43.79, 41.21, 38.65, 36.06, 35.45, 34.27, 32.25, 28.17; HRMS (ESI) *m/z* calcd for C$_{26}$H$_{30}$O$_4$SNa (M+Na)$^+$ 461.1757, found 461.1764.
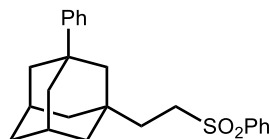
**1-Phenyl-3-(2-(phenylsulfonyl)ethyl)adamantane** (**2.57**)

Prepared according to General Procedure using 1-phenyladamantane and phenyl vinyl sulfone as the substrates. Reaction time: 24 h. The crude residue was purified by column chromatography on silica gel (EtOAc/Hexanes = 1/5) to afford **2.57** (136.8 mg, 72% yield), IR (film) 2898, 2846, 1495, 1446, 1303, 1146, 1086, 931, 741, 688, 617, 532 cm^{-1}; ^{1}H NMR (400 MHz, CDCl$_3$) δ 7.94-7.91 (m, 2H), 7.66 (t, J = 7.4 Hz, 1H), 7.57 (t, J = 7.7 Hz, 2H), 7.36-7.32 (m, 4H), 7.21-7.18 (m, 1H), 3.13-3.09 (m, 2H), 2.18 (p, J = 3.0 Hz, 2H), 1.89-1.42 (m, 14H); ^{13}C NMR (100 MHz, CDCl$_3$) δ 150.13, 139.24, 133.66, 129.30, 128.23, 128.03, 125.84, 124.77, 51.31, 47.80, 42.26, 41.11, 36.88, 35.91, 35.65, 32.94, 29.04; HRMS (ESI) m/z calcd for C$_{24}$H$_{28}$O$_2$SNa (M+Na)$^+$ 403.1702, found 403.1709.
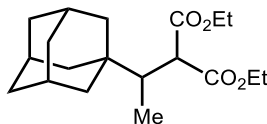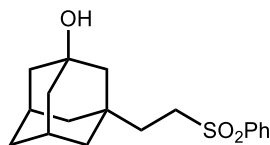

3-(2-(Phenylsulfonyl)ethyl)adamantan-1-ol (**2.56**)

Prepared according to General Procedure using adamantan-1-ol and phenyl vinyl sulfone as the substrates. Reaction time: 24 h. The crude residue was purified by column chromatography on silica gel (EtOAc/Hexanes = 1/1) to afford **2.56** (114.7 mg, 72% yield), IR (film) 3348, 2971, 2905, 2850, 1447, 1301, 1147, 1086, 1047, 727, 688, 617, 533 cm^{-1};

^{1}H NMR (400 MHz, CDCl$_3$) δ 7.85 (d, J = 7.7 Hz, 2H), 7.62 (t, J = 7.4 Hz, 1H), 7.53 (t, J = 7.7 Hz, 2H), 3.03-2.99 (m, 2H), 2.11 (brs, 2H), 1.94 (brs, 1H), 1.62-1.40 (m, 8H), 1.30-1.21 (m, 6H); ^{13}C NMR (100 MHz, CDCl$_3$) δ 139.01, 133.72, 129.30, 127.94, 68.50, 51.28, 49.30, 44.41, 40.52, 35.38, 35.22, 34.83, 30.39; HRMS (ESI) m/z calcd for C$_{18}$H$_{24}$O$_3$SNa (M+Na)$^+$ 343.1338, found 343.1345.
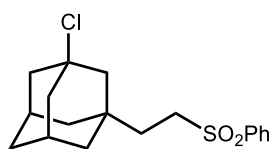
1-Chloro-3-(2-(phenylsulfonyl)ethyl)adamantane (**2.59**)

Prepared according to General Procedure with slight modification (DCE was replaced by CH$_3$CN), using 1-chloroadamantane and phenyl vinyl sulfone as the substrates. Reaction time: 48 h. The crude residue was purified by column chromatography on silica gel (EtOAc/Hexanes = 1/5) to afford **2.59** (118.0 mg, 70% yield), IR (film) 2972, 2904, 2861, 1445, 1302, 1147, 1086, 1046, 804, 739, 688, 602, 534 cm^{-1}; ^{1}H NMR (400 MHz, CDCl$_3$) δ 7.88-7.86 (m, 2H), 7.64 (t, J = 7.4 Hz, 1H), 7.55 (t, J = 7.6 Hz, 2H), 3.04-3.00 (m, 2H), 2.14 (brs, 2H), 2.04 (d, J = 12.1 Hz, 2H), 1.94 (d, J = 12.1 Hz, 2H), 1.75 (s, 2H), 1.60-1.46 (m, 4H), 1.36-1.35 (m, 4H); ^{13}C NMR (100 MHz, CDCl$_3$) δ 139.07, 133.79, 129.37, 128.00, 67.92, 51.69, 51.13, 46.82, 40.00, 36.23, 34.78, 34.72, 31.35; HRMS (ESI) m/z calcd for C$_{18}$H$_{23}$ClO$_2$SNa (M+Na)$^+$ 361.0999, found 361.1006.
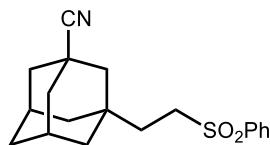
3-(2-(Phenylsulfonyl)ethyl)adamantane-1-carbonitrile (**26.58**)

Prepared according to General Procedure with slight modification (DCE was replaced by CH$_3$CN), using adamantane-1-carbonitrile and phenyl vinyl sulfone as the substrates. Reaction time: 48 h. The crude residue was purified by column chromatography on silica gel (EtOAc/Hexanes = 1/3) to afford **2.58** (104.8 mg, 64% yield), IR (film) 2972, 2905, 2860, 2233, 1444, 1301, 1140, 1085, 1047, 880, 806, 740, 687, 604, 531, 435 cm^{-1}; ^{1}H NMR (400 MHz, CDCl$_3$) δ 7.88-7.86 (m, 2H), 7.67-7.62 (m, 1H), 7.55 (t, *J* = 7.6 Hz, 2H), 3.03-2.98 (m, 2H), 2.06 (brs, 2H), 1.95 (d, *J* = 12.6 Hz, 2H), 1.85 (d, *J* = 12.6 Hz, 2H), 1.65-1.61 (m, 3H), 1.55-1.51 (m, 3H), 1.43-1.36 (m, 4H); ^{13}C NMR (100 MHz, CDCl$_3$) δ 138.97, 133.84, 129.39, 127.97, 124.47, 50.83, 43.95, 40.10, 39.16, 34.93, 34.85, 31.73, 30.75, 27.32; HRMS (ESI) *m/z* calcd for C$_{19}$H$_{23}$NO$_2$SNa (M+Na)$^+$ 352.1342, found 352.1348.
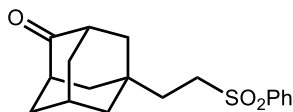
5-(2-(Phenylsulfonyl)ethyl)adamantan-2-one (**2.60**)

Prepared according to General Procedure with slight modification (Reaction vial was placed approximately 2 inches away from two Kessil® LEDs which led to a higher temperature (38 °C) and DCE was replaced by CH$_3$CN), using adamantan-2-one and

phenyl vinyl sulfone as the substrates. Reaction time: 96 h. The crude residue was purified by column chromatography on silica gel (EtOAc/DCM = 1/10) to afford **2.60** (95.0 mg, 60% yield), IR (film) 2973, 2921, 2856, 1708, 1446, 1297, 1139, 1086, 1048, 880, 807, 740, 688, 585, 522, 474 cm^{-1}; ^{1}H NMR (400 MHz, CDCl$_3$) δ 7.88-7.84 (m, 2H), 7.63 (t, *J* = 8.0 Hz, 1H), 7.54 (t, *J* = 8.0 Hz, 2H), 3.03-2.99 (m, 2H), 2.47 (brs, 2H), 2.08 (brs, 1H), 1.93-1.86 (m, 4H), 1.68-1.54 (m, 8H); ^{13}C NMR (100 MHz, CDCl$_3$) δ 217.11, 138.96, 133.84, 129.38, 127.97, 51.31, 46.06, 42.81, 40.55, 38.50, 34.06, 31.92, 27.58; HRMS (ESI) *m/z* calcd for C$_{18}$H$_{22}$O$_3$SNa (M+Na)$^+$ 341.1182, found 341.1188.
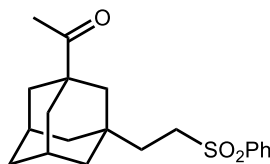
1-(3-(2-(Phenylsulfonyl)ethyl)adamantan-1-yl)ethenone (2.61)

Prepared according to General Procedure with slight modification (DCE was replaced by CH$_3$CN), using 1-(adamantan-1-yl)ethanone and phenyl vinyl sulfone as the substrates. Reaction time: 48 h. The crude residue was purified by column chromatography on silica gel (EtOAc/Hexanes = 1/3) to afford **2.61** (129.6 mg, 75% yield), IR (film) 2916, 2854, 1695, 1446, 1298, 1150, 1085, 806, 741, 688, 586, 533 cm^{-1}; ^{1}H NMR (400 MHz, CDCl$_3$) δ 7.85 (d, *J* = 7.6 Hz, 2H), 7.61 (t, *J* = 7.4 Hz, 1H), 7.52 (t, *J* = 7.7 Hz, 2H), 3.04-2.99 (m, 2H), 2.05 (brs, 2H), 2.02 (s, 3H), 1.74-1.70 (m, 2H), 1.58-1.48 (m, 6H), 1.39-1.29 (m, 6H); ^{13}C NMR (100 MHz, CDCl$_3$) δ 213.20, 139.09, 133.69, 129.29, 127.96, 51.10, 47.08, 42.21, 40.83, 37.64, 35.66, 35.42, 32.22, 28.09, 24.46; HRMS (ESI) *m/z* calcd for C$_{20}$H$_{26}$O$_3$SNa (M+Na)$^+$ 369.1495, found 369.1502.
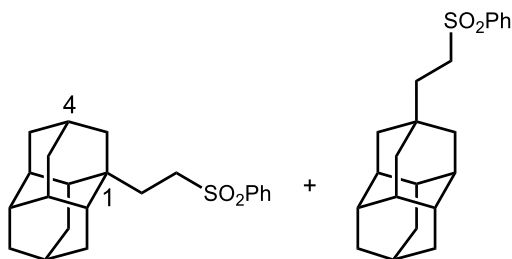
1-(2-(Phenylsulfonyl)ethyl)diamantine + **4-(2-(phenylsulfonyl)ethyl)diamantane** (**2.68 and 2.68'**)

Prepared according to General Procedure with slight modification (**Ir 2.25** + **Q 2.17** were replaced by **Ir 2.24**+**Q 2.19**), using diamantane and phenyl vinyl sulfone as the substrates. Reaction time: 24 h. The crude residue was purified by column chromatography on silica gel (EtOAc/Hexanes = 1/5) to afford **2.68** and **2.68'** (97.5 mg, 62% yield, 1.2:1 ratio of regioisomers). 1-(2-(Phenylsulfonyl)ethyl)diamantane was synthesized via debromo-alkylation of 1-bromo diamantane, and 1-(2-(phenylsulfonyl)ethyl)diamantane was determined as the major isomer via ^{1}H NMR spectra comparison of pure 1-(2-(phenylsulfonyl)ethyl)diamantane and regioisomers. ^{1}H NMR (400 MHz, CDCl$_3$) δ 7.93-7.89 (m, 2H), 7.65 (t, J = 7.4 Hz, 1H), 7.57 (t, J = 7.6 Hz, 2H), 3.08-3.04 (m, 2H), 3.01-2.96 (m, 2H), 1.87-1.25 (m, 21H); ^{13}C NMR (100 MHz, CDCl$_3$) δ 139.28, 133.62, 129.28, 128.03, 51.57, 50.98, 42.64, 41.86, 39.63, 38.76, 38.25, 37.92, 37.71, 37.65, 37.62, 36.88, 35.78, 34.96, 32.44, 29.94, 29.60, 27.42, 25.62, 25.48; HRMS (ESI) *m/z* calcd for C$_{22}$H$_{28}$O$_2$SNa (M+Na)$^+$ 379.1702, found 379.1709.
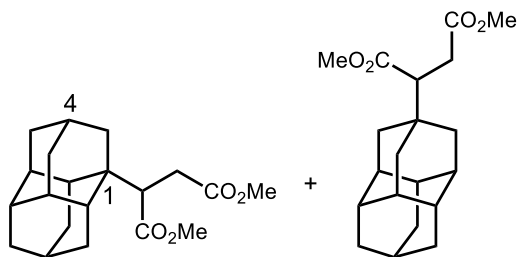
1-(2-(Dimethylsuccinate)diamantane + 4-(2-(dimethylsuccinate)diamantane (2.69 and 2.69')

Prepared according to General Procedure with slight modification (**Ir 2.25** + **Q 2.17** were replaced by **Ir 2.24**+**Q 2.19**), using diamantane and dimethylmaleate as the substrates. Reaction time: 24 h. The crude residue was purified by column chromatography on silica gel (EtOAc/Hexanes = 1/5) to afford **2.69** and **2.69'** (108 mg, 65% yield), IR (film) 2989, 2900, 2848, 1729, 1160 cm^{-1}; ^{1}H NMR (400 MHz, CDCl$_3$) δ 3.64 (d, J = 2.8 Hz, 6H), 3.62 (d, J = 3.28 Hz, 6H), 2.80-2.65 (m, 2H), 2.55-2.42 (m, 2H), 2.41 (d, J = 13.6 Hz, 1H), 2.32 (dd, J = 2.9 Hz, 16.7 Hz, 1H), 1.95-1.30 (m, 18 H); ^{13}C NMR (100 MHz, CDCl$_3$) δ 174.56, 174.48, 173.67, 173.39, 51.78, 51.49, 51.38, 51.31, 44.50, 40.75, 39.12, 39.01, 38.71, 38.61, 37.95, 37.75, 37.60, 37.41, 37.14, 36.80, 32.65, 32.54, 32.32, 31.28, 30.21, 27.22, 25.61, 25.50; HRMS (ESI) *m/z* calcd for C$_{20}$H$_{28}$O$_4$Na (M+Na)$^+$ 355.1880, found 355.1887.
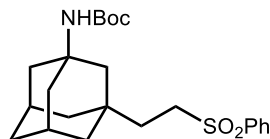
tert-Butyl (3-(2-(phenylsulfonyl)ethyl)adamantan-1-yl)carbamate (2.62)

Prepared according to General Procedure using tert-butyl adamantan-1-ylcarbamate and phenyl vinyl sulfone as the substrates. Reaction time: 24 h. The crude residue was purified by column chromatography on silica gel (EtOAc/Hexanes = 1/2) to afford **2.62** (133.2 mg, 63% yield), IR (film) 3338, 2975, 2910, 2863, 1685, 1523, 1448, 1362, 1302, 1146, 1086, 1046, 879, 739, 687, 613, 552, 532 cm^{-1}; ^{1}H NMR (400 MHz, CDCl$_3$) δ 7.84 (d, J = 7.7 Hz, 2H), 7.61 (t, J = 7.4 Hz, 1H), 7.51 (t, J = 7.6 Hz, 2H), 4.39 (brs, 1H), 3.02-2.98 (m, 2H), 2.05 (brs, 2H), 1.80 (d, J = 12.0 Hz, 2H), 1.68 (d, J = 12.0 Hz, 2H), 1.57-1.43 (m, 6H), 1.35-1.29 (m, 13H); ^{13}C NMR (100 MHz, CDCl$_3$) δ 154.12, 139.09, 133.66, 129.27, 127.98, 78.78, 51.24, 50.90, 45.57, 41.20, 40.70, 35.60, 35.04, 33.89, 29.28, 28.44; HRMS (ESI) m/z calcd for C$_{23}$H$_{33}$NO$_4$SNa (M+Na)$^+$ 442.2023, found 442.2030.
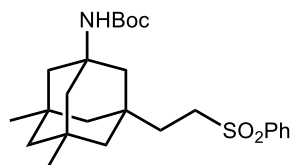
**_tert_-Butyl   (3,5-dimethyl-7-(2-(phenylsulfonyl)ethyl)adamantan-1-yl)carbamate (2.63)**

Prepared according to General Procedure with slight modification (Reaction vial was placed approximately 2 inches away from two Kessil® LEDs which led to a higher

temperature (38 °C) and DCE was replaced by CH₃CN), using Boc-protected Memantine and phenyl vinyl sulfone as the substrates. Reaction time: 48 h. The crude residue was purified by column chromatography on silica gel (EtOAc/DCM = 1/100-1/30) to afford **2.63** (165.7 mg, 74% yield), IR (film) 3368, 2971, 2896, 2864, 1697, 1499, 1448, 1364, 1302, 1151, 1086, 916, 880, 732, 689, 610, 534 cm⁻¹; ¹H NMR (400 MHz, CDCl₃) δ 7.88 (d, *J* = 7.2 Hz, 2H), 7.65 (t, *J* = 7.4 Hz, 1H), 7.56 (t, *J* = 7.6 Hz, 2H), 4.38 (brs, 1H), 3.06-3.01 (m, 2H), 1.59-1.53 (m, 2H), 1.49 (d, *J* = 11.2 Hz, 3H), 1.40-1.37 (m, 12H), 1.12-0.95 (m, 6H), 0.82 (s, 6H); ¹³C NMR (100 MHz, CDCl₃) δ 154.29, 139.22, 133.75, 129.36, 128.10, 78.97, 52.56, 51.50, 50.07, 47.38, 47.32, 44.45, 35.16, 34.53, 32.77, 29.70, 28.53; HRMS (ESI) *m/z* calcd for $C_{25}H_{37}NO_4SNa$ (M+Na)⁺ 470.2336, found 470.2343
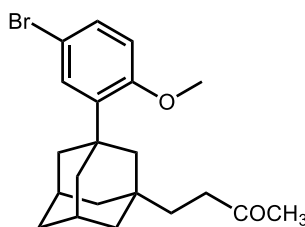
4-(3-(5-Bromo-2-methoxyphenyl)adamantan-1-yl)butan-2-one (**2.64**)

Prepared according to General Procedure with slight modification (**Ir 2.25** + **Q 2.17** were replaced by **Ir 2.24**+**Q 2.19**), using defferin precursor and methyl vinyl ketone as the substrates. Reaction time: 48 h. The crude residue was purified by column chromatography on silica gel (EtOAc/Hexanes = 1/5) to afford **2.64** (100.2 mg, 51% yield), IR (film) 2900, 2846, 1712, 1482, 1356, 1280, 1231, 1177, 1093, 1026, 868, 805, 731, 621, 491 cm⁻¹; NMR data are in accordance with literature values[38]: ¹H NMR (400 MHz, CDCl₃) δ 7.19-7.16 (m, 2H), 6.64 (d, *J* = 8.5 Hz, 1H), 3.71 (s, 3H), 2.33 (t, *J* = 8.2 Hz, 2H), 2.10-2.04 (m, 5H),

1.92-1.86 (m, 4H), 1.65-1.61 (m, 3H), 1.54 (d, J = 12.4 Hz, 1H), 1.42-1.33 (d, J = 14.2 Hz, 6H); ^{13}C NMR (100 MHz, CDCl$_3$) δ 209.82, 157.86, 140.18, 129.69, 129.49, 113.40, 113.29, 55.27, 44.87, 41.48, 39.86, 37.90, 37.70, 37.54, 36.41, 32.73, 29.99, 29.27.
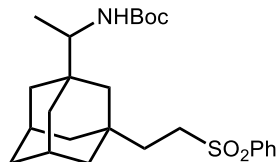
_t_ert-Butyl (1-((3-(2-(phenylsulfonyl)ethyl)adamantan-1-yl)ethyl)carbamate

(2.65)

Prepared according to General Procedure using Boc-protected Rimantadine and phenyl vinyl sulfone as the substrates. Reaction time: 48 h. The crude residue was purified by column chromatography on silica gel (EtOAc/Hexanes = 1/5) to afford **2.65** (152 mg, 68% yield), IR (film) 3395, 2902, 2849, 1733, 1165 cm^{-1}; ^{1}H NMR (400 MHz, CDCl3) δ 7.92-7.84 (m, 2H), 7.64 (t, J = 7.4 Hz, 1H), 7.55 (t, J = 7.9 Hz, 2H), 4.3 (d, J = 9.8 Hz, 1H), 3.33 (m, 1H), 3.05 (m, 2H), 2.02 (s, 2H), 1.60-1.20 (m, 21H), 1.13 (d, J = 12.1 Hz, 1H), 1.08 (d, J = 12.0 Hz, 1H) 0.97 (d, J = 6.84 Hz, 3H); ^{13}C NMR (100 MHz, CDCl$_3$) δ 155.81, 139.27, 133.71, 129.34, 128.09, 79.04, 60.45, 54.22, 51.37, 42.92, 41.42, 41.39, 37.82, 37.34, 36.97, 36.25, 35.69, 32.49, 28.52, 15.04; HRMS (ESI) _m/z_ calcd for C$_{25}$H$_{37}$NO$_4$SNa (M+Na)$^+$ 470.2336, found 470.2343.
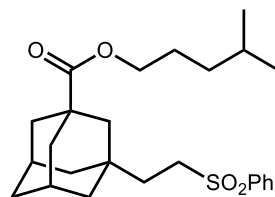
4-Methylpentyl 3-(2-(phenylsulfonyl)ethyl)adamantane-1-carboxylate (**2.66**)

Prepared according to General Procedure, using 4-methylpentyl adamantane-1-carboxylate and phenyl vinyl sulfone (0.2 mmol scale) as the substrates. Reaction time: 48 h. The crude residue was purified by column chromatography on silica gel (EtOAc/Hexanes = 1/4) to afford **2.66** (60.9 mg, 70% yield), ^{1}H NMR (400 MHz, CDCl$_3$) δ 7.89 (d, J = 7.1 Hz, 2H), 7.65 (t, J = 7.5 Hz, 1H), 7.56 (t, J = 7.6 Hz, 2H), 3.99 (t, J = 6.8 Hz, 2H), 3.07-3.03 (m, 2H), 2.06 (brs, 2H), 1.83 (d, J = 11.8 Hz, 2H), 1.71 (d, J = 12.6 Hz, 2H), 1.65-1.51 (m, 9H), 1.42-1.34 (m, 4H), 1.24-1.16 (m, 2H), 0.87 (*d*, J = 6.6 Hz, 6H); ^{13}C NMR (100 MHz, CDCl$_3$) δ 177.20, 139.28, 133.77, 129.39, 128.12, 64.80, 51.29, 43.07, 41.47, 41.02, 38.30, 35.77, 35.48, 35.09, 32.33, 28.26, 27.77, 26.58, 22.63. HRMS (ESI) *m/z* calcd for C$_{25}$H$_{37}$O$_4$S (M+H)$^+$ 433.2407, found 433.2401.
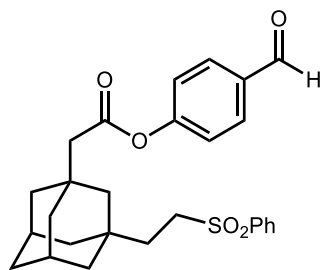
4-Formylphenyl 2-(3-(2-(phenylsulfonyl)ethyl)adamantan-1-yl)acetate (2.67)

Prepared according to General Procedure (DCE was replaced by CH$_3$CN), using 4-formylphenyl 2-(adamantan-1-yl)acetate and phenyl vinyl sulfone as the substrates. Reaction time: 24 h. The crude residue was purified by column chromatography on silica gel (EtOAc/Hexanes = 2/1) to afford **2.67** (163.2 mg, 70% yield), ^{1}H NMR (400 MHz, CDCl$_3$) δ 9.96 (s, 1H), 7.90-7.83 (m, 4H), 7.63 (t, J = 7.4 Hz, 1H), 7.54 (t, J = 7.8 Hz, 2H), 7.22 (d, J = 8.3 Hz, 2H), 3.06-3.02 (m, 2H), 2.31 (s, 2H), 2.06 (brs, 2H), 1.70-1.50 (m, 8H), 1.41-1.31 (m, 6H); ^{13}C NMR (100 MHz, CDCl$_3$) δ 190.88, 169.10, 155.18, 139.10, 133.89, 133.64, 131.12, 129.25, 127.92, 122.41, 51.14, 47.90, 46.60, 41.48, 40.86, 35.69, 35.32, 33.76, 32.65, 28.57. HRMS (ESI) m/z calcd for C$_{27}$H$_{31}$O$_5$S (M+H)$^+$ 467.1887, found 467.1892.
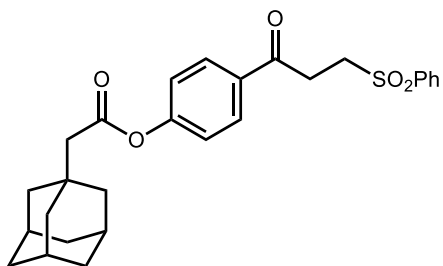
4-(3-(Phenylsulfonyl)propanoyl)phenyl 2-(adamantan-1-yl)acetate

Obtained from the formyl alkylation of 4-formylphenyl 2-(adamantan-1-yl)acetate and purified by column chromatography on silica gel (EtOAc/Hexanes = 5/1, 7.0 mg, 3% yield), ^{1}H NMR (400 MHz, CDCl$_3$) δ 7.96-7.95 (m, 4H), 7.67 (t, J = 7.5 Hz, 1H), 7.58 (t, J = 7.7 Hz, 2H), 7.21 (d, J = 8.0 Hz, 2H), 3.58-3.54 (m, 2H), 3.49-3.45 (m, 2H), 2.32 (s, 2H), 2.02 (brs, 3H), 1.78-1.64 (m, 12H); ^{13}C NMR (100 MHz, CDCl$_3$) δ 194.32, 169.62, 155.08, 139.12, 134.12, 133.32, 129.82, 129.58, 128.12, 122.31, 51.10, 48.81, 42.57, 36.78, 33.46, 31.47, 28.70. HRMS (ESI) *m/z* calcd for C$_{27}$H$_{31}$O$_5$S (M+H)$^+$ 467.1887, found 467.1881.

2.10.6 - Characterization of byproducts
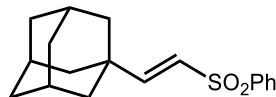
1-((*E*)-2-(Phenylsulfonyl)vinyl)adamantane (2.32)

Obtained as a mixture of compound **2.32** and **2.09**. NMR data are in accordance with literature values[52]: ^{1}H NMR (400 MHz, CDCl$_3$) δ 7.87-7.84 (m, 2H), 7.62-7.59 (m, 1H), 7.54-7.50 (m, 2H), 6.83 (d, *J* = 15.3 Hz, 1H), 6.13 (d, *J* = 15.3 Hz, 1H), 2.00 (brs, 3H), 1.74-1.60 (m, 12H); ^{13}C NMR (100 MHz, CDCl$_3$) δ 156.17, 141.03, 133.22, 127.59, 126.51, 40.80, 36.44, 36.21, 27.95.
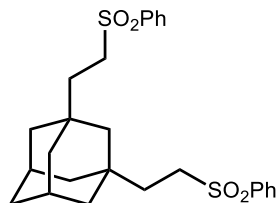
1,3-Bis(2-(phenylsulfonyl)ethyl)adamantane

^{1}H NMR (400 MHz, CDCl$_3$) δ 7.91-7.88 (m, 4H), 7.66 (td, t, *J* = 7.7, 1.3 Hz, 2H), 7.56 (t, *J* = 7.7 Hz, 4H), 3.02-2.97 (m, 4H), 2.00 (brs, 2H), 1.52-1.46 (m, 6H), 1.35 (d, *J* = 12.2 Hz, 4H), 1.23 (d, *J* = 13.1 Hz, 4H), 1.02 (s, 2H); ^{13}C NMR (100 MHz, CDCl$_3$) δ 139.20, 133.77, 129.38, 128.06, 51.25, 46.44, 41.15, 35.94, 35.40, 32.64, 28.55; HRMS (ESI) *m/z* calcd for C$_{26}$H$_{32}$O$_4$S$_2$Na (M+Na)[+] 495.1634, found 495.1641.

PhO$_2$S$\diagdown\diagup\diagdown$SO$_2$Ph
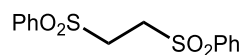
1,2-Bis(phenylsulfonyl)ethane (2.33)

IR (film) 2988, 2900, 2845, 1447, 1299, 1144, 1082, 742, 685, 616, 569 cm^{-1}; ^{1}H

NMR (400 MHz, CDCl$_3$) δ 7.88 (d, J = 7.7 Hz, 4H), 7.72 (t, J = 7.5 Hz, 2H), 7.61 (t, J =

7.7 Hz, 4H), 3.44 (s, 4H); ^{13}C NMR (100 MHz, CDCl$_3$) δ 138.16, 134.73, 129.88, 128.23,

49.65; HRMS (ESI) *m/z* calcd for C$_{14}$H$_{14}$O$_4$S$_2$Na (M+Na)$^+$ 333.0226, found 333.0232.

2.10.7 - Kinetic Isotope Effects Experiment

Dideuterated adamantane and tetradeuterated adamantane were prepared according to previous procedure[53,54]. **Dideuterated adamantane 2.87**: ^{1}H NMR (400 MHz, CDCl3) δ 1.88 (p, J = 3.1 Hz, 2H), 1.76-1.74 (m, 12H); ^{13}C NMR (100 MHz, CDCl3) δ 37.91, 37.78, 37.65, 28.43, 27.95 (t, J = 20.3 Hz); **Tetradeuterated adamantane 2.90**: ^{1}H NMR (400 MHz, CDCl3) δ 1.75-1.73 (m, 12H); ^{13}C NMR (100 MHz, CDCl3) δ 37.66, 27.88 (t, J = 20.0 Hz).
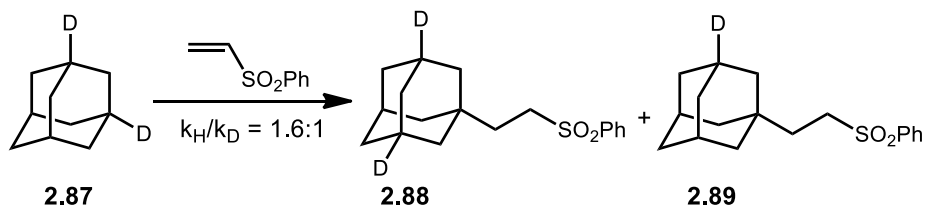
Intramolecular KIE experiment: To an 8-mL glass vial equipped with magnetic stir bar were sequentially added **Ir 2.25** (4.58 mg, 0.004 mmol, 2 mol%), **Q 2.17** (10.69 mg, 0.040 mmol, 20 mol%), dideuterated adamantane **2.87** (83.0 mg, 0.600 mmol, 3.0 equiv), phenyl vinyl sulfone (33.6 mg, 0.200 mmol, 1.0 equiv), water (7.2 µL, 0.400 mmol, 2.0 equiv) and DCE (2.0 mL). The resulting mixture was degassed via three cycles of "freeze, pump, thaw" operation. The vial was placed approximately 4 inches away from two Kessil® LEDs (456 nm) for 8 h. The internal temperature was maintained at approximately 28 °C by an electric fan placed approximately 5 inches above the vial. The products were isolated by flash column chromatography (5/1 hexanes/EtOAc). No deuterium was detected at the α position of the sulfonyl group according to ^{1}H-NMR analysis. So, the ratio of **2.88** to **2.89** can be calculated via MS-ESI analysis. MS-ESI[+]

observed abundances: **2.89** [328.1458 (M+Na)] = 112. Theoretical isotopic natural

abundance ratio of M+1/M+2 for **2.89** = 100/19.5. To account for the contribution of **2.89**

M+2 in the **2.88** M+H, the following formula was used: [329.1520 (M+Na)] = 205-

(112×0.195) = 183. k_H/k_D = 183/112 = 1.6.

2.90   **2.01**   **2.91**   **2.09**
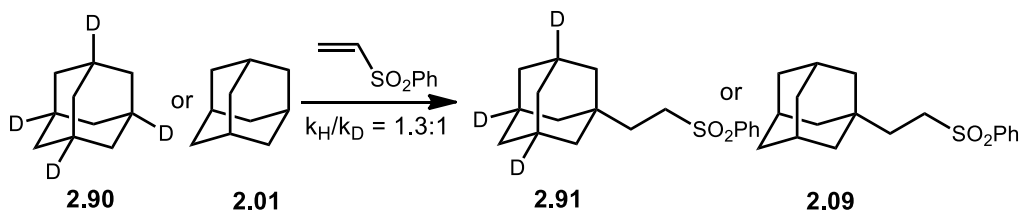
Intermolecular KIE experiment: To an 8-mL glass vial equipped with magnetic

stir bar were sequentially added **Ir 2.25** (4.58 mg, 0.004 mmol, 2 mol%), **Q 2.17** (10.69

mg, 0.040 mmol, 20 mol%), adamantane (81.7 mg, 0.600 mmol, 3.0 equiv) (tetradeuterated

adamantane **2.90** (105.3 mg, 0.600 mmol, 3.0 equiv，80% purity)), phenyl vinyl sulfone

(33.6 mg, 0.200 mmol, 1.0 equiv), naphthalene (25.6 mg, 0.200 mmol, 1.0 equiv, internal

standard), water (7.2 μL, 0.400 mmol, 2.0 equiv) and DCE (2.0 mL). The resulting mixture

was degassed via three cycles of "freeze, pump, thaw" operation. The vial was placed

approximately 4 inches away from two Kessil® LEDs (456 nm). The internal temperature

was maintained at approximately 28 °C by an electric fan placed approximately 5 inches

above the vial. At the indicated time points, the reaction mixture was placed in the dark

and an aliquot was removed by syringe and analyzed by GC (same GC condition as in the

section of **Optimization details.** Retention time: t(naphthalene) = 3.33, Relative response

factor: Rf (**2.91**) = 1.939). Each data point represents an average value determined from

two separate experiments. Linear regression of product yield against time is done in Microsoft Excel. k_H/k_D (1.3) was calculated based on ratio of slopes.

Note: The reaction was kept under positive N_2 pressure during these experiments. The rate of the reaction became slower when O_2 was introduced.

KIE experiment

$y = 0.4254x - 0.7321$
$R^2 = 0.9941$

$y = 0.3229x - 0.6429$
$R^2 = 0.9951$

Yield (8 or 8-D3, %)

time (min)

■ 1

▲ 1-D4

⋯⋯ Linear (1)
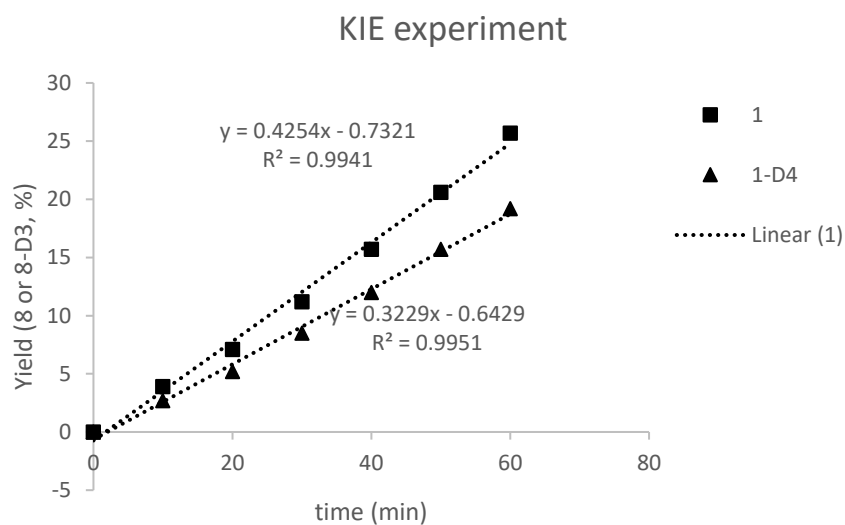
2.10.8 - Probing the reversibility of C–H abstraction
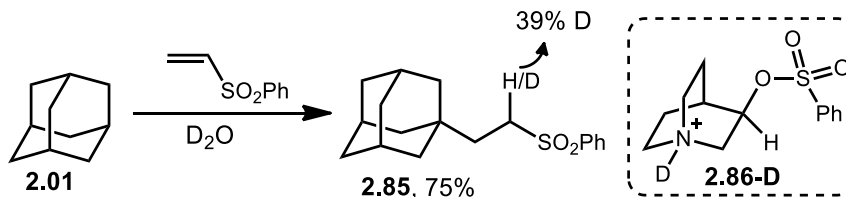
To an 8-mL glass vial equipped with magnetic stir bar were sequentially added **Ir 2.25** (4.58 mg, 0.004 mmol, 2 mol%), **Q 2.17** (10.69 mg, 0.040 mmol, 20 mol%), adamantane (81.7 mg, 0.600 mmol, 3.0 equiv), phenyl vinyl sulfone (33.6 mg, 0.200 mmol, 1.0 equiv), D_2O (7.2 μL, 0.400 mmol, 2.0 equiv) and DCE (2.0 mL). The resulting mixture was degassed via three cycles of "freeze, pump, thaw" operation. The vial was placed approximately 4 inches away from two Kessil® LEDs (456 nm) for 8 h. The internal temperature was maintained at approximately 28 °C by an electric fan placed approximately 5 inches above the vial.

Because the proton exchange between ammonium salt **2.86** resulting from **Q 2.17** and D_2O will yield the corresponding ammonium salt **2.86-D**, the tertiary position in the adamantane motif of starting material or product will be partially deuterated if C–H abstraction is a reversible process. However, we didn't detect obvious deuterium at that positions based on NMR analysis which demonstrated the C–H abstraction step was likely irreversible.

2.10.9 - Intermolecular competitive experiments between adamantane and compound incorporating weaker C(sp³)–H

To an 8-mL glass vial equipped with magnetic stir bar were sequentially added **Ir-2.25** (4.58 mg, 0.004 mmol, 2 mol%), **Q 2.17** (10.69 mg, 0.040 mmol, 20 mol%), adamantane (81.74 mg, 0.600 mmol, 3.0 equiv), compound incorporating weaker C(sp³)–H (0.600 mmol, 3.0 equiv), phenyl vinyl sulfone (33.64 mg, 0.200 mmol, 1.0 equiv), water (7.2 µL, 0.400 mmol, 2.0 equiv) and DCE (2.0 mL). The vial was sealed with a Teflon septum. The resulting mixture was degassed via three cycles of "freeze, pump, thaw" operation. The vial was further sealed with parafilm and placed approximately 4 inches away from two Kessil® LEDs (456 nm). The reaction mixture was stirred and irradiated for 24 h. The internal temperature was maintained at approximately 28 °C by an electric fan placed approximately 5 inches above the vial. The yield was determined by GC using Bn₂O as an internal standard. The samples were performed in the same GC condition as the section of **Optimization details**.
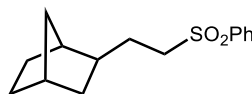
(1S,4R)-2-(2-(phenylsulfonyl)ethyl)bicyclo[2.2.1]heptane **(2.72)**

IR (film) 3054, 2959, 2930, 1264, 730 cm⁻¹; ¹H NMR (400 MHz, CDCl₃) δ 7.90 (d, *J* = 7.5 Hz, 2H), 7.65 (t, *J* = 7.4 Hz, 1H), 7.57 (t, *J* = 7.7 Hz, 2H), 3.07 – 3.01 (m, 2H), 2.18 (s, 1H), 1.89 (s, 1H), 1.72 – 1.62 (m, 1H), 1.52 – 1.18 (m, 7H), 1.12 – 1.04 (m, 3H), 0.97 – 0.86 (m, 2H). ¹³C NMR (100 MHz, CDCl₃) δ 133.74, 129.39, 128.15, 55.22, 41.18, 40.99,

37.80, 36.60, 35.30, 29.95, 29.11, 28.63. HRMS (ESI) *m/z* calcd for $C_{15}H_{21}O_2S$ (M+H)$^+$ 265.1257, found 265.1248
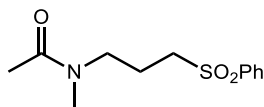
N-Methyl-N-(3-(phenylsulfonyl)propyl)acetamide (2.74)

^{1}H NMR (400 MHz, CDCl$_3$) δ 7.90-7.85 (m, 2H), 7.69-7.53 (m, 3H), 3.45-3.40 (m, 2H), 3.09-3.04 (m, 2H), 2.95 (s, 3H), 2.84 (s, 3H), 2.05-1.92 (m, 5H); ^{13}C NMR (100 MHz, CDCl$_3$) δ 171.06, 170.51, 139.12, 138.88, 134.17, 133.90, 129.61, 129.45, 128.07, 128.03, 53.89, 53.13, 48.96, 45.74, 36.14, 33.06, 21.90, 21.59, 21.37, 20.71. HRMS (ESI) *m/z* calcd for $C_{12}H_{18}NO_3S$ (M+H)$^+$ 256.1002, found 256.1008
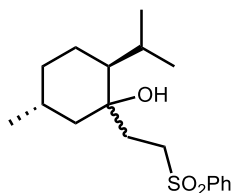
(2S,5R)-2-Isopropyl-5-methyl-1-(2-(phenylsulfonyl)ethyl)cyclohexanol (2.78)

^{1}H NMR (400 MHz, CDCl$_3$) δ 7.90-7.86 (m, 2H), 7.74-7.55 (m, 3H), 3.04-3.00 (m, 2H), 2.26-2.21 (m, 1H), 2.07-1.60 (m, 8H), 1.46-1.25 (m, 3H), 0.98 (d, *J* = 6.3 Hz, 6H), 0.92 (d, *J* = 6.9 Hz, 6H), 1.01-0.75 (m, 2H); ^{13}C NMR (100 MHz, CDCl$_3$) δ 139.19, 138.15, 134.72, 133.79, 129.87, 129.40, 128.21, 128.18, 57.69, 52.48, 52.40, 49.64, 36.36, 34.74, 34.02, 31.86, 28.21, 24.64, 24.49, 22.41. HRMS (ESI) *m/z* calcd for $C_{18}H_{29}O_3S$ (M+H)$^+$ 325.1832, found 325.1828

2.10.10 - Stern-Volmer Fluorescence Quenching Experiment

Stern-Volmer experiments were conducted on a QuantaMaster[TM] 400 Fluorometer, using a 0.3 mM solution of **Ir 2.25** (or **Ir 2.24**) in 1,2-dichloroethane and variable concentrations (0, 3.0, 6.0, 9.0 and 12.0 mM) of quencher. The samples were prepared in 3.0 mL quartz cuvettes equipped with PTFE stoppers, purged with N_2 for 10 min and then sealed with Parafilm. The solutions were irradiated at 420 nm and luminescence was measured at 585 nm (**Ir 2.25**) or 469 nm (**Ir 2.24**). Linear regression of I_0/I against concentration is done in Microsoft Excel. These experiments indicated that only **Q 2.17** (or **Q 2.19**) will quench excited state of **Ir 2.25** (or **Ir 2.24**).

Rates of quenching (k_q) were determined using Stern-Volmer kinetics (eq 1).

$$I_0/I = k_q\tau_0[\text{Quencher}] \quad (1)$$

Where I_0 is the luminescence intensity without the quencher, I is the intensity with the quencher, and τ_0 is the lifetime of the photocatalyst (279 ns for **Ir 2.25**[47]and 2300 ns for **Ir 2.24**[60]).

Constant [Ir(dF(CF$_3$)ppy)$_2$(d(CF$_3$)bpy)]PF$_6$ **Ir 2.25** (0.3 mM) and varied phenyl vinyl sulfone **2.31** (0, 3.0, 6.0, 9.0 and 12.0 mM).

[**2.31**] (mM)	0	3.0	6.0	9.0	12.0
I_0/I	1.0000	1.0074	0.9954	1.026	0.9945

Ir 2.25 + 2.31
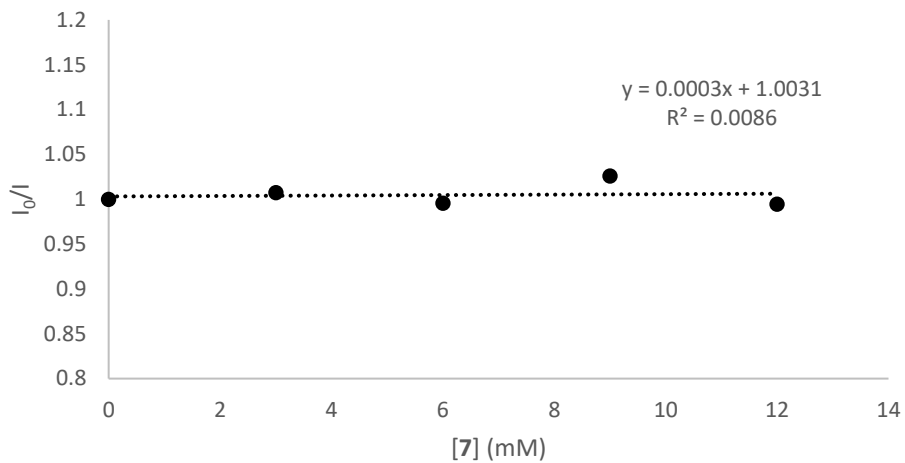
Stern-Volmer plot of $[Ir(dF(CF_3)ppy)_2(d(CF_3)bpy)]PF_6$ and variable phenyl vinyl sulfone **2.31**.

Constant $[Ir(dF(CF_3)ppy)_2(d(CF_3)bpy)]PF_6$ **Ir 2.25** (0.3 mM) and varied adamantane **2.01** (0, 3.0, 6.0, 9.0 and 12.0 mM).

[**2.01**] (mM)	0	3.0	6.0	9.0	12.0
I_0/I	1.0000	1.0176	1.0115	1.0199	1.0307

Ir 2.25 + 2.01
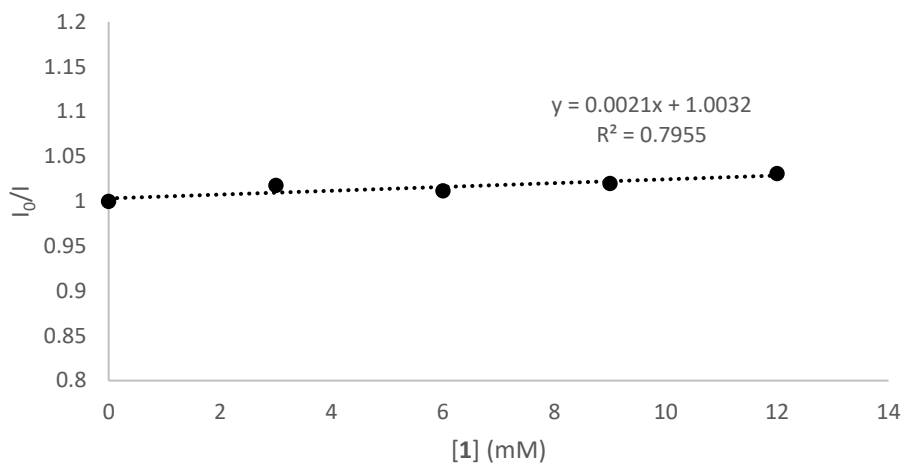
Stern-Volmer plot of $[Ir(dF(CF_3)ppy)_2(d(CF_3)bpy)]PF_6$ and variable adamantane **2.01**.

Constant $[Ir(dF(CF_3)ppy)_2(d(CF_3)bpy)]PF_6$ **Ir 2.25** (0.3 mM) and varied **Q 2.17** (0, 3.0, 6.0, 9.0 and 12.0 mM).

[**2.17**] (mM)	0	3.0	6.0	9.0	12.0
I_0/I	1.0000	2.0399	3.1498	4.4757	5.9478
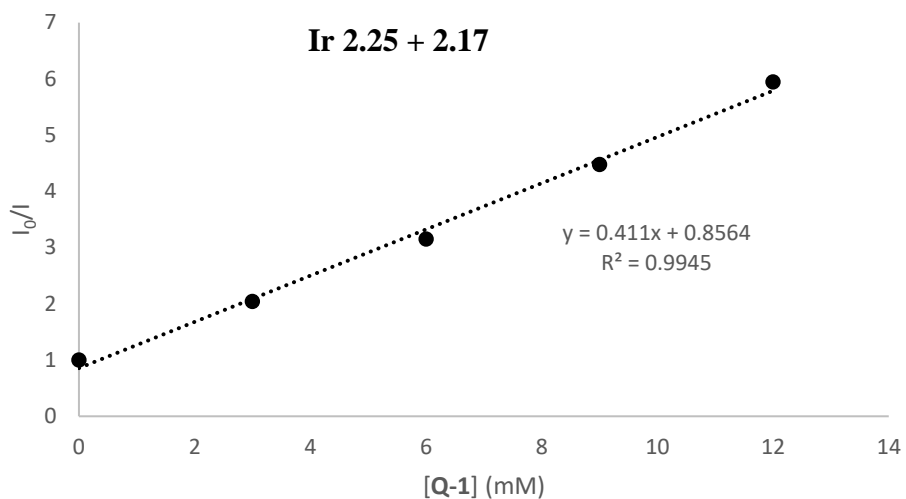
Stern-Volmer plot of $[Ir(dF(CF_3)ppy)_2(d(CF_3)bpy)]PF_6$ and variable **Q 2.17** ($k_q = 1.47 \times 10^9 \text{ M}^{-1} \text{ s}^{-1}$).

Constant $[Ir(dF(CF_3)ppy)_2(dtbbpy)]PF_6$ **Ir 2.24** (0.3 mM) and **Q 2.19** (0, 3.0, 6.0, 9.0 and 12.0 mM).

[**2.19**] (mM)	0	3.0	6.0	9.0	12.0
I_0/I	1.0000	4.3944	8.7857	12.3013	15.6163

Ir 2.24 + 2.19
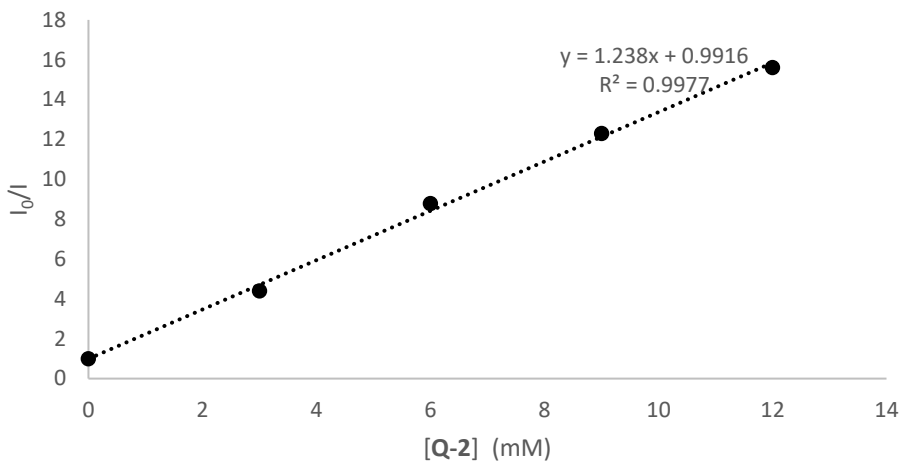
Stern-Volmer plot of $[Ir(dF(CF_3)ppy)_2(dtbbpy)]PF_6$ and variable **Q 2.19** ($kq = 5.38 \times 10^8$ $M^{-1} s^{-1}$).

2.10.11 - Cyclic voltammetry experiment

Cyclic voltammetry experiments were performed using a Pine AFP1 potentiostat. The cell consisted of a glassy carbon working electrode, a Pt wire auxiliary electrode and a Pt wire pseudo-reference electrode. All potentials are measured in a MeCN solution of tetrabutylammonium hexafluorophosphate, using the Fc/Fc+ couple as an internal standard. The data was subsequently adjusted to the saturated calomel electrode (SCE) by addition of +0.38 V[61]. The oxidative potential of quinuclidine increases with the introduction of electron-withdrawing group at 3-position of quinuclidine.

2.19
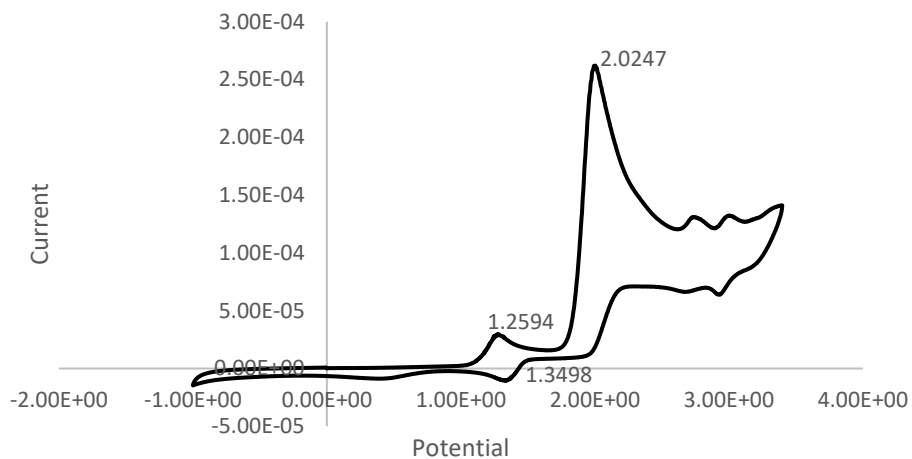
CV of **Q 2.19** ($E_{1/2}^{red}$ = +0.72 V vs Fc/Fc+ in CH_3CN; $E_{1/2}^{red}$ = +1.10 V vs SCE in CH_3CN; This value matches the literature[33]).
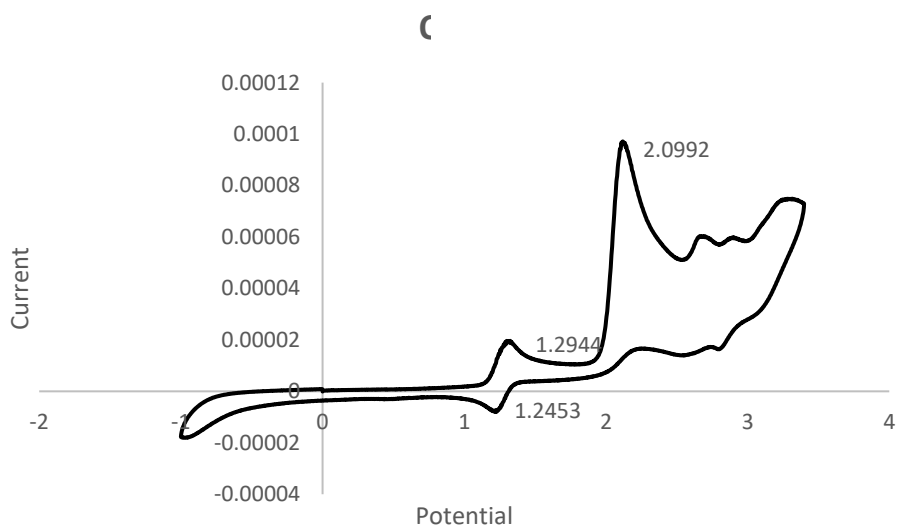
CV of **Q 2.18** ($E_{1/2}^{red}$ = +0.83 V vs Fc/Fc+ in CH_3CN; $E_{1/2}^{red}$ = +1.21 V vs SCE in CH_3CN; This value matches the literature[34]).
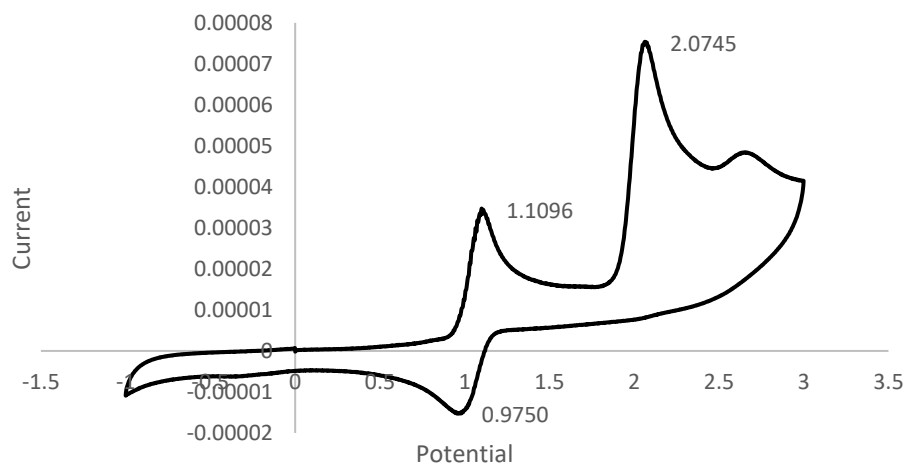
CV of **Q 2.17** ($E_{1/2}^{red}$ = +1.03 V vs Fc/Fc+ in CH_3CN; $E_{1/2}^{red}$ = +1.41 V vs SCE in CH_3CN)

2.11 - References

[1]   G. A. Mansoori, in *Adv. Chem. Phys.*, John Wiley & Sons, Ltd, **2008**, pp. 207–258.

[2]   G. H. Kruppa, J. L. Beauchamp, *J. Am. Chem. Soc.* **1986**, *108*, 2162–2169.

[3]   P. von R. Schleyer, *J. Am. Chem. Soc.* **1957**, *79*, 3292–3292.

[4]   E. I. Bagrii, A. I. Nekhaev, A. L. Maksimov, *Pet. Chem.* **2017**, *57*, 183–197.

[5]   P. R. Schreiner, N. A. Fokina, B. A. Tkachenko, H. Hausmann, M. Serafin, J. E. P. Dahl, S. Liu, R. M. K. Carlson, A. A. Fokin, *J. Org. Chem.* **2006**, *71*, 6709–6720.

[6]   H. Schwertfeger, A. A. Fokin, P. R. Schreiner, *Angew. Chem. Int. Ed.* **2008**, *47*, 1022–1036.

[7]   T. P. Stockdale, C. M. Williams, *Chem. Soc. Rev.* **2015**, *44*, 7737–7763.

[8]   L. Wanka, K. Iqbal, P. R. Schreiner, *Chem. Rev.* **2013**, *113*, 3516–3604.

[9]   "Physicochemical prediction of a brain–blood distribution profile in polycyclic amines - ScienceDirect," can be found under https://www.sciencedirect.com/science/article/pii/S0968089603003651, **n.d.**

[10] J. G. Henkel, J. T. Hane, G. Gianutsos, *J. Med. Chem.* **1982**, *25*, 51–56.

[11] U. Radhakrishnan, M. Schweiger, P. J. Stang, *Org. Lett.* **2001**, *3*, 3141–3143.

[12] Q. Li, C. Jin, P. A. Petukhov, A. V. Rukavishnikov, T. O. Zaikova, A. Phadke, D. H. LaMunyon, M. D. Lee, J. F. W. Keana, *J. Org. Chem.* **2004**, *69*, 1010–1019.

[13] Q. Fang, S. Gu, J. Zheng, Z. Zhuang, S. Qiu, Y. Yan, *Angew. Chem. Int. Ed.* **2014**, *53*, 2878–2882.

[14] K. Nasr, N. Pannier, J. V. Frangioni, W. Maison, *J. Org. Chem.* **2008**, *73*, 1056–1060.

[15] D. Beaudoin, T. Maris, J. D. Wuest, *Nat. Chem.* **2013**, *5*, 830–834.

[16] I. B. Perry, T. F. Brewer, P. J. Sarver, D. M. Schultz, D. A. DiRocco, D. W. C. MacMillan, *Nature* **2018**, *560*, 70.

[17] I. Tabushi, S. Kojo, K. Fukunishi, *J. Org. Chem.* **1978**, *43*, 2370–2374.

[18] S. Kato, T. Iwahama, S. Sakaguchi, Y. Ishii, *J. Org. Chem.* **1998**, *63*, 222–223.

[19] K. Fukunishi, I. Tabushi, *Synthesis* **1988**, *1988*, 826–827.

[20] A. M. González-Cameno, M. Mella, M. Fagnoni, A. Albini, *J. Org. Chem.* **2000**, *65*, 297–303.

[21] G. Campari, M. Fagnoni, M. Mella, A. Albini, *Tetrahedron Asymmetry* **2000**, *11*, 1891–1906.

[22] B. A. Arndtsen, R. G. Bergman, T. A. Mobley, T. H. Peterson, *Acc. Chem. Res.* **1995**, *28*, 154–162.

[23] J. F. Hartwig, M. A. Larsen, *ACS Cent. Sci.* **2016**, *2*, 281–292.

[24] A. E. Shilov, G. B. Shul'pin, *Chem. Rev.* **1997**, *97*, 2879–2932.

[25] W. R. Gutekunst, P. S. Baran, *Chem. Soc. Rev.* **2011**, *40*, 1976–1991.

[26] S. J. Pastine, D. V. Gribkov, D. Sames, *J. Am. Chem. Soc.* **2006**, *128*, 14220–14221.

[27] K. M. Engle, T.-S. Mei, M. Wasa, J.-Q. Yu, *Acc. Chem. Res.* **2012**, *45*, 788–802.

[28] J. He, S. Li, Y. Deng, H. Fu, B. N. Laforteza, J. E. Spangler, A. Homs, J.-Q. Yu, *Science* **2014**, *343*, 1216–1220.

[29] R. Hrdina, *Synthesis* **2019**, *51*, 629–642.

[30] T. Newhouse, P. S. Baran, *Angew. Chem. Int. Ed.* **2011**, *50*, 3362–3374.

[31] H.-B. Yang, A. Feceu, D. B. C. Martin, *ACS Catal.* **2019**, *9*, 5708–5715.

[32] I. Tabushi, S. Kojo, P. v R. Schleyer, T. M. Gund, *J. Chem. Soc. Chem. Commun.* **1974**, 591–591.

[33] J. L. Jeffrey, J. A. Terrett, D. W. C. MacMillan, *Science* **2015**, *349*, 1532–1536.

[34] M. H. Shaw, V. W. Shurtleff, J. A. Terrett, J. D. Cuthbertson, D. W. C. MacMillan, *Science* **2016**, *352*, 1304–1308.

[35] C. Le, Y. Liang, R. W. Evans, X. Li, D. W. C. MacMillan, *Nature* **2017**, *547*, 79–83.

[36] X. Zhang, D. W. C. MacMillan, *J. Am. Chem. Soc.* **2017**, *139*, 11353–11356.

[37] K. L. Skubi, T. R. Blum, T. P. Yoon, *Chem. Rev.* **2016**, *116*, 10035–10074.

[38] K. A. Margrey, W. L. Czaplyski, D. A. Nicewicz, E. J. Alexanian, *J. Am. Chem. Soc.* **2018**, *140*, 4213–4217.

[39] S. Mukherjee, B. Maji, A. Tlahuext-Aca, F. Glorius, *J. Am. Chem. Soc.* **2016**, *138*, 16200–16203.

[40] A. Kolocouris, K. Dimas, C. Pannecouque, M. Witvrouw, G. B. Foscolos, G. Stamatiou, G. Fytas, G. Zoidis, N. Kolocouris, G. Andrei, et al., *Bioorg. Med. Chem. Lett.* **2002**, *12*, 723–727.

[41] N. V. Makarova, M. N. Zemtsova, I. K. Moiseev, A. A. Ozerov, V. I. Petrov, I. A. Grigor'ev, *Pharm. Chem. J.* **2000**, *34*, 293–296.

[42] I. Tabushi, Y. Aoyama, *J. Org. Chem.* **1973**, *38*, 3447–3454.

[43] A. A. Fokin, P. A. Gunchenko, A. A. Novikovsky, T. E. Shubina, B. V. Chernyaev, J. E. P. Dahl, R. M. K. Carlson, A. G. Yurchenko, P. R. Schreiner, *Eur. J. Org. Chem.* **2009**, *2009*, 5153–5161.

[44] "Redesign of a Pyrylium Photoredox Catalyst and Its Application to the Generation of Carbonyl Ylides," can be found under https://pubs.acs.org/doi/pdf/10.1021/acs.orglett.7b01222, **n.d.**

[45] M. A. Miranda, H. Garcia, *Chem. Rev.* **1994**, *94*, 1063–1089.

[46] D. A. Nicewicz, D. W. C. MacMillan, *Science* **2008**, *322*, 77–80.

[47] G. J. Choi, Q. Zhu, D. C. Miller, C. J. Gu, R. R. Knowles, *Nature* **2016**, *539*, 268–271.

[48] M. S. Lowry, W. R. Hudson, R. A. Pascal, S. Bernhard, *J. Am. Chem. Soc.* **2004**, *126*, 14129–14135.

[49] V. K. Aggarwal, I. Emme, S. Y. Fulford, *J. Org. Chem.* **2003**, *68*, 692–700.

[50] N. P. Ramirez, J. C. Gonzalez-Gomez, *Eur. J. Org. Chem.* **2017**, *2017*, 2154–2163.

[51] F. Recupero, A. Bravo, H.-R. Bjørsvik, F. Fontana, F. Minisci, M. Piredda, *J. Chem. Soc. Perkin Trans. 2* **1997**, *0*, 2399–2406.

[52] D. H. R. Barton, J. Boivin, E. Crépon (née da Silva), J. Sarma, H. Togo, S. Z. Zaid, *Tetrahedron* **1991**, *47*, 7091–7108.

[53] G. A. Olah, P. Ramaiah, C. B. Rao, G. Sandford, R. Golam, N. J. Trivedi, J. A. Olah, *J. Am. Chem. Soc.* **1993**, *115*, 7246–7249.

[54] J. L. Roizen, D. N. Zalatan, J. Du Bois, *Angew. Chem. Int. Ed.* **2013**, *52*, 11343–11346.

[55] S. Sumino, I. Ryu, *Org. Lett.* **2016**, *18*, 52–55.

[56] B. K. Peters, T. Zhou, J. Rujirawanich, A. Cadu, T. Singh, W. Rabten, S. Kerdphon, P. G. Andersson, *J. Am. Chem. Soc.* **2014**, *136*, 16557–16562.

[57] X.-Z. Fan, J.-W. Rong, H.-L. Wu, Q. Zhou, H.-P. Deng, J. D. Tan, C.-W. Xue, L.-Z. Wu, H.-R. Tao, J. Wu, *Angew. Chem. Int. Ed.* **2018**, *57*, 8514–8518.

[58] N. Shapiro, M. Kramer, I. Goldberg, A. Vigalok, *Green Chem.* **2010**, *12*, 582–584.

[59] "Comprehensive Handbook of Chemical Bond Energies," can be found under https://www.crcpress.com/Comprehensive-Handbook-of-Chemical-Bond-Energies/Luo/p/book/9780849373664, **n.d.**

[60] M. S. Lowry, J. I. Goldsmith, J. D. Slinker, R. Rohl, R. A. Pascal, G. G. Malliaras, S. Bernhard, *Chem. Mater.* **2005**, *17*, 5712–5719.

[61] N. G. Connelly, W. E. Geiger, *Chem. Rev.* **1996**, *96*, 877–910.

Chapter 3 - Total Synthesis of Earthworm Metabolite Malylglutamate

3.1 - Introduction

Soil health can be negatively affected by factors such as pesticides, pollutants and other soil contaminants and they must be monitored closely to avoid serious environmental damage. By studying the metabolism of earthworms, it is possible to monitor ecotoxicity and ecological stress.[1] Recently, Larive *et. al*[2] studied the metabolic material in earthworm coelomic fluid, coelomocytes, and tissue from the species *Eisenia fetida* using NMR spectroscopy and high-resolution MS/MS. Fifty-nine metabolites, with some shown in Figure 3.1, were identified from the earthworm species and one newly discovered metabolite, known as malylglutamate (**3.01**, Figure 3.1). Due to the current limited scope of NMR-based metabolic profiling for earthworms, this new metabolite was further studied to expand the utility of this approach and also to investigate the metabolites' association with environmental stress. Malylglutamate is hypothesized to be a store for glutamic acid and malic acid, and may also be involved in chelation due to its similarity in structure to β-citrylglutamate **3.03**, a known chelator.[3,4] It is a relatively abundant metabolite, present at an average of 7 µg/mg in whole-earthworm extracts, and is similar in structure to metabolites like *N*-acetylaspartylglutamate (NAAG) **3.02.**

α-malylglutamate (3.01)
(reported structure)

N-acetylaspartylglutamate (3.02)
(NAAG)

β-citrylglutamate (3.03)

trigonelline (3.04)
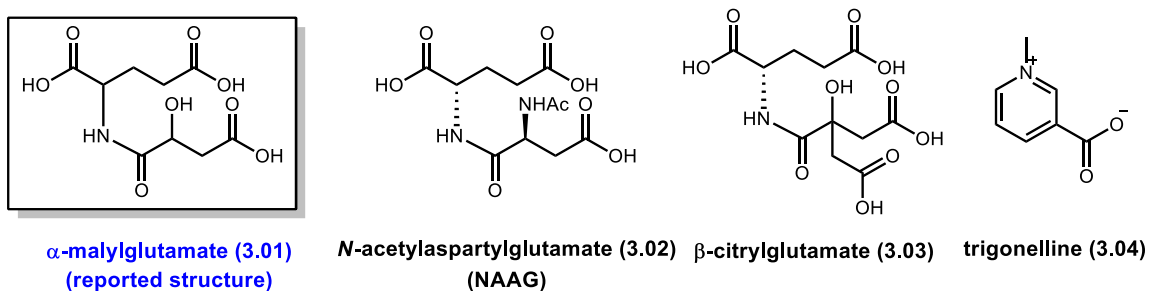
Figure 3.1 Proposed malylglutamate structure and other discovered metabolites

Malylglutamate is prominent in the NMR metabolite profiles of earthworm coelomic fluid and coelomocyte extracts. Coelomic fluid is a biofluid that fills the body cavity of the worm and is critical for movement, excretion, metabolism, and nutrient storage, while coelomocytes are free-moving immune and liver-like cells in the coelomic fluid.[2] Malyglutamate is a suggested anionic osmolyte, acting as a charge-balance counterpart to betaine analogs in earthworms, which are known cationic osmolytes and helps provide electrolyte balance in earthworms.[5] Due to the difficulty in isolating a pure naturally sourced sample and the complexity of the NMR spectra of the earthworm, we sought to confirm the proposed structure **3.01** and fully assign the relative and absolute configuration of malylglutamate synthetically.

3.2 - Results and Discussion

3.2.1 - Retrosynthesis of Originally Proposed Structure

The proposed structure of malylglutamate possesses two chiral centers thus all diastereomeric and enantiomeric possibilities must be carefully considered and controlled. We envisioned the synthesis of malylglutamate to involve a traditional peptide coupling as the key step where both enantiopure L- and D-isomers of the corresponding amino acid starting materials can be incorporated. The retrosynthetic plan for the proposed structure is shown in Scheme 3.1. Beginning with the reported target molecule **3.01**, we propose it is derived from a fully benzylated intermediate **3.05** which is subjected to a global deprotection by hydrogenolysis. This is followed by a peptide coupling reaction (main disconnection shown in Scheme 3.1) between di-benzylated glutamic acid **3.06** and mono-benzylated malic acid **3.08**. A Fischer esterification of L- and D-glutamic acid **3.07** with

benzyl alcohol gives the double protected intermediate as the tosylate salt. The malic acid

intermediate is obtained after selective mono-benzylation. With this plan in hand, we set

out for the initial synthesis.
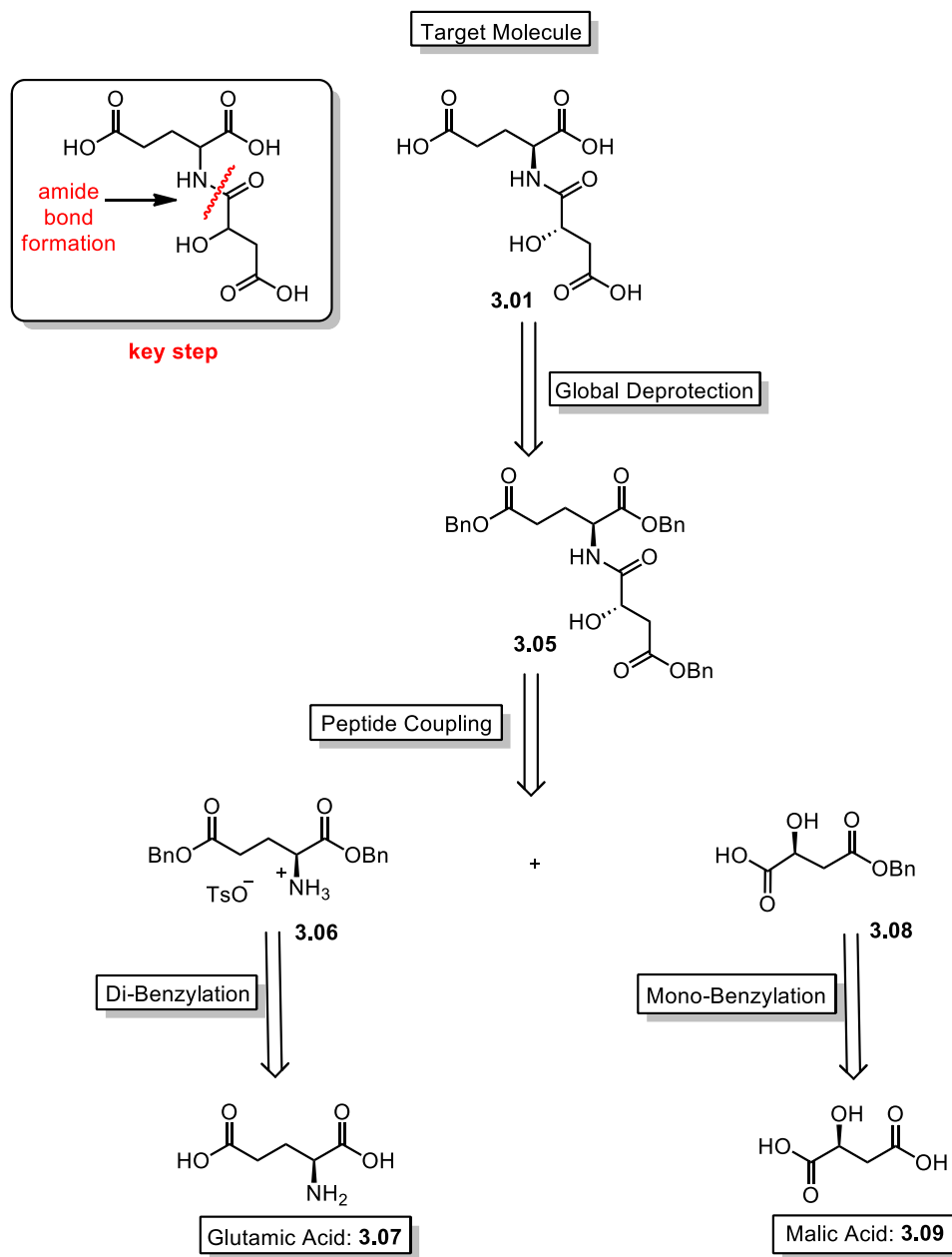
Scheme 3.1 Retrosynthesis of proposed structure

3.2.2 - Synthesis and Optimization of Proposed Metabolite

We began the synthesis with an acid catalyzed benzylation of both L- and D-isomers

of glutamic acid **3.07** using 2.0 equivalents of benzyl alcohol in toluene to give the doubly

protected tosylate salts in good yields (**3.06** and **3.06'**, Scheme 3.2Scheme 3.2).[6] We then

focused our attention on selectively mono-protecting the L-malic acid isomer **3.09** using

2,2-dimethoxypropane and *p*-toluenesulfonic acid. Fortunately, we were able to selectively

protect malic acid in good yields preferentially giving the desired five membered acetonide

protected product **3.10** over the six.[7] This was followed by a benzylation of the free acid

to give protected intermediate **3.11** in an 86% yield. Selective hydrolysis of the acetonide

intermediate **3.11** with a 3:1 ratio of acetic acid and water gave the mono-benzyl ester **3.12**

in 79% yield.
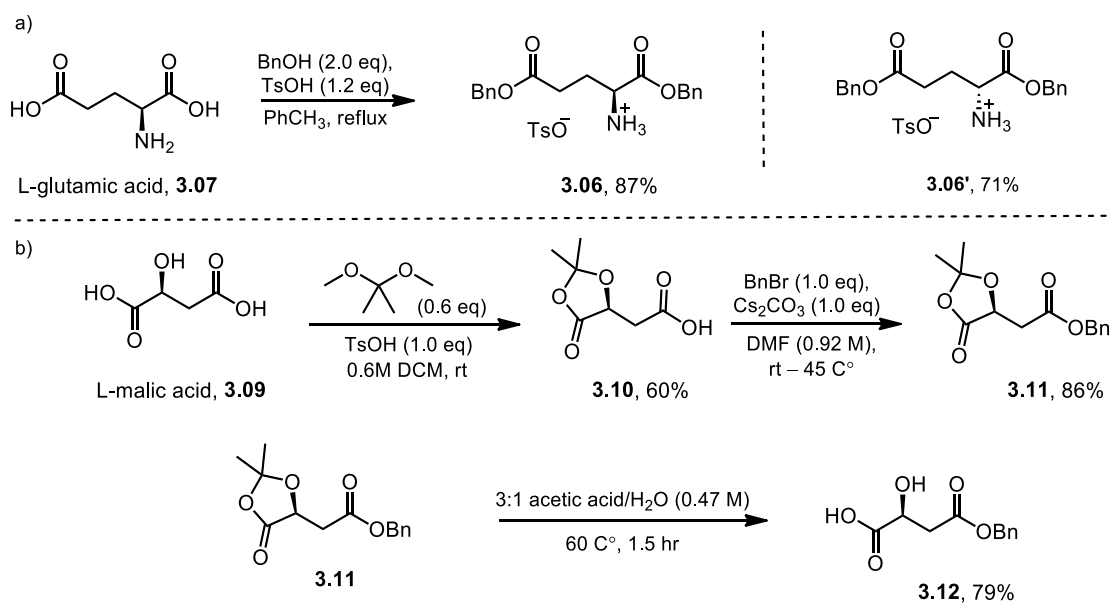
Scheme 3.2 Benzylation of amino acid starting materials

With both benzylated intermediates in hand, **3.06** and **3.12**, we investigated different known peptide coupling conditions shown in Table 3.1. Ye *et. al.* used *N,N,N′,N′*-tetramethylchloroformamidinium hexafluorophosphate (TCFH) and *N*-methylimidazole (NMI) as a mild method for in situ generation of highly reactive acyl imidazoliums which can then be used to make peptide bonds in high yields.[8] We attempted the peptide coupling reaction using TCFH with and without the imidazole. No reaction was observed in the absence of NMI, however with both TCFH and NMI, the reaction proceeded in a modest 51% yield. Commonly used coupling reagents, such as DIC and DCC, were tested with HOBT; however, only low yields were obtained. When using HCTU as a coupling reagent the yield increased slightly to 32%. Ultimately, using both EDCI and HOBT in the presence of Et$_3$N gave the desired fully benzylated amide **3.05** in an acceptable 73% yield.

Table 3.1 Optimization of peptide coupling reaction
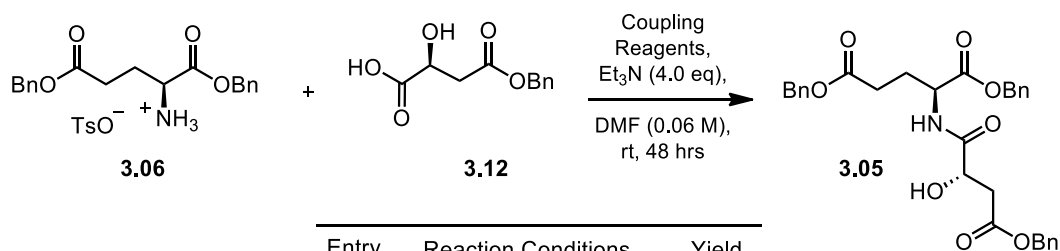
Entry	Reaction Conditions	Yield
a	TCFH	0
b	TCFH + NMI	51
c	DCC + HOBT	5
d	DIC +HOBT	13
e	EDCI + HCTU	32
f	EDCI + HOBT	73

138
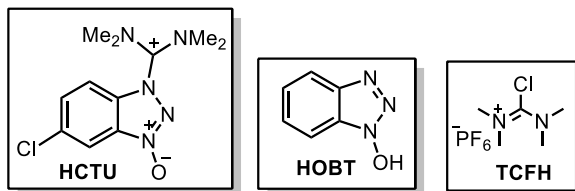
Following the peptide coupling reaction, global deprotection of the fully benzylated species **3.05** using hydrogen and palladium on carbon gave the proposed malylglutamate **3.01** in good yields (Scheme 3.3). Deprotection of each ester was monitored conveniently by mass spectrometry. Initially, 5.0 mol% of Pd/C in various solvents were tested however optimal conditions involved 10 mol% Pd/C in degassed ethanol and required no further purification. Both L, L- and L,D -malylglutamate were synthesized in 73% and 71% yields, respectively.
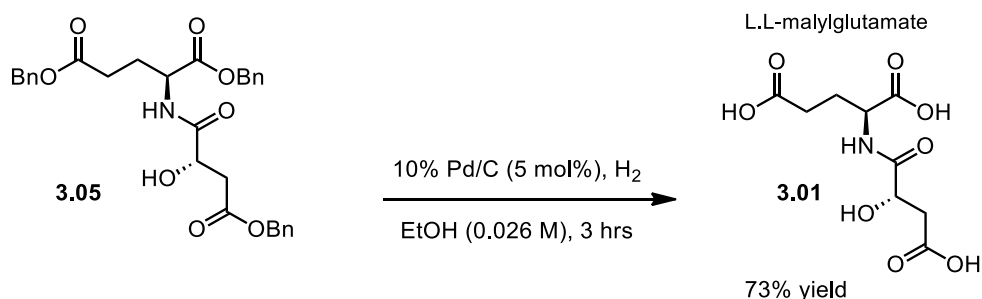
Scheme 3.3 Hydrogenation of fully benzylated compound

Once synthesized and isolated, the proton NMR of both synthetic samples and the natural samples were compared in D_2O as the deuterated solvent. Unfortunately, neither synthetic compounds matched that of the natural one. Based on NMR studies performed by our collaborator, Dr. Corey Griffith, the glutamate carbonyl peaks showed the correct assignment however the malyl moiety of the synthetic samples did not correspond to the natural samples. This indicated that the malyl moiety is possibly attached to the glutamate in the β position as opposed to the proposed α position. Based on the NMR data, a similar yet alternative structure was proposed, compound **3.15**. This revised structure was

therefore synthesized using a different protecting group strategy for both malic acid isomers (Scheme 3.4).

3.2.3 - Synthesis of Both Diastereomers of Revised Malylglutamate

Although the glutamate moiety remained the same in the revised synthesis, the α-hydroxy acid of malic acid now needed to be mono-benzylated instead of the β-hydroxy acid as was done previously. Selective benzylation of the β-hydroxy acid **3.13** was achieved using a known procedure with trifluoroacetic acid and benzyl alcohol (Scheme 3.4).[9] This was followed by a peptide coupling to give the fully benzylated intermediates **3.14** and finally deprotection of the benzyl groups to give **3.15**, similar to the procedures for the synthesis of the first proposed structure. Purification of the intermediates proved to be easier in these cases most likely due to the reduced steric hindrance of the hydroxyl group.

Both the L,L- and D,L - malylglutamate isomers were synthesized and used for comparison with the natural product. The natural sample was once again spiked against both isomers of malylglutamate in D_2O. With the revised synthesis, the synthetic L,L-malylglutamate **3.15** isomer matched in chemical shift and *J*-coupling. Comparisons of the natural sample, synthetic sample and spiked samples are shown in Figure 3.2. Once synthesized and confirmed, the absolute configuration of L,L-malylglutamate was determined using liquid chromatography-mass spectrometry (LC-MS) via a chiral phase chromatography method. This method allowed for excellent separation of the L,L- and D,D-isomers. Finally, the specific rotation of synthetic L,L-malylglutamate was determined to be $[\alpha]^{25}_D$ -13.6 (c 1.0, MeOH) establishing the correct natural product to be (-)-β-L-malyl-L-glutamate.
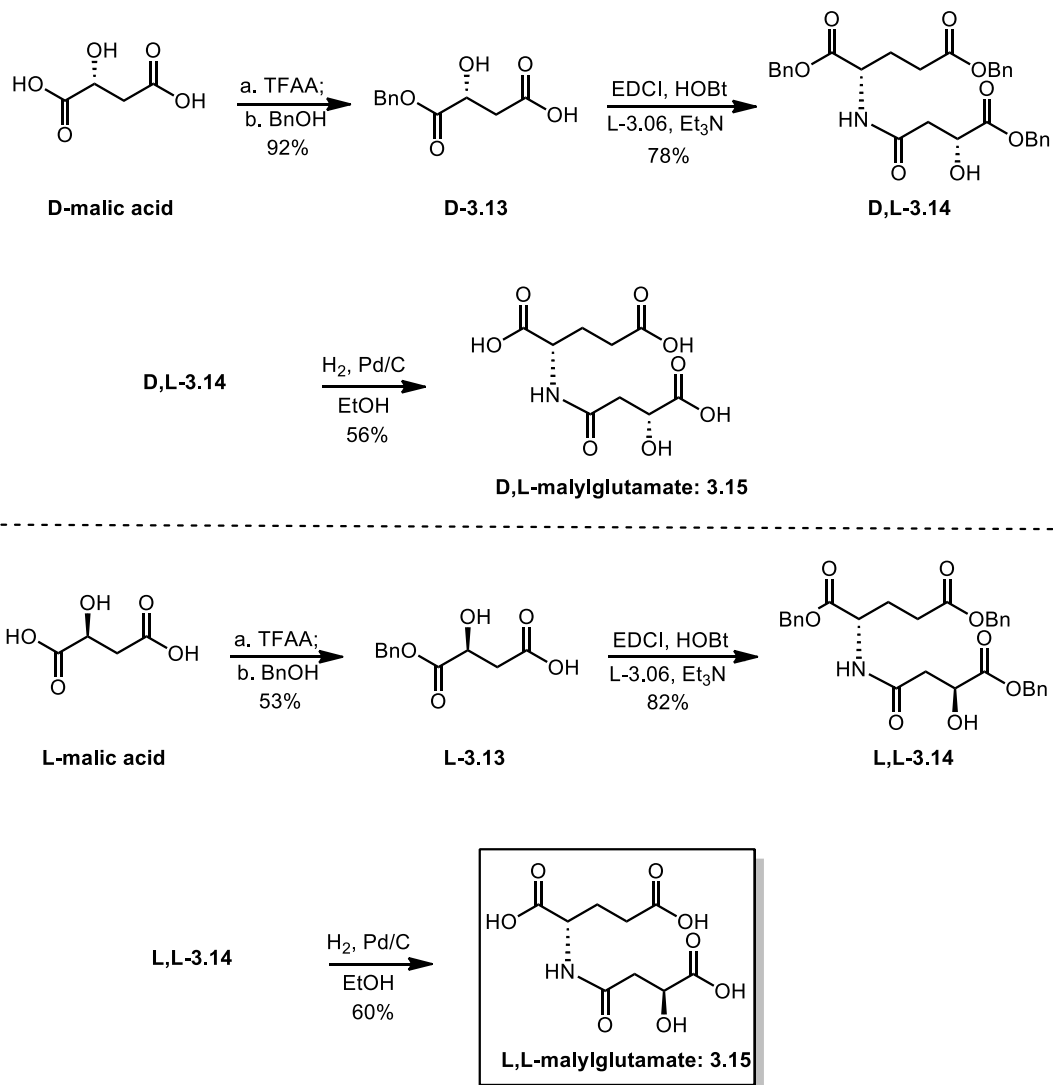
Scheme 3.4 Alternative synthesis of malylglutamate
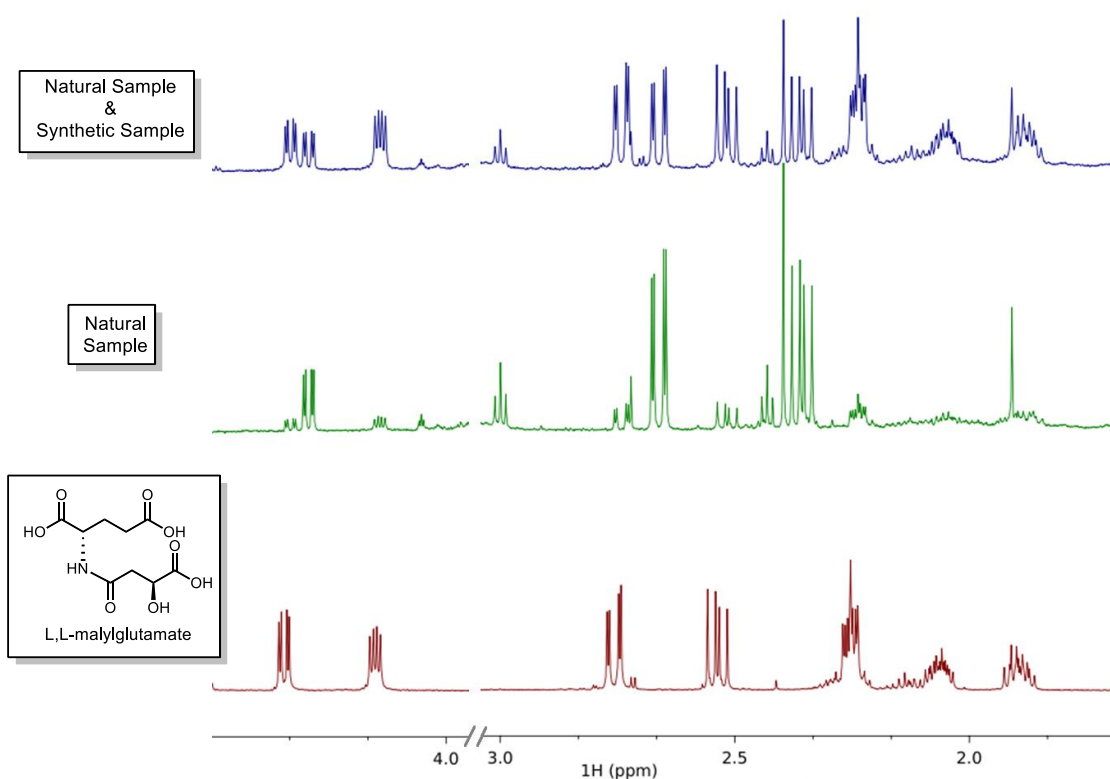
Figure 3.2 NMR's of natural and synthetic samples

3.3 - Conclusion

The synthesis of the metabolite from the earthworm species *Eisenia Fetida*, malylglutamate, was of interest due to the correlation between earthworm metabolites and ecological stress. The synthesis of the metabolite involved selective benzylations, a key peptide coupling and a hydrogenation of a fully benzylated intermediate. The initial synthesis of both stereoisomers of the proposed structure proved to be incorrect once compared and spiked with the natural sample. An alternative synthesis was devised and was similar to that of the first synthesis but involved selective benzylation of the opposite carboxylic acid in the amino acid malic acid. Reaction conditions for the peptide coupling and hydrogenation remained the same. Both isomers L,L- D,L-malylglutamate were

142

synthesized leading to a total of four proposed isomers of malylglutamate to be synthesized (Figure 3.3). When the samples were compared to the natural sample and both the absolute configuration and optical rotation were determined, the correct isomer of the natural product was (-)-β-L-malyl-L-glutamate.
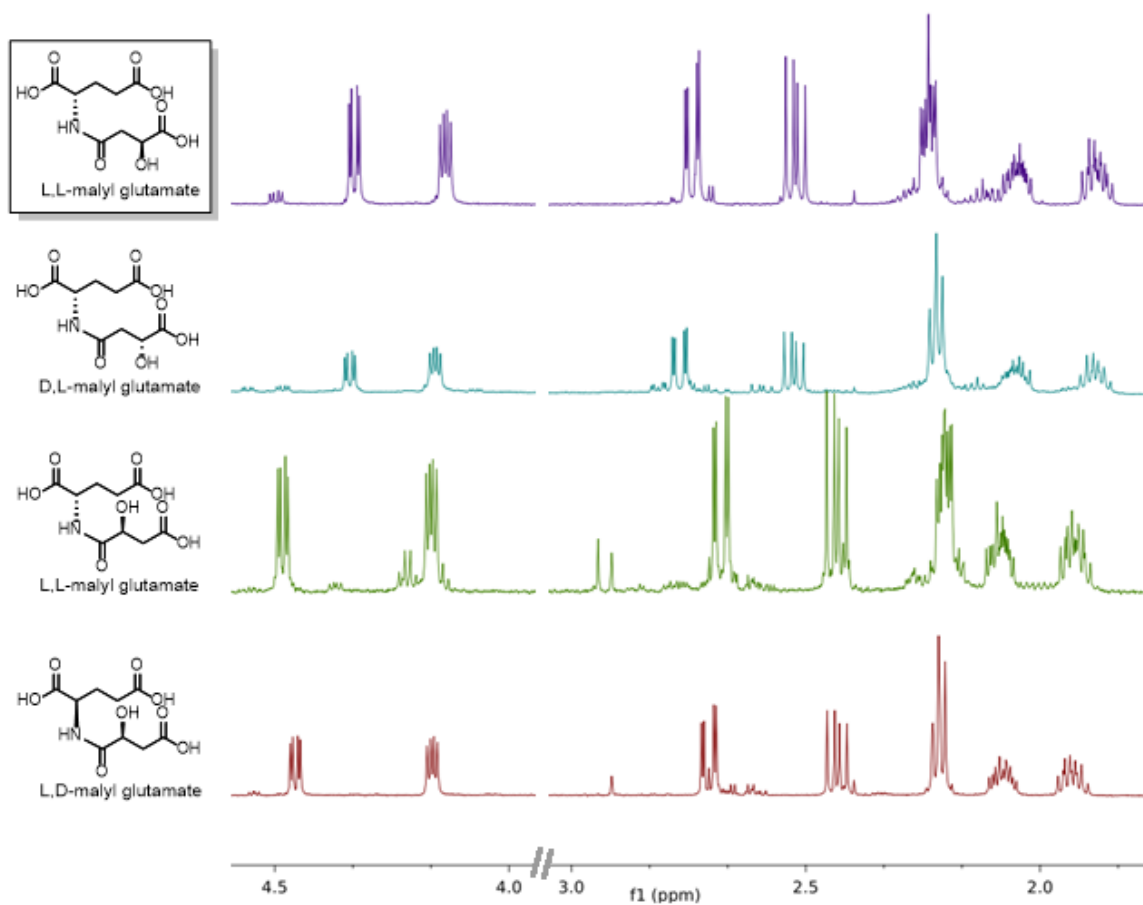
Figure 3.3. NMR's of synthesized malylglutamate

3.4 - Experimental Section

3.4.1 - Materials and Methods

All reactions were carried out under an inert atmosphere of nitrogen in oven dried or flame dried glassware with magnetic stirring, unless otherwise noted. Solvents were dried by passage through columns of activated alumina. All starting materials were prepared according to known literature procedures or used as obtained from commercial sources, unless otherwise indicated. Reactions were monitored by thin-layer chromatography (TLC) and carried out on 0.25 mm coated commercial silica gel plates (Analtech TLC Uniplates, F_{254} precoated glass plates with organic fluorescent binder) using UV light as visualizing agent and $KMnO_4$ and heat as a developing agent. Flash chromatography was performed on silica gel (Silicycle, SiliaFlash P60, 230-400 mesh). Hydrogenation was monitored using Mass Spectrometry

3.4.2 - Synthesis and Characterization of Benzylated Compounds

General Procedure for Peptide Coupling Reactions (A): To a flame dried flask equipped with a magnetic stir bar were sequentially added acid (1.0 eq), amine (1.2 eq), HOBT (1.2 eq), EDCI (2.0 eq) and DMF (60 mM). The vial was sealed with a septum and degassed. The reaction mixture was stirred for 10 minutes followed by addition of Et_3N (4.0 eq) dropwise. The reaction was stirred for 24 hours followed by extraction with EtOAc and dried over Na_2SO_4. The solvent was removed in vacuo and the crude residue was purified using silica gel chromatography to provide benzylated products as a white solid.
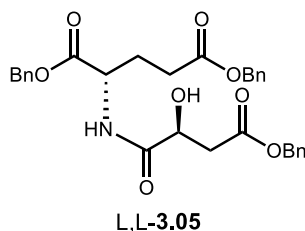
L,L-**3.05**

(*S*)-Dibenzyl 2-(((*S*)-4-(benzyloxy)-2-hydroxy-4-oxobutanamido)pentanedioate (3.05)

Prepared according to General Procedure A using acid **L-3.12** (22 mg, 0.10 mmol) and amine **L-3.06** (60 mg, 0.12 mmol) as the substrates. Reaction time: 24 h. The crude residue was purified by column chromatography on silica gel using EtOAc to afford **L,L-3.05** as a white solid (22 mg, 42% yield). IR (film) 3388, 3063, 3032, 1735, 1731 cm^{-1}; ^{1}H NMR (400 MHz, CDCl$_3$) δ 1.98-2.10 (m, 1H), 2.20-2.34 (m, 1H), 2.35-2.50 (m, 2H), 2.82 (dd, *J* = 7.88, 17.44 Hz, 1H), 2.94 (dd, *J* = 3.88, 17.48 Hz, 1H), 3.60-3.66 (m, 1H), 4.40-4.42 (m, 1H), 4.64-4.72 (M, 1H), 5.10 (s, 2H), 5.13 (s, 2H), 5.16 (s, 2H), 7.27-7.39 (m, 15H); ^{13}C NMR (100 MHz, CDCl$_3$) δ 172.6, 172.4, 172.2, 171.4, 135.9, 135.4, 135.3, 133.9, 128.8, 128.7, 128.7, 128.6, 128.5, 128.4, 128.4, 77.5, 77.2, 76.9, 72.2, 68.6, 67.5, 67.5, 67.0, 66.7, 51.6, 38.8, 38.4, 30.3, 29.3, 27.4, 27.3; HRMS (ESI) *m/z* calcd. for C$_{30}$H$_{32}$NO$_8$ (M+H)$^+$ 534.2122, found 534.2140.

L,D-**3.05**
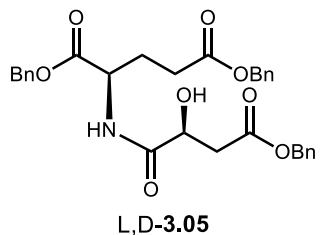
(*R*)-Dibenzyl 2-((*S*)-4-(benzyloxy)-2-hydroxy-4-oxobutanamido)pentanedioate (3.05)

Prepared according to General Procedure A using acid **L-3.12** (100 mg, 0.446 mmol) and amine **D-3.06** (267 mg, 0.535 mmol). Reaction time: 24 h. The crude residue was purified by column chromatography on silica gel with EtOAc to afford **L,D-3.05** as a white solid (63 mg, 26% yield). IR (film) 3389, 3033, 2948, 1731, 1715 cm^{-1}; ^{1}H NMR (400 MHz, CDCl$_3$) δ 2.00-2.10 (m, 1H), 2.20-2.33 (m, 1H), 2.35-2.50 (m, 2H), 2.74 (dd, *J* = 8.72, 17.44 Hz, 1H), 2.94 (dd, *J* = 3.6, 17.56 Hz, 1H), 3.65 (d, *J* = 4.92 Hz, 1H), 4.40-4.48 (m, 1H), 4.62-4.72 (m, 1H), 5.09 (s, 2H), 5.15 (s, 2H), 5.16 (s, 2H), 7.28-7.40 (m, 15H); ^{13}C NMR (100 MHz, CDCl$_3$) δ 172.6, 172.0, 171.4, 164.9, 138.6, 135.9, 135.4, 133.9, 128.8, 128.7, 128.7, 128.6, 128.5, 128.5, 128.4, 128.0, 127.8, 77.5, 77.2, 76.9, 72.3, 68.6, 67.6, 67.3, 67.1, 66.7, 51.6, 38.3, 29.9, 27.4; HRMS (ESI) *m/z* calcd. for C$_{30}$H$_{32}$NO$_8$ (M+H)$^+$ 534.2122, found 534.2137.

146

L,L-**3.14**
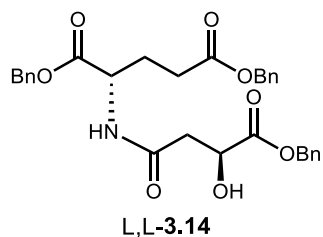
(*S*)-Dibenzyl 2-((*S*)-4-(benzyloxy)-3-hydroxy-4-oxobutanamido)pentanedioate

(3.14)

Prepared according to General Procedure A using acid **L-3.13** (500 mg, 2.23 mmol) and amine **L-3.06** (1.34 g, 2.67 mmol). Reaction time: 24 h. The crude residue was purified by column chromatography on silica gel using EtOAc to afford **L,L-3.14** as a white solid (868 mg, 73% yield). IR (film) 3360, 2915, 1745, 1715, 1170 cm^{-1}; ^{1}H NMR (400 MHz, CDCl$_3$) δ 1.94-2.06 (m, 1H), 2.16-2.27 (m, 1H), 2.33-2.48 (m, 1H), 2.62 (dd, J = 7.16, 15.32 Hz, 1H), 2.72 (dd, J = 3.68, 15.32 Hz, 1H), 3.61 (bs, 1H), 4.50 (dd, J = 3.72, 7.12 Hz, 1H), 4.63-4.70 (m, 1H), 5.09 (s, 2H), 5.15 (s, 2H), 5.20 (s, 2H), 6.56 (d, J = 7.84, 1H), 7.28-7.39 (m, 15H); ^{13}C NMR (100 MHz, CDCl$_3$) δ 173.3, 172.8, 171.6, 170.0, 135.8, 135.2, 128.8, 128.7, 128.7, 128.6, 128.5, 128.5, 77.5, 77.2, 67.9, 67.8, 67.8, 67.6, 66.7, 51.9, 40.0, 31.0, 30.3, 27.3; HRMS (ESI) *m/z* calcd. for C$_{30}$H$_{32}$NO$_8$ (M+H)$^+$ 534.2122, found 534.2119.

D,L-**3.14**
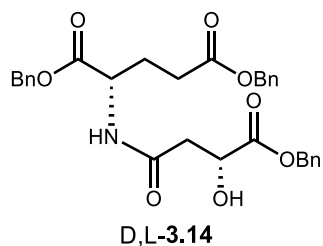
(*S*)-Dibenzyl 2-((*R*)-4-(benzyloxy)-3-hydroxy-4-

oxobutanamido)pentanedioate (3.14)

Prepared according to General Procedure A using acid **D-3.13** (400 mg, 1.78 mmol) and amine **L-3.06** (1.07 g, 2.14 mmol). Reaction time: 24 h. The crude residue was purified by column chromatography on silica gel EtOAc to afford **D,L-3.14** as a white solid (683 mg, 72% yield). IR (film) 3352, 3065, 2853, 1733 cm^{-1}; ^{1}H NMR (400 MHz, CDCl$_3$) δ 1.94-2.06 (m, 1H), 2.16-2.28 (m, 1H), 2.32-2.48 (m, 2H), 2.63 (dd, *J* = 7.12, 15.28 Hz, 1H), 2.72 (dd, *J* = 3.72, 15.32 Hz, 1H), 3.55 (d, *J* = 5.52 Hz, 1H), 4.47-4.53 (m, 1H), 4.62-4.70 (m, 1H), 5.09 (s, 2H), 5.15 (s, 2H), 5.21 (s, 2H), 6.53 (d, *J* = 7.92 Hz, 1H), 7.30-7.39 (m, 15H); ^{13}C NMR (100 MHz, CDCl$_3$) δ 177.7, 173.3, 172.3, 170.4, 135.5, 135.1, 128.70, 128.6, 128.5, 128.4, 128.4, 128.3, 77.5, 77.3, 76.9, 67.7, 67.4, 66.8, 66.8, 51.8, 38.8, 30.8, 30.2, 27.2, 23.5; HRMS (ESI) *m/z* calcd. for C$_{30}$H$_{32}$NO$_8$ (M+H)$^+$ 534.2122, found 534.2130.

3.4.3 - Synthesis and Characterization of Natural Products

General Procedure for Hydrogenolysis (B): To a flame dried flask equipped with a magnetic stir bar were sequentially added fully benzylated precursor and Pd/C (10%, 5.0 mol%). The vial was sealed with a septum and pumped and back filled 3 times with nitrogen. This was followed by addition of dry ethanol (0.026 M) and careful addition of H_2 via balloon. The reaction mixture was stirred for 6 hours and then filtered through celite with DCM. Solvent was removed in vacuo without further purification.
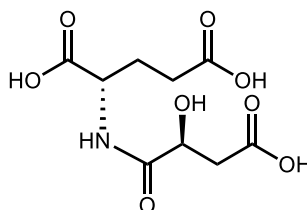
L,L-malylglutamate: **3.01**

(*S*)-2-((*S*)-3-Carboxy-2-hydroxypropanamido)pentanedioic acid (3.01)

Prepared according to General Procedure B using **L,L-3.05** (126 mg, 0.236 mmol) to afford **LL-3.01** as a white solid (46 mg, 73% yield). IR (film) 3396, 2844, 1710, 1450, 1361 cm^{-1}; ^{1}H NMR (400 MHz, D$_2$O) δ 4.58 (dd, *J* = 4.0, 8.0 Hz, 1H), 4.47 (dd, *J* = 4.0, 8.0 Hz, 1H), 2.90 (dd, *J* = 4.0, 16 Hz, 1H), 2.79 (dd, *J* = 4.0, 16 Hz), 2.50 (t, *J* = 8.0 Hz, 2 H), 2.22-2.32 (m, 1H), 2.00-2.12, (m, 1H); ^{13}C NMR (100 MHz, D$_2$O) δ 177.1, 176.8, 174.6, 71.4, 66.9, 38.5, 28.7; HRMS (ESI) *m/z* calcd. for C$_9$H$_{14}$NO$_8$ (M+H)$^+$ 264.0714, found 264.0710.
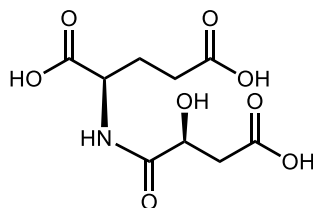
L,D-malylglutamate: **3.01**

(*R*)-2-((*S*)-3-Carboxy-2-hydroxypropanamido)pentanedioic acid (3.01)

Prepared according to General Procedure B using **L,L-3.05**(63 mg, 0.118 mmol) to afford **LL-3.01** (22 mg, 71% yield). IR (film) 3396, 2844, 1710, 1450, 1361, cm[-1]; ^{1}H NMR (400 MHz, D$_2$O) δ 4.57 (dd, *J* = 4.0, 8.0 Hz, 1H), 4.48 (dd, *J* = 4.0, 8.0 Hz, 1H), 2.90 (dd, *J* = 4.0, 16 Hz, 1H), 2.77 (dd, *J* = 4.0, 16 Hz), 2.50 (t, *J* = 8.0 Hz, 2 H), 2.22-2.32 (m, 1H), 2.04-2.12, (m, 1H); ^{13}C NMR (100 MHz, D$_2$O) δ 177.1, 176.7, 174.6, 133.7, 127.1, 71.4, 66.9, 38.6, 28.8; HRMS (ESI) *m/z* calcd. for C$_9$H$_{14}$NO$_8$ (M+H)[+] 264.0714, found 264.0719
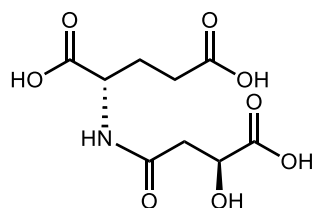
L,L-malylglutamate: **3.15**

(*S*)-2-((*S*)-3-Carboxy-3-hydroxypropanamido)pentanedioic acid (3.15)

Prepared according to General Procedure B using **L,L-3.14** (20 mg, 0.038 mmol) to afford **LL-3.15** (9 mg, 82% yield). IR (film) 3352, 3034, 1733, 1536, 1386, cm[-1]; ^{1}H NMR (400 MHz, D$_2$O) δ 4.60 (dd, *J* = 4.5, 7.8 Hz, 1H), 4.46 (dd, *J* = 4.7, 8.2 Hz, 1H), 3.20-3.33 (m, 1H), 2.82 (dd, *J* = 4.5, 15.2, 1H), 2.70-2.77 (m, 1H), 2.35-2.55 (m, 3H), 2.15-2.34 (m, 1H), 1.90-2.05 (m, 1H); ^{13}C NMR (100 MHz, D$_2$O) δ 177.2, 175.3, 174.9,

174.5, 67.9, 66.9, 57.5, 51.9, 48.9, 38.6, 29.9, 16.8.; HRMS (ESI) *m/z* calcd for $C_9H_{14}NO_8$

$(M+H)^+$ 264.0714, found 264.0721. The specific rotation $[\alpha]^{24}_D$ = -13.6° (*c* 0.1, MeOH).

D,D-malylglutamate: **3.15**
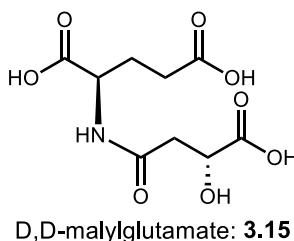
(*R*)-2-((*R*)-3-Carboxy-3-hydroxypropanamido)pentanedioic acid (3.15)

Prepared according to General Procedure B using **D,D-3.14** (20 mg, 0.038 mmol)

to afford **D,D-3.15** (8 mg, 80% yield). IR (film) 3352, 3034, 1733, 1536, 1386, cm^{-1}; ^{1}H

NMR (400 MHz, D$_2$O) δ 4.60 (dd, *J* = 4.5, 7.8 Hz, 1H), 4.46 (dd, *J* = 4.7, 8.2 Hz, 1H),

3.20-3.33 (m, 1H), 2.82 (dd, *J* = 4.5, 15.2, 1H), 2.70-2.77 (m, 1H), 2.35-2.55 (m, 3H),

2.15-2.34 (m, 1H), 1.90-2.05 (m, 1H); ^{13}C NMR (100 MHz, D$_2$O) δ 177.2, 175.3, 174.9,

174.5, 67.9, 66.9, 57.5, 51.9, 48.9, 38.6, 29.9, 16.8.; HRMS (ESI) *m/z* calcd for $C_9H_{14}NO_8$

$(M+H)^+$ 264.0714, found 264.0718.

D,L-malylglutamate: **3.15**
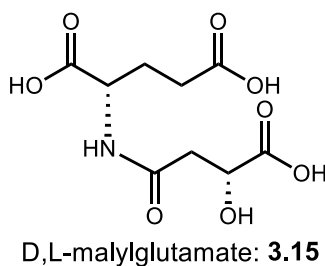
(*S*)-2-((*R*)-3-Carboxy-3-hydroxypropanamido)pentanedioic acid (3.15)

Prepared according to General Procedure B using **D,L-3.14** (10 mg, 0.019 mmol)

to afford **D,L-3.15** (3.8 mg, 78% yield). IR (film) 3350, 2853, 1730, 1260, 1170, cm^{-1}; ^{1}H

NMR (400 MHz, D$_2$O) δ 4.59 (dd, J = 4.4, 7.8 Hz, 1H), 4.46 (dd, J = 5.1, 9.0 Hz, 1H),

2.83 (dd, J = 4.5, 15.2, 1H), 2.77 (dd, J = 7.9, 15.2, 1H), 2.51 (t, J = 7.5, 2H), 2.15-2.28;

^{13}C NMR (100 MHz, D$_2$O) δ 177.1, 175.3, 174.8, 174.5, 67.9, 57.4, 51.7, 38.5, 29.9, 25.6,

16.7; HRMS (ESI) m/z calcd for C$_9$H$_{14}$NO$_8$ (M+H)$^+$ 264.0714, found 264.0720.

3.5 - References

[1]   B. P. Lankadurai, E. G. Nagato, M. J. Simpson, *Environ. Rev.* **2013**, *21*, 180–205.

[2]   C. M. Griffith, P. B. Williams, L. W. Tinoco, M. M. Dinges, Y. Wang, C. K. Larive, *J. Proteome Res.* **2017**, *16*, 3407–3418.

[3]   M. Hamada-Kanazawa, M. Kouda, A. Odani, K. Matsuyama, K. Kanazawa, T. Hasegawa, M. Narahara, M. Miyake, *Biol. Pharm. Bull.* **2010**, *33*, 729–737.

[4]   M. Narahara, M. Hamada-Kanazawa, M. Kouda, A. Odani, M. Miyake, *Biol. Pharm. Bull.* **2010**, *33*, 1938–1943.

[5]   M. Liebeke, J. G. Bundy, *Biochem. Biophys. Res. Commun.* **2013**, *430*, 1306–1311.

[6]   Z. Du, Y. Lu, X. Dai, D. Zhang-Negrerie, Q. Gao, *J. Chem. Res.* **2013**, *37*, 177–180.

[7]   T.-M. Chan, J. Kong, P. McNamara, J. K. Wong, *Synth. Commun.* **2008**, *38*, 2252–2260.

[8]   G. L. Beutner, I. S. Young, M. L. Davies, M. R. Hickey, H. Park, J. M. Stevens, Q. Ye, *Org. Lett.* **2018**, *20*, 4218–4222.

[9]   R. Schobert, C. Jagusch, *Synthesis* **2005**, *2005*, 2421–2425.

Chapter 4 - Investigations Toward the Synthesis of the Flavalin Family of Natural

Products

4.1 - Introduction

4.1.1 - Background

Neurodegenerative diseases are debilitating conditions that result in the degeneration and/or death of nerve cells.[1] Disorders like Alzheimer's, Huntington's, and Parkinson's disease affect an estimated 22 million people world-wide with symptoms that can include memory loss, cognitive decline and movement impairment.[2,3] The devastating effects of neurodegenerative diseases and their prevalence in today's aging population make the search for effective treatments critical. Many natural products have displayed neuroprotective properties against neurodegeneration, making them desirable candidates for therapeutic treatment.[4] Thus, there is a strong interest in developing new synthetic methods to access bioactive natural products as effective therapeutic leads.

common dimethyl-decalin core: **4.01**   eremophilane skeleton: **4.02**   nardosinane skeleton: **4.03**   (+)-nootkatone: **4.04** (eremophilane)   (-)-flavalin E: **4.05** (nardosinane)
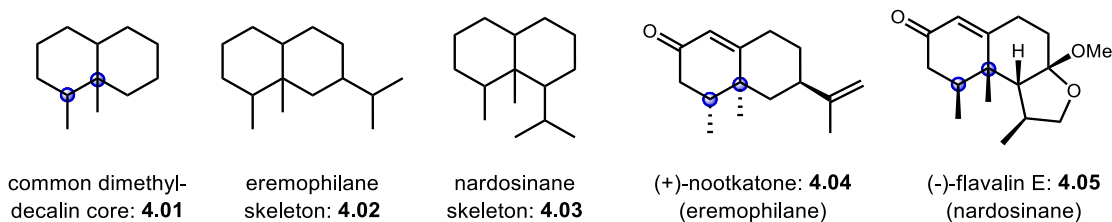
Figure 4.1 *Cis*-dimethyldecalin core found in many terpenes including eremophilare and nardosinane sesquiterpenes

A wide variety of terpene natural products that commonly have diverse bioactivity contain a decalin substructure. These decalins often possess methyl or isopropyl substituents along with additional rings and various patterns of oxidative modification. In particular, many natural products share a vicinal *cis*-dimethyldecalin core structure **4.01** (>15000 natural products), including a significant number of sesquiterpenes (Figure 4.1). Sesquiterpenoids are a diverse class of natural products and are comprised of C_{15}

compounds that are formed by the condensation of three isoprene units. This class includes the eremophilane skeleton **4.02** and nardosinane skeleton **4.03** which are represented by nootkatone (**4.04**) and flavalin E (**4.05**).[4–6]

4.1.2 - Biosynthesis of *cis*-dimethyldecalin Sesquiterpenes

Sesquiterpenoids are derived biosynthetically from the 15-carbon precursor, farnesyl pyrophosphate (FPP) **4.06,** Scheme 4.1.[5] FPP undergoes a cyclase phase, specifically a set of carbocation cascade reactions where a diverse range of these polycyclic hydrocarbon structures are formed. This is followed by an oxidase phase where functionality is introduced in the sesquiterpenoid natural products. An example of the biosynthesis of the eremophilane skeleton, a well-known class of sesquiterpenes, is shown in Scheme 4.1a and involves loss of pyrophosphate to make carbocation intermediates followed by hydride shifts, a cyclization and methyl migrations to give the eremophilane core (**4.06-4.11**). This polycyclic structure can then be further functionalized to give natural products like (+)-nootkatone (**4.04**).[5]

A plausible biosynthetic pathway to nardosinane natural products, particularly those from the flavalin family, is shown in Scheme 4.1b.[6] Beginning with the natural product aristolene (**4.12**)**,** a proposed precursor of the nardosinanes,[7] an oxidative cleavage gives ketone intermediate **4.13.** A hydration or treatment with methanol followed by lactolization gives dihydrofuran nardosinanol A (**4.14**)**.** This is followed by an oxidation/acetalization reaction to give flavalin E (**4.05**) with its *cis*-dimethyl stereochemistry intact. Intermediate **4.13** can also be epoxidized at the less hindered double bond followed by a rearrangement and an allylic oxidation to give nardosinanol C (**4.15**)**.**

From this intermediate, an allylic rearrangement followed by a cyclization reaction gives the structurally complicated flavalin B (**4.18).** An alternative pathway to synthesizing another member of the flavalin family begins with nardosinanol C and involves reduction of the ketone to give the alcohol intermediate which can then cyclize to give the lactol intermediate followed by an allylic rearrangement to give elongatol E (**4.16).** Finally, a cyclization reaction of the lactol gives flavalin A (**4.17).**

a)

farnesyl pyrophosphate

4.06

OPP

4.07

H+

4.08

4.09

4.10

4.11

eremophilane skeleton: **4.02**

b)

aristolene: **4.12**

oxidative cleavage

4.13

1.hydration or methanolation
2. lactolization

1. epoxidation
2. rearrangement
3. oxidation

1. oxidation
2. acetalization

flavalin E: **4.05**

nardosinanol A: **4.14**

nardosinanol C: **4.15**

1. reduction
2. cyclization
3. allylic rearrangement

1. allylic rearrangement
2. cyclization

cyclization

flavalin A: **4.17**

elongatol E: **4.16**

flavalin B: **4.18**

Scheme 4.1 Biosynthesis of eremophilane core and proposed biosynthesis of flavalin natural products

4.1.3 - Previous syntheses of *cis*-dimethyldecalin compounds

Previous syntheses of nardosinane and eremophilane sesquiterpenes have classically involved a Robinson annulation to construct one 6-membered ring, however other different and creative strategies for synthesizing individual members of this family have also been reported.[8–12] For example, in 1984 Valenta *et. al.* [13] synthesized dimethyldecalin **4.21** and **4.22** *via* a Diels-Alder reaction using trans-piperylene **(4.19)** and 2-methyl-2-cyclohexenone **(4.20)** (Scheme 4.2a). By using excess diene and stirring in BF₃-etherate for 48 hours at 20 °C, they obtained a mixture of the vicinal dimethyl adducts in an 80% yield, albeit favoring *trans*-product **4.21** over the *cis*-dimethyl motif **4.22**. Ketone **4.22**, was isolated when eluted with 5% ether in hexane on a silver nitrate impregnated silica gel column in a 25% yield. AlCl₃ has also been employed as the catalyst however the reaction time increased to 72 hours. Following an identical purification as above, the dimethyl decalins **4.21** and **4.22** were isolated in 62% and 18% yield, respectively.

More recently, Pipelier and coworkers[12] investigated the stereoselective synthesis of nardosinane derivatives (Scheme 4.2b). Starting from (*S*)-(+)-carvone **4.23**, the methyl group was introduced to the β-position *via* a diastereoselective Michael addition using lithium dimethyl cuprate. The isopropenyl group was then removed using a Criegee rearrangement by ozonolysis and treatment of the peroxy ester intermediate with cupric acetate and ferric sulfate. This gave a mixture of unsaturated ketones but upon treatment with DBU, enone **4.24** was ultimately isolated in an overall 50% yield from (*S*)-(+)-carvone. An α-allylation with intermediate **4.24** was quite tedious and typically resulted in

low yields however optimal results were achieved with sequential addition of LDA at −78℃ followed by warming up to −40℃ and adding HMPA. Finally, after an hour, allyl iodide was added and stirred for 12 hours to give the *cis*-dimethyl enone **4.25** with 90:10 d.r. in an 80% yield. After allylation, a total of six steps are needed to form the desired *cis*-dimethyl diene **4.26** in an overall 14% yield.
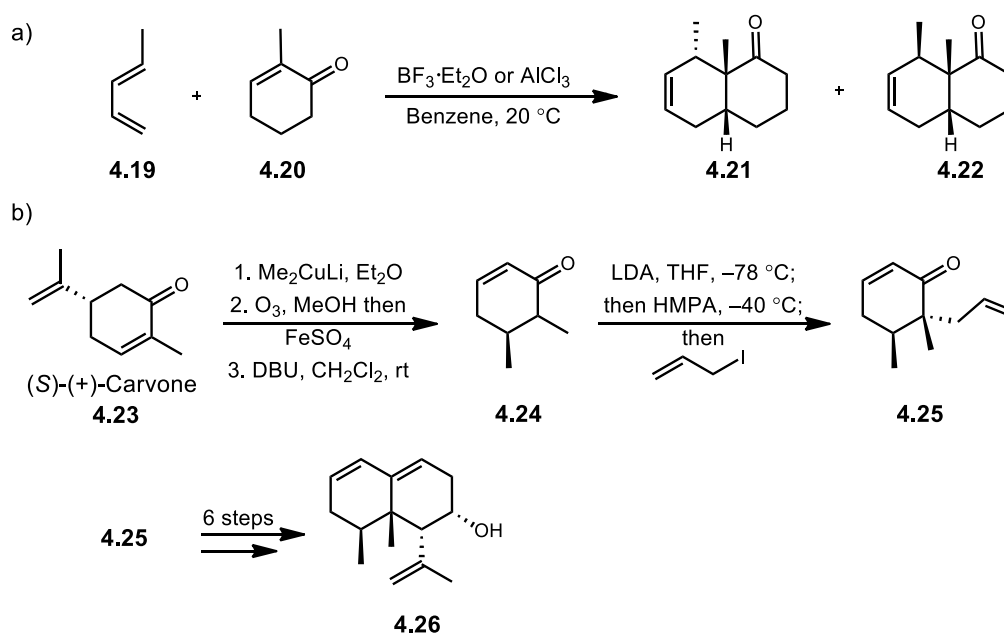
Scheme 4.2 Relevant synthetic approaches for *cis*-dimethyldecalin motif

Other natural products containing *cis*-dimethyl moieties, such as the eremophilane (+)-nootkatone (**4.04**), are abundant, yet introduction of this specific dimethyl stereochemistry has proven difficult because of complicated syntheses, toxic reagents and low yields. Previous syntheses of (+)-nootkatone (**4.04**) have been shown to be dangerous if not carefully monitored and carried out at low temperatures.[14] Although there have been several representative literature examples for synthesizing dimethyl motifs, most give mixtures of inseparable products, generally have a high step count and are typically low

yielding. The stereoselective construction of the *cis*-dimethyldecalin core **4.01** still poses a challenge and new, more efficient synthetic approaches would be of significant value.

4.1.4 - 6π-Electrocyclization

Although there are previous methods to synthesize natural products with the decalin core, we were attracted to the possibility of generating the nardosinane *cis*-dimethyldecalin substructure using a 6π-electrocyclization reaction. A 6π-electrocyclization is a pericyclic reaction in which the net result is the intramolecular conversion of a π-bond to a σ-bond *via* an acyclic ring closure. Such reactions have been shown to display high regio- and stereocontrol in making complicated polycyclic molecules.[15] According to the Woodward-Hoffman rules, the stereochemical outcome is dependent on the symmetry of the orbitals involved in the electrocyclization reaction.[16]

In Figure 4.2, the HOMO and the LUMO are shown for both a 4π-system and a 6π-system. For a 4π-system, the HOMO has the proper symmetry to undergo a conrotatory ring closure to achieve constructive orbital overlap. When the molecule is excited by absorption of a photon to promote one electron from the HOMO to the LUMO, the LUMO dictates that the electrocyclization will occur in a disrotatory fashion. Conversely, in order to have proper orbital overlap, the 6π-system will undergo a disrotatory ring closure from the ground state (thermal manifold) but when excited, it does a conrotatory ring closure (photochemical manifold).
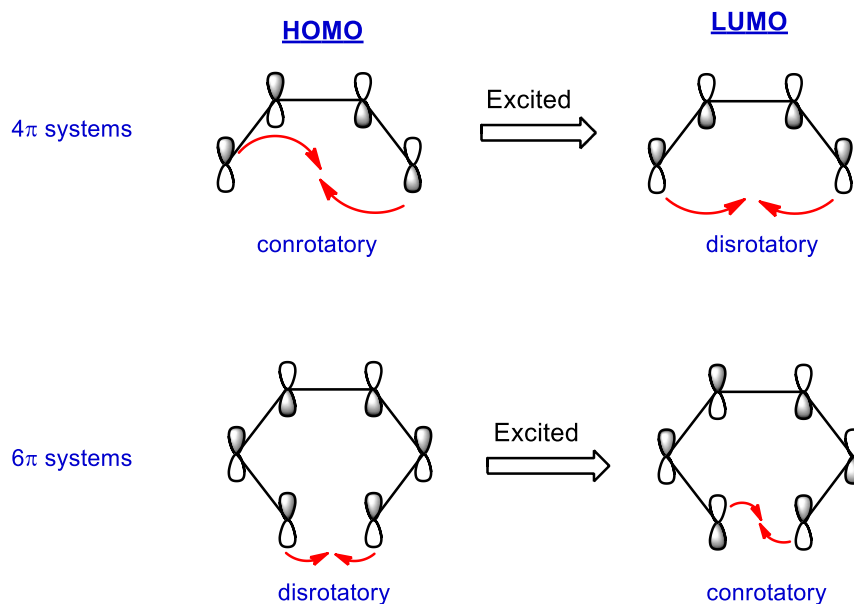
Figure 4.2 Woodward-Hoffmann rules in electrocyclization reactions

Nature efficiently utilizes biosynthetically facilitated 6π-electrocyclizations to produce complex natural products. Compounds like the endriandric acids undergo 8π- followed by 6π- electrocyclizations to generate their complex cores[17,18] while the biosynthesis of vitamin D involves a conrotatory 6π-electrocyclic ring-opening reaction.[19,20] Quite a few natural products recently have been synthesized using 6π-electrocyclizations as the key step *via* thermal and photochemical methods.[15,21–23]

Scheme 4.3a describes the synthesis of the natural product rubriflordilactone A (**4.32**) which begins with cyclopentenone **4.27**.[15,21] Following a series of steps, the triene core **4.30** is synthesized *via* a Stille-Migita cross-coupling reaction between iodo ester **4.28** and tin intermediate **4.29** in great yields. It then undergoes a thermal 6π-electrocyclization when heated to 145℃ in DMSO followed by aromatization in one pot procedure to give the arene intermediate **4.31** in 73% yield. After 3 subsequent steps, the final stage of the synthesis of rubriflordilactone A was completed.

162

Another example of a 6π-electrocyclization was reported by Li and coworkers in their total synthesis of the natural product alkaloid, daphenylline (**4.38**) (Scheme 4.3b).[15,22] Although complicated in structure, the Li group was able to synthesize the daphenylline core structure using a photochemical 6π-electrocyclization as the key step. Beginning with hydroxy enone **4.33**, the triene precursor **4.34** was constructed in 8 steps. Upon irradiation using a 500 W Hg lamp at low temperatures, intermediate **4.35** was in the proper *cis* configuration to do a 6π-electrocyclization. After irradiating for 15 mins, diene **4.36** was obtained as a single diastereomer in 71% yield. Aromatization was achieved using DBU and air to give arene **4.37** in 67% yield followed by 9 steps to give the desired natural product, daphenylline.

Finally, a concise total synthesis of calothrixin A (**4.44**) is shown in Scheme 4.3c which was done by Ishikura and co-workers in 2011. The synthesis utilizes a cyclization/cross-coupling cascade reaction to obtain the 6π-precursor.[15,23] Treatment of borate salt **4.40**, which is generated *in situ* from 1-methoxyindole and *n*-BuLi followed by Et$_3$B, with diene intermediate **4.41** generates triene **4.42** in 68% yield. After removal of the THP group with camphorsulfonic acid (CSA), the triene efficiently underwent a copper(II) triflate catalyzed 6π-electrocyclization/aromatization to give carbazole **4.43** in 75% yield. An additional 4 steps give the natural product calothrixin A. As these examples show, the 6π-electrocyclization is a powerful transformation and was used as the key step in the aromatization of these complex natural products.
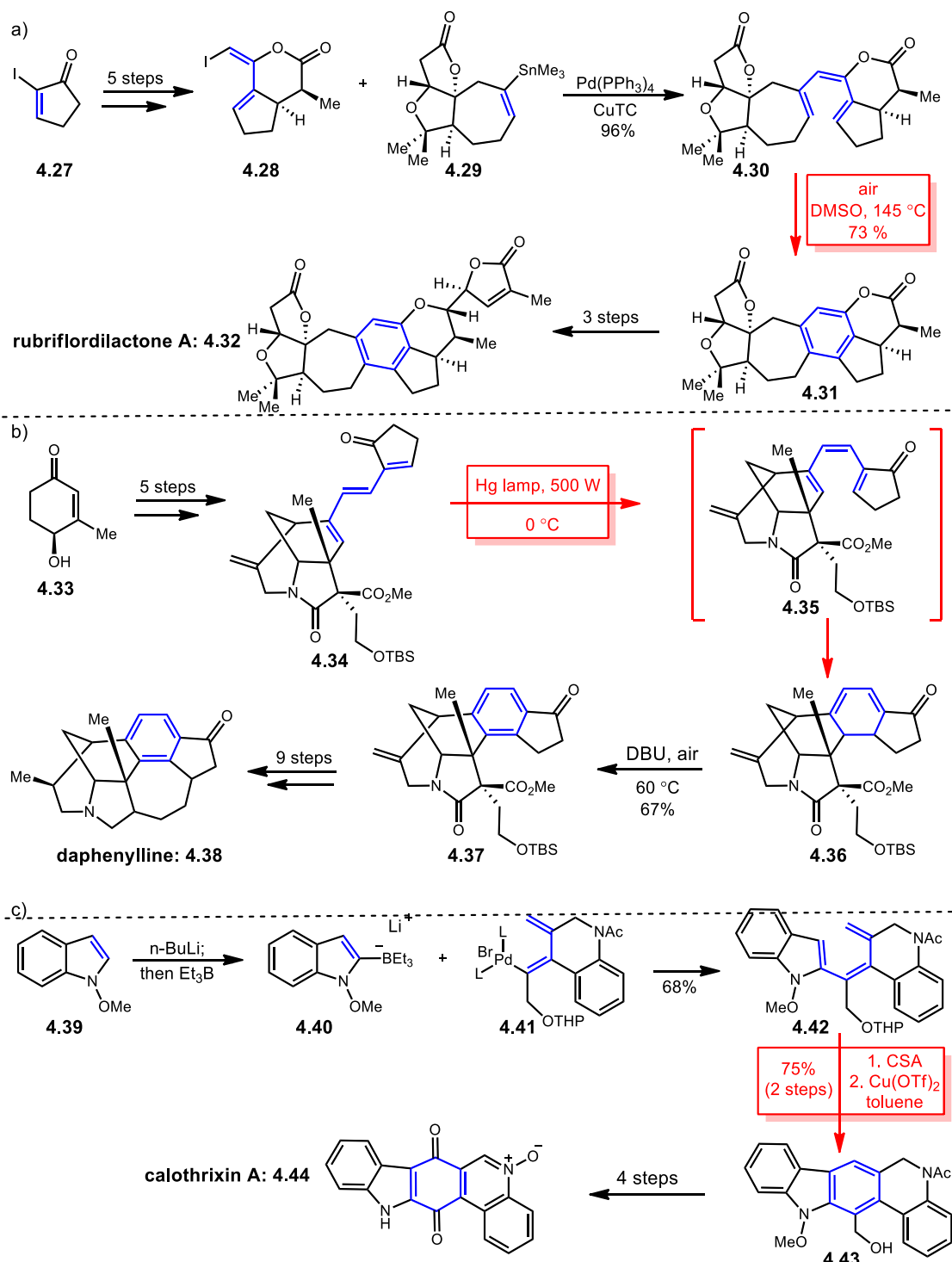
Scheme 4.3 Examples of 6π-electrocyclizations in natural product synthesis

4.1.5 - Visible light [2+2] cycloaddition *via* Energy Transfer

Typically pericyclic reactions allow for efficient regio- and stereocontrol for complex molecules. However, syntheses using this strategy require the use of high energy ultraviolet (UV) light. The need for UV light in most organic photochemical reactions not only limits the practicality, due to specialized glassware and safety concerns, but is not beneficial when used on industrial scales.[24] UV light is high energy which can cause unwanted decomposition of complex molecules. An alternative and attractive method to using UV light is the usage of visible light because it is benign to humans, generates no inherent waste, is readily renewable and poses a lower risk of molecular decomposition.[24,25] In the past ten years there has been a surge in the area of visible light photocatalysis.[26–30] Unfortunately, most organic compounds do not absorb visible light, however, this has been overshadowed with the rising use of transition metal complexes as visible light absorbing photocatalysts. Despite the practicality of using photocatalysis as a strategy to synthesize complex molecules, visible light-mediated pericyclic reactions provide a safer and more convenient alternative and are not well investigated.
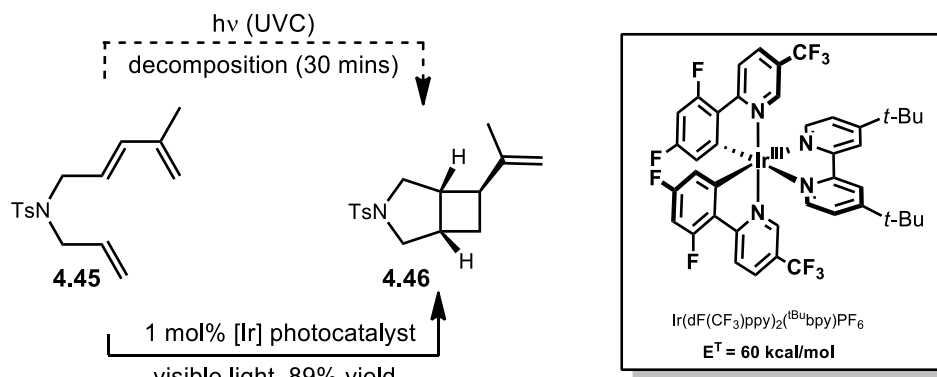
Figure 4.3 Energy transfer mediated [2+2] cycloaddition

In 2014, Tehshik Yoon and coworkers introduced a photocatalytic strategy for a [2+2] cycloaddition of 1,3-dienes (Figure 4.3).[31] Typically, the direct photoexcitation of dienes requires high energy UV light. However, this poses an issue when these high energy photons are not compatible with organic substrates that are highly functionalized. As predicted, the use of high-energy UVC radiation resulted in decomposition of the dienes after 30 minutes. However, when an iridium photocatalyst and visible light was used, they obtained their [2+2] cyclized product **4.46** in 89% yield. The proposed mode of action is based on an energy transfer mechanism. Energy transfer relies on the triplet state energies of the catalyst and substrate(s).[28] Most visible light reactions use photoredox activation with a transition metal photocatalyst, which relies on the redox potentials of the photocatalyst and the substrate(s) of interest.

Yoon and coworkers took advantage of the incompatabilty of the redox potentials, because the lowest lying triplet states of the photocatalyst and diene were quite similar (55-60 kcal/mol) allowing the reaction to proceed efficiently *via* energy transfer.[32] Overall, they were able to synthesize a variety of cycloadducts using dienes with different functional groups well tolerated under the visible light conditions which would otherwise be prone to decomposition under UV conditions. With this in mind, we wondered whether transition metal-mediated visible light catalysis *via* energy transfer could also be applied as the key step in the synthesis of the flavalin family of natural products.

4.2 - Motivation

4.2.1 - Flavalin Natural Products

We were attracted to synthesizing nardosinane-type natural products containing the *cis*-dimethyldecalin core. One particular family of sesquiterpenoid marine natural products, known as flavalins, has recently been discovered and all new members contain this *cis*-dimethyl motif (

Figure 4.4). Flavalins were extracted from the Formosan soft coral *Lemnalia flava* off the coast of Taiwan by Sheu and his team, and although they have not been explored synthetically, some of the natural products have shown promising bioactivity.[6,33] After testing several of the flavalins for biological activity, flavalin A **(4.17)** and B **(4.18)** were shown to possess cytotoxic, anti-inflammatory and neuroprotective properties. In a neuroprotective assay, using a toxic dose of 6-hydroxydopamine in neuroblastoma cells, cytotoxicity of the cells was significantly reduced after pre-treatment with flavalin A and B.[6]

The structures of flavalins are comprised of two different classes: flavalins A-D **(4.17, 4.18, 4.47, 4.48)** possess an oxa-cage ring system core while all members of the second class, flavalins E-H **(4.05, 4.49-4.51)** all contain a fused tetrahydrofuran-type functional group. These natural products are complex due to their multiple quaternary and fully-substituted centers, contiguous stereogenic centers, and *cis*-dimethyl stereochemistry. The biosynthesis of selected flavalins is shown in Scheme 4.1 and in all cases the common intermediate for both classes is ketone **4.13.** A series of oxidations and a lactolization give the tetrahydrofuran flavalin core while cyclization reactions give the oxa-cage core.

Although these natural products are bioactive and have interesting structures, making them synthetically poses an issue due to the complexity of the structures and the poor outcomes in previous syntheses of *cis*-dimethyl natural products. An alternative route in which the flavalin core can be generated in few steps stereoselectively would be highly desirable.
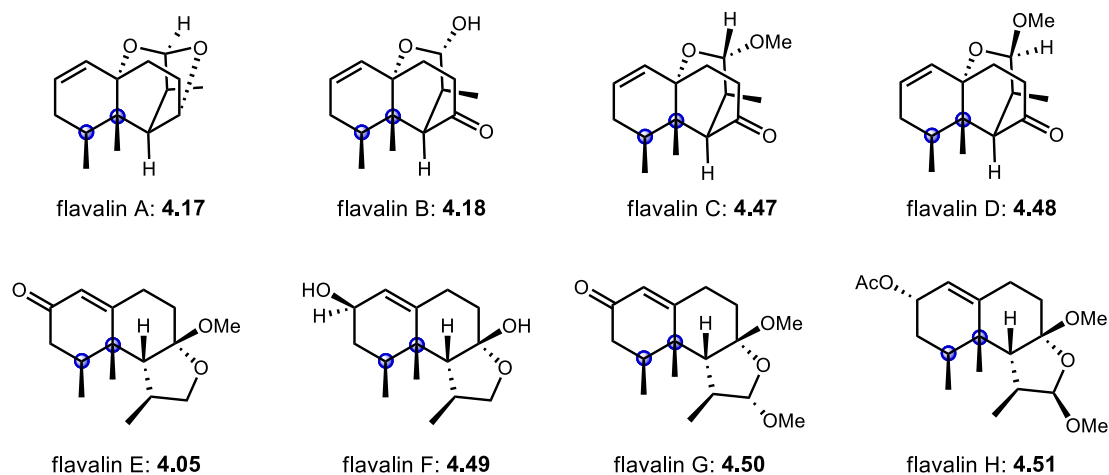
Figure 4.4 Newly discovered nardosinane-type sesquiterpenoids: flavalins

We were interested in the possibility of generating the dimethyldecalin substructure *via* a 6π-electrocyclization using visible light which would substantially simplify the target. The proposed 6π-electrocyclization reaction would allow for the introduction of both the tertiary and quaternary stereocenters in a single step, where the stereochemical outcome would be predictable based on the choice of reaction conditions (thermal or photochemical) based on the Woodward–Hoffmann rules.

Figure 4.5 shows the two potential *trans* products, **4.53** and **4.54**, when triene **4.52** is placed under thermal conditions which theoretically undergoes disrotatory ring closure while under photochemical conditions, it undergoes conrotatory ring closure giving the two *cis* cyclohexadiene products, **4.55** and **4.56**. This powerful strategy would hypothetically

facilitate the synthesis of a variety of eremophilane, nardosinane and related sesquiterpenes through a unified approach.
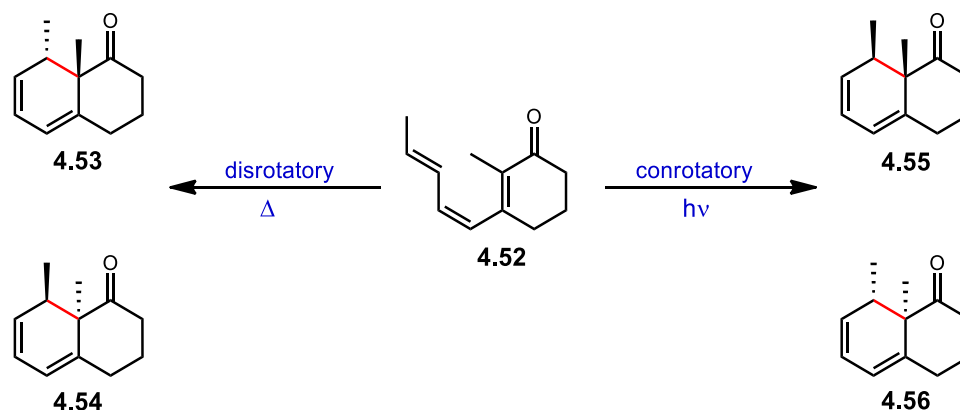
Figure 4.5 Thermal and photochemical outcomes for triene core **4.52**

Figure 4.6shows the proposed mechanism for the 6π-electrocyclization. $Ru(bpy)_3^{2+}$, which is a commonly used visible light absorbing transition metal photocatalyst, is irradiated to generate the singlet exited state. After undergoing metal to ligand charge transfer (MLCT) and intersystem crossing (ISC) the excited triplet state is generated. The catalyst can then excite the ground state of the substrate of interest to its lowest lying triplet state while decaying back to its original ground state. The excited substrate then undergoes a 6π-electrocyclization to give the desired cyclized product. With this in mind, prior to synthesizing the flavalin core, the photochemical 6π-electrocyclization strategy was tested on a simplified model system.
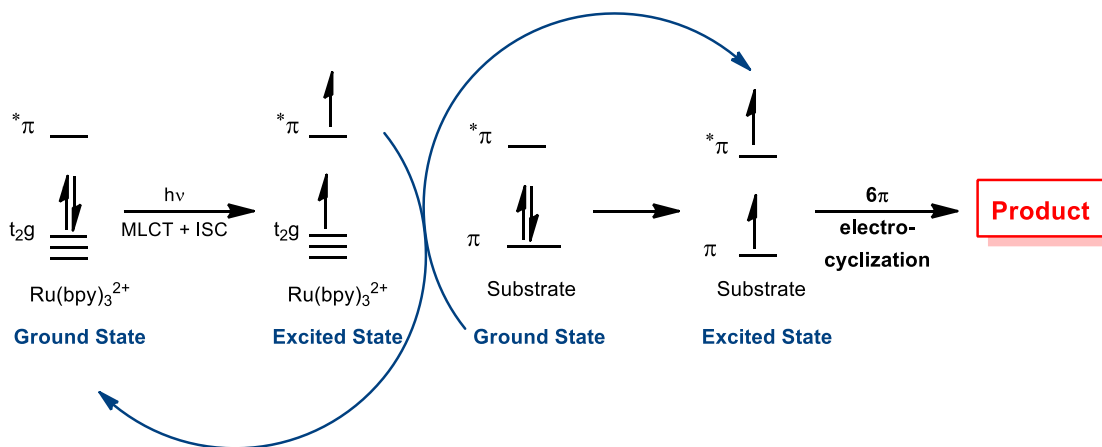
Figure 4.6 Proposed mechanism *via* energy transfer

4.3 - Results and Discussion for First Model System

4.3.1 - First Model System: Testing the Photochemical Electrocyclization

A simplified model system was developed to determine the feasibility of the photochemical electrocyclization using energy transfer. Scheme 4.4a shows the two potential cyclohexadiene products **4.58** and **4.59** when subjected under different reaction conditions, thermal and photochemical, and the two key disconnections in the proposed synthesis; a Wittig olefination generates the central alkene and a Horner-Wadsworth-Emmons olefination followed by a DIBAL-H reduction gives the *E*-alkene selectively. The synthetic plan, shown in Scheme 4.4b, uses known procedures to make the triene. The synthesis begins with commercially available and inexpensive starting material, 1,4-butanedione (**4.60**). Following mono-benzylation with benzyl bromide and a Swern oxidation, benzyl protected hydroxybutanal **4.61** was synthesized in 86% yield. A Horner-Wadsworth-Emmons olefination with triethyl phosphonoacetate gave the α,β-unsaturated ester **4.62** which led to a DIBAL-H reduction at low temperatures to give the desired allylic

170

alcohol **4.63** in 94% yield. Afterwards, a MnO$_2$ oxidation in hexanes gave the *E*-α,β-unsaturated enal **4.64** in 88% yield. In order to synthesize the desired triene **4.57**, a Wittig olefination involving crotyl triphenylphosphonium bromide was used. A mixture of both inseparable isomers (81:19 ratio of *E/Z*) of the crotyl salt were made using triphenylphosphine and crotyl bromide. Despite the inability to separate these two isomers, we moved forward to the next step.
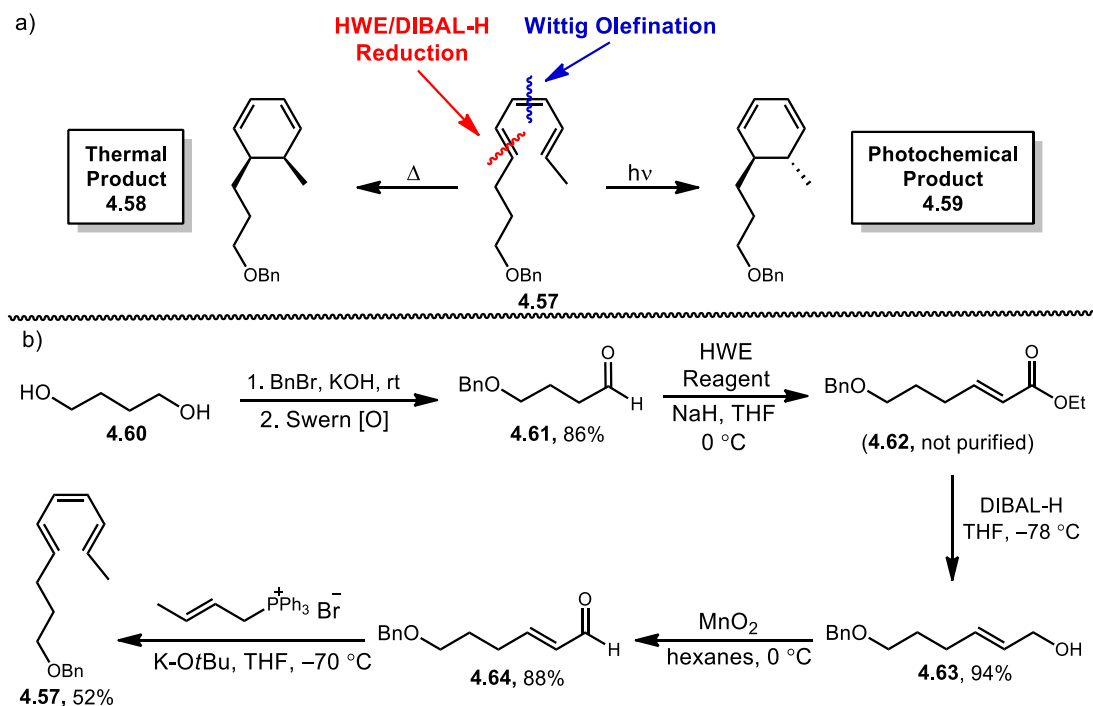
Scheme 4.4 Potential diene products and first model system

Triene **4.57** was obtained by a Wittig olefination using the crotyl salt to give a modest 52% yield. Analysis by gas chromatography (GC) indicated the presence of three products in a 45:50:5 ratio, which are the triene isomers. Table 4.1b shows the mixture of isomers that were predicted based on the mechanism of Wittig olefinations. The enal precursor **4.64** was set to the *E*-isomer however the crotyl salt was a mixture of two isomers

171

favoring the *E*-alkene. We suspected the major product to be the *E,Z,E* isomer with the minor two to be the *E,E,E* and the *E,E,Z* isomer. By lowering the temperature of the reaction, the selectivity improved to a 66:31:3 ratio at −70℃ (Table 4.1a). Ultimately, it was necessary to isolate the *E,Z,E* isomer as it is the only isomer with the proper geometry to do the 6π-electrocyclization. Impregnated silver nitrate was employed to separate the alkene isomers with no success, as well as a variety of other separation techniques (alumina, etc).

After testing a variety of high boiling solvents including toluene, DMF and xylenes to induce the thermal electrocyclization, DMF proved to be the most optimal solvent for this task. The thermal 6π-electrocyclization reaction gave an authentic sample of the cis diene product **4.65** in a 26% yield 4.1c. Although the triene contained three different isomers, it is expected that the thermal cyclized product can only be obtained through a thermal 6π-electrocyclization with the *E,Z,E* isomer, GC analysis showed the consumption of one of the three isomeric peaks and the appearance of a new peak corresponding to the product. After isolation by column chromatography, the new GC peak was confirmed to be the cyclized product by GC and 2D NMR techniques. COSY NMR was used to assign proper chemistry of the cis diene and NOESY NMR showed that the methylene and the methyl group adjacent to the cyclized diene had an nOe correlation with each other.

a)

b)

c)

Entry	Temp (°C)	E,Z,E Ratio (%)	E,E,E Ratio (%)	Other Isomer (%)
1	rt	40	55	5
2	0	44	51	5
3	−10	45	50	5
4	−20	50	46	4
5	−40	52	44	4
6	−60	59	38	3
7	−70	64	33	3
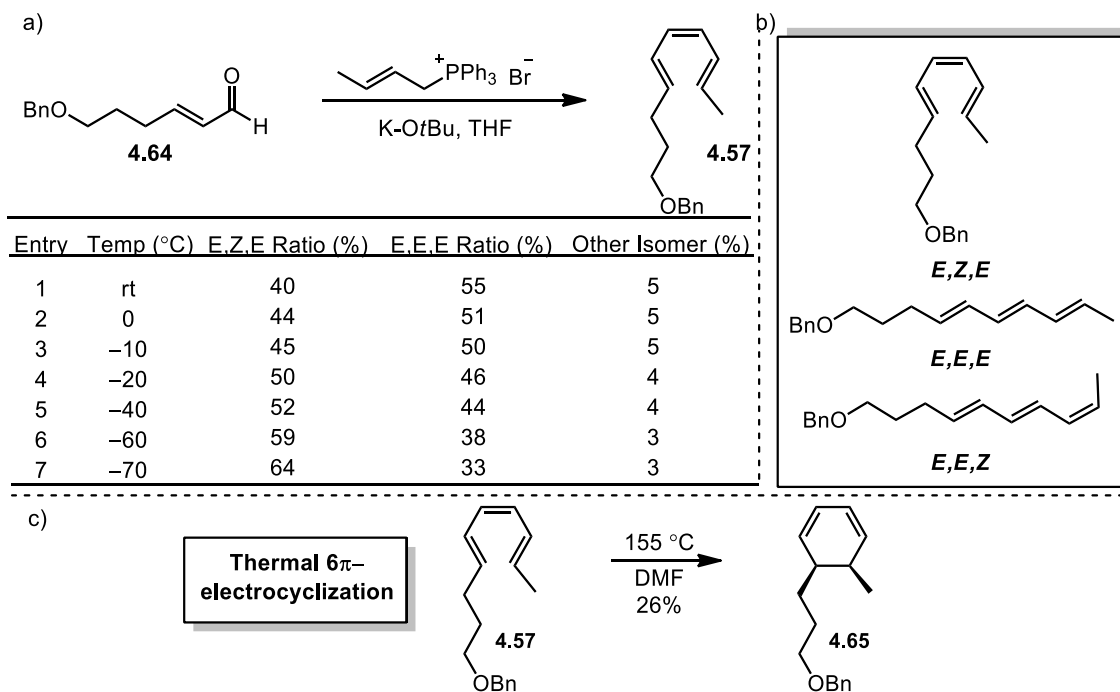
Table 4.1 Temperature controlled Wittig olefinations, triene isomers and thermal electrocyclization

To obtain the photochemical product, a photocatalyst must absorb light at the appropriate wavelength. Initial conditions for the photochemical reactions were: 10 mol% of $[Ru(bpy)_3](Cl_2)$ which absorbs light at 452 nm, DMSO as solvent and blue LED lights (emission maximum = 450 nm). The photochemical reactions showed a relatively small new peak by GC that did not correspond to the thermal product but had a similar retention time. Similar to the thermal electrocyclization reaction, the consumption of one of the isomers occurred by GC. The new peak was hypothesized to be the photochemical product since without a light source or photocatalyst, this new GC peak did not form. Although, the other alkene isomers could not be separated out, we performed a set of optimization reactions varying the solvent, photocatalyst and temperature.

Unfortunately, when the reaction was subjected to photochemical conditions, the main reaction was the isomerization of the alkene trienes to the more thermodynamically favorable isomer, the *E,E,E* triene isomer which was confirmed by the increase in area of one of the major GC peaks, and the larger coupling constant for the alkene protons in the proton NMR. After using different concentrations of silver nitrate, solvents for impregnation, and solvents for thin layer chromatography, isolation of any potential product, particularly the smallest peak by GC, could not be achieved. With this in mind, we decided that a more efficient and stereoselective synthesis must be devised and a new model system more closely related to the flavalins would be more valuable.

4.4 - Flavalin Core Model System

4.4.1 - Previous Synthesis of triene precursor

The lack of *E/Z*-selectivity and inability to isolate the product in the alkyl model system led to a search for a more selective synthetic strategy. We set out to develop an efficient synthesis of conjugated triene precursor **4.52** because of its similarity to the nardosinane flavalin core. Ketotriene **4.52** was previously synthesized by Ramage and Satter using the Stork-Danheiser protocol (Scheme 4.5).[34] Ramage's synthesis begins with the reaction between vinylogous ester **4.66** and the Grignard derivative of alkyne **4.67** followed by acid treatment to give acetylenic alcohol **4.68**. A two-step dehydration with POCl₃–pyridine followed by treatment with Oediger's base gave intermediate **4.69** as a mixture of products in a 4:1 ratio (shown in step 3, Scheme 4.5). The *trans* isomer, Product B, was much less stable than the *cis* isomer and degraded rapidly when stored at 0℃ however the *cis* isomer was separated from the *trans* isomer by g.l.c. A partial

hydrogenation using Lindlar's catalyst in heptane gave an inseparable mixture of the desired all *cis*-trienone **4.52**, 20% starting material XX and 10% of the over reduced product.
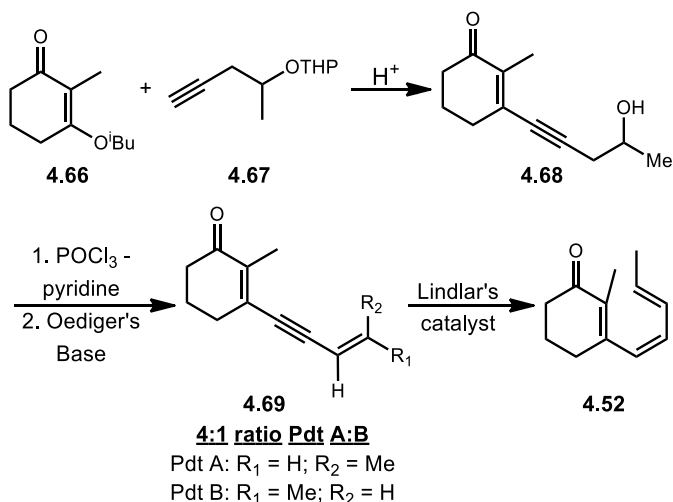
Scheme 4.5 Synthesis of ketotriene by Ramage and Sattar

We devised an alternative synthesis for trienone **4.52** using recent developments in cross-coupling to stereospecifically synthesize the ketotriene through a Suzuki coupling beginning with stereodefined alkene building blocks.[35] We were inspired by Martin Burke *et al.*'s research involving the stereoselective synthesis of polyene natural products using iterative cross coupling reactions.[36,37,37,38] Burke and co-workers developed a strategy that utilizes *N*-methyliminodiacetic acid (MIDA) boronates (Scheme 4.6) due to their high benchtop stability, easy purification and commercial availability. We envisioned using these MIDA boronates as the building blocks to synthesize the triene precursor stereoselectively with the flavalin core in mind as the final target. Stereospecificity is critical to ensure the Z-geometry about the central alkene which is necessary for the 6π-

electrocyclization and using MIDA boronates as the building blocks in Suzuki cross coupling reactions seemed like the ideal strategy for accomplishing this. Once the triene with the correct stereochemistry is synthesized, the photochemical 6π-electrocyclization can be tested followed by further functionality to make the flavalin natural products.

4.4.2 - Synthesis of ketotriene *via* Suzuki cross-coupling reactions using MIDA boronates

Scheme 4.6 shows a retrosynthetic route for the triene precursor. It relies on utilizing the MIDA boronates as the building blocks and performing Suzuki cross-coupling reactions to control the stereochemistry of the triene. The triene **4.52** results from a Suzuki reaction between vinyl bromide **4.70** that has an *E*-alkene incorporated in its structure along with diene MIDA boronate **4.71**. The diene is the result of another Suzuki cross coupling reaction between a boronic acid **4.72** and a *Z*-vinyl bromide **4.73**. The vinyl bromide comes from bis-borylated alkene **4.74** and finally the starting material, commercially available ethynyl MIDA boronate **4.75**.[39,40]
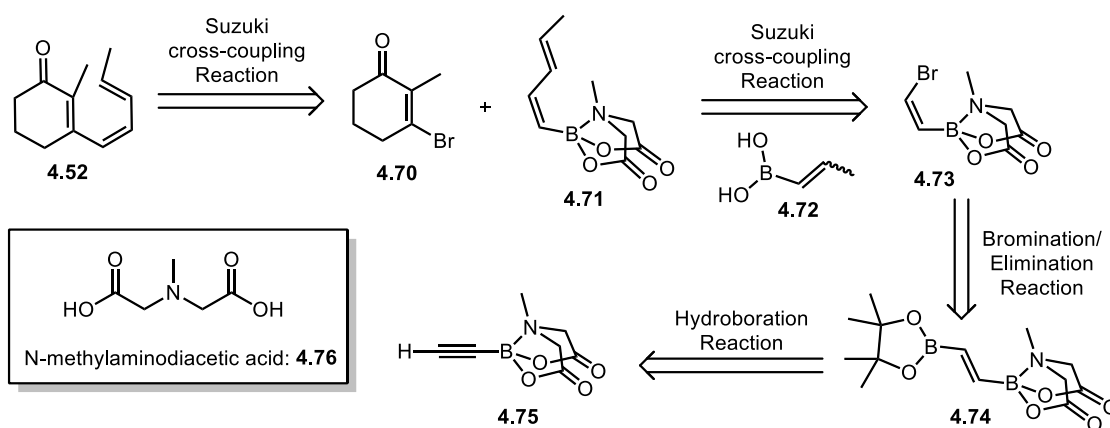
Scheme 4.6 Retrosynthesis of triene core

The synthesis began with the hydroboration of ethynyl MIDA boronate **4.75** using dicyclohexyl borane (synthesized from cyclohexene and borane) and pinacol borane (Scheme 4.7a). Bis-borylated alkene intermediate **4.74** undergoes a two-step bromination/elimination to give *Z*-MIDA boronate **4.73** in 81% yield and high *Z*-selectivity. Optimal yields occurred when Na_2HPO_4 was used as the base as opposed to K_3PO_4. This was followed by the first Suzuki cross-coupling reaction to generate diene MIDA boronate **4.71** using propenyl boronic acid, $Pd(OAc)_2$ and XPhos. Two isomers are formed (in a 1:1 ratio which resulted from the mixture of *E*- and *Z*-propenyl Grignard reagent used to generate the *E,Z*-propenylboronic acid **4.72**. We attempted to separate the two dienyl MIDA boronate isomers *via* crystallization and chromatography but with no success. This four-step sequence proceeded in an overall 63% yield.
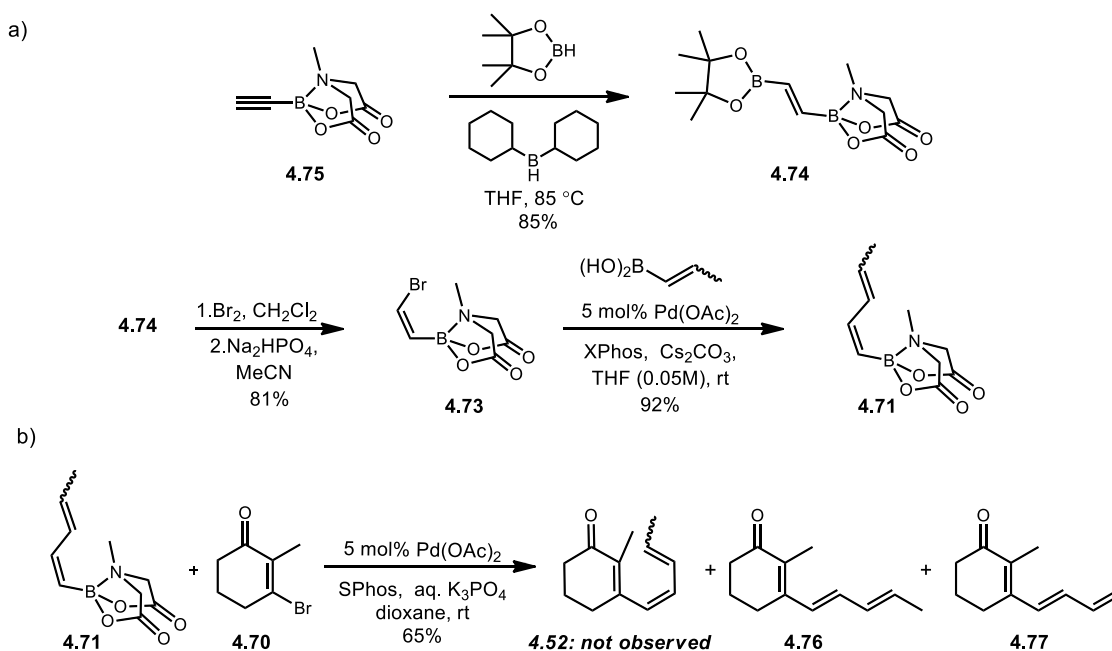
Scheme 4.7 Synthesis of diene and triene precursors

As shown in Scheme 4.7b, we focused our attention on optimizing the Suzuki coupling involving the dienyl MIDA boronate **4.71** and β-bromoenone **4.70**. We employed optimized conditions reported by Burke and coworkers for in situ hydrolysis/coupling with catalytic $Pd(OAc)_2$, SPhos, and aqueous K_3PO_4 in dioxane at room temperature. Under these conditions, we observed two different triene isomers that were isolated in a 65% yield. The two isomers differed at the double bond distal to the carbonyl group, as was expected starting from the mixture of E- and Z-MIDA boronates.

After inspecting the ^{1}H NMR spectra, we noticed a large *J*-value ($J_{HH} = 15.6$ Hz) in the alkene region corresponding to the central alkene, suggesting it has *E*-stereochemistry. Although the stereochemistry for the central alkene should have been Z-selective based on its precursor, the NMR showed no indication that the desired *E,Z*-triene **4.52** was formed. These results indicated that a triene was generated but contained alkenes with a higher coupling constant most likely corresponding to the *E,E* isomer **4.76**. Ultimately, we discovered that during the Suzuki cross-coupling reaction between the β-bromoenone and the dienyl MIDA boronate, the previously set *Z*-alkene in the diene had isomerized to the *E*-alkene. Although we were unable to isolate an authentic sample of the desired triene in order to test the 6 π-electrocyclization reaction using this strategy, we were interested in determining the cause of the isomerization of the double bonds in the Suzuki reaction.

4.4.3 - Suzuki Cross Coupling Experiments

The isomerization of the *Z*-alkene to the *E*-alkene was of interest not only because it inhibited us from moving forward with the synthesis, but also because of the surprising outcome when placed under standard, widely-employed Suzuki coupling conditions. To verify the outcome, we synthesized an authentic sample of the *E,E* triene in order to compare it to the previously made sample (Scheme 4.8).
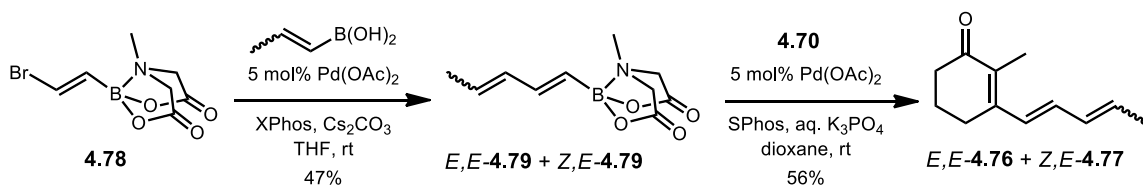
Scheme 4.8 Synthesis of authentic *E,E* triene

We began the synthesis with commercially available *E*-bromo MIDA boronate **4.78** and cross-coupled it with the previously synthesized propenyl boronic acid. This gave us two isomeric dienes, E,E-**4.79** and Z,E-**4.79,** however in this case, the alkene adjacent to the B(MIDA) was set as the *E*-isomer as opposed to the *Z*-isomer from the previous synthesis. When performing the second Suzuki reaction, the same two triene products which were both isomeric at the alkene distal to the ketone were obtained, ultimately confirming the structure of the *E,E* triene. Also, carrying out the reaction with the rigorous exclusion of light had no effect on this isomerization process, suggesting that it is not a photochemical isomerization.
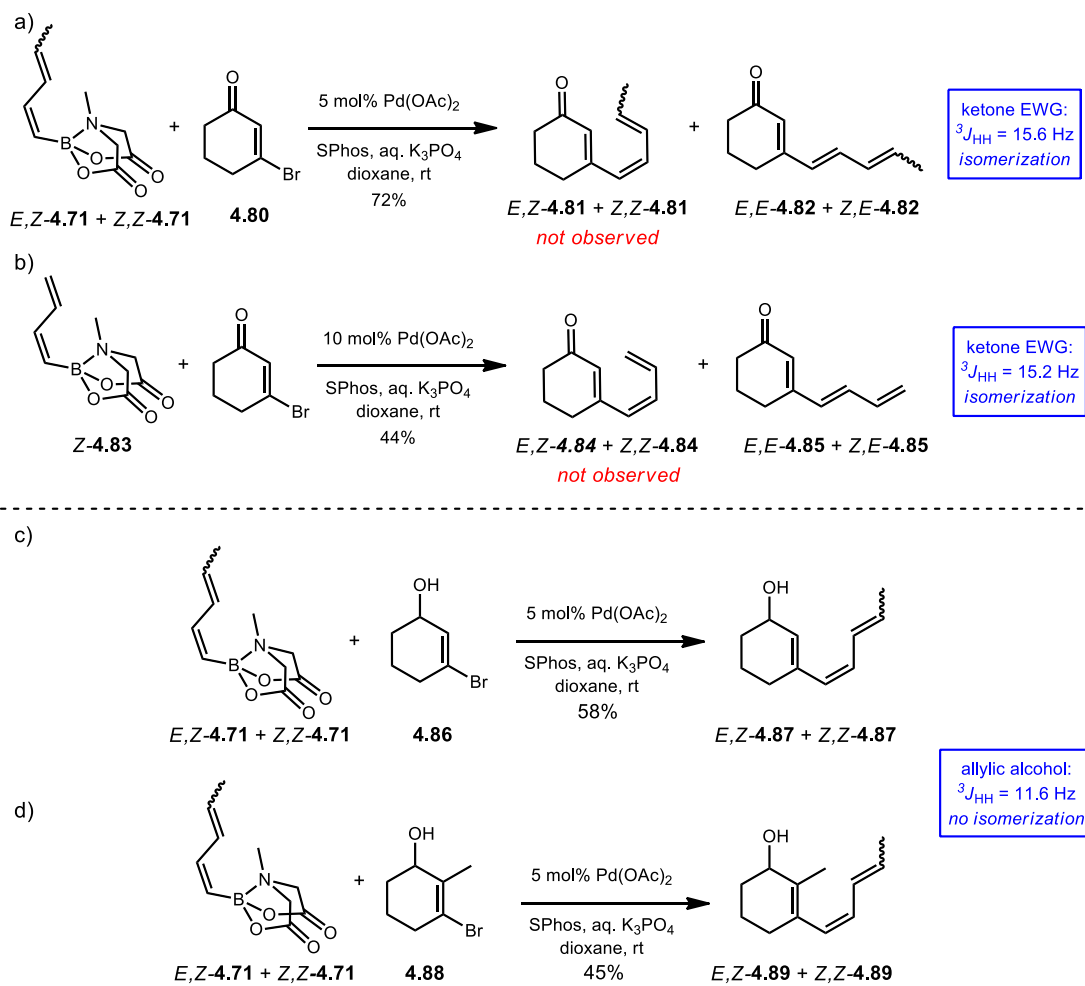
Scheme 4.9 Related structures for standard Suzuki coupling

The Suzuki cross-coupling reactions were then tested under standard conditions using variations of the vinyl bromide coupling partner. In Scheme 4.9a, the less hindered bromoenone **4.80**, which lacks the α-methyl substituent, was cross-coupled with the dienyl MIDA boronate **4.71** and gave **4.82** in 72% yield. Once again, we did not observe the desired *E,Z* triene but the isomerized product (**4.82**). The J_{HH} value obtained by NMR was 15.6 Hz indicating isomerization of the *Z*-alkene to the *E*-alkene. These results suggest that steric hinderance α to the carbonyl in the triene does not cause the isomerization. One

possible mechanism for isomerization is a deprotonation/reprotonation of the moderately acidic methyl group in conjugated products **4.81** and **4.82**, which is a process that would require the presence of the ketone to acidify the position. We synthesized the simpler *Z*-dienyl MIDA boronate **4.83** in Scheme 4.9b which lacks the terminal methyl group. After subjecting it to typical Suzuki conditions with bromoenone **4.80**, we again observed isomerization where the J_{HH} value obtained by NMR was 15.2 Hz suggesting that deprotonation is not required for isomerization.

We synthesized a more electron-rich vinyl bromide by replacing the ketone with an allylic alcohol group to investigate whether isomerization was due to an electronic effect as opposed to a steric effect (Scheme 4.9c,d). The Suzuki reaction with the dienyl MIDA boronate **4.71** and the allylic alcohol without the methyl group **4.86** gave the desired *E,Z*- and *Z,Z*- triene **4.87** in a 58% yield. When testing the allylic alcohol with the methyl group **4.88**, we obtained the *E,Z*- and *Z,Z*-triene in a 45% yield. Both reactions proceeded with retention of stereochemistry and sterics slightly effected the yield for allyl alcohol **4.89**. The J_{HH} value obtained by NMR was 11.6 Hz for both alcohols **4.87** and **4.89** indicating the *Z*-alkene at the central position had not isomerized.
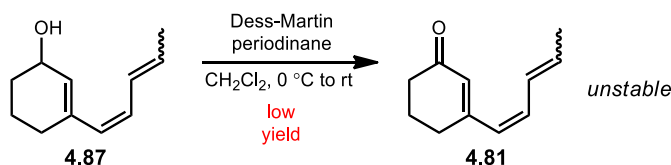

Scheme 4.10 Attempted synthesis of desired trienone **4.81**

With access to the *cis*-allylic alcohol products, we sought to reach the target trienones by an alternative route (Scheme 4.10). The allylic alcohol intermediates were

somewhat unstable and decomposed under a variety of oxidation conditions as evidenced by the lower yields. A Dess-Martin oxidation of the alcohol **4.87** appeared to give E,Z and Z,Z **4.81** which was one of the original target trienones, however in low yield. These two isomeric products differed from the previously synthesized-*E,E* and *Z,E*-**4.82**, however we were unable to obtain a pure sample and measure the coupling constants accurately due to the instability of this compound.

Cis/trans isomerization, although rarely observed in Pd catalyzed cross-coupling reactions, have in some cases been shown where electron deficient conjugated π-systems are used.[41–45] An early report by Mavrov discusses the synthesis of dienoate **4.92** using catechol borane **4.90** and alkenyl halide **4.91** under Suzuki conditions. (Scheme 4.11)[35] The reaction with (*Z*)-β-bromoacrylate gave a mixture of stereoisomers, however by changing the ligand source, temperature, and the reaction time, isomerization was significantly reduced favoring the expected *E,Z* isomer over the *E,E* isomer.
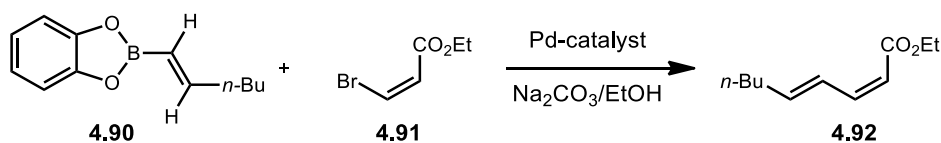
Scheme 4.11 Example of Pd catalyzed isomerization

4.5 - Conclusions

The decomposition of *cis*-trienes supports the hypothesis that isomerization of the double bonds occurs post Suzuki coupling which is facilitated by the electron withdrawing ketone and is driven by the formation of the more stable *trans* products. Based on previous reports and the results of the synthesis, we favor isomerization of the electron-deficient

product *via* a palladium hydride species or a Pd(II) species.[46–48] Although the unexpected isomerization of polyenes is not new, the process observed here defines a current challenge for the synthesis of conjugated polyenes that are electron deficient using the iterative cross-coupling strategy. Overall, the synthesis of a variety of trienes and trienones using an iterative Suzuki coupling strategy is described. We observed an unexpected isomerization of electron-poor conjugated trienones under mild Suzuki conditions. This isomerization led to loss of stereoselectivity and complicated the exploration of an electrocyclization strategy to making the dimethyldecalin substructure present in flavalin natural products. In the face of these challenges, we decided to pursue other, more fruitful investigations.

4.6 - Experimentals

4.6.1 - Materials and Methods:

^{1}H and ^{13}C NMR spectra were recorded on a Varian Inova 400 MHz or Bruker 700 MHz spectrometer unless otherwise indicated and were internally referenced to residual protio solvent signal (note: CDCl$_3$ referenced at δ7.26 ppm for ^{1}H NMR and δ77.1 ppm for ^{13}C NMR, respectively. Acetone-D$_6$ referenced at δ2.05 ppm for ^{1}H NMR and δ29.3 ppm for ^{13}C NMR, respectively). Data for ^{1}H NMR are reported as follows: chemical shift (δ ppm), integration, multiplicity (s = singlet, d = doublet, t = triplet, q = quartet, m = multiplet), and coupling constant (Hz). Data for ^{13}C NMR are reported in terms of chemical shift and no special nomenclature is used for equivalent carbons. IR spectra were recorded on a Bruker Alpha FT-IR Spectrometer. High-resolution mass spectrometry data were recorded on an Agilent LCTOF instrument using direct injection of samples in dichloromethane into the electrospray source (ESI) with positive ionization.

All reactions were carried out under an inert atmosphere of nitrogen in oven dried or flame dried glassware with magnetic stirring, unless otherwise noted. Solvents were dried by passage through columns of activated alumina. All starting materials were prepared according to known literature procedures or used as obtained from commercial sources, unless otherwise indicated. Reactions were monitored by thin-layer chromatography (TLC) and carried out on 0.25 mm coated commercial silica gel plates (Analtech TLC Uniplates, F254 precoated glass plates) using UV light as the visualizing agent and KMnO$_4$ and heat as a developing agent. Flash chromatography was performed on silica gel (Silicycle, SiliaFlash P60, 230-400 mesh).

4.6.2 - Experimental Procedures:

General Procedure A: Suzuki Cross-Coupling to form Dienes:

To a flask containing 5 mol% Pd(OAc)$_2$ and 10 mol% XPhos was added THF (0.05M). The resulting solution was stirred for 15 minutes and then added to a flask containing bromo MIDA boronate **(4.73)** (1 equiv), propenyl boronic acid (1.2 equiv), and Cs$_2$CO$_3$ (3.55 equiv). The reaction was stirred for 24 hours at room temperature. The reactions were tracked by TLC (100% EtOAc). Upon completion, the crude reaction mixture was filtered through celite, concentrated, and then diluted with EtOAc. The organic layer was washed with brine and dried with Na$_2$SO$_4$. Volatiles were removed under reduced pressure to afford a crude yellow oil. The crude material was purified using silica gel chromatography with 100% EtOAc.

General Procedure B: Suzuki Cross-Coupling to form Trienes:

To a flask containing vinylbromide (1 equiv)**,** diene MIDA boronate **(4.71)** (1.2 equiv), 5 mol% Pd(OAc)$_2$ and 10 mol% SPhos was added dioxane (0.08M). The resulting solution was sparged with nitrogen for 30 minutes at room temperature. Aqueous K$_3$PO$_4$ (3M) was then added and the reaction was stirred for 24 hours at room temperature. The reactions were tracked by TLC. Upon completion, the crude reaction mixture was filtered through celite, concentrated, and then diluted with EtOAc. The organic layer was washed with brine and dried with Na$_2$SO$_4$. Volatiles were removed under reduced pressure to afford

a crude yellow oil. The crude material was purified using silica gel chromatography with 1:5 EtOAc/hexanes.
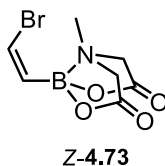
Z-**4.73**

Modified procedure for MIDA boronate Z-4.73

Synthesis conducted according to literature procedure[39] using *E*-diboronate **E-4.74** (1 g, 3.24 mmol), substituting K$_3$PO$_4$ with anhydrous Na$_2$HPO$_4$ (4.27 g, 30.78 mmol) in the elimination step, to give the desired product **Z-4.73** (0.685 g, 81%). Spectral data were consistent with literature values.
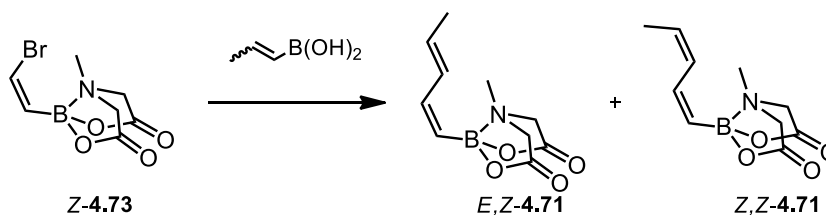
MIDA boronate (E,Z-4.71 + Z,Z-4.71)

Prepared according to general procedure A using 5 mol% Pd(OAc)$_2$ (28 mg, 0.127 mmol), 10 mol% XPhos (121 mg, 0.254 mmol), Z-MIDA boronate (**Z-4.73**) (666 mg, 2.54 mmol, 1 equiv), propenyl boronic acid (570 mg, 6.64 mmol, 2.61 equiv), Cs$_2$CO$_3$ (2.94 g, 9.02 mmol, 3.55 equiv) in THF (51 mL). Purification afforded the product as a pale yellow solid (524 mg, 2.34 mmol, 92%) in a 1:1 ratio of isomers as determined by ^{1}H NMR. IR (film) 2998, 1758, 1739, 1639, 1450, 983 cm^{-1}; ^{1}H NMR (400 MHz, CDCl$_3$) δ 7.11 (t, *J* = 13.2 Hz, 1H), 6.73 (t, *J* = 12.8 Hz, 1H), 6.50 (m, 2H), 5.82 (dq, *J* = 13.7, 6.8 Hz, 1H), 5.70 (dtt, *J* = 10.8, 7.2, 1.4 Hz, 1H), 5.27 (d, *J* = 14.4 Hz, 1H), 5.13 (d, *J* = 13.6 Hz, 1H), 3.88

(dd, J = 16.4, 2.8 Hz, 2H), 3.71 (dd, J = 16.4, 0.8 Hz, 2H), 2.86 (d, J = 1.6 Hz, 3H), 1.78 (dt, J = 4.8, 1.4 Hz, 3H); ^{13}C NMR (100 MHz, CDCl$_3$) δ 167.7, 146.3, 140.4, 134.8, 130.6, 130.1, 127.3, 61.7, 46.9, 18.4, 13.0; HRMS (ESI) m/z calcd for C$_{10}$H$_{15}$BNO$_4$ (M+H)$^+$ 224.1050, found 224.1059.
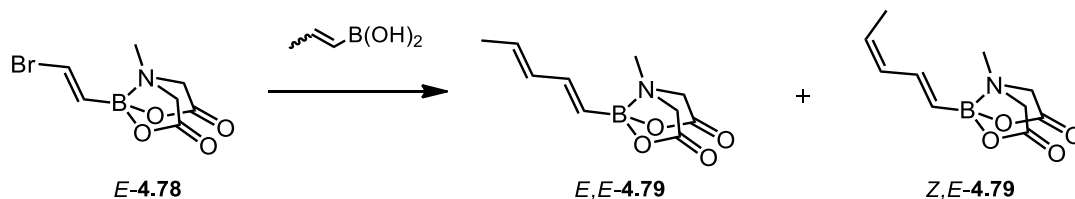

MIDA boronate (E,E-4.79 + Z,E-4.79)

Prepared according to general procedure A using 5 mol% Pd(OAc)$_2$ (4 mg, 0.019 mmol), 10 mol% XPhos (18 mg, 0.038 mmol), E-MIDA boronate (**E-4.78**) (100 mg, 0.382 mmol, 1 equiv), propenyl boronic acid (86 mg, 0.996 mmol, 2.61 equiv), Cs$_2$CO$_3$ (442 mg, 1.356 mmol, 3.55 equiv) in THF (8 mL). Purification afforded the product as a pale yellow solid (40 mg, 0.015 mmol, 47%) in a 1:1 ratio of isomers as determined by ^{1}H NMR. IR (film) 3058, 2961, 1762, 1641, 1449 cm^{-1}; ^{1}H NMR (700 MHz, CDCl$_3$) δ 7.01 (dd, J = 17.5, 10.5 Hz, 1H), 6.64 (dd, J = 17.5, 10.5 Hz, 1H), 6.13 (dd, J = 14.7, 10.5 Hz, 1H), 6.08 (dt, J = 11.2, 1.4 Hz, 1H), 5.83 (dq, J = 14.7, 7 Hz, 1H), 5.61 (dq, J = 10.5, 7 Hz, 1H), 5.54 (d, J = 16.8 Hz, 1H), 5.42 (d, J = 17.5 Hz, 1H), 3.82 (d, J = 16.1 Hz, 2H) 3.68 (d, J = 16.8 Hz, 2H), 2.85 (s, 3H), 1.79 (dd, J = 7, 1.4 Hz). ^{13}C NMR (176 MHz, Acetone-d$_6$) δ 168.9, 168.9, 144.70, 138.8, 132.75, 131.9, 129.1, 128.6, 62.3, 47.2, 18.23, 12.8.; HRMS (ESI) m/z calcd for C$_{10}$H$_{15}$BNO$_4$ (M+H)$^+$ 224.1050, found 224.1058.
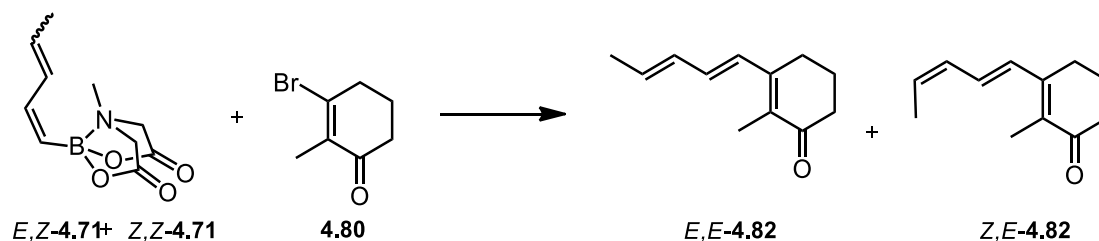
2-methyl-3-penta-1,3-dien-1-yl)cyclohex-2-enone (*E,E*-4.82 + *Z,E*-4.82)

Prepared according to general procedure B using 3-bromo-2-methylcyclohex-2-enone **(4.80)** (46 mg, 0.244 mmol, 1 equiv)**,** diene MIDA boronate **(*E,Z*-4.71 + *Z,Z*-4.71)** (66 mg, 0.292 mmol, 1.2 equiv), 5 mol% Pd(OAc)$_2$ (2.7 mg, 0.012 mmol), 10 mol% SPhos (0.024mmol, 10 mg), and 3.05 mL of dioxane. After sparging with nitrogen for 30 minutes at room temperature, aqueous K$_3$PO$_4$ (3M, 1.83 mmol, 7.5 equiv) was added. Purification afforded the product as a pale yellow oil (28 mg, 0.159 mmol, 65%) in a 39:61 ratio of isomers as determined by ^{1}H NMR. IR (film) 3053, 2957, 1652, 1596, 1264 cm^{-1}; ^{1}H NMR (700 MHz, CDCl$_3$) δ 6.93 (dd, *J* = 15.4, 11.2 Hz, 1H), 6.71 (d, *J* = 15.4 Hz, 1H), 6.61 – 6.58 (m, 1H), 6.26 – 6.21 (m, 1H), 6.19 (dt, *J* = 10.5, 0.9 Hz, 1H), 5.94 (dq, *J* = 15.4, 7 Hz, 1H), 5.74 (dq, *J* = 10.5, 7.7 Hz), 2.57 – 2.39 (m, 4H), 2.03 – 1.80 (m, 8H); ^{13}C NMR (176 MHz, CDCl$_3$) δ 199.4, 149.9, 149.8, 135.4, 134.2, 132.2, 131.8, 131.3, 130.7, 129.9, 129.8, 129.7, 127.9, 37.8, 26.0, 22.0, 18.5, 13.8, 10.5; HRMS (ESI) *m/z* calcd for C$_{12}$H$_{17}$O (M+H)$^+$ 177.1279, found 177.1285.
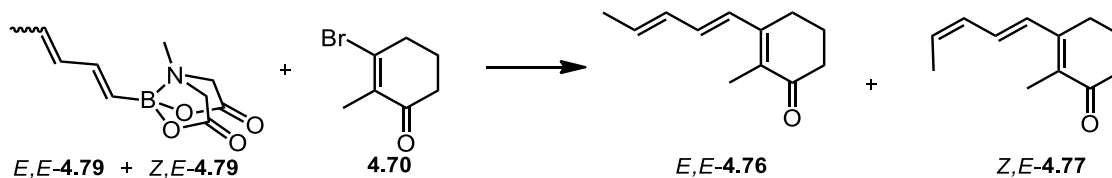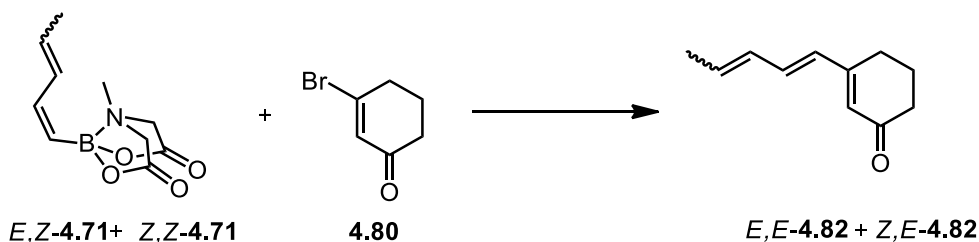
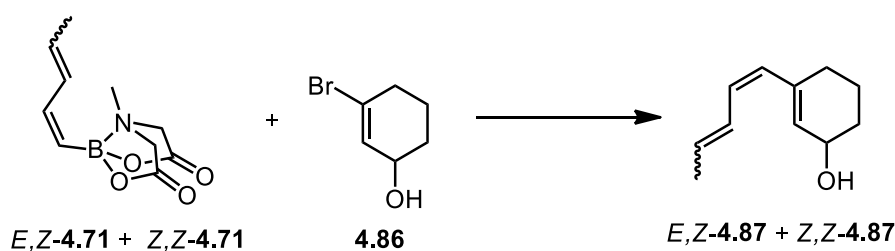**2-methyl-3-penta-1,3-dien-1-yl)cyclohex-2-enone (*E,E*-4.76 + *Z,E*-4.77)**

Prepared according to general procedure B using 3-bromo-2-methylcyclohex-2-enone **(4.70)** (28 mg, 0.148 mmol, 1 equiv)**,** diene MIDA boronate (*E,E*-**4.79** + *Z,E*-**4.79)** (40 mg, 0.179 mmol, 1.2 equiv), 5 mol% Pd(OAc)₂ (1/7 mg, 0.008 mmol), 10 mol% SPhos (6 mg, 0.015 mmol), and 1.86 mL of dioxane. After sparging with nitrogen for 30 minutes at room temperature, aqueous K_3PO_4 (3M, 1.12 mmol, 7.5 equiv) was added. Purification afforded the product as a pale yellow oil (15 mg, 0.08 mmol, 56%) as a mixture of triene isomers. The characterization data matches that of the products of the reaction between the same vinyl bromide (**4.70**) and diene MIDA boronate (**E,Z-4.71** + **Z,Z-4.71).**

E,Z-**4.71** + *Z,Z*-**4.71**   **4.80**   *E,E*-**4.82** + *Z,E*-**4.82**

3-((1E)-penta-1,3-dien-1-yl)cyclohex-2-enone (4.82)

Prepared according to general procedure B using 3-bromocyclohex-2-enone (**4.80**) (123 mg, 0.703 mmol, 1 equiv), diene MIDA boronate (**E,Z-4.82** + **Z,Z-4.82**) (189 mg, 0.843 mmol, 1.2 equiv), 5 mol% Pd(OAc)₂ (8 mg, 0.035 mmol), 10 mol% SPhos (29 mg, 0.070 mmol) and 9 mL of dioxane. After sparging with nitrogen for 30 minutes at room temperature, aqueous K_3PO_4 (3M, 5.27 mmol, 7.5 equiv) was added. Purification afforded the product as a pale yellow oil (85 mg, 0.521 mmol, 72%). IR (film) 3026, 2931, 2867, 1657, 986 cm⁻¹; ¹H NMR (400 MHz, CDCl3) δ 6.95 (dd, *J* = 15.6, 11.2 Hz, 1H), 6.62 (dd,

J = 15.6, 10.4 Hz, 1H), 6.29 (d, J = 15.6 Hz, 1H), 6.22 – 6.07 (m, 1H), 6.02-5.85 (m, 1H),

5.75 (dq, J = 10.8, 7.2 Hz, 1H) 2.55 – 2.30 (m, 4H), 2.08 – 1.95 (m, 2H), 1.88 – 1.75 (m,

2H); ^{13}C NMR (100 MHz, CDCl$_3$) δ 200.1, 157.5, 157.4, 136.1, 135.2, 132.7, 131.7, 131.5,

130.6, 130.4, 129.1, 127.5, 127.1, 37.7, 24.9, 22.4, 18.6, 13.9; HRMS (ESI) m/z calcd for

C$_{11}$H$_{15}$O (M+H)$^+$ 163.1117, found 163.1119.

E,Z-**4.71** + Z,Z-**4.71**   **4.86**   E,Z-**4.87** + Z,Z-**4.87**

3-((1Z)-penta-1,3-dien-1-yl)cyclohex-2-enol (4.87)

Prepared according to general procedure B using 3-bromocyclohex-2-enol (**4.86**)

(88 mg, 0.288 mmol, 1 equiv), 134 mg diene MIDA Boronate (**E,Z-4.71** + **Z,Z-4.71**)

(0.596 mmol, 1.2 equiv.), 5 mol% Pd(OAc)$_2$ (3 mg, 0.144 mmol), 10 mol% SPhos (12 mg,

0.029 mmol), and 3.60 mL of dioxane After sparging with nitrogen for 30 minutes at room

temperature, aqueous K$_3$PO$_4$ (3M, 2.16 mmol, 7.5 equiv) was added. Purification afforded

the product as a pale yellow oil (47 mg, 0.288 mmol, 58%). IR (film) 3333, 2933, 2861,

1646, 956 cm^{-1}; ^{1}H NMR (400 MHz, CDCl$_3$) δ 6.65 – 6.43 (m, 2H), 6.28 (t, J = 11.8 Hz,

1H), 6.17 – 6.12 (m, 1H), 5.95 (t, J = 11.6 Hz, 1H), 5.82 – 5.68 (m, 3H), 5.62 (d, J = 11.6

Hz, 1H), 5.61 – 5.50 (m, 1H), 4.31 (s, 1H), 2.28 – 2.10 (m, 2H), 1.89 – 1.55 (m, 10H); ^{13}C

NMR (100 MHz, CDCl$_3$) δ 139.1, 131.9, 131.5, 131.0, 130.4, 129.8, 129.6, 129.1, 128.6,

128.1, 126.2, 124.2, 67.2, 66.2, 35.3, 31.7, 30.7, 29.2, 20.6, 19.3, 18.4, 13.1; HRMS (ESI) m/z calcd for $C_{11}H_{17}O$ (M+H)$^+$ 164.1201, found 164.1196.

E,Z-**4.71** + Z,Z-**4.71**   **4.88** E,Z-**4.89** + Z,Z-**4.89**
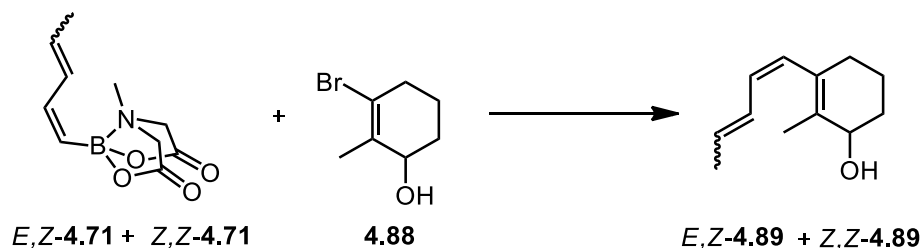
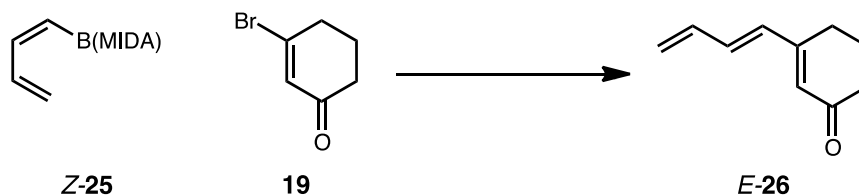**2-methyl-3-((1Z)-penta-1,3-dien-1-yl)cyclohex-2-enol (4.89)**

Prepared according to general procedure B using 3-bromo-2-methylcyclohex-2-enol (**4.88**) (90 mg, 0.470 mmol, 1 equiv.), 126 mg diene MIDA boronate (**E,Z-4.89 + Z,Z-4.89**) (0.564 mmol, 1.2 equiv.), 5 mol% Pd(OAc)$_2$ (5.3 mg, 0.024 mmol), 10 mol% SPhos (19 mg, 0.047 mmol), and 5.89 mL of dioxane. After sparging with nitrogen for 30 minutes at room temperature, aqueous K$_3$PO$_4$ (3M, 3.53 mmol, 7.5 equiv) was added. Purification afforded the product as a pale yellow oil (38 mg, 0.213 mmol, 45%). IR (film) 3433, 3054, 2933, 2852, 1659 cm^{-1}; ^{1}H NMR (700 MHz, CDCl$_3$) δ 6.30 (t, J = 11.2 Hz, 1H), 6.10 (t, J = 12.6 Hz, 1H), 6.03 (t, J = 11.2 Hz, 1H), 5.96 (t, J = 11.2 Hz, 1H), 5.87 (d, J = 11.2 Hz, 1H), 5.77 – 5.68 (m, 2H), 5.59 – 5.49 (m, 1H), 4.10 (s, 1H), 2.57 – 2.43 (m, 2H), 2.12 – 1.95 (m, 2H), 1.80 – 1.60 (m, 10H); ^{13}C NMR (176 MHz, CDCl$_3$) δ 134.0, 132.7, 131.3, 130.7, 130.3, 129.4, 128.8, 128.2, 127.1, 126.4, 124.7, 124.0, 70.0, 69.4, 36.7, 32.1, 31.6, 30.3, 20.5, 20.0, 18.4, 17.5; HRMS (ESI) m/z calcd for $C_{12}H_{19}O$ (M+H)$^+$ 178.1358, found 178.1353.
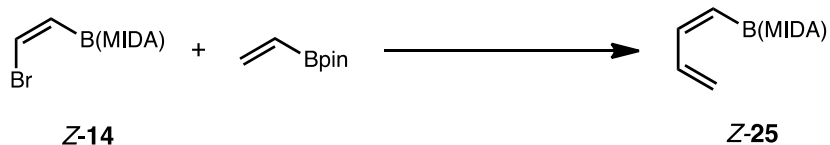
MIDA boronate Z-4.83

To a Schlenk flask containing Pd(OAc)$_2$ (8.6 mg, 10 mol%), XPhos (36.2 mg, 20 mol%), Cs$_2$CO$_3$ (436 mg, 3.5 equiv), bromo MIDA boronate **(4.73)** (100 mg, 1 equiv), was added DMSO (7.6 mL, 0.05M). The resulting solution was stirred for 15 minutes and then added to a flask containing vinyl boronic acid (133 µL, 2 equiv), and the reaction was stirred for 24 hours at room temperature. The reactions were tracked by TLC (100% EtOAc). Upon completion, the crude reaction mixture was filtered through celite, concentrated, and then diluted with EtOAc. The organic layer was washed with brine and dried with Na$_2$SO$_4$. Volatiles were removed under reduced pressure to afford a crude yellow oil. The crude material was purified using silica gel chromatography with 100% Et$_2$O, then 1.5% MeOH/Et$_2$O, then 50% acetone/hexanes to give a light yellow oil (15.2 mg, 0.073 mmol, 19%). Spectral data were consistent with literature values.

Z-25   19   E-26

(E)-3-(buta-1,3-dien-1-yl)cyclohex-2-enone (4.85)

Prepared according to general procedure B using 3-bromocyclohex-2-enone **(4.80)** (10 mg, 0.058 mmol, 1 equiv), diene MIDA boronate (**Z-4.83**) (14 mg, 0.069 mmol, 1.2 equiv), 10 mol% Pd(OAc)$_2$ (1.3 mg, 0.006 mmol), 20 mol% SPhos (4.7 mg, 0.070 mmol) and 723 µL of dioxane. After sparging with nitrogen for 30 minutes at room temperature, aqueous K$_3$PO$_4$ (3M, 0.4335 mmol, 7.5 equiv) was added. Purification afforded the product as a pale yellow oil (3.8 mg, 44%). IR (film) 2929, 2852, 1667, 1590, 1250 cm^{-1}; ^{1}H NMR (400 MHz, CDCl$_3$) δ 6.70 – 6.55 (m, 1H), 6.44 (dt, J = 10.4 Hz, 1H), 6.37 (d, J = 15.2 Hz, 1H), 5.97 (s, 1H), 5.47 (d, J = 16.8 Hz, 1H), 5.36 (d, J = 10.0 Hz, 1H), 2.50 (t, J = 6.4 Hz, 2H), 2.43 (t, J = 6.4 Hz, 2H), 2.10 – 2.00 (m, 2H); HRMS (ESI) m/z calcd for C$_{10}$H$_{13}$O (M+H)$^+$ 149.0961, found 149.0959.

4.7 - References

[1]   D. J. Newman, G. M. Cragg, *J. Nat. Prod.* **2012**, *75*, 311–335.

[2]   R. Scatena, G. E. Martorana, P. Bottoni, G. Botta, P. Pastore, B. Giardina, *Expert Opin. Investig. Drugs* **2007**, *16*, 59–72.

[3]   P. M. Joyner, R. H. Cichewicz, *Nat. Prod. Rep.* **2010**, *28*, 26–47.

[4]   D. J. Newman, G. M. Cragg, *J. Nat. Prod.* **2012**, *75*, 311–335.

[5]   K. T. Yuyama, D. Fortkamp, W.-R. Abraham, *Biol. Chem.* **2017**, *399*, 13–28.

[6]   Y. Lu, P.-J. Li, W.-Y. Hung, J.-H. Su, Z.-H. Wen, C.-H. Hsu, C.-F. Dai, M. Y. Chiang, J.-H. Sheu, *J. Nat. Prod.* **2011**, *74*, 169–174.

[7]   B. F. Bowden, J. C. Coll, S. J. Mitchell, *Aust. J. Chem.* **1980**, *33*, 885–890.

[8]   J. A. Marshall, H. Faubl, T. M. Warne, *Chem. Commun. Lond.* **1967**, 753–754.

[9]   K. P. Dastur, *J. Am. Chem. Soc.* **1974**, *96*, 2605–2608.

[10] M. Pesaro, G. Bozzato, P. Schudel, *Chem. Commun. Lond.* **1968**, 1152–1154.

[11] R. Liffert, A. Linden, K. Gademann, *J. Am. Chem. Soc.* **2017**, *139*, 16096–16099.

[12] O. Selaïmia-Ferdjani, A. Kar, S. P. Chavan, M. Horeau, G. Viault, J. Pouessel, X. Guillory, V. Blot, A. Tessier, A. Planchat, et al., *Eur. J. Org. Chem.* **2013**, *2013*, 7083–7094.

[13] J. Das, M. Kakushima, Z. Valenta, K. Jankowski, R. Luce, *Can. J. Chem.* **1984**, *62*, 411–416.

[14] C. W. Wilson, P. E. Shaw, *J. Agric. Food Chem.* **1978**, *26*, 1430–1432.

[15] M. Bian, L. Li, H. Ding, *Synthesis* **2017**, *49*, 4383–4413.

[16] R. B. Woodward, R. Hoffmann, *Angew. Chem. Int. Ed. Engl.* **1969**, *8*, 781–853.

[17] K. C. Nicolaou, *J. Org. Chem.* **2009**, *74*, 951–972.

[18] E. E. Anagnostaki, A. L. Zografos, *Chem. Soc. Rev.* **2012**, *41*, 5613–5625.

[19] G.-Dong. Zhu, W. H. Okamura, *Chem. Rev.* **1995**, *95*, 1877–1952.

[20] G. H. Posner, M. Kahraman, *Eur. J. Org. Chem.* **2003**, *2003*, 3889–3895.

[21] W.-L. Xiao, L.-M. Yang, N.-B. Gong, L. Wu, R.-R. Wang, J.-X. Pu, X.-L. Li, S.-X. Huang, Y.-T. Zheng, R.-T. Li, et al., *Org. Lett.* **2006**, *8*, 991–994.

[22] Z. Lu, Y. Li, J. Deng, A. Li, *Nat. Chem.* **2013**, *5*, 679–684.

[23] T. Abe, T. Ikeda, R. Yanada, M. Ishikura, *Org. Lett.* **2011**, *13*, 3356–3359.

[24] T. P. Yoon, M. A. Ischay, J. Du, *Nat. Chem.* **2010**, *2*, 527–532.

[25] D. M. Schultz, J. W. Sawicki, T. P. Yoon, *Beilstein J. Org. Chem.* **2015**, *11*, 61–65.

[26] D. A. Nicewicz, D. W. C. MacMillan, *Science* **2008**, *322*, 77–80.

[27] J. Ma, K. Harms, E. Meggers, *Chem. Commun.* **2016**, *52*, 10183–10186.

[28] C. K. Prier, D. A. Rankic, D. W. C. MacMillan, *Chem. Rev.* **2013**, *113*, 5322–5363.

[29] J. M. R. Narayanam, J. W. Tucker, C. R. J. Stephenson, *J. Am. Chem. Soc.* **2009**, *131*, 8756–8757.

[30] Y.-Q. Zou, L.-Q. Lu, L. Fu, N.-J. Chang, J. Rong, J.-R. Chen, W.-J. Xiao, *Angew. Chem. Int. Ed.* **2011**, *50*, 7171–7175.

[31] A. E. Hurtley, Z. Lu, T. P. Yoon, *Angew. Chem. Int. Ed Engl.* **2014**, *53*, 8991–8994.

[32] T. Ni, R. A. Caldwell, L. A. Melton, *J. Am. Chem. Soc.* **1989**, *111*, 457–464.

[33] J.-H. Su, Y. Lu, W.-Y. Hung, C.-Y. Huang, M. Y. Chiang, P.-J. Sung, Y.-H. Kuo, J.-H. Sheu, *Chem. Pharm. Bull. (Tokyo)* **2011**, *59*, 698–702.

[34] R. Ramage, A. Sattar, *J. Chem. Soc. Chem. Commun.* **1970**, 173–175.

[35] Norio. Miyaura, Akira. Suzuki, *Chem. Rev.* **1995**, *95*, 2457–2483.

[36] E. P. Gillis, M. D. Burke, *Aldrichimica Acta* **2009**, *42*, 17–27.

[37] J. Li, A. S. Grillo, M. D. Burke, *Acc. Chem. Res.* **2015**, *48*, 2297–2307.

[38] J. W. Lehmann, D. J. Blair, M. D. Burke, *Nat. Rev. Chem.* **2018**, *2*, DOI 10.1038/s41570-018-0115.

[39] E. M. Woerly, J. E. Miller, M. D. Burke, *Tetrahedron* **2013**, *69*, 7732–7740.

[40] E. M. Woerly, J. R. Struble, N. Palyam, S. P. O'Hara, M. D. Burke, *Tetrahedron* **2011**, *67*, 4333–4343.

[41] N. K. Chehal, P. H. M. Budzelaar, P. G. Hultin, *Org. Biomol. Chem.* **2018**, *16*, 1134–1143.

[42] K. A. Mack, A. McClory, H. Zhang, F. Gosselin, D. B. Collum, *J. Am. Chem. Soc.* **2017**, *139*, 12182–12189.

[43] M. Christensen, A. Nolting, M. Shevlin, M. Weisel, P. E. Maligres, J. Lee, R. K. Orr, C. W. Plummer, M. T. Tudge, L.-C. Campeau, et al., *J. Org. Chem.* **2016**, *81*, 824–830.

[44] C. Molinaro, J. P. Scott, M. Shevlin, C. Wise, A. Ménard, A. Gibb, E. M. Junker, D. Lieberman, *J. Am. Chem. Soc.* **2015**, *137*, 999–1006.

[45] G.-P. Lu, K. R. Voigtritter, C. Cai, B. H. Lipshutz, *J. Org. Chem.* **2012**, *77*, 3700–3703.

[46] P. V. Ramachandran, W. Mitsuhashi, *Org. Lett.* **2015**, *17*, 1252–1255.

[47] J. Yu, M. J. Gaunt, J. B. Spencer, *J. Org. Chem.* **2002**, *67*, 4627–4629.

[48] J. E. Moses, J. E. Baldwin, R. Marquez, R. M. Adlington, A. R. Cowley, *Org. Lett.* **2002**, *4*, 3731–3734.